

d'A (rchief)

Closure of the Shiwa Tidal Basin

July 1993

A.F.Kooij

Volume I Main Report

Volume I: Main Report
Volume II: Preliminary Model Investigation


TU Delft
Delft University of Technology

Faculty of Civil Engineering
Hydraulic and Geotechnical Engineering Division
Hydraulic Engineering Group



Thesis Report

Student: A.F. Kooij

Student number: 466274

Thesis subject: Design of the bottom protection length of the closure dam of the Shiwa Tidal Basin

Supervisors: prof. ir. K. d'Angremond

ir. F. C. van Roode

ir. C. Verspuy

Preface

This report describes the results of my thesis study on the design of the bottom protection length of the closure dam of the Shiwa tidal basin in South Korea. This study is the final stage of my Civil Engineering study at the Delft University of Technology. I have been working on this subject from October 1992 until July 1993 at the Delft University of Technology. I experienced this period and mainly the process of doing a thesis study as very positive and I would therefore like to thank ir. F.C. van Roode who supported me during this thesis study. I also would like to thank ir C. Verspuy who helped me with the DUFLOW modelling of the Shiwa tidal basin and last but not least prof. ir. K. d'Angremond for being chairman of my thesis committee.

Arjan Kooij, July 1993

Abstract

South Korea suffers from a high population density and stands therefore in need of agricultural and industrial land. The Koreans are seeking for solutions to solve this problem. One of the possibilities is to reclaim land from the sea. Several land-reclamation projects have already been carried out and one of the projects that is at the moment under construction is the closure of the Shiwa tidal basin. This project has been studied by the NEDECO and it appeared that the bottom protection length of 30 meter, designed by the Koreans is not sufficient according to Dutch design rules.

In this thesis study, the bottom protection length has been determined according to Dutch design standards. Therefore, first a mathematical model of the region has been made to obtain the local conditions. This model is described in the sub report on the preliminary model investigation on the closure of the Shiwa tidal basin. With the model, several closure methods have been simulated. With the thus obtained local hydraulic data, the decisive D_{50} of the closure dam, depending on the closure method has been determined. Subsequently, the time needed for the construction of the dam has been determined with an estimation of the production capacity. With the flow velocities during every closure phase and the time during which the bottom is exposed to these flow velocities, the bottom protection length could be determined. The bottom protection length needed to avoid failure of the closure dam due to extensive scouring appeared to have a length of 15 to 300 meter. The maximum bottom protection is ten times more than the length designed by the Koreans.

The report consists of two separate volumes:

Volume I	Main report
Volume II	Preliminary model investigation

Table of contents

Preface

Abstract

1 Introduction	1
1.1 Current state	1
1.2 Objectives	1
1.3 Limitations	1
1.4 Methodology	2
2 Dam alignment	5
3 Closure methods	9
3.1 Introduction	9
3.2 Vertical closure	9
3.2.1 Hydraulic conditions	9
3.2.1 Construction method	10
3.3 Horizontal closure	11
3.3.1 Hydraulic conditions	11
3.3.2 Construction method	12
3.4 Combination of a vertical and a horizontal closure	12
3.4.1 Hydraulic conditions	12
4 Design of the construction profile of the closure dam	15
4.1 Introduction	15
4.2 Slope angle	15
4.3 Crest width	16
4.4 Crest level	16
4.4.1 Functional crest level	17
4.4.2 Workable crest level	17
4.4.2.1 Wind set-up	18
4.4.2.1 Wave run-up	19
4.5 Construction profile	22
5 Micro stability of the closure dam	25
5.1 Introduction	25
5.2 Flow induced loads	25
5.2.1 Flow conditions during a vertical closure	25
5.2.1.1 Low dam flow	25

5.2.1.2 Intermediate flow	28
5.2.1.3 High dam flow	28
5.2.1.4 Through flow	29
5.2.2 Flow conditions during a horizontal closure	29
5.2.3 Flow conditions during a combined closure	30
5.3 Wave conditions during closure	31
6 Bottom protection design	33
6.1 Introduction	33
6.2 Theory	33
6.3 Determination of the maximum scour depth	35
6.3.1 Influence of the flow velocities on the scour	35
6.3.2 Time depending scour	37
6.3.2 Resulting scour depth	39
6.4 Resulting slope angle after slide	39
6.5 Determination of the bottom protection length	40
6.6 Final results	40
7 Conclusions and recommendations	47
Bibliography	48
Annex A General data	
Annex B Set-up and run-up at the closure site	
Annex C C1: D_{50} during a vertical closure	
C2: D_{50} during a horizontal closure	
C3: D_{50} during a combined closure	
Annex D D1: Scour depth during a vertical closure	
D2: Scour depth during a horizontal closure	
D3: Scour depth during a combined closure	

Closure of the Shiwa Tidal Basin

1 Introduction

1.1 Current state

South Korea suffers from a high population density at the surroundings of the capital Seoul and the harbour Inch'On. This country therefore stands in need of agricultural and industrial land. As the inland and east coast are inapt for any expansion because they are mountainous, a solution has to be found at the west coast where a coastal plane is situated. Here, several land reclamation projects have already been carried-out by the Koreans. These closures were mainly based on a horizontal closure method where rock was dumped over the roundheads with dump trucks. This method was applied as a result of the large tidal range and the big storage areas implying very high flow velocities in the final closure stage.

One of the possibilities for land reclamation is the closure of the Shiwa tidal basin, situated approximately 50 km. at the south of Inch'On (see figure 1.2). The storage of the tidal basin including shoals is 160 km². After closure, 60 % of the reclaimed area will be used to create new land while 40 % will be used as a fresh-water basin. This project has been designed by the Koreans. At the moment the closure dam is under construction but as a result of protesting fishermen who see the dam as a threat of their profession, it has an undetermined delay.

1.2 Objectives

NEDECO, an organization of Dutch consulting Engineers carried-out a study on various land reclamation projects in South Korea, evaluating each project on its economical and technical aspects. One of the largest projects, (Shiwa) has been examined more thoroughly. It appeared that the bottom protection with a length of ± 30 meter, designed by the Koreans seems to be rather short concerning Dutch design standards. The bottom of the Shiwa basin consists of fine-grained sand which erodes easily.

My thesis study consists of designing the closure dam for the Shiwa Tidal Basin and the bottom protection, according to Dutch design standards. The result will be compared with the actual design that is made by the Koreans.

1.3 Limitations

The lay-out of the reclaimed land goes beyond this thesis study as well as the design of

the sluices for shipping and for discharging water into the Yellow Sea.

The small connections near Bul Do and Son Gam Do, are already closed, and will therefore not be considered.

As my thesis study consists of designing the bottom protection for the closure of the Shiwa Tidal Basin only the construction profile of the closure dam will be determined. The final dam profile has no influence on the scour and the size of the bottom protection.

1.4 Methodology

Before being able to design the closure dam and its bottom protection, the local hydraulic conditions at the site must be determined. These local hydraulic conditions depend on the geometry of the region and the general hydraulic conditions, such as the prevailing tide, the wave climate and the upland flow. The required local hydraulic data can be obtained by making a model of the region in accordance with the geometry of the region, using the general hydraulic conditions as boundary conditions. With the one dimensional computer program DUFLOW a model of the region is made and is discussed separately in the sub-report Preliminary Model Investigation on the Closure of the Shiwa Tidal Basin.

In this report, the construction profile of the closure dam and its bottom protection are designed using the local hydraulic conditions, obtained with the DUFLOW model. First the dam alignment is determined in chapter 2. In chapter 3, three possible closure methods are discussed. Chapter 4 describes the stability of the stones and the required stone sizes under all closure phases. Then the construction profile of the closure dam is determined in chapter 5, after which the scour depth and the length of the bottom protection is discussed in chapter 6. Chapter 7 finally describes the conclusions and recommendations.

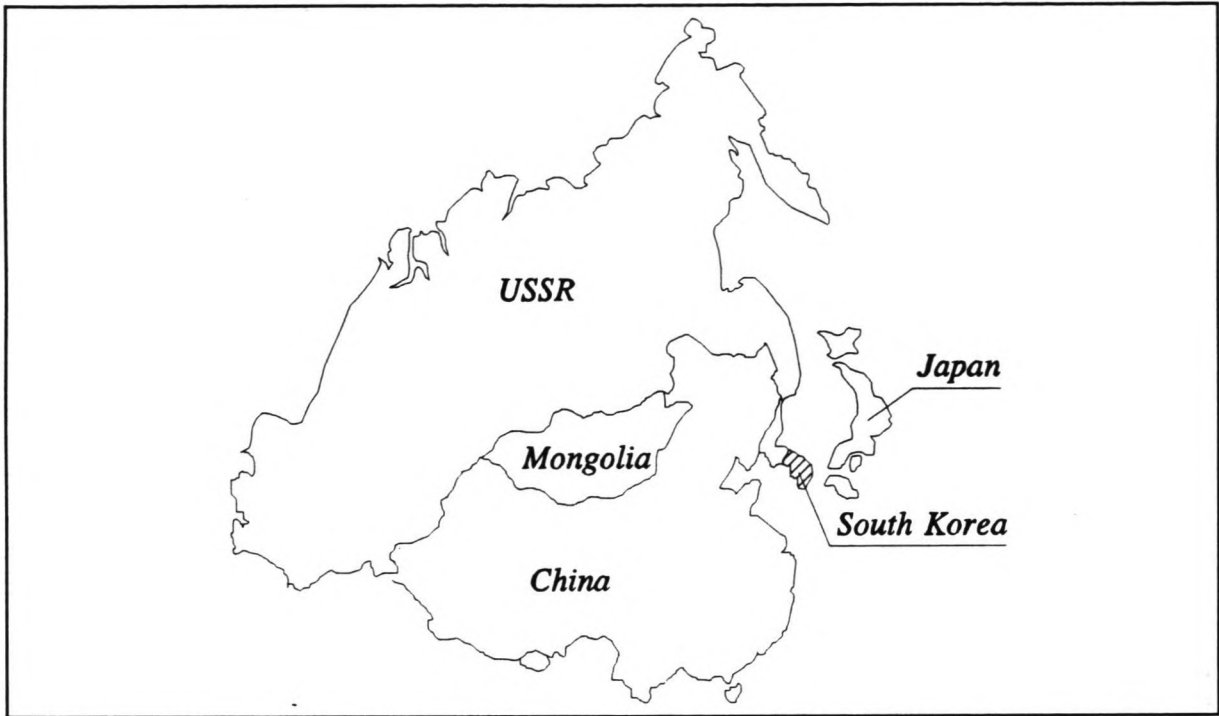


Figure 1.1: Map of East Asia



Figure 1.2: Korea

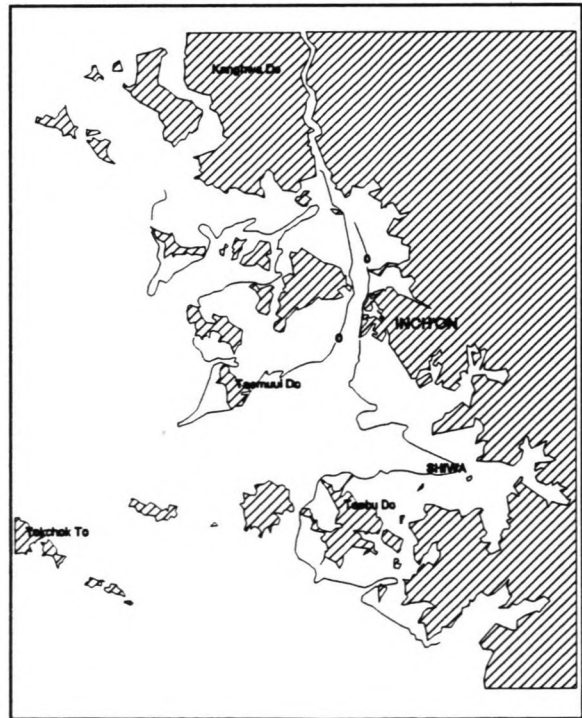


Figure 1.3: The Shiwa Tidal Basin

2 Dam alignment

As a result of the comparative nature of this thesis study, the same dam-alignment as proposed in the study on the closure of the Shiwa tidal basin, carried out for NEDECO by the Delta Department of the Dutch Ministry of Transport and Public Works [4] will be used. This chapter describes the factors that determined the chosen dam alignment.

As can be seen in Figure 2.1, various alternatives for the dam alignment in the main gullies (near Oheido) are generated. The choice of the best alignment of the closure dam should be based on a number of criteria. The seven main criteria are discussed below.

I Length of the dam:

A minimum length of the dam is preferable with respect to costs and time. A short dam alignment saves time and material. This depends however also on the depth of the gully, the deeper the gully, the more material is needed.

II Size of the reclaimed area:

Depending on the aims for reclaiming new land, the maximum size of the area to be reclaimed can be determined. The bigger the reclaimed area, the higher the costs will be to construct the closure dam. The dam will be constructed in much deeper water, thus needing much more material. There is an optimum for which the profit of extra gained land does not equal the extra costs for a bigger closure dam. In the case of the Shiwa Tidal Basin, a maximum area is preferred.

III Use of natural points of support:

When constructing the closure dam, it is attractive to use islands, located at the dam alignment. These points can be used as material depots. From a logistic perspective it is also very attractive to have such natural points of support, because they can be used as a starting point to build-out the roundheads. This way the construction time can be reduced considerably.

IV Angle between dam- and gully-axis:

In order to minimize both the required amount of material and the construction time, a perpendicular crossing of the gullies is best. Another advantage of crossing the gullies perpendicular is that a minimum amount of material is submitted to heavy current attack.

V Location of the dam in relation with wave direction:

The maximum run-up at a slope occurs when the waves approach perpendicular to the slope. Therefore it is favourable to have a dam alignment not perpendicular to the main wave direction. This way the elevation of the crest can be reduced which is profitable concerning costs and time.

VI Alignment dam versus alignment coast:

The final structure will form a part of the coast. As the dam can be considered as a disturbance of the natural coastline, the morphological situation is likely to alter. In order to avoid problems with undesirable erosion or accretion, a smooth fitting of the dam alignment with the existing coastline is recommended.

VII Depth of the final closure gap:

In case of closing a number of gaps, it is recommended to close the smaller ones first, see section 3.3. When applying a horizontal closure, it is attractive to close the final gap in a shallow part of the gully.

To determine the best dam alignment, a multi criteria analysis, demonstrated below has been carried out. In this analysis one other criterion is considered namely VIII, the location of the sluices. The best dam alignment, according to this multi criteria analysis is 1a, see Figure 2.1.

Table (2.2): Selection of main dam alignment, according to the NEDECO study [4]

Criteria	1	2	3	4	5	6	7	8
Alternative								
1a	+	++	+	0	0	-	-	+
1b	+	+	+	+	-	--	0	0
2	-	0	+	+	-	--	+	+
3	0	0	0	+	0/-	0	+	0
4	-	-	+	+	+	-	+	0

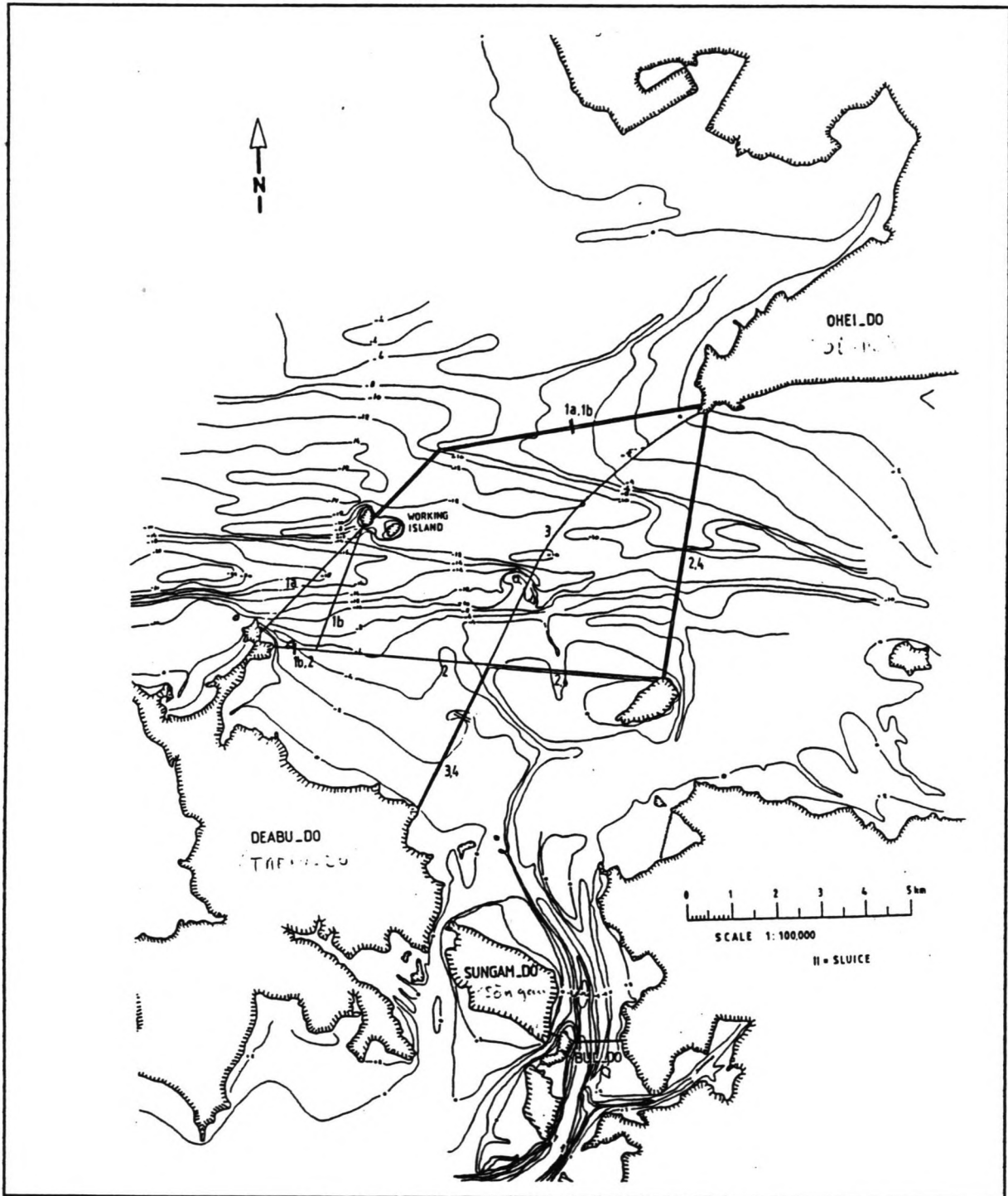


Figure 2.1: Dam alignment (source: ref [4])

3 Closure methods

3.1 Introduction

There are several methods to close a tidal basin. Depending on the hydraulic conditions and the available material and equipment, a choice for the best closure method can be made. In this chapter, three closure methods will be discussed, a vertical, a horizontal and a combination of both a horizontal and a vertical closure. Each of these methods differ in the hydraulic conditions during closure and the construction method. As the Korean design of the closure dam is a rock fill dam, a sudden closure with caissons will not be considered. In Figure 3.1, the cross section of the closure gap is displayed. This cross section is schematized into 4 sections, called S1, S2, S3 and S4.

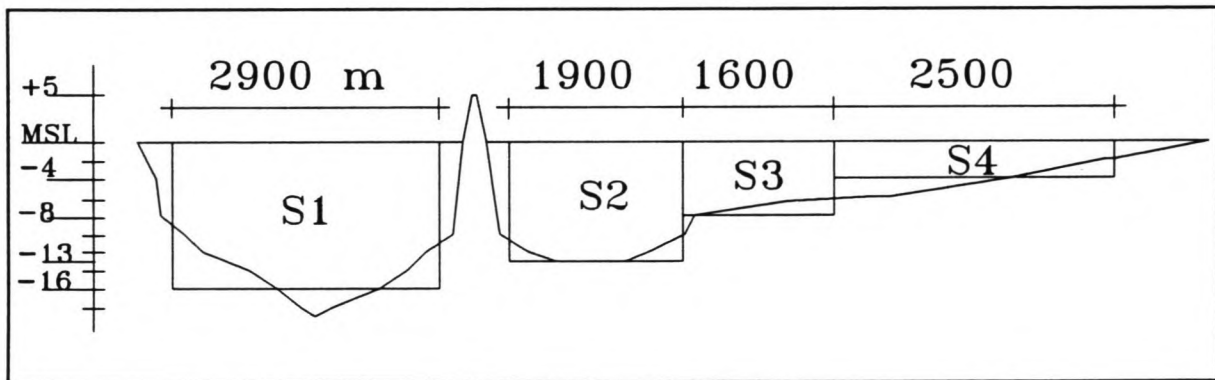


Figure 3.1: Cross section over dam alignment 1a

3.2 Vertical closure

3.2.1 Hydraulic conditions

When applying a vertical closure method, demonstrated in Figure 3.2, a sill will be build-up over the entire length of the cross section. As a consequence of the reduction of the cross section, the flow velocities increase. With this increase of the flow velocities, the weight of the material that is used to close the gap must increase as well. The increase of the maximum velocity will stop when the flow over the crest of the sill becomes supercritical. This stage of supercritical flow is reached when the downstream water level above the crest of the sill is less than $\frac{2}{3}$ of the upstream water level above the crest of the sill. Further heightening of the sill will decrease the maximum flow velocities until the

dam has reached its attained height. In case of the closure of the Shiwa tidal basin, the flow velocities that occur during a vertical closure are determined by dividing the closure into a number of phases, see Annex C1 figure 1. Here it can be seen that the sill is built up to the same height in all sections. This is done to have the maximum profit of the restricted flow velocities during the situation of free flow. During closure, the sill level is gradually in-creased until in the final phase the crest level of MSL +5m is reached. With the DUFLOW model, the flow velocities as a function of time are calculated and the results are demonstrated in Figure 3.3. An advantage of a vertical closure method is the diminution of the velocities at the bottom of the gully during the heightening of the sill. This way scour is minimum and less extensive bottom protection is needed.

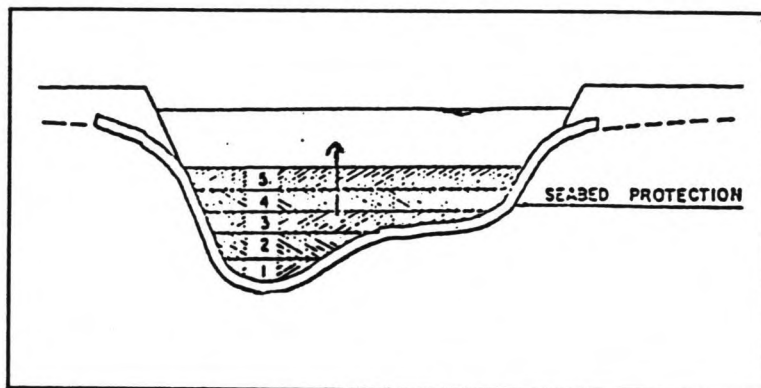


Figure 3.2: Vertical closure method

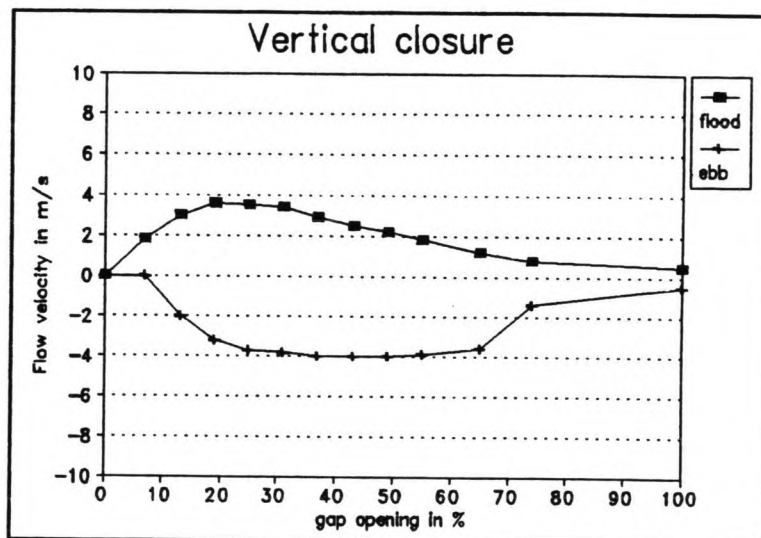


Figure 3.3: Flow velocities as function of gap opening

3.2.1 Construction method

First, after the bottom has been protected, the shallow parts of the gully will be closed by building out a dam section from one of the banks. In this case this will be S4, see Figure 3.1. In the remaining gap, a sill is built up in horizontal layers. This can be done by dumping flow resistant material such as gravel, stones, concrete blocks or rock units by:

- I: Manual labour or trucks on a causeway
- II: Floating equipment such as stone dumping vessels or floating cranes

- III: Cableway
- IV: Helicopters
- V: Trucks on a bridge

Dumping material by means of manual labour or trucks on a causeway is relatively cheap, but only applicable in relatively shallow channels. In case of the closure of the Shiwa tidal basin the high tidal range is an extra disadvantage for applying this method.

When using stone dumping vessels the capacity is low because the production decreases until zero when the closure reaches its final stage. Due to the draught and the highly increased flow velocities, stone dumping vessels are able to float over the retaining dam at high tide only and when the flow velocities are sufficiently low. Floating cranes have a relatively low dumping capacity and need to be anchored with special mooring pontoons behind the closure gap, due to the high flow velocities. Both types of dumping material are relatively cheap.

A cableway, helicopters or trucks on a bridge are all very expensive methods. The advantage is however that a high dumping capacity can be attained with almost no bad weather delay. In case of large closure operations, and Shiwa can be considered as large with its total length of almost twelve kilometers, it can be profitable to use one of these methods. The construction time is considerably reduced and the bottom protection is minimum as the scour is reduced as well.

3.3 Horizontal closure

3.3.1 Hydraulic conditions

In case of a horizontal closure, the gap will be closed by building out the roundheads from both sides, see Figure 3.4. As a result of decreasing the cross section horizon-tally, the flow velocities will increase continuously up to the final closure stage. No stage of free overflow will be reached as during a vertical closure. These high flow velocities in the final stage demand large closing elements such as concrete cubes, gabions or large rock units. This method can therefore only be applied in cases where the head over the closure gap is not too great.

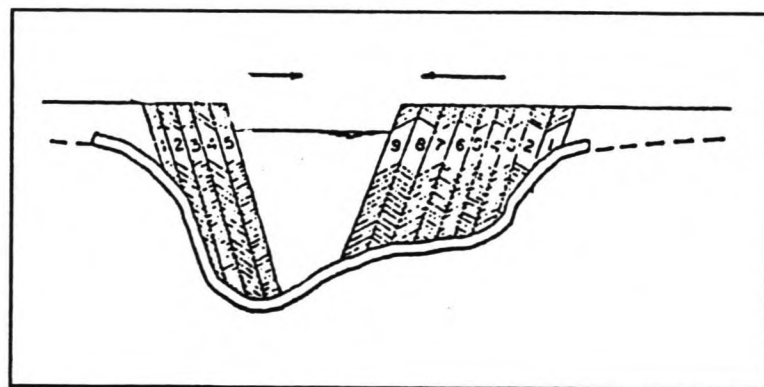


Figure 3.4: Horizontal closure method

In this case, the flow velocities that occur during a horizontal closure are determined by dividing the closure into a number of phases. This is demonstrated in Annex C2, figure 36. During every phase, the section width is reduced until in the last phase the basin is closed. With the DUFLOW model, the flow velocities as a function of time are calculated during every phase and the results are demonstrated in Figure 3.5. The calculations made with the DUFLOW model show, that the maximum flow velocities increase up to 9.3 m/s during the ebb flow.

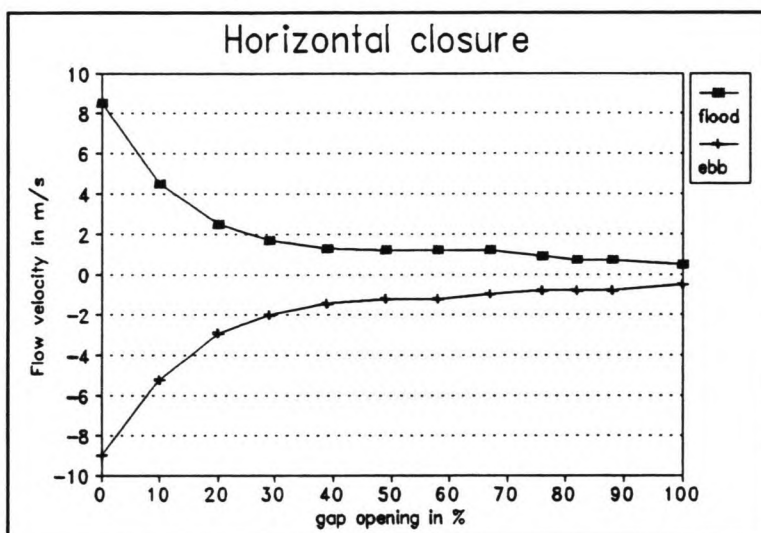


Figure 3.5: Flow velocities as function of gap opening

3.3.2 Construction method

In case of a horizontal closure, the roundheads of the dam are build-out from the sides, thus narrowing the gap until zero. This can be done by dumping gravel, clay, rubble or bags filled with either sand or clay over the head of the dam section by manual labour, trucks or cranes. When thus constricting a closure gap, the ultimate closure gap must be sufficiently small to be closed during one low tide, while still being large enough to avoid very high flow velocities. These high flow velocities would cause scouring of the bottom and the dam heads

3.4 Combination of a vertical and a horizontal closure

3.4.1 Hydraulic conditions

When applying a combination of a horizontal and a vertical closure, see Figure 3.6, the advantage of creating a situation of free overflow by constructing a sill is combined with building out the roundheads from the sides. Although the flow velocities are higher than during a complete vertical closure method, the flow velocities are reduced because the situation of free overflow will be reached. As a result of the horizontal constriction in the final phase of the closure, the water level inside the basin will increase thus causing an

increasing head over the structure. Consequently, the flow velocities will increase until the final stage up to 6.5 m/s, which is not as much as during a complete horizontal closure. Figure 3.7 shows the flow velocities as a function of gap opening. These values are obtained by simulating the closure with the DUFLOW model. Therefore, the closure is divided into thirteen phases, see Annex C3 figure 62. At first a sill is build-up until MSL -2 meter after which the cross section is horizontally constricted until zero.

3.4.2 Construction method

As has already been mentioned in section 3.4.1, first a sill is constructed up to MSL -2. This is the maximum level that can be constructed by using floating equipment. Subsequently, the gap will be closed in a

horizontal way by building out the dam from the sides with dump trucks. Constructing the sill level up to the highest possible level gives the best results in regions with a small tidal range. As we are dealing here with a very large amplitude of the tide of approximately 8 meter, the sill level must be determined by optimizing the closure operation. In this thesis study, this optimization has not been carried out. A sill level of MSL -2 meter is applied, in accordance with the NEDECO study [4].

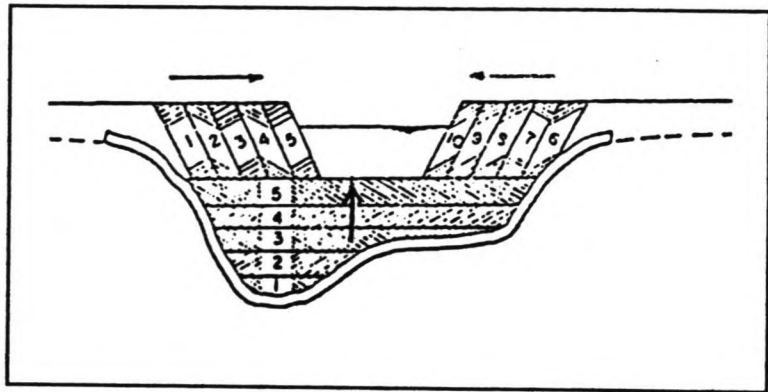


Figure 3.6: Combined closure method

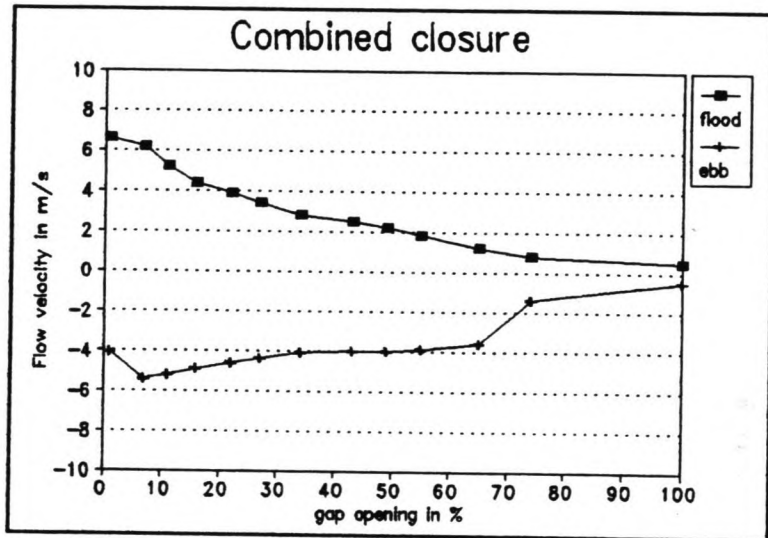


Figure 3.7: Flow velocities as function of gap opening

4 Design of the construction profile of the closure dam

4.1 Introduction

The cross sectional profile of the closure dam consists of a construction profile and a final profile. The construction profile has the function of closing the tidal basin so the basin is not influenced anymore by the tidal motion of the sea. Figure 4.1 shows this profile, that depends on the required crest level H , crest-width B and the slope-angles α and β . In this chapter, these parameters will successively be discussed.

The final dam profile that will be constructed over the construction profile, has the function of protecting the new obtained area behind the dam from inundation. This profile has however no effect on the design of the bottom protection and shall therefore not be considered.

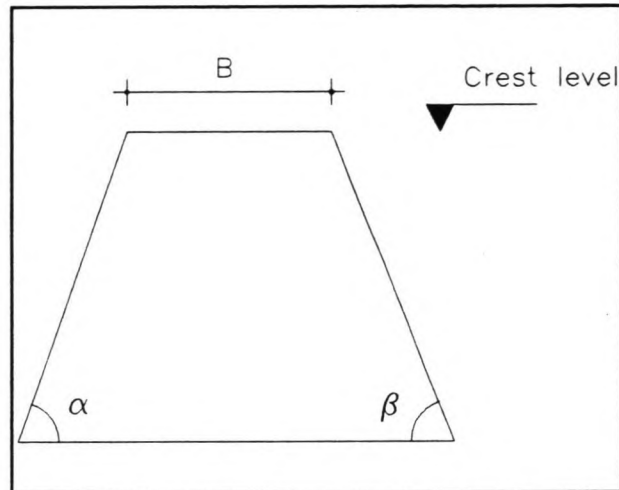


Figure 4.1: Cross sectional profile

4.2 Slope angle

The slope angles α and β mainly depend on the applied construction method. When a sill is constructed by dumping stones from barges, any angle between almost flat and the maximum angle of natural dumped stones can be obtained, see Figure 4.2. As the construction profile needs to be constructed as quick as possible thus keeping the scour minimum, the stones will be dumped continuously in a line in order to minimize the total amount of m^3 needed to close the basin. Consequently, the $\cot \alpha$ and $\cot \beta$ become 1.5 which is the maximum natural slope for dumped rubble mound.

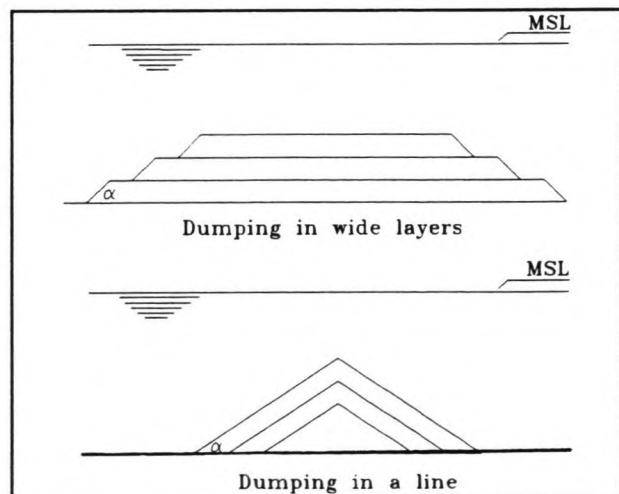


Figure 4.2: Slope angle when using barges

When constructing the closure dam by tipping the stones over the roundheads with dump trucks, see Figure 4.3, the cot α and cot β become also 1.5.

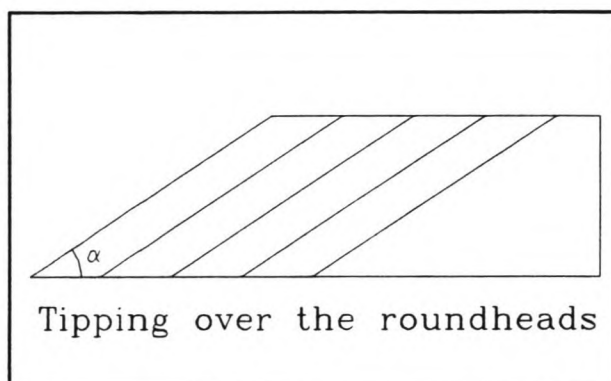


Figure 4.3: *Slope angle when tipping over the roundheads*

4.3 Crest width

The crest width of the construction profile, is mainly depending on the construction method. When a complete vertical closure method is applied, the crest width can be very small, approximately equal to the D_{50} of the material dumped in the final phase. When applying a horizontal or a combined closure, dump trucks need to drive on the crest. The crest width depends on how many trucks need to drive on the crest, if they need to pass by and if so, how many times this will happen. When the production does not need to be high and the closure dam is short, one lane on the crest will do. In case of larger closure operations, at several places a widening can be constructed so the trucks can pass by. In a situation where trucks drive on the dam with a very high frequency, two lanes are recommended. In this case, two lanes seem to be best. The longest construction dam is almost 6 km. and with only one lane on the crest, a high production is not possible. The assumed crest width therefore becomes 10 meter which is sufficient for two trucks passing by.

4.4 Crest level

The crest level depends on two types of parameters namely the functional and the workability parameters.

The functional parameters are:

- tidal level
- settlement

The workability parameters are:

- wind set-up
- wave run-up

Each of these parameters will be discussed in this section.

The effect of long term settlement, sea level rise and extremities such as tornados and tsunamis will not be discussed. The construction time of the construction profile is relatively short compared to the return-periods of these phenomena. When designing the final dam profile however, these factors must be considered.

4.4.1 Functional crest level

When the crest of the construction profile is elevated up to the maximum tidal level that will be reached plus the settlement of the dam, no water will enter the basin anymore and the construction profile fulfills its primary function.

The maximum water level at the closure site, due to tide can be expected during spring tide. Using the tidal constituents given by the Admiralty Tide Tables at the station Tokchok To a calculation is carried out with the DUFLOW modeling. It shows that the range of a spring tide is from MSL -4.25 m. up to MSL +4.45 m.

4.4.2 Workable crest level

The workability depends on the applied construction method of the closure dam. In case of a vertical closure almost no interruption due to bad sea conditions is expected. This is also the case when constructing the sill for the combined closure method.

When using a closure method where dump-trucks are used to build-out the roundheads, these trucks must be able to drive on the crest of the dam. This crest may not be flooded during the time that the weather is fair enough to drive on the dam. It must also be avoided that the fill layer is flushed away. This fill layer is a layer of fine graded material that is spread over the large stones at the top of the crest to smoothen the surface so the truck can drive on the crest. The crest level of the construction profile depends on the damage that is acceptable. Assuming that the time needed to construct the dam above MSL is 6 months, a storm that occurs about once a year is taken as design storm. Looking at the three most important wind directions, demonstrated in table 4.1, learns that the NW storm with a maximum speed of 15 m/s occurred 87 times in a period of 71 years. This storm is therefore taken as design storm. The extra water-level rise that is caused by a storm can be divided into wind set-up and wave run-up. These two phenomena will be discussed in the next sections.

Table 4.1: Wind direction and velocities at Inch'On, 1905-1976

Wind direction	appearance		wind velocity in m/s						
	no	rate	< 5	5-10	10-15	15-20	20-25	25-30	> 30
WNW	90	10.6%		2	43	38	5	1	1
NW	222	26.2%	1	115	87	18		1	
NNW	111	13.1%		3	63	40	4	1	

4.4.2.1 Wind set-up

When wind blows over a water surface, shear stresses occur at the interface between the water and the air. The forces that act on a column of water with width Δs and height d , is demonstrated in Figure 4.4. With the help of this figure, these forces can be derived:

$$f_1 = c_1 \rho_1 U^2 \Delta s \quad (4.1)$$

$$f_2 = \rho_w g d i \Delta s \quad (4.2)$$

When neglecting bottom friction,

$$f_1 = f_2 \text{ and } i = c \frac{U^2}{gd} \quad (4.3)$$

where:

- f_1 = wind force [N/m]
- f_2 = hydrostatic force [N/m]
- c_1 = friction coefficient
- ρ_1 = density of air [kg/m³]
- ρ_w = density of water [kg/m³]
- d = water depth [m]
- i = gradient
- c = $3.5 \text{ à } 4.0 \times 10^{-6}$
- U = wind speed [m/s]

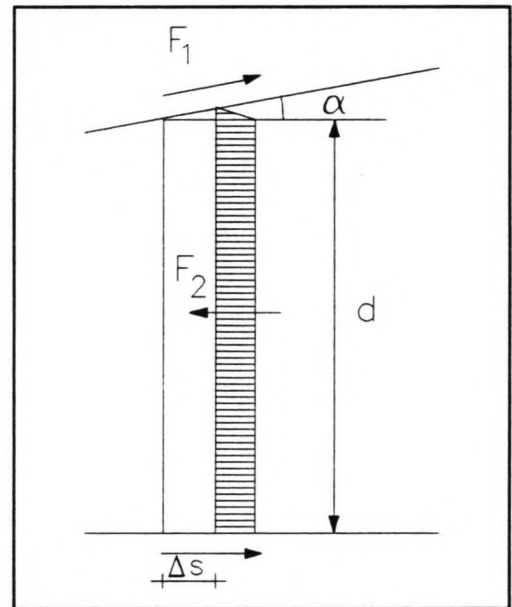


Figure 4.4: Set-up gradient

With the relation: $\Delta h = F \cdot i$

where F = the fetch length of the basin, the wind set-up Δh can be determined as demonstrated in equation (4.4):

$$\Delta h = \frac{cU^2F}{gd} \quad (4.4)$$

With the help of the Bathymetric Chart of Annex A, for all wind directions the fetch and the water depth is determined. The results of the calculations, carried out with this equation, are displayed in Annex B. It can be seen that the NW design storm gives the highest set-up of 0.33 m.

4.4.2.1 Wave run-up

When waves break on a slope, a part of their momentum results in a tongue of water, rushing up the slope. The run-up R (see Figure 4.5) is defined as the maximum vertical elevation reached by this tongue, related to the still water level.

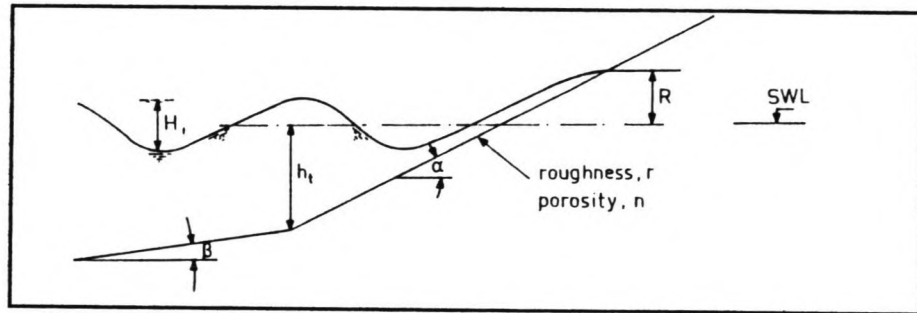


Figure 4.5: Run-up on a slope

Recent investigation and combination of many data from other research have led to, see CUR/CIRIA [7]:

$$R_{u2\%} = 1.5 H_s \frac{\tan \alpha}{\sqrt{H_s/L_0}} \quad (4.5)$$

With a maximum $R_{u2\%}$ of $3H_s$,

Where:

- $R_{u2\%}$ = 2% wave run-up
- H_s = significant wave height
- α = slope angle
- L_0 = wave length

This formula however is only valid for slopes of 1:3 or gentler. For steeper slopes an imaginary slope of 1:2.5 must be taken.

The run-up is maximum when the direction of the incoming waves is perpendicular to the crest of the dam. Therefore, the orientation of the dam in relation with the wind directions must be determined first. Looking at Figure 2.1, the dam alignment can be divided into two directions: One dam is orientated perpendicular to the North-West and the South-East and the other to the North and the South. Taking into account that waves propagate towards the dam at an angle β , see Figure 4.6, equation (4.5) changes into:

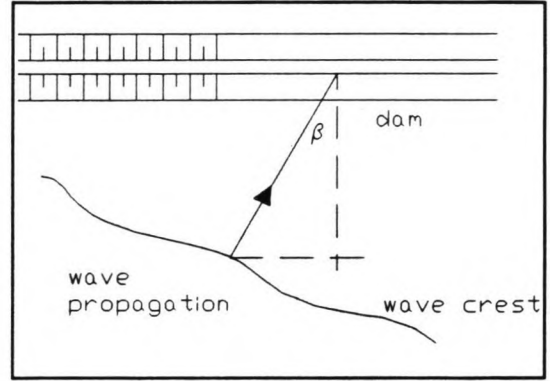


Figure 4.6: Oblique approaching waves

$$R_{u2\%} = 1,5 H_s \frac{\tan \alpha}{\sqrt{H_s/L_0}} \cos \beta \quad (4.6)$$

where:

β = angle between wave crest and dam axis

Equation (4.6) and (8) have been derived for wave run-up at slopes covered with grass or basalt. When applying this formula for a rubble mound slope, a reduction factor of 0.5-0.6, (see [7]) has to be taken into account. Once H_s and T_s are known, the run-up can be determined.

With the next formulas, derived by Bretschneider (Shore Protection Manual volume 1,p 3.55), wave height and wave period can be calculated:

$$H_{\frac{1}{3}} = 0.283 \left(\frac{U^2}{g} \right) \tanh \left[0.0125 \left(\frac{gF}{U^2} \right)^{0.42} \right] \quad (4.7)$$

$$T_{\frac{1}{3}} = 2.4\pi \left(\frac{U}{g} \right) \tanh \left[0.077 \left(\frac{gF}{U^2} \right)^{0.25} \right] \quad (4.8)$$

in case of deep water and:
in case of shallow water.

where:

$$H_{\frac{1}{3}} = 0.283 \left(\frac{U^2}{g} \right) \tanh \left[0.530 \left(\frac{gd}{U^2} \right)^{0.75} \right] \quad (4.9)$$

$$T_{\frac{1}{3}} = 2.4\pi \left(\frac{U}{g} \right) \tanh \left[0.833 \left(\frac{gd}{U^2} \right)^{0.375} \right] \quad (4.10)$$

U	= wind speed	[m/s]
g	= acceleration due to gravity	[m/s ²]
F	= fetch	[m]
d	= water depth	[m]
H _{1/3}	= mean height of the highest one-third part of all observed waves.	[m]
T _{1/3}	= mean period of the highest one-third part of all observed waves.	[s]

As the formulas 4.5 - 4.8 are only valid in situations where either the water depth d or the fetch F is predominant for the development of the waves, other calculations have been carried out in order to find out what wave height is decisive.

Bretschneider therefore gives combination formulas, demonstrated below:

$$\frac{gH_s}{u^2} = 0.283 \tanh \left[0.530 \left(\frac{gd}{u^2} \right)^{0.75} \right] \tanh \frac{0.0125 \left(\frac{gF}{u^2} \right)^{0.42}}{\tanh \left[0.530 \left(\frac{gd}{u^2} \right)^{0.750} \right]} \quad (4.11)$$

$$\frac{gT}{u} = 2\pi \cdot 1.2 \tanh \left[0.833 \left(\frac{gd}{u^2} \right)^{0.375} \right] \tanh \frac{0.077 \left(\frac{gF}{u^2} \right)^{0.25}}{\tanh \left[0.833 \left(\frac{gd}{u^2} \right)^{0.375} \right]} \quad (4.12)$$

The International Hydraulic Institute in Delft, (IHE) developed a computer program CRESS which calculates among others the significant wave height H_s and period T_s, considering the influence of depth and fetch. The results are displayed in Annex B.

With the thus obtained H_s and T_s, the run-up can be determined. Using equation (4.6), the run-up for the NW storm with a wind speed of 15 m/s the run-up is 4.20 meter for dam 1 and 3.10 meter for dam 2. As the construction dam is a porous dam, it can be assumed that part of the tongue that rushes up the slope flows into the dam body before it reaches

the other side of the dam. The total crest elevation above MSL now becomes for

	dam 1:	dam 2:
- Maximum Spring Tide + settlement	4.85 m.	4.85 m.
- wind set-up	0.33 m.	0.33 m.
- wave run-up	1.70 m. +	1.20 m. +
	<hr/>	
	6.88 m.	6.33 m.

4.5 Construction profile

With the obtained data the construction profile can be determined, depending on the closure method and the orientation of the dam.

In case of a horizontal or a combined closure method, the crest level must be elevated above the functional crest level of MSL + 4.45 m. + settlement. As it is not necessary to have this height over the complete width of the crest, only a small lip with a width of 1.00 meter is elevated at the sea side up to the maximum needed level of MSL +6.88 meter for dam 1 and MSL +6.33 meter for dam 2. The advantage of creating this lip is that the dump trucks need to dump less material so the dam can be constructed in a shorter period of time. The extra material that is needed to construct the lip will be placed by cranes on pontoons so they do not bother the trucks. Due to the wave attack on these pontoons, the production of the cranes is low. It is assumed that these pontoons are available. They can be situated just outside of the constricted flow. Figure 4.7, Figure 4.8 and Figure 4.9 show the different profiles.

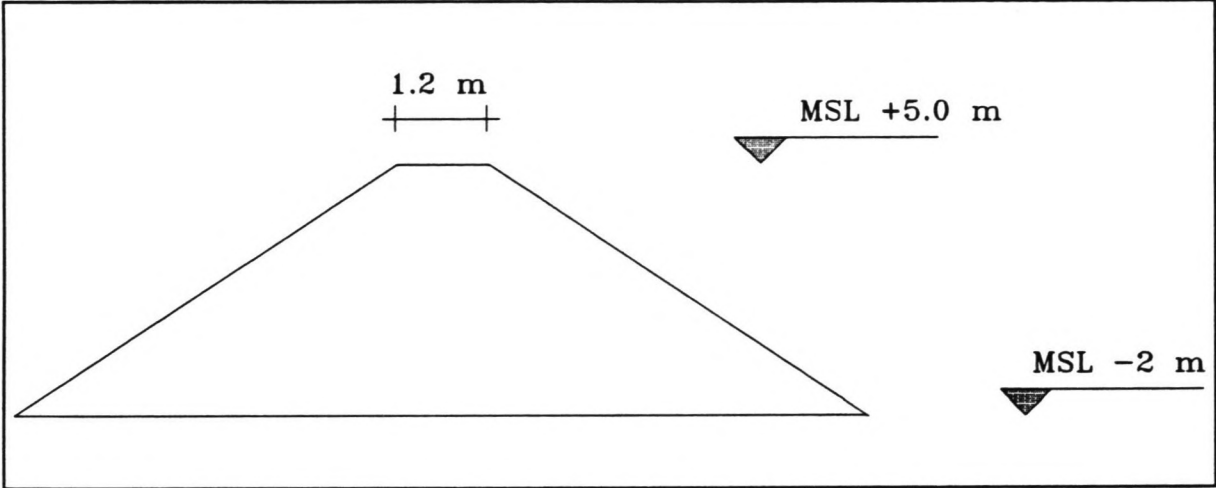


Figure 4.7: Construction profile of dam 1 and 2 with a vertical closure method

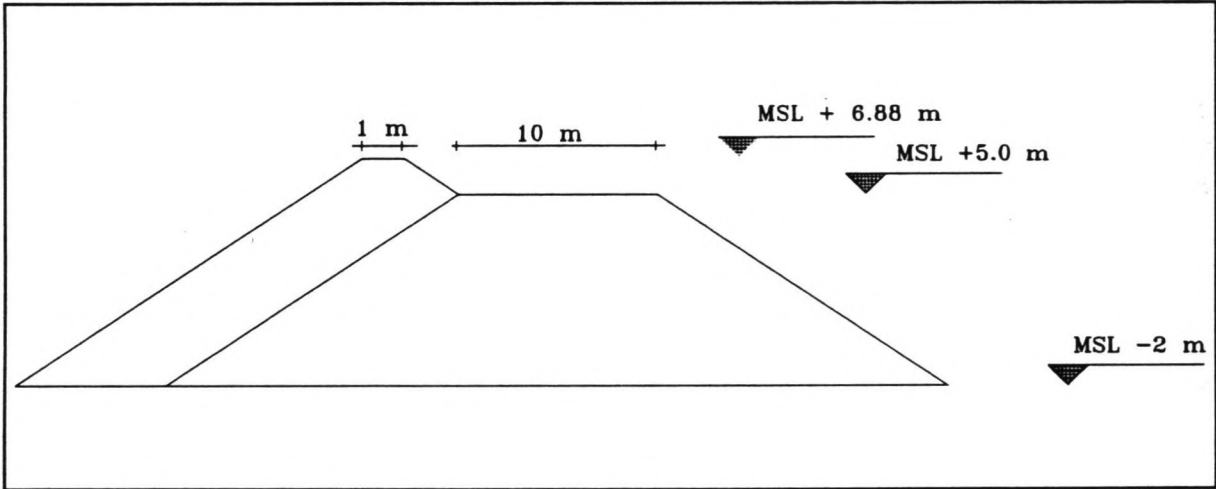


Figure 4.8: Construction profile of dam 1 and 2 with a horizontal closure method

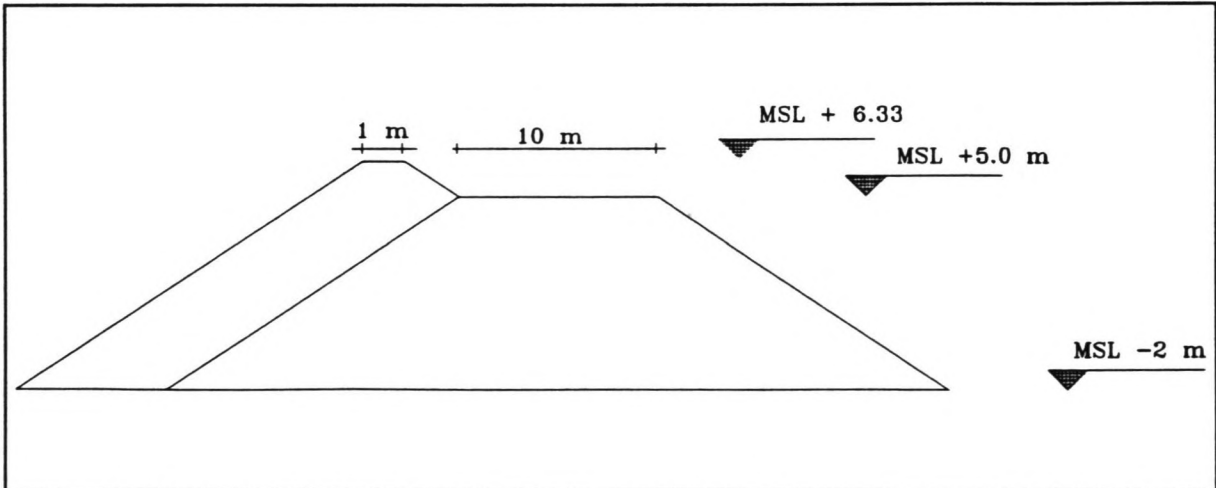


Figure 4.9: Construction profile of dam with a horizontal closure method

5 Micro stability of the closure dam

5.1 Introduction

The stability of the closure dam depends on the stability of the dam material, the micro stability and the stability of the sub-soil, the macro stability. In this chapter, the micro stability of the construction profile is discussed. The macro stability will be discussed in chapter 6, as this stability depends on the location and depth of the scour hole.

The dam material is submitted to two types of loads, flow induced and wave induced. The flow induced loads depend on the closure method and the closure phase. The stone stability under flow attack is discussed in paragraph 5.2. Paragraph 5.3 describes the stability of the stones under wave attack.

5.2 Flow induced loads

Every closure method and construction phase has its own characteristic values for the head over the constructions, the flow velocities and discharges in the closure gap and over the sill.

In this paragraph, the stability of the stones under all flow conditions will be discussed.

5.2.1 Flow conditions during a vertical closure

According to an investigation of Akkerman and Konter at DHL [9], four phases can be distinguished in case of a vertical closure method: Low dam flow, intermediate flow, high dam flow and through flow. See Figure 5.1.

5.2.1.1 Low dam flow

Low dam flow occurs, when $h_b/\Delta D > 4$. For uniform flow conditions, a widely used expression for relating the critical velocity u_c to the stone diameter D , is expression (5.1), derived by Shields,

$$\frac{u_c}{\sqrt{g\Delta D}} = C \frac{\sqrt{\psi}}{\sqrt{g}} \quad (5.1)$$

in which:

- g = gravitational acceleration
- ψ = Shields parameter
- $C = 18 \log(12h/k)$, White Colebrook.
- $k = 2D$ for natural dumped rockfill.

At the crest of an overflow, however, the current is not uniformly distributed. Therefore, a current velocity adaption factor k_* is introduced to take this influence into account. This factor has to be determined experimentally. With rockfill overflow dams the downstream crest experiences the heaviest current attack, and so the vertically-averaged current velocity u_0 is taken as the reference velocity.

The critical local current velocity u_0 now reads:

$$\frac{k_* u_0}{\sqrt{g\Delta D}} = C \frac{\sqrt{\psi}}{\sqrt{g}} \quad (5.2)$$

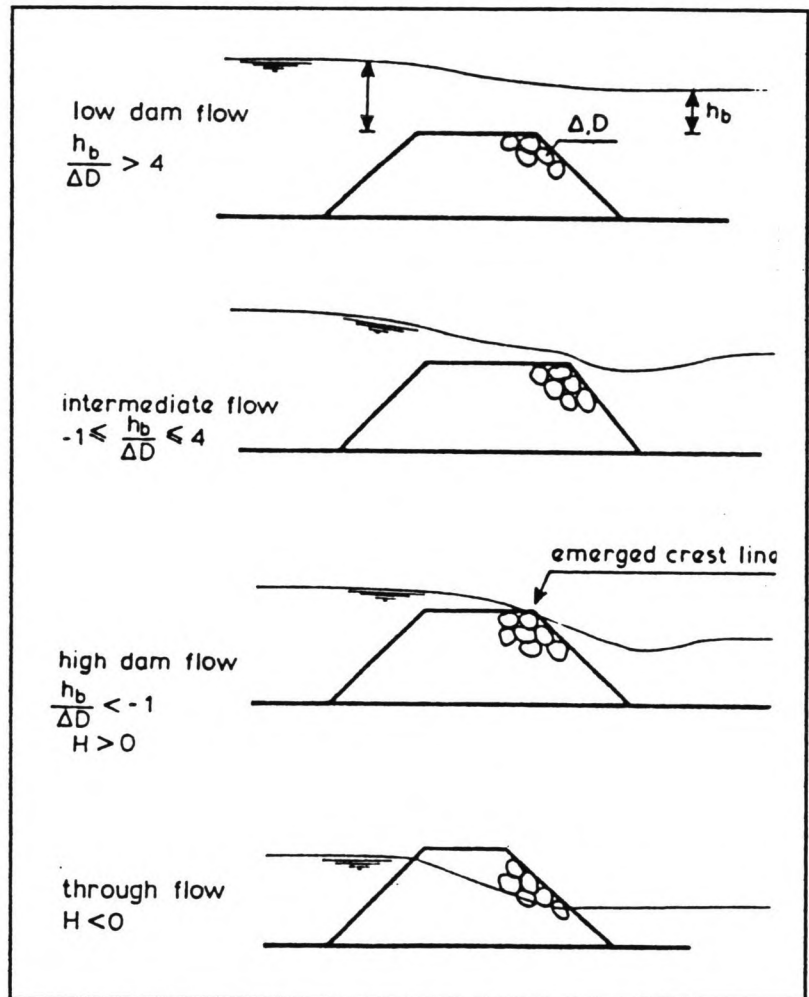


Figure 5.1: Decisive dam flow situations

Additional to a current velocity approach, the general relationship (5.2) can be expressed in terms of a water level difference over the dam, $H-h$, by introducing a coefficient μ_2 :

$$u_0 = \mu_2 \sqrt{2g(H-h_b)} \quad (5.3)$$

Combining equations (5.2) and (5.3) yields:

After some damage has occurred, the remaining dam body

$$\frac{H-h_b}{\Delta D} = \frac{C^2 \psi}{2g\mu_2^2 k_*^2} \quad (5.4)$$

becomes more stable than before because of the geometrical deformation. This implies that for stable dam design the value of Ψ may be somewhat higher than its minimum value of 0.02.

DHL [9] performed investigations, which resulted in the following formulae:

$$\frac{u_0}{\sqrt{g\Delta D}} = 1.4 \log \left(3.5 \frac{h_0}{D} \right) \quad (5.5)$$

for a broad crested dam with a relative crest width of $B/d > 5$ and:

$$\frac{u_0}{\sqrt{g\Delta D}} = 1.4 \log \left(1.5 \frac{h_0}{D} \right) \quad (5.6)$$

for a sharp crested dam.

It must be noted, that (5.5) and (5.6) originate from (5.1), using the White Colebrook relation for the Chézy-value. With the Shields parameter $\psi = 0.06$, the value 1.4 is obtained. Depending on whether a horizontal bottom, a broad crest or a sharp crest is present, the factor $\left(\frac{12h}{2D} \right)$ differs respectively from 6, 3.5 to 1.5.

Izbash also derived a relationship for the critical current velocity for threshold damage:

$$\frac{u}{\sqrt{g\Delta D}} = 1.7 \quad (5.8)$$

for a well embedded stone and:

$$\frac{u}{\sqrt{g\Delta D}} = 1.2 \quad (5.9)$$

for an isolated stone on top of a dam.

The influence of the roughness, related to the water depth however is ignored and therefore these formulae will not be applied.

5.2.1.2 Intermediate flow

Intermediate flow occurs when $-1 < h_b/\Delta D < 4$. When a sill of a closure dam is raised further, the flow regime will become supercritical. The flow velocity at the downstream crest increases in excess of the critical flow velocity as the dam is subsequently raised, by flow penetration into the porous top layer(s). The investigation of Akkerman and Konter [9], showed that the relative flow velocity enlargement, expressed in a factor γ , proved to be a function of the tailwater depth parameter.

Approximating γ by:

$$\gamma = \sqrt{2.40 - 0.35 \frac{h_b}{\Delta D}} \quad (5.10)$$

They found a relationship between u_0 , H and $h_b/\Delta D$:

$$\frac{u_0}{\sqrt{\Delta g D}} = \sqrt{A + 0.375 \frac{h_b}{\Delta D}} \quad (5.11)$$

with $A = 2.7$ for the broad crested dam and $A = 2.0$ for the narrow crested dam.

5.2.1.3 High dam flow

When the downstream water level becomes lower than the crest level of the dam, the stability of the dam must be checked with respect to the overflow conditions. For the no-damage protection of the downstream-slope of the dam with a relatively impervious core and in the case of free overflow conditions, the formula of Hartung and Scheuerlein simplified by Knauss can be applied. This formula defines the maximum unit discharge over the dam as a function of slope angle (α):

$$q_{\max} = 0.84 \sqrt{G_{50}} (1.9 + 0.8\phi - 3 \sin \alpha) \quad (5.12)$$

Where:

- q = critical specific discharge
- G_{50} = average stone weight
- ϕ = packing factor, ranging from 0.625 (natural packing) to 1.125 (manual packing)
- α = downstream slope-angle

Using D_{50} and Δ instead of G_{50} , this formula becomes:

$$q_{\max} = 1.95 (\Delta D_{50})^2 (1.9 + 0.8\phi - 3 \sin \alpha) \quad (5.13)$$

where D_{50} is the equivalent diameter.

5.2.1.4 Through flow

A through flow situation is reached after the closure is completed. This stage is in practice not a critical stage for stone stability. The stone sizes applied in the preceding phases are larger than the size needed to resist the forces due to through flow.

The results of the calculations demonstrated in Annex C1 are displayed in Figure 5.2.

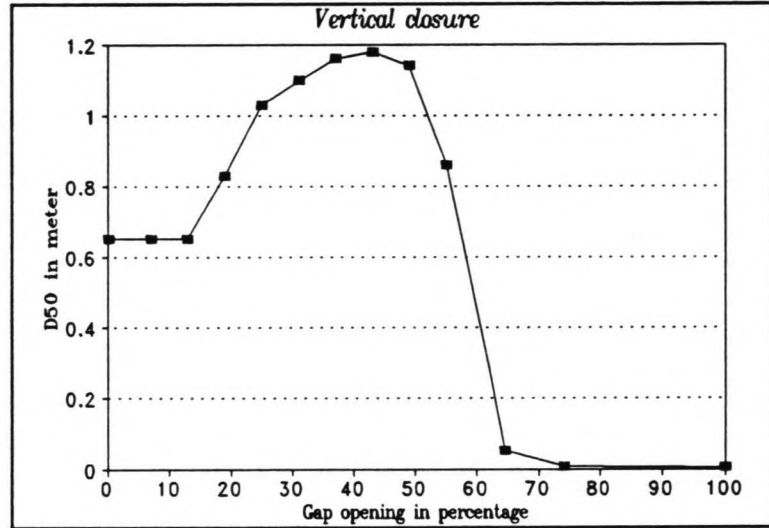


Figure 5.2: D_{50} as a function gap opening

5.2.2 Flow conditions during a horizontal closure

When applying a horizontal closure, the decisive D_{50} of every phase can be determined by using the following formula:

where ψ_{cr} is taken as 0.06 so limited stone transport is accepted.

$$\frac{u_{cr}}{\sqrt{g\Delta D_s}} = 6\sqrt{\psi_{cr}} \left(\frac{h}{D_s}\right)^{\frac{1}{6}} \quad (5.14)$$

When calculating u_{cr} with the DUFLOW model, the decisive D_{50} during every closure phase can be determined. The D_{50} as a function of gap opening is demonstrated in Figure 5.3. The calculations are displayed in Annex C2.

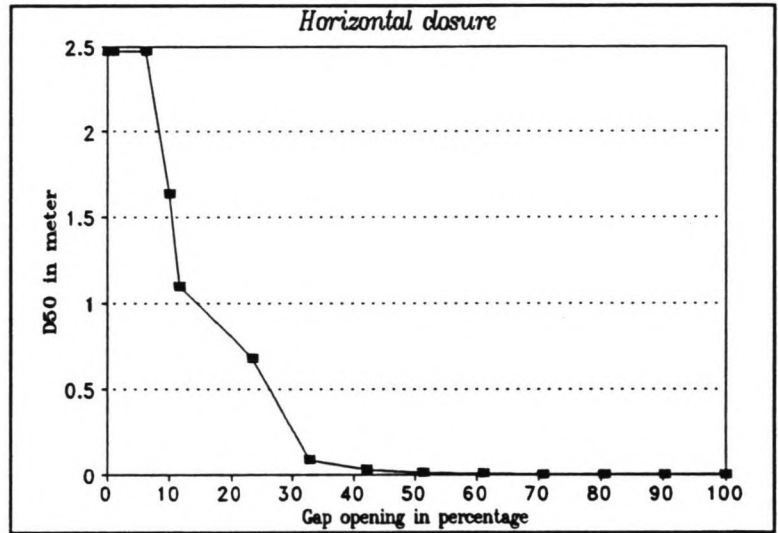


Figure 5.3: D_{50} as a function of gap opening

5.2.3 Flow conditions during a combined closure

When applying a combined closure, normally a horizontal closure can be superimposed upon a vertical closure. In this case however the water level outside the basin reaches a level that is 2 meter below the level of the sill. Therefore the formula that is used in section 5.2.2 to determine the D_{50} of the material to be used is not sufficient. The situation of intermediate flow and high dam flow as have been described in the sections 5.2.1.2 and 5.2.1.3 must be considered as well. The

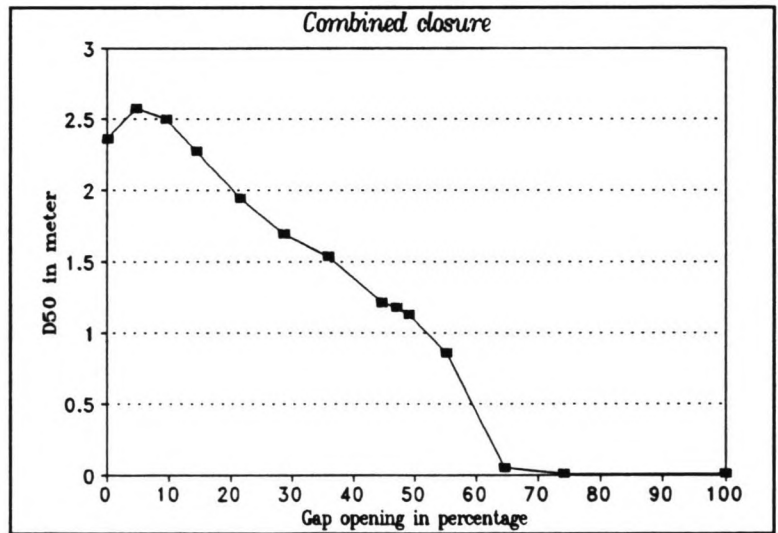


Figure 5.4: D_{50} as a function of gap opening

first 5 phases in which the sill is elevated in a vertical way, the same calculations have been carried out as in the case of a complete vertical closure method, until the sill level is raised up to the level of MSL- 2.0 meter. The results of the calculations, demonstrated in Annex C3, are displayed in Figure 5.4.

5.3 Wave conditions during closure

The main governing variables by which the static stability of a rubble mound structure under wave attack is determined are: H_s , T_s , N , h , D_{50} , Δ , α and P .

Van der Meer [13] derived two formulae to determine the static stability of rubble mound structures:

$$\frac{H_s}{\Delta D_{50}} \sqrt{\xi_m} = 6.2P^{0.18} \left[\frac{S}{\sqrt{N}} \right]^{0.2} \quad (5.15)$$

for plunging waves and:

$$\frac{H_s}{\Delta D_{50}} = 1.0P^{-0.13} \left[\frac{S}{\sqrt{N}} \right]^{0.2} \sqrt{\cot\alpha} \xi_m^P \quad (5.16)$$

for surging waves, where: $\xi_m =$ surf similarity parameter, $= \sqrt{\frac{\tan\alpha}{\frac{H_s}{L_0}}}$

$P =$ permeability of the structure
 $S =$ damage level

Taking the NW design storm with a wind speed of 15 m/s, the H_s is 1.25 m., T_s is 4.3 s. and L_0 is 27.54 m. (See chapter 3.) With $\cot\alpha = 1.5$, ξ_m becomes 3.12. Plunging breakers occur when $0.5 < \xi < 3.3$ so in this case equation (5.15) can be used to determine the stability of the construction dam.

With a mean storm duration of 6 hours and a T_s of 4.3 seconds the number of waves N becomes 5023. The permeability of a rubble mound structure is 0.4 and when accepting no damage, the damage level S is 2.

With these values the D_{50} becomes 0.52 m., using equation (5.15).

This value is much smaller than the maximum D_{50} determined with the flow induced loads. The top layer of the construction profile of the dam does not consist of the maximum D_{50} over the complete length in case of a horizontal or a combined closure. Therefore the two graphs of D_{max} by flow induced and wave induced loads are combined to determine the minimum required D_{50} .

6 Bottom protection design

6.1 Introduction

As a result of constructing a sill in the gully, a constriction of the flow occurs and therefore the flow-velocities will increase. A further increase of the flow-velocities can be expected when building out the roundheads from the sides thus forcing a horizontal constriction as well.

This increase in flow-velocity will cause deep scour-holes near the closure-dam, at both the sea side and the basin side, as a result of the flood and ebb flow.

Instability of the subsoil may be the result of these scour holes and this can lead to the failure of the structure. To ensure the stability of the dam, seabed protection is necessary. The function of this sea bed protection is to keep the scour hole that will be formed as far as necessary from the toe of the construction. The length of this protection depends on several parameters such as: Maximum depth of the scour hole, (which depends on the flow velocities and the period of time these velocities occur) and the slope gradient β . These parameters and the resulting length of the seabed-protection are discussed in this chapter.

6.2 Theory

In general, four phases can be distinguished in the development of a scour hole. See Figure 6.1. In phase I, the increased transport capacity of the flow results in sediment transport along the original bottom and hence a gradual erosion downstream from the end of the bottom protection. This phase can be described by existing equations for sediment transport. This first phase is very short and therefore of little practical interest.

In phase II, the scour hole is large enough to initiate flow separation. As a result of this, a bottom eddy is formed, see Figure 6.2. The direction of the bottom-velocity inside the eddy is towards the construction but outside it in the direction of the main flow. This se-

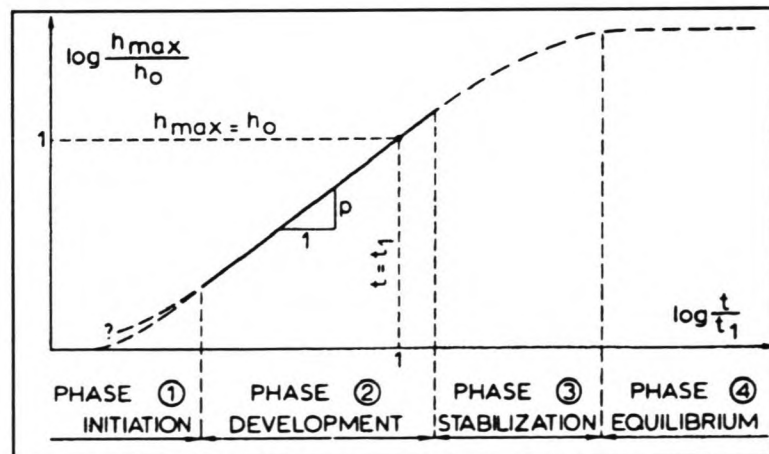


Figure 6.1: Different phases of the scouring process

cond phase generally lasts much longer than the first and is of great practical interest. The end of phase II is more or less marked by the point where $H_{\max} = H_0$ where H_0 is the water depth

In the third phase, the bottom-velocities almost reach the critical velocity of incipient motion because of an increase in depth of the scour hole.

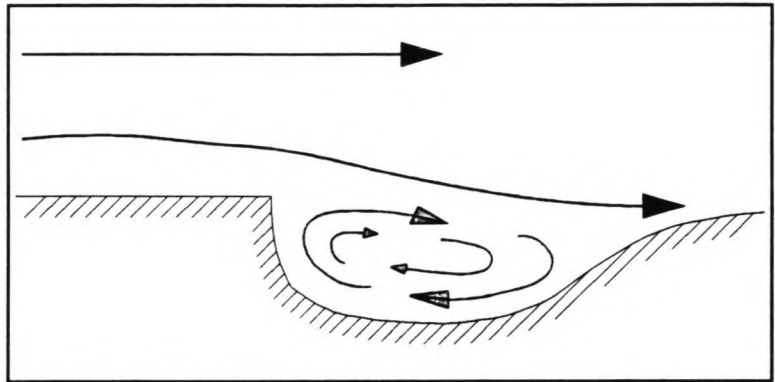


Figure 6.2: Bottom-eddy at the end of the bottom protection

Therefore scour progress is very slow. In the final phase, the bottom-velocity is nearly equal to the velocity of incipient motion. There may still be a certain transport of sediment, but the flow is not capable of transporting this sediment out of the scour-hole. So more or less a stable situation is reached. The maximum depth of the scour-hole in this state is called the equilibrium depth. To determine the maximum scour depth, an empirical formula has been developed by Breusers and Raudkivi:

$$h_{\max}(t) = \frac{(\alpha \bar{u} - u_c)^{1.7} h_0^{0.2}}{10 \Delta^{0.7}} t^{0.4} \quad (6.1)$$

- Where:
- h_{\max} = the maximum scour depth as a function of time.
 - h_0 = the original water depth.
 - t = the time in hours.
 - α = a factor that represents, among other things, turbulence and is related to the geometry of the flow.
 - u_c = the critical flow velocity, at which a grain is no longer in equilibrium and starts to move.

As the flow is cyclic because of the tidal motion, the relation $(\alpha \bar{u}(t) - u_c)^{1.7}$ has to be replaced by:

$$\frac{1}{T} \int_0^T (\alpha u - u_c)^{1.7} dt \quad (6.2)$$

The critical flow-velocity u_c can be determined by using the formula derived by Shields:

$$\frac{u_c}{\sqrt{g\Delta d}} = C\sqrt{\psi} \tag{6.3}$$

The factor ψ

in this formula can be determined with the Shields diagram, shown in Figure 6.3. To use this diagram, first the shear stress u_* must be determined with the following relation:

$$u_* = \bar{u}_m \sqrt{\frac{g}{C}} \tag{6.4}$$

Where: \bar{u}_m = the depth averaged velocity

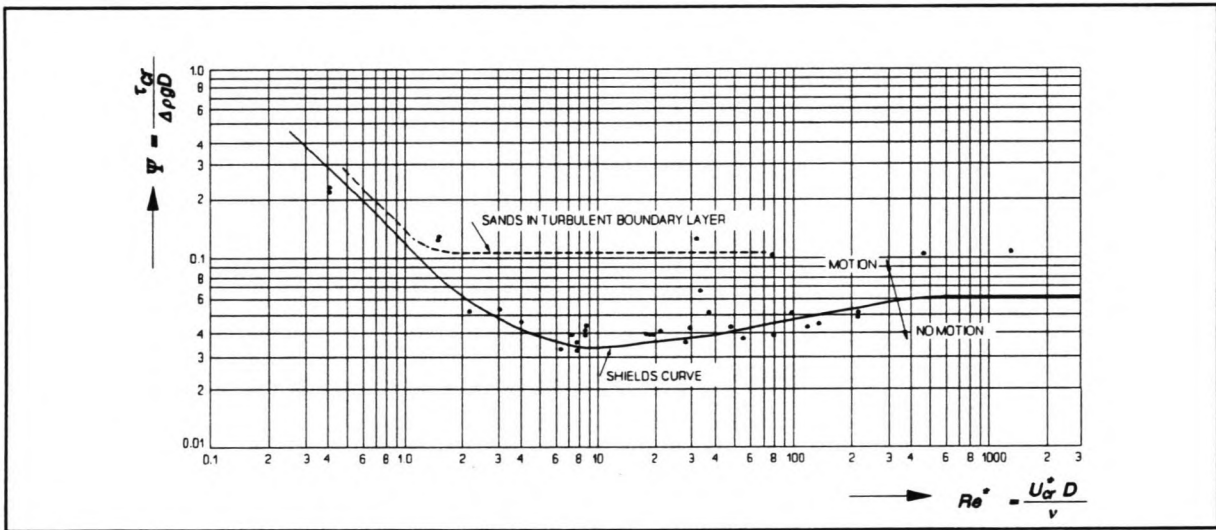


Figure 6.3: Shields diagram

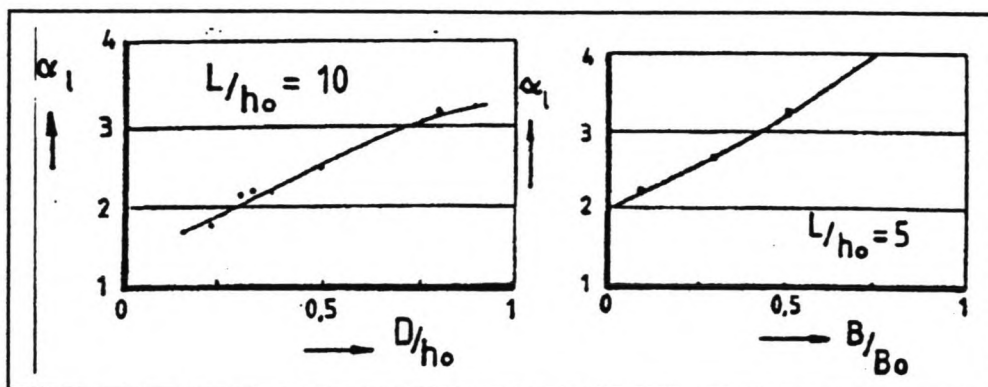
6.3 Determination of the maximum scour depth

6.3.1 Influence of the flow velocities on the scour

As can be seen in equation (6.3), the flow velocity u at the end of the bottom protection must be multiplied by α . This factor α is a rather important parameter representing the influence of turbulence on the flow velocity. It is determined by means of model investigation where u , u_c , h_0 and Δ are known and where h_{max} is measured as a function of time. Then α can be determined by using equation (6.1). For preliminary design purpose, α can be predicted with the help of Figure 6.4 that shows a relation between α and the degree of horizontal or vertical constriction. Since the factor α depends on the geometry

of the structure, it has to be determined for every phase of the closure.

Looking at the diagram it can be seen that α is related to $L/h_0 = 10$. In case that L is related to α other than 10 times h_0 , this figure can not be used.

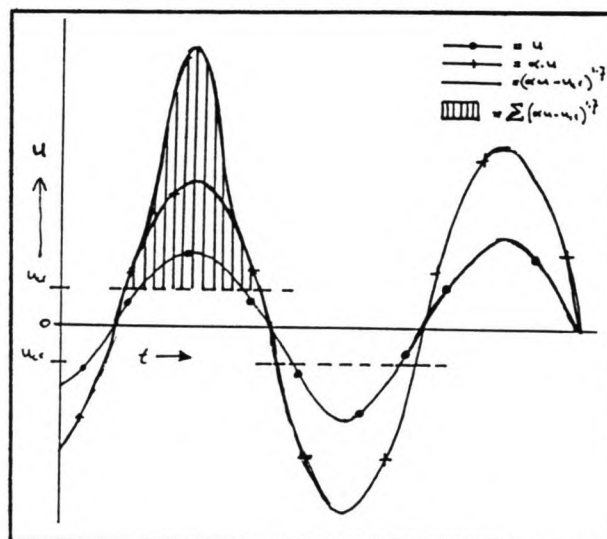


Equation (6.6) enables to transform α_{10} to an α according to any value of L/h_0 . **Figure 6.4:** α as a function of bed protection length and geometry.

transform α_{10} to an α according to any value of L/h_0 .

$$\alpha\left(\frac{L}{h_0}\right) = 1.5 + (1.57 \alpha_{10} - 2.35) e^{(-0.045 \frac{L}{h_0})} \tag{6.6}$$

With the help of the DUFLOW model, for every phase the flow velocities in every weir are determined. These calculations have been carried out with a Mean-Tide as input which is considered as a representative tide over a longer period of time. As the flow velocities must be elevated to the power 1.7, a Mean Tide is not exactly the representative tide but gives a slightly lower mean value. Therefore the biggest surface below the velocity curve is taken, without taking the mean value between the two surfaces, see Figure 6.5.



With equation (6.5) and Figure 6.3, u_c can be determined. When for every closure **Figure 6.5:** Integral of $(\alpha u - u)^{1.7}$ over T .

phase, α is determined, the total term $\frac{1}{T} \int_0^T (\alpha u - u)^{1.7} dt$ is known. Figure 6.5 shows

an example of how this term has been determined. The result of the calculations for all closure phases is displayed in Annex D.

6.3.2 Time depending scour

Time is a very important parameter for the determination of h_{max} . Depending on the duration of the considered period in which erosion of the bottom is expected to take place, the development of the scour hole is in phase I, II, III or IV, see therefore Figure 6.1.

Every construction phase has its own characteristic flow velocity. For every construction phase therefore the time needed for construction must be known. Once this time is known, the $h_{max i}$ can be determined. In the next phase (i+1), however, equation (6.1) can not be used without considering that an initial scour hole is already present following from a flow velocity and duration of phase i. Therefore, first a new calculation of the time (t_{i+1}), needed to generate a scour hole with a depth of $h_{max i}$ must be made. This is done with the flow velocities of the actual construction phase (i+1). Once this time (t_{i+1}) is known, the calculation of $h_{max i+1}$ can be started with $t_{i+1} + t_{c i+1}$ which is the construction time of phase i+1. Thus calculating the scour depth for every construction phase, the total h_{max} can be determined.

It must be noted that equation (6.1) is not valid anymore when $\alpha u - u_c < 0.1$ m/s. as than the scour process is in phase III.

The time t for every construction phase depends on the amount of material needed to construct the dam and the equipment that is applied. These factors depend of the construction method that has been applied. In Annex D, the construction time for all construction phases has been determined. The resulting scour depth for every structure and for every closure method is displayed in Annex D as well.

As the construction of the closure dam takes more or less half a year, reduction of the scour depth has to be taken into account. This reduction is a result of the cyclic nature of the flow. Every time the flow direction is from the scour hole towards the weir, sediment from upstream is transported into the hole thus decreasing the scour depth. The difference in geometry of a scour hole with or without tidal motion is demonstrated in Figure 6.6.

A stationary phase is reached when the flow of sediment into the hole equals the outflow. Schematizing the hole as demonstrated in Figure 6.6, the volume of the scour-hole per meter width is:

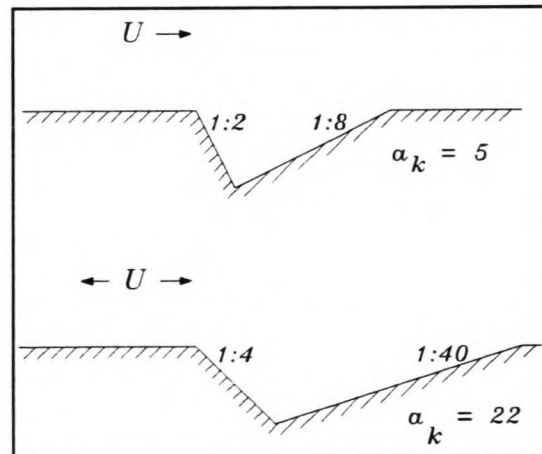


Figure 6.6: Geometry of a scour hole in none cohesive material

$$I = \frac{1}{2}(\cot\beta_1 + \cot\beta_2) h_{\max}^2 = 0.005(\cot\beta_1 + \cot\beta_2) \Delta^{-1.4} h_0^{0.4} (\alpha u - u_c)^{3.4} t^{0.8} = K t^{0.8} \quad (6.8)$$

With sediment supply this becomes:

$$I_{red} = K.t^{0.8} - S.t \rightarrow h_{\max red} = \sqrt{\frac{I_{red}}{\frac{1}{2}(\cot\beta_1 + \cot\beta_2)}} \quad (6.9)$$

Equilibrium is reached when:

$$\frac{dI}{dt} = 0 \rightarrow 0.8K.t^{-0.2} = S \rightarrow t_{eq} = \left[\frac{0.8K}{S} \right]^5 \rightarrow h_{\max\infty} = \sqrt{\frac{K.t_{eq}^{0.8} - S.t_{eq}}{\frac{1}{2}(\cot\beta_1 + \cot\beta_2)}} \quad (6.10)$$

With the help of a sediment transport formula, S can be approximated. Engelund and Hansen derived a formula for the total amount of sediment that is transported per meter width that reads:

$$S = 0.03 \left(\frac{g}{C^2} \right)^{\frac{3}{2}} \frac{U^5}{g^2 D_{50}} \quad (6.11)$$

Equation (6.10) shows however that t_{eq} is rather sensible for S, represented in this formula to the fifth power. It is therefore questionable to determine the reduction supply without any measured data on the sediment transport inside the basin.

6.3.3 Resulting scour depth

With the help of a spread-sheet program Quattro, the scour depth for every closure phase during every closure method and for every weir has been determined. The results of these calculations which are displayed in Annex D are demonstrated in Table 6.1.

Table 6.1: Maximum scour depth

Weir:	1		2		3		4	
Method:	H _{max} [m] basin	H _{max} [m] sea						
vertical	0.97	2.56	1.04	3.14	1.35	3.65	2.95	10.52
horizontal	2.81	3.7	10.65	13.5	19.9	28.85	146	158
combined	5.8	5.9	2.03	4.27	2.67	5.48	4.04	8.97

6.4 Resulting slope angle after slide

The slope angle β is the slope angle that results after sliding of the inner slope of the scour hole. This sliding occurs after the slope has lost its stability. This loss of stability can be induced by waves or by progressive scouring. The resulting slope is dependent upon whether or not liquefaction of the subsoil occurs.

In general, liquefaction occurs at places where loosely packed marine sediment is present, ending with steep slope under water. When liquefaction occurs, the sand turns into quicksand and flows away, coming to rest under a much flatter slope of approximately 1:15. Although not so much is known about this phenomenon, three conditions under which liquefaction may occur are known.

- I The sand is loosely packed
- II The permeability coefficient k is sufficiently low
- III There is an initiating force

When the sand is submitted to a shear stress, it will show a change in volume. This shear stress can be a result of a sand slide into the scour hole or a ship passing by, etc. In case of dense packed sand, this will be an increase in volume and in case of loose packed sand a decrease. A decrease in volume will cause high water pressures when the water is not capable of flowing quickly out of the pores. This is the case when the k of the sand is

very low. When the water is still present in the pores, the water pressure will increase and take over the tension between the grains of the sand. Now the sand is more or less a thick fluid and flows away. In case of the Shiwa tidal basin it can be said that liquefaction is likely to occur. The first ten meter of the subsoil consists of very loose packed sand with a SPT value from 1 to 14, see Annex A. As a result of the very small grain size of the sand, 50 μm ., the k-value is very low, approximately $1 \cdot 10^{-6}$. Combining this with the presence of a scour hole near the closure dam, liquefaction is likely to occur. A slope angle β of 1:15 is therefore recommended.

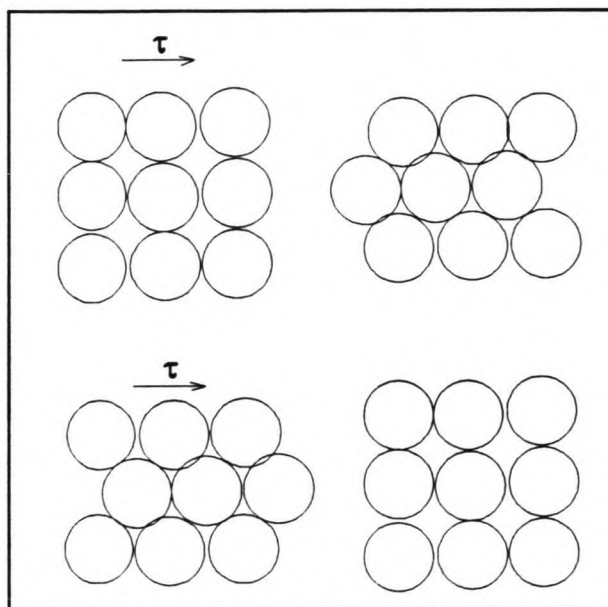


Figure 6.7: Dilatancy of sand

6.5 Determination of the bottom protection length

With β and H_{max} known, the bottom protection length can be determined. This is an iterative process as H_{max} depends on the factor α which depends on L_0/D . The resulting L_0 for every closure method and every weir at both sides of the dam are displayed in table 6.2. An example of the calculation of L_0 and more detailed data on the calculations are displayed in Annex D.

Table 6.2: Bottom protection length for all closure phases

weir nr	1		2		3		4	
Closure method	L_0 [m] basin	L_0 [m] sea						
vertical	15	38	16	47	20	55	44	158
horizontal	42	55	160	203	300	300	300	300
combined	87	88	30	64	40	82	61	135

6.6 Final results

On the following pages, Figure 6.8 to Figure 6.13 show the scour depth as a function of time in all weirs, and during all closure methods. Figure 6.14 and Figure 6.15 show the plan of the bottom protection mattresses in case of a vertical, a combined or a horizontal closure method. In these figures, only the dam axis is demonstrated, so the bottom protection length must be extended by the width of the closure dam at the bottom.

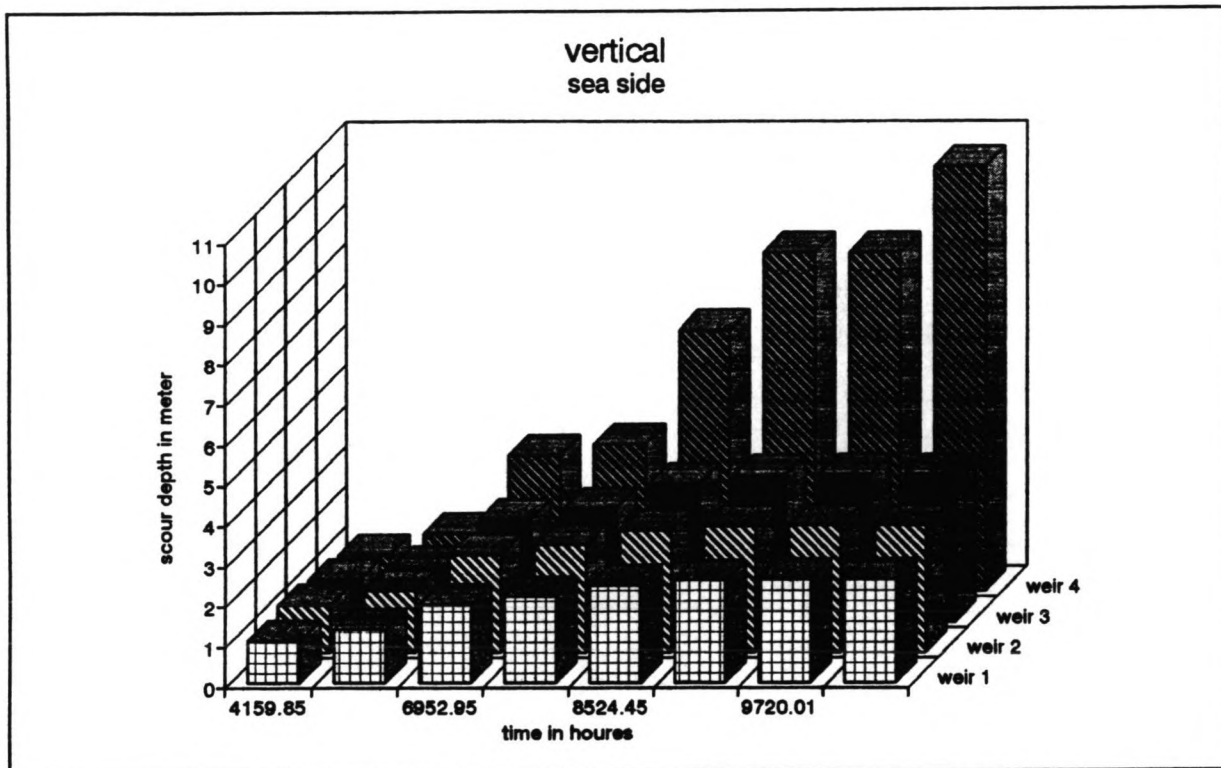


Figure 6.8: Scour depth as a function of time in all weirs during a vertical closure at the sea side

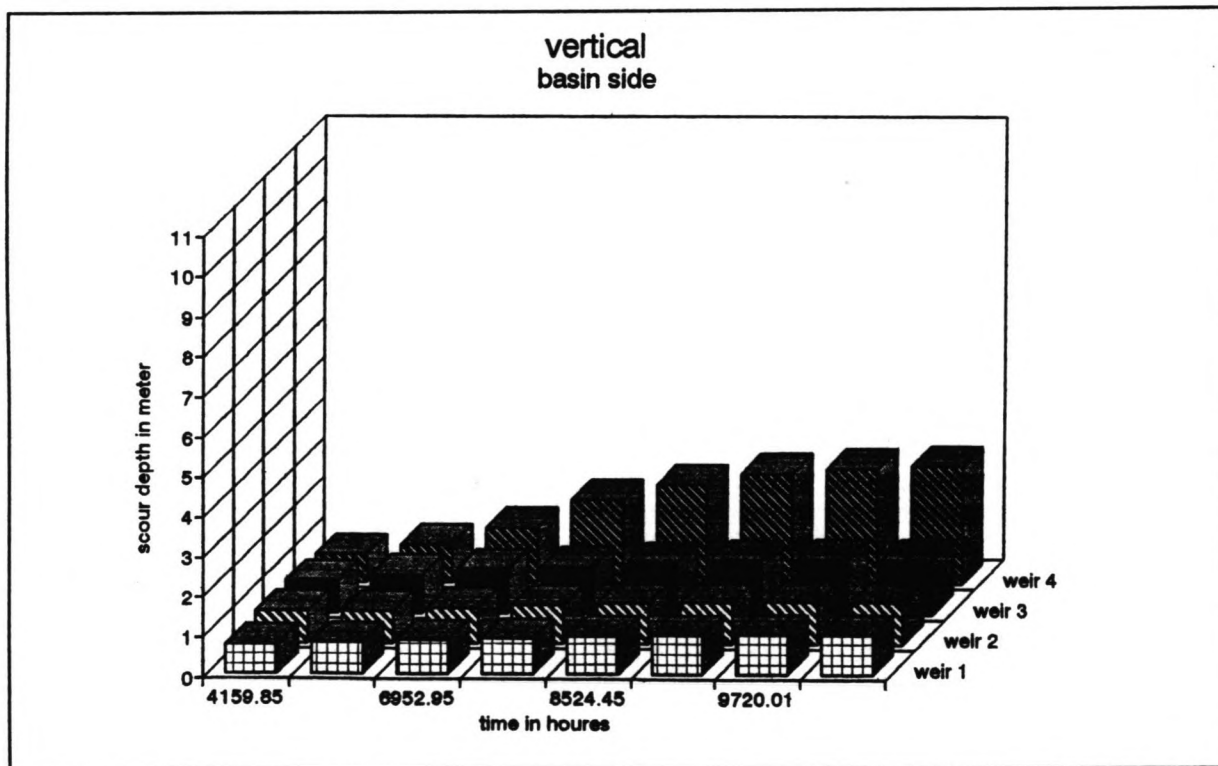


Figure 6.9: Scour depth as a function of time in all weirs during a vertical closure at the basin side

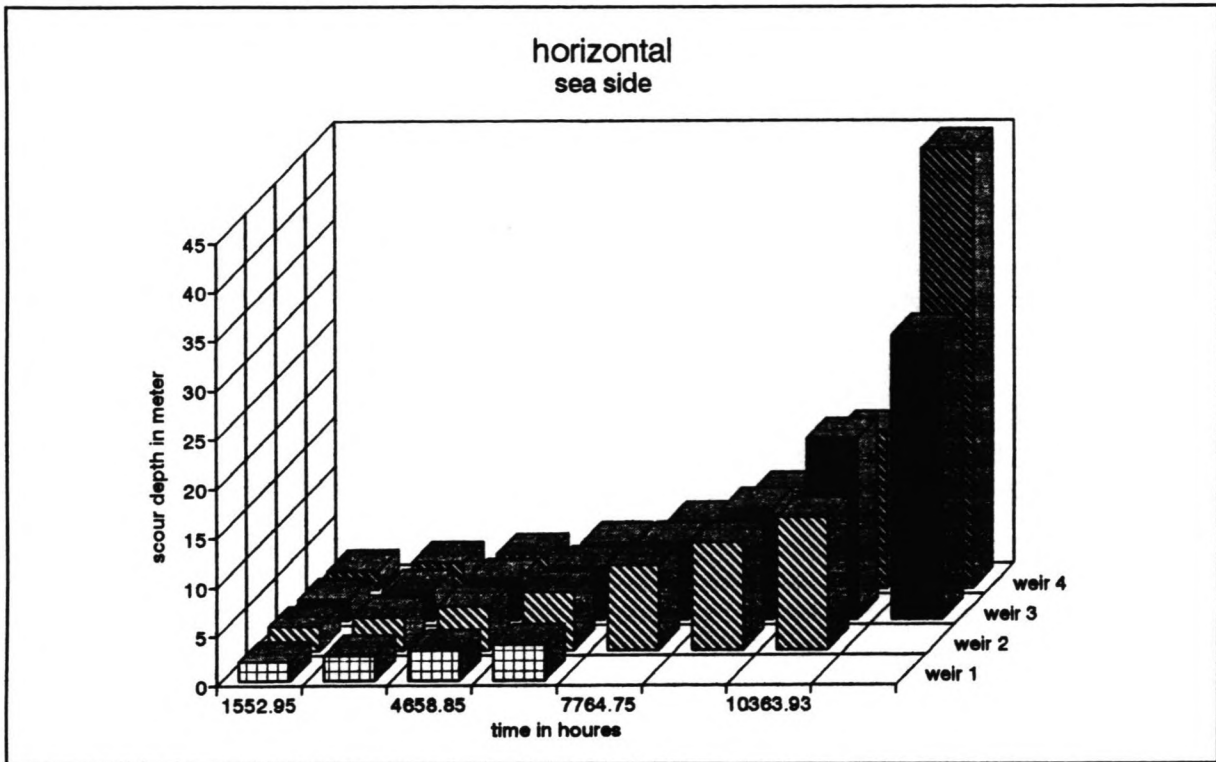


Figure 6.10: Scour depth as a function of time in all weirs during a horizontal closure at the sea side

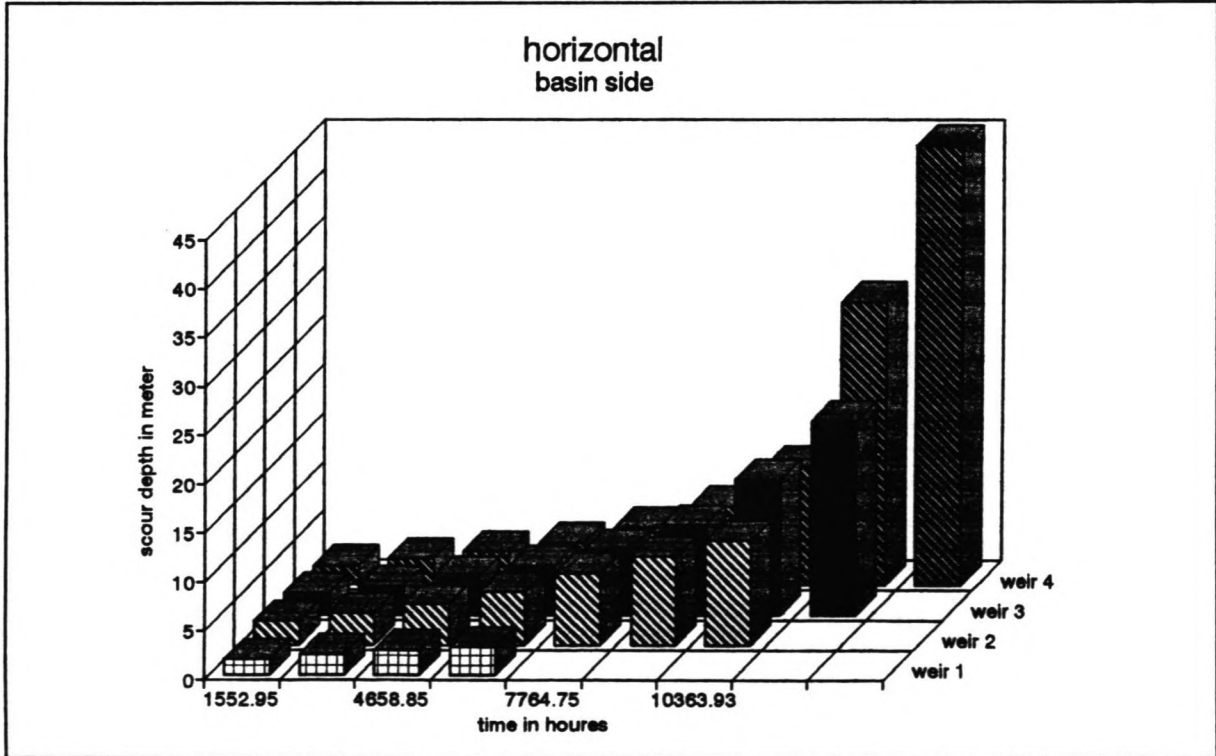


Figure 6.11: Scour depth as a function of time in all weirs during a horizontal closure at the basin side

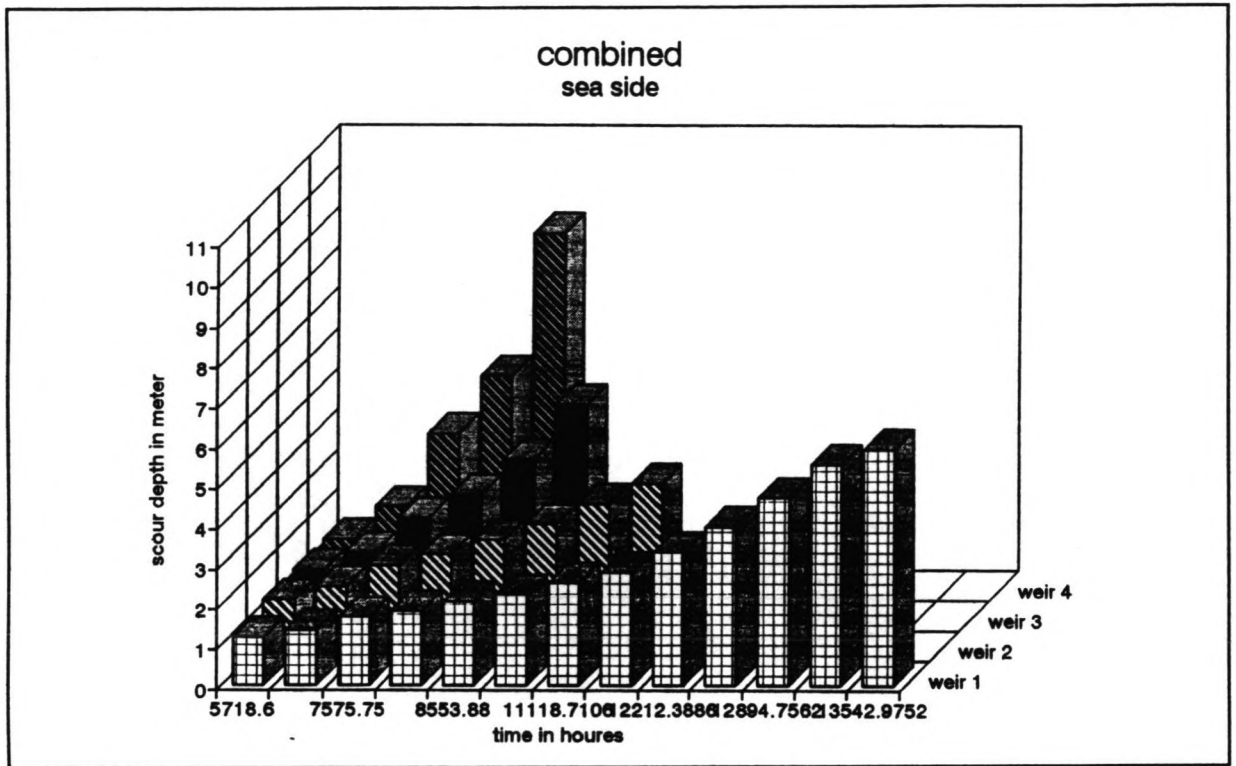


Figure 6.12: Scour depth as a function of time in all weirs during a combined closure at the sea side

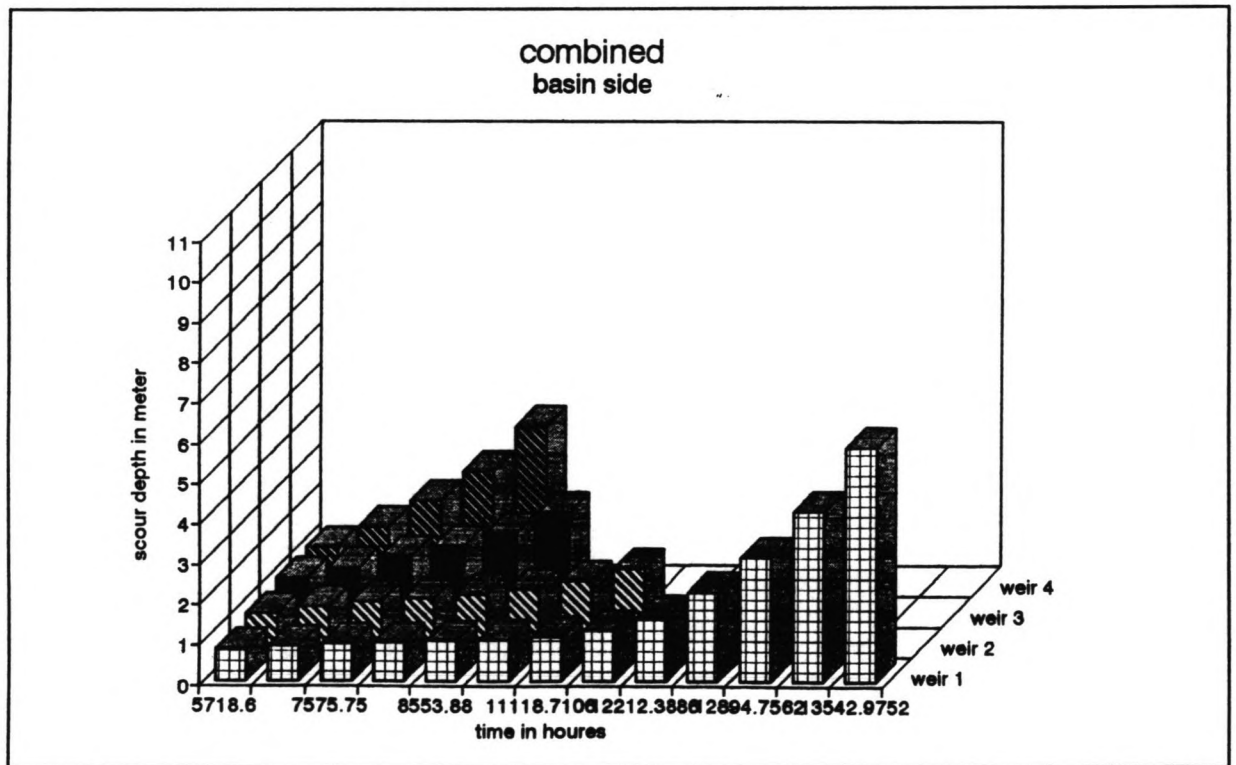


Figure 6.13: Scour depth as a function of time in all weirs during a combined closure at the basin side

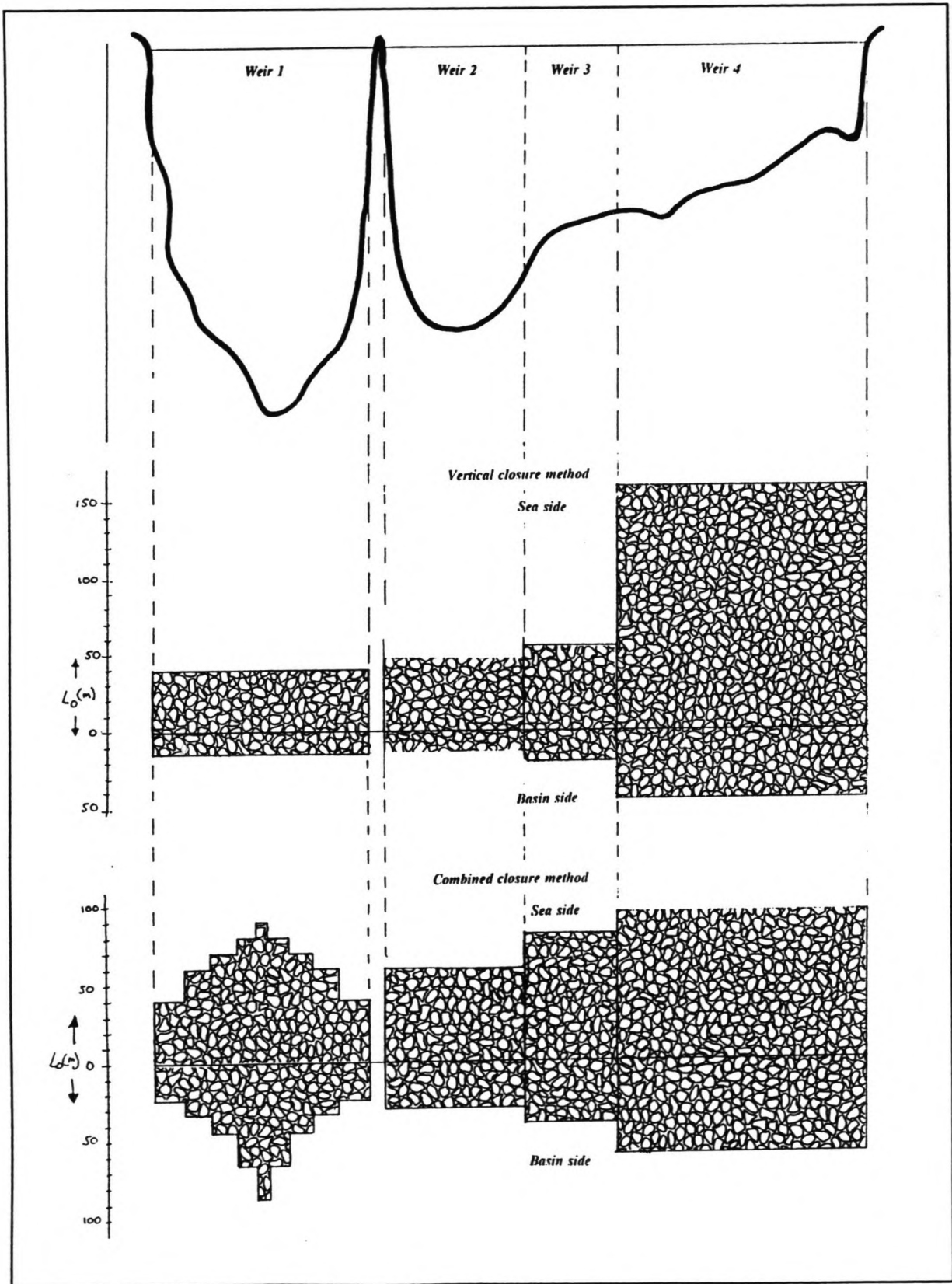


Figure 6.14: Top view of the bottom protection length with a vertical and a combined closure method

Closure of the Shiwa Tidal Basin

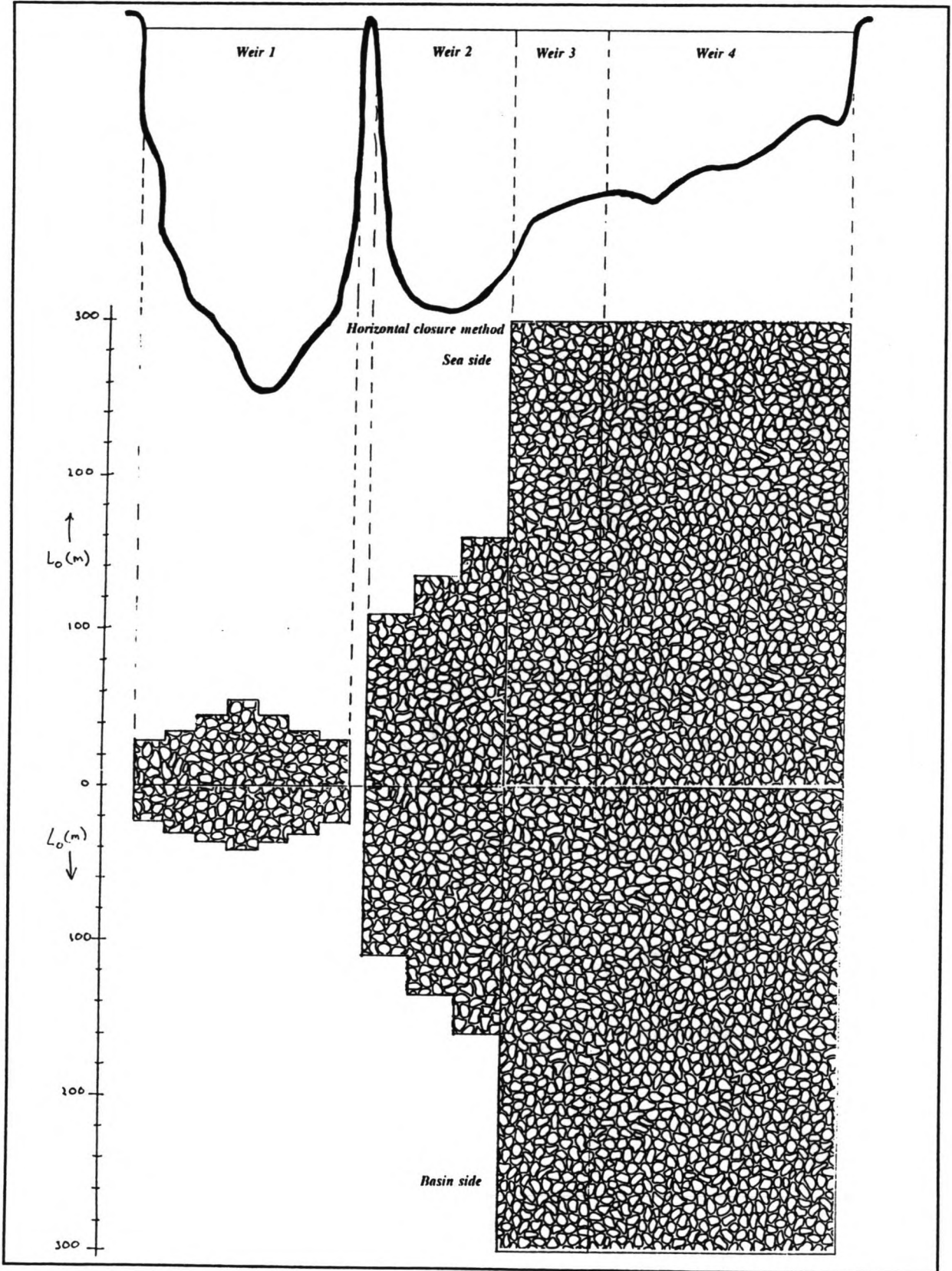


Figure 6.15: Top view of the bottom protection length with a horizontal closure method

7 Conclusions and recommendations

The bottom protection length, calculated in accordance with Dutch design standards appeared to be larger than the bottom protection designed by the Koreans in case of a horizontal closure method in case liquefaction occurs.

From table 6.2 can be concluded that a vertical closure method is best concerning the amount of bottom protection material. In this case it is recommended to close weir number 4 first as this saves a lot of bottom protection material.

It is recommended to do some extra penetration tests to obtain more data about the subsoil. Measurements on the transport of sediment in the basin resulting from the tidal flow is recommended as well. Thus a better prediction of the reduction of the scour hole can be made, which can result in a more reliable estimation of the bottom protection length.

Bibliography

- [1] Verspuy C.: Handleiding lange golven, Delft University of Technology, April 1987
- [2] DUFLOW manual
- [3] Admiralty Tide Tables, vol. 3, Hydrographer of the navy, 1992
- [4] Shiwa, the closure of the tidal basin. Netherlands Ministry of Transport and Public Works, Delta Department, November 1984
- [5] Roode F.C. van: Lecture notes F11-C: Afsluitingen van waterlopen Delft University of Technology, April 1987
- [6] Huis in 't Veld et al: The Closure of Tidal Basins Delft University Press, 1987
- [7] Rapport 155: Handboek voor dimensionering van gezette taludbekleding. CUR Gouda, March 1992
- [8] Konter J.L.M. and Meulen T. van der: Influence of upstream sand-transport on local scour. RWS, Delft Hydraulic laboratory
- [9] Akkerman G.J. and Konter J.L.M.: Hydraulic design criteria for rockfill closure of tidal gaps. Vertical closure methods. D.H.L., July 1985
- [10] Schiereck G.J.: Introduction to bed, bank and shore protection. Lecture notes F4. Delft University of Technology, October 1992
- [11] Velden E.T.J.M. van der: Coastal engineering,. Lecture notes F7. Delft University of Technology, February 1989
- [12] Massie W.W.: Lecture notes F5N, Coastal Engineering, Volume III: Breakwater Design, Department of Civil Engineering, Delft University of Technology, 1986.
- [13] Meer J.W. van der: Rock Slopes and Gravel Beaches under Wave Attack. Delft Hydraulics Communication No. 396, 1988.
- [14] Breusers and Raudkivi: Scouring, Balkema, Rotterdam, 1991

- [15] Verruijt A, Soilmechanics (in Dutch), lecture notes B22, D.U.M., 1987
- [16] Lindenberg J.L.: Liquefaction of sand, Landslides in Zeeland (in Dutch), I²-Bouwkunde en Civiele Techniek no. 11, 1986
- [17] Lindenberg J.L.: Liquefaction abroad (in Dutch), I²-Bouwkunde en Civiele Techniek no. 12, 1986
- [18] Kuitert C: Liquefaction of berms, Safety of the Oosterschelde dikes (in Dutch), Pt/C 1986 (41) 3

Annex A

This Annex contains:

- a map of the region
- wind data
- the tidal constituents at the three nearest stations
- the local hydraulic data, obtained with the duflow MODEL
- soil mechanical data

Table A1: Wind directions and velocities at Inch On station, 1905-1976

Wind direction	appearance		wind velocity in m/s						
	no	rate	< 5	5-10	10-15	15-20	20-25	25-30	> 30
N	19	2.3			12	6		1	
NNE	17	2.0			12	5			
NE	7	0.8		1	4	2			
ENE	7	0.8		3	4				
E	19	2.3		2	12	5			
ESE	8	0.9			3	5			
SE	36	4.3		2	12	20	2		
SSE	63	7.4		4	30	23	6		
S	66	7.8	1	2	28	24	9	2	
SSW	72	8.5		5	37	25	4	1	
SW	23	2.7		3	14	5	1		
WSW	36	4.3		3	16	15	2		
W	51	6.0	1	2	25	20	2	1	
WNW	90	10.6%		2	43	38	5	1	1
NW	222	26.2%	1	115	87	18		1	
NNW	111	13.1%		3	63	40	4	1	

Table A2: Tidal data

	Time differences	Z_0	M_2		S_2		K_1		O_1	
	hh.mm	m.	g°	H.m.	g°	H.m.	g°	H.m.	g°	H.m.
Inch'On	00.00	4.64	138	2.84	196	1.09	305	0.39	265	0.28
Taemuui Do	-00.06	4.53	136	2.78	197	1.05	303	0.40	263	0.30
Tokchok To	-00.18	4.25	130	2.48	189	0.96	294	0.43	257	0.32

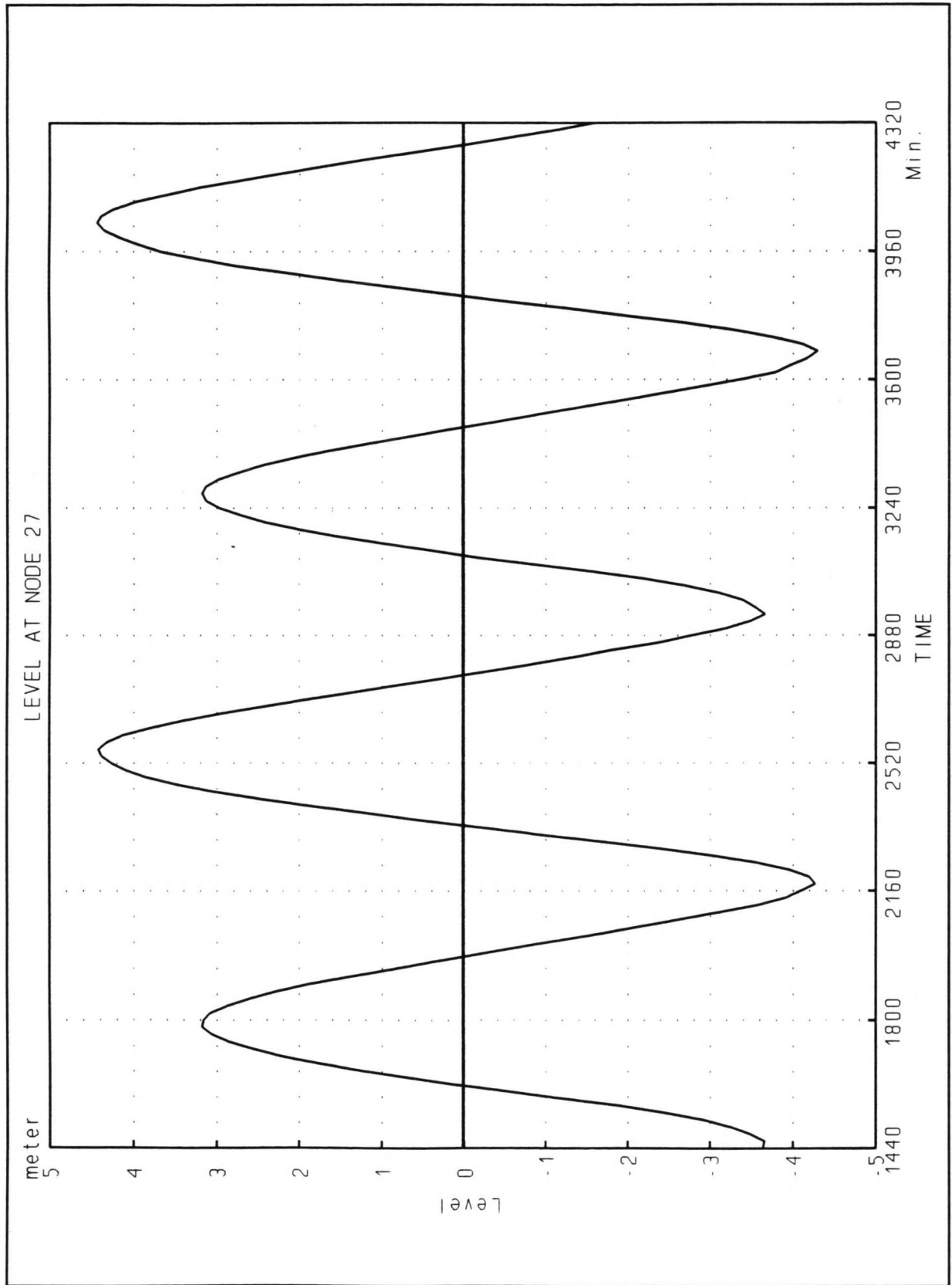


Figure A1: Spring tide at the closure site

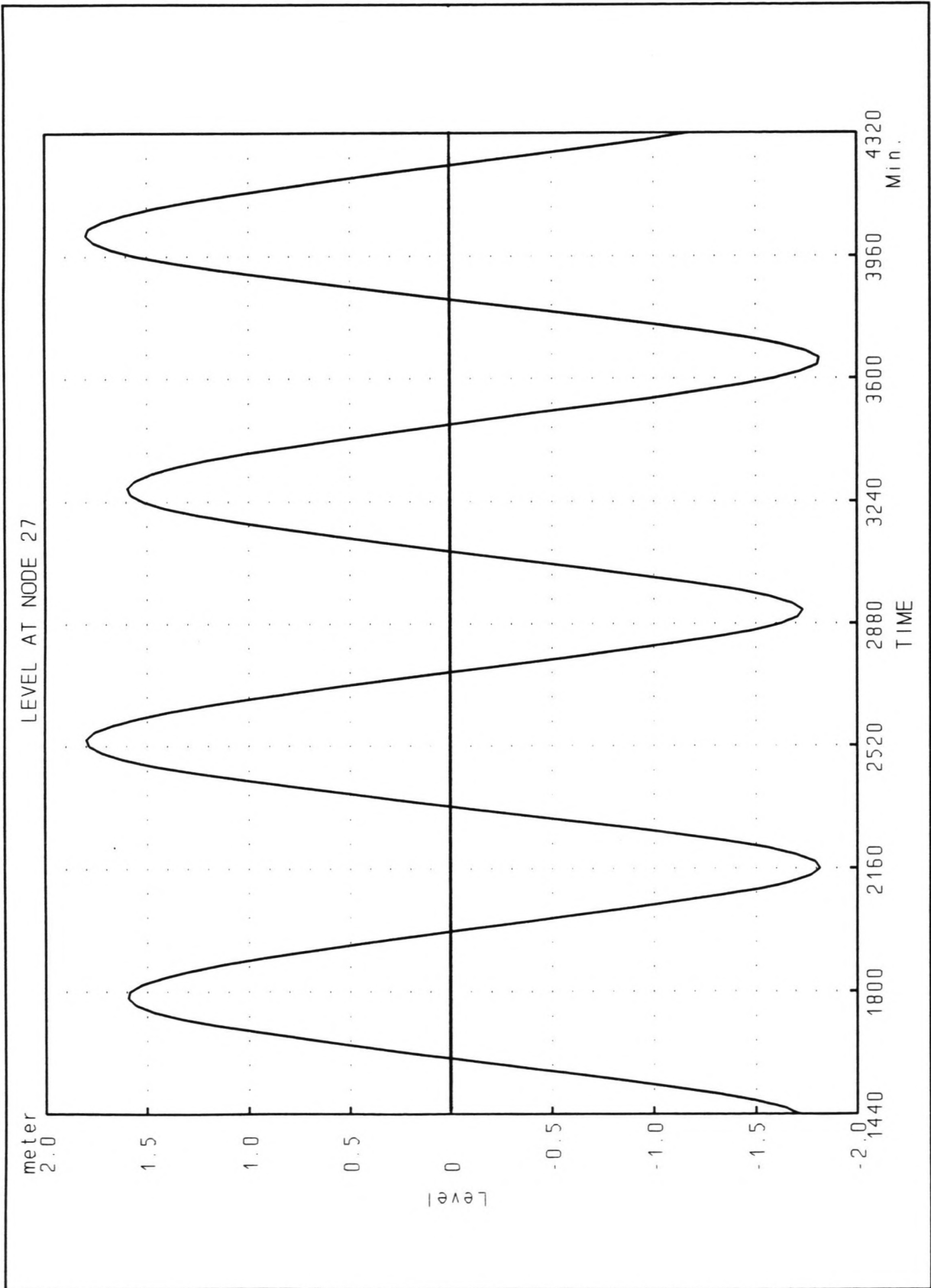


Figure A2: Neap tide at the closure site

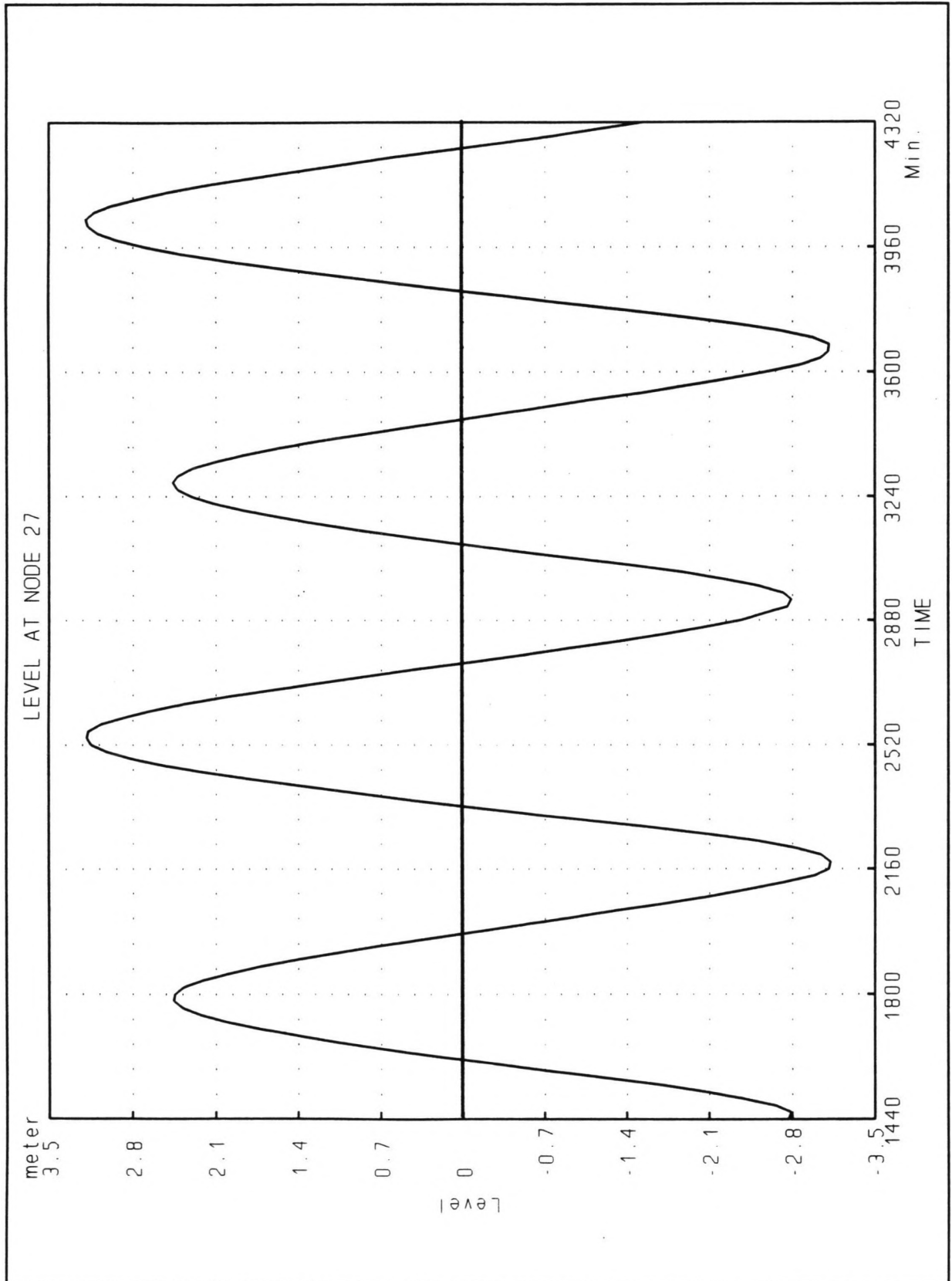


Figure A3: Mean tide at the closure site

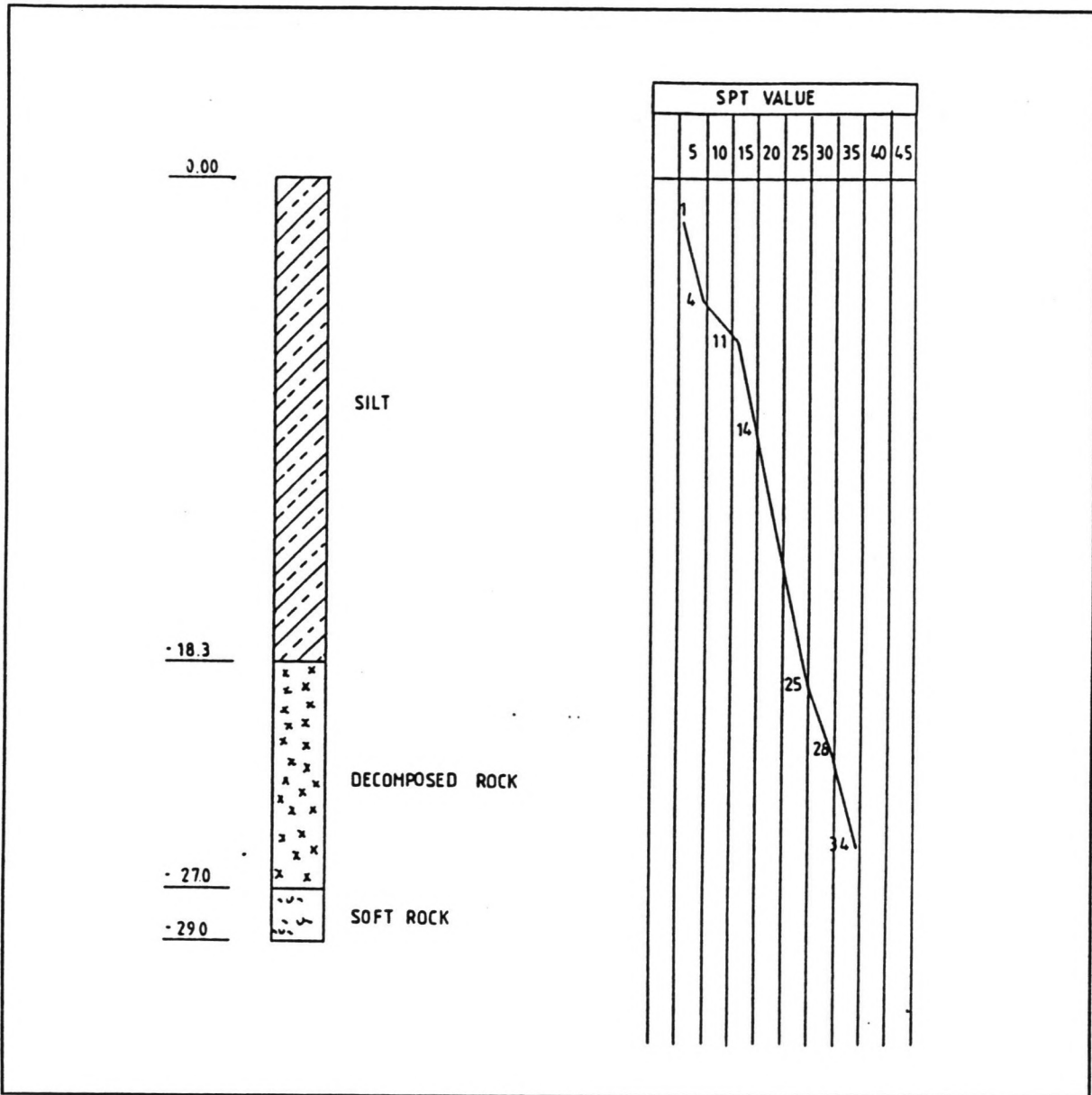


Figure A4: Example of bore hole results

Annex B

This Annex contains:

-set-up at the closure site

-run up at the closure site

Table B1: Wind set-up

<i>wind direction</i>	<i>wind speed</i>	<i>d</i>	<i>F</i>	ΔH
	[m/s]	[m]	[m]	[m]
<i>N</i>	15	6	20000	0.26
<i>E</i>	15	8	19000	0.19
<i>ESE</i>	15	5	16000	0.25
<i>SE</i>	15	6	11000	0.14
<i>SSE</i>	15	5	10000	0.16
<i>S</i>	15	7	10000	0.11
<i>WSW</i>	15	10	11000	0.09
<i>W</i>	15	20	50000	0.20
<i>WNW</i>	15	10	16000	0.13
<i>NW</i>	15	8	34000	0.33
<i>NNW</i>	15	6	20000	0.26

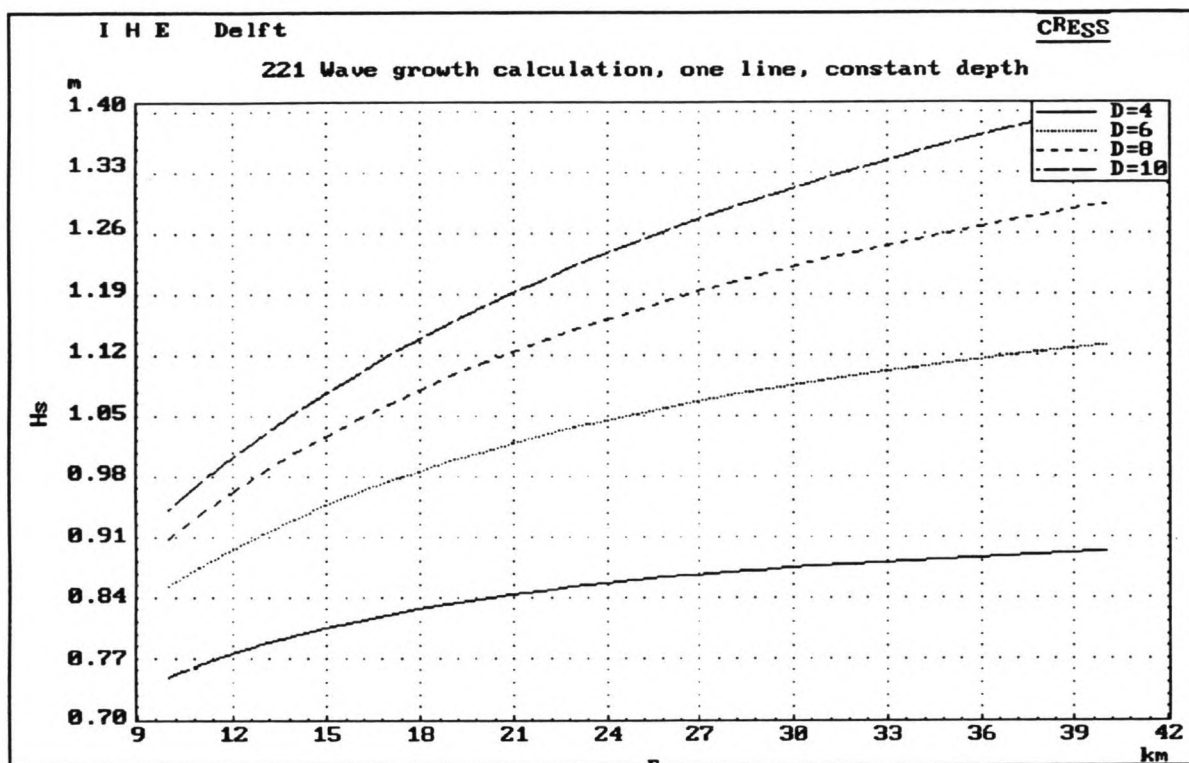


Figure B1: H_s as a function of fetch and depth with $u = 15$ m/s

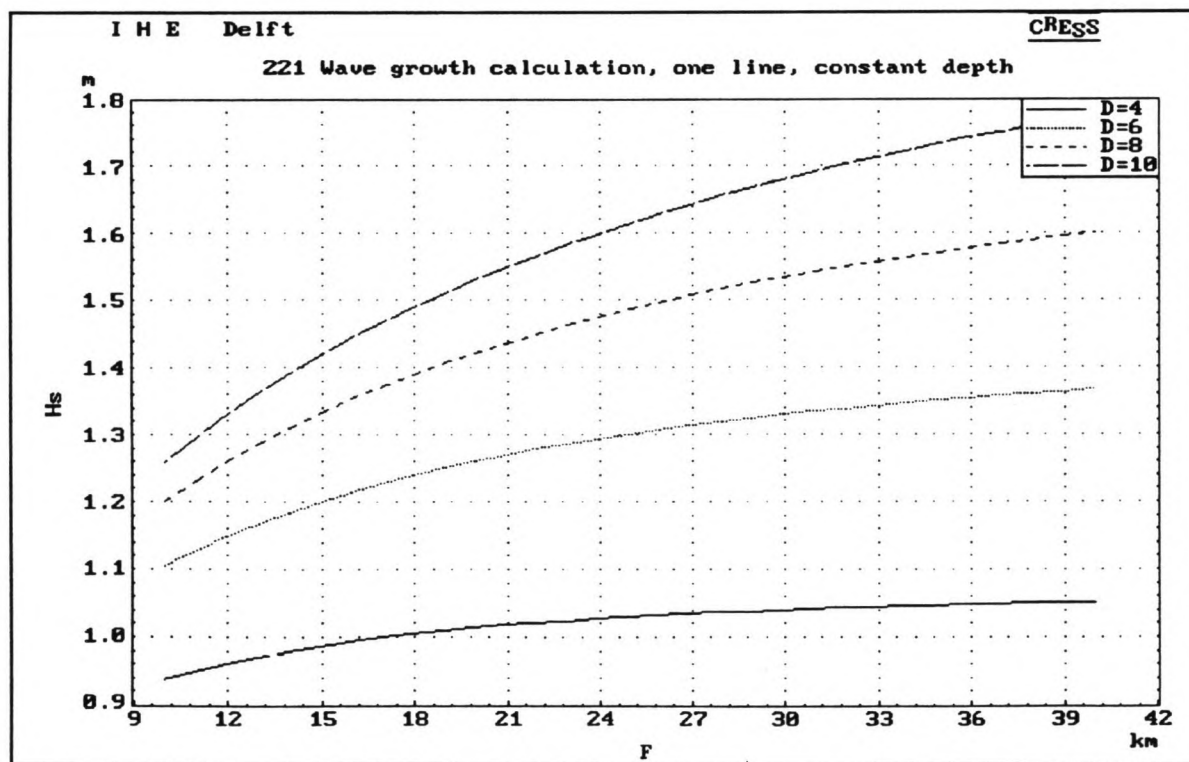


Figure B2: H_s as a function of fetch and depth with $u = 20$ m/s

Table B2: Wave run-up

wind direction	u [m/s]	F [km]				run-up	
					dam	cos α	R _{2%} [m]
N	15	20000	H 1/3 =	1.37	1	0.7071	0.971
			T 1/3 =	4.56	2	1	1.373
E	15	19000	H 1/3 =	1.34	1	0.7071	0.95
			T 1/3 =	4.51	2	0	0
ESE	15	16000	H 1/3 =	1.25	1	0.3827	0.48
			T 1/3 =	4.34	2	0.3827	0.48
SE	15	11000	H 1/3 =	1.07	1	1	1.07
			T 1/3 =	3.98	2	0.7071	0.76
SSE	15	10000	H 1/3 =	1.03	1	0.3827	0.40
			T 1/3 =	3.90	2	0.9239	0.95
S	15	10000	H 1/3 =	1.03	1	0.7071	0.73
			T 1/3 =	3.90	2	1	1.03
WSW	15	11000	H 1/3 =	1.07	1	0.3827	0.41
			T 1/3 =	3.98	2	0.3827	0.41
W	15	50000	H 1/3 =	1.98	1	0.7071	1.4
			T 1/3 =	5.56	2	0	0
WNW	15	16000	H 1/3 =	1.25	1	0.3827	0.48
			T 1/3 =	4.34	2	0.3827	0.48
NW	15	34000	H 1/3 =	1.70	1	1	1.7
			T 1/3 =	5.12	2	0.7071	1.2
NNW	15	20000	H 1/3 =	1.37	1	0.3827	0.53
			T 1/3 =	4.56	2	0.9239	1.27

Annex C

- This Annex contains
- C1: Calculation of the D_{50} during a vertical closure
 - C2: Calculation of the D_{50} during a horizontal closure
 - C3: Calculation of the D_{50} during a combined closure

Annex C1: Vertical closure

In case of a vertical closure the closure is divided into 12 phases see Figure 1:

Phase 1:	S 1, 2 and 3 at MSL -8 m., sill 4 at MSL -4 m.
Phase 2:	S 1, 2 and 3 at MSL -6 m., sill 4 at MSL -4 m.
Phase 3:	All sill levels at MSL -4 m.
Phase 4:	All sill levels at MSL -3 m.
Phase 5:	All sill levels at MSL -2 m.
Phase 6:	All sill levels at MSL -1 m.
Phase 7:	All sill levels at MSL.
Phase 8:	All sill levels at MSL +1 m.
Phase 9:	All sill levels at MSL +2 m.
Phase10:	All sill levels at MSL +3 m.
Phase11:	All sill levels at MSL +4 m.
Phase12:	All sill levels at MSL +5 m.

For every phase, a Duflow-calculation is made. Figure 4 to 35 show the water level at the beginning and at the end of every weir, together with the flow velocities and discharges that occur in every weir as a function of time.

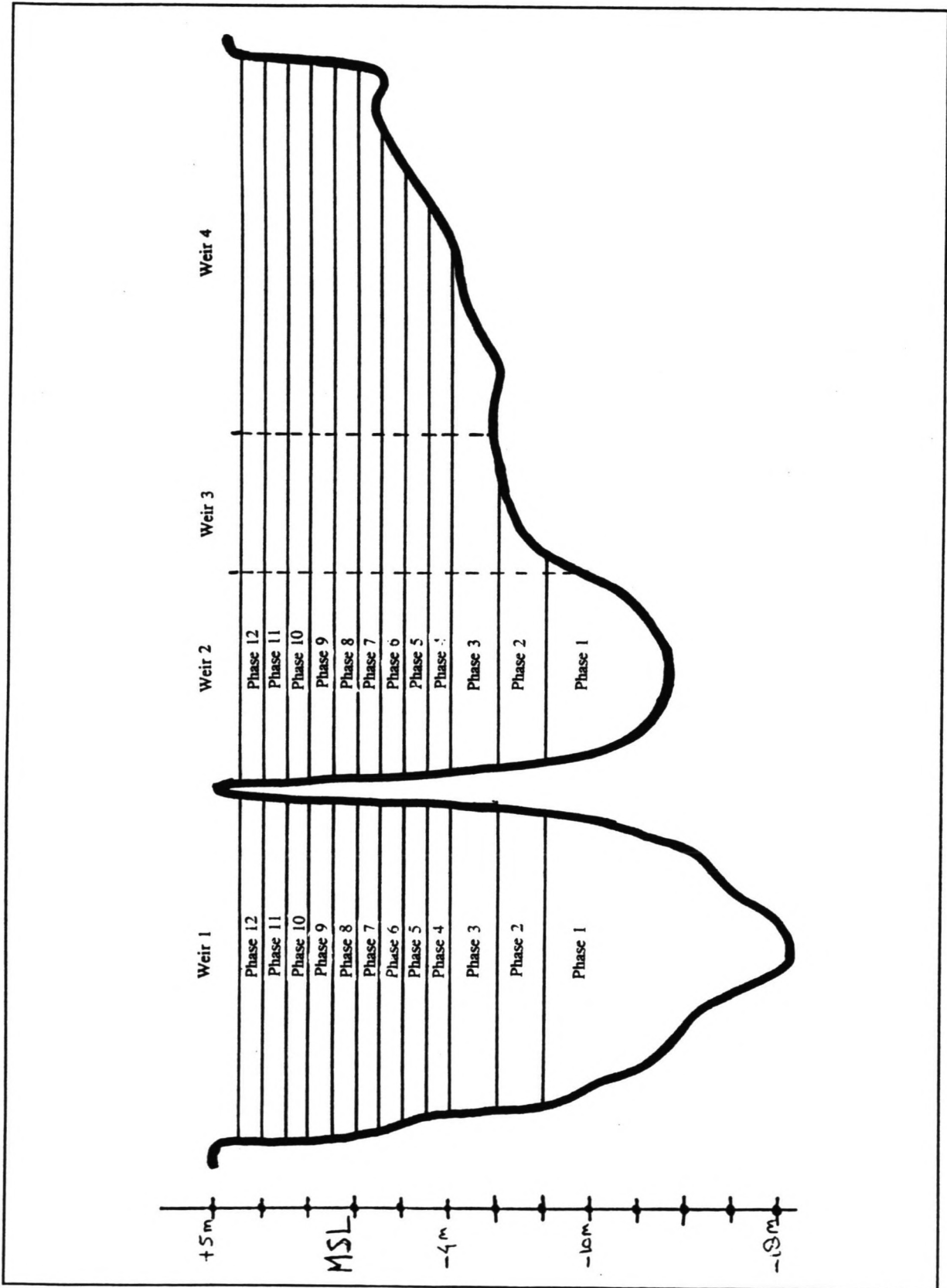


Figure C1: Phases of a vertical closure method

Phase 1:

In this phase, the sill will be constructed upto MSL -8.0 m. in structure 1, 2 and 3. Assuming a crest heigth at MSL +5 m., and a bottom level at MSL -16 m., (see Figure 1), $B/d = 40/8 = 5$. This means that the equations for broad crested dams may be applied.

Low dam flow:

$$\frac{u_0}{\sqrt{g\Delta D}} = 1.4 \log \left(3.5 \frac{h_0}{D} \right)$$

with: $u_0 = -1.5$ m/s
 $\Delta = 1.65$
 $h_0 = 3.99$ m

D_{50} becomes 0.008 m.

Intermediate Flow: With $h_b/\Delta D \gg \gg 4$, intermediate flow does not occur.

Phase 2:

In this phase, the sill of structure 1,2 and 3 will be constructed upto MSL -6.0 m. $B/d = 34/10 = 3.4$. As this is smaller than 5, the equations for sharp crested sills may be applied:

Low dam flow:

$$\frac{u_0}{\sqrt{g\Delta D}} = 1.4 \log \left(1.5 \frac{h_0}{D} \right)$$

with: $u_0 = -2.7$ m/s
 $\Delta = 1.65$
 $h_0 = 2.11$ m

D_{50} becomes 0.052 m.

Intermediate Flow: With $h_b/\Delta D = 22$, intermediate flow does not occur.

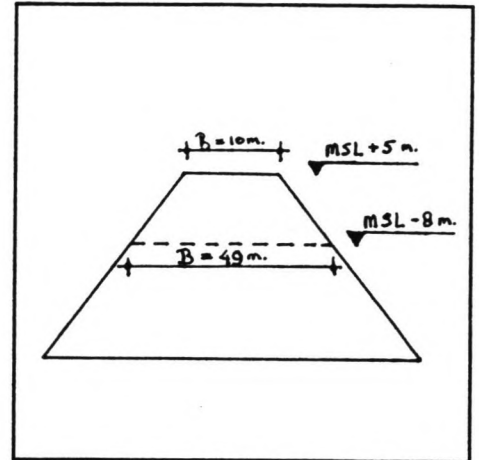


Figure C2: Crest width

Phase 3:

In this phase, the sill will be constructed upto MSL -4.0 m. , $B/d = 28/12 = 2.33$. As this is smaller than 5, the equations for a sharp crested sill may be applied:

Low dam flow: As $h_b/\Delta D = 0.8$, the equations who describe low dam flow are not valid anymore.

Intermediate flow: With $h_b/\Delta D = 0.8$, the intermediate flow situation is valid.

$$\frac{u_0}{\sqrt{\Delta g D}} = \sqrt{A + 0.375 \frac{h_b}{\Delta D}}$$

with: $A = 2$, (sharp crested dam)
 $u_0 = -3.86$ m/s
 $\Delta = 1.65$
 $h_0 = 1.08$ m

D_{50} becomes 0.86 m.

High dam flow: As the crest of the dam is not emerged yet, high dam flow does not occur.

Phase 4:

In this phase, the sill will be constructed upto MSL -3.0 m., $B/d = 28/13 = 2.15$. As this is smaller than 5, the equations for a sharp crested sill may be applied.

Intermediate flow: With $h_b/\Delta D = 0.57$, the intermediate flow situation is valid.

$$\frac{u_0}{\sqrt{\Delta g D}} = \sqrt{A + 0.375 \frac{h_b}{\Delta D}}$$

with: $A = 2$, (sharp crested dam)
 $u_0 = -3.93$ m/s
 $\Delta = 1.65$
 $h_0 = 1.11$ m

D_{50} becomes 0.95 m.

High dam flow:

$$q_{\max} = 1.95 (\Delta D_s)^{\frac{3}{2}} (1.9 + 0.8\phi - 3\sin\alpha)$$

with $q_{\max} = 3.44 \text{ m}^2/\text{s}$

D_{50} becomes 1.14 m.

As the the high dam flow criterion gives a higher value than the intermediate flow criterion, the value of 1.14 m. is decisive.

Phase 5:

In this phase, the sill will be constructed upto MSL -2.0 m., $B/d < 5$, so the equations for a sharp crested sill may be applied.

Intermediate flow: with $h_b/\Delta D = 0.58$, the intermediate flow situation is valid.

$$\frac{u_0}{\sqrt{\Delta g D}} = \sqrt{A + 0.375 \frac{h_b}{\Delta D}}$$

with: $A = 2$, (sharp crested dam)
 $u_0 = -3.96 \text{ m/s}$
 $\Delta = 1.65$
 $h_0 = 0.92 \text{ m}$

D_{50} becomes 0.96 m.

High dam flow:

$$q_{\max} = 1.95 (\Delta D_s)^{\frac{3}{2}} (1.9 + 0.8\phi - 3\sin\alpha)$$

with $q_{\max} = 3.9 \text{ m}^2/\text{s}$

D_{50} becomes 1.18 m.

As the the high dam flow criterion gives a higher value than the intermediate flow criterion, the value of 1.18 m. is decisive.

Phase 6:

In this phase, the sill will be constructed upto MSL -1.0 m., $B/d < 5$, so the equations for a sharp crested sill may be applied.

Intermediate flow: With $h_b/\Delta D = 0.52$, the intermediate flow situation is valid.

$$\frac{u_0}{\sqrt{\Delta g D}} = \sqrt{A + 0.375 \frac{h_b}{\Delta D}}$$

with: $A = 2$, (sharp crested dam)
 $u_0 = -4.15$ m/s
 $\Delta = 1.65$
 $h_0 = 0.93$ m

D_{50} becomes 1.07 m.

High dam flow:

$$q_{\max} = 1.95 (\Delta D_s)^{\frac{3}{2}} (1.9 + 0.8\phi - 3\sin\alpha)$$

With $q_{\max} = 3.73$ m²/s
 D_{50} becomes 1.16 m.

As the the high dam flow criterion gives a higher value than the intermediate flow criterion, the value of 1.16 m. is decisive.

Phase 7:

In this phase, the sill will be constructed upto MSL, $B/d < 5$, so the equations for a sharp crested sill may be applied.

Intermediate flow: With $h_b/\Delta D = 1.15$, the intermediate flow situation is valid.

$$\frac{u_0}{\sqrt{\Delta g D}} = \sqrt{A + 0.375 \frac{h_b}{\Delta D}}$$

with: $A = 2$, (sharp crested dam)

$$\begin{aligned}u_0 &= -3.65 \text{ m/s} \\ \Delta &= 1.65 \\ h_0 &= 1.28 \text{ m}\end{aligned}$$

D_{50} becomes 0.80 m.

High dam flow:

$$q_{\max} = 1.95 (\Delta D_s)^{\frac{3}{2}} (1.9 + 0.8\phi - 3\sin\alpha)$$

With $q_{\max} = 3.51 \text{ m}^2/\text{s}$

D_{50} becomes 1.10 m.

As the the high dam flow criterion gives a higher value than the intermediate flow criterion, the value of 1.10 m. is decisive.

Phase 8:

In this phase, the sill will be constructed upto MSL +1.0 m., $B/d < 5$, the equations for a sharp crested sill may be applied.

Intermediate flow: With $h_b/\Delta D = 0.5$, the intermediate flow situation is valid.

$$\frac{u_0}{\sqrt{\Delta g D}} = \sqrt{A + 0.375 \frac{h_b}{\Delta D}}$$

with: $A = 2$, (sharp crested dam)

$$\begin{aligned}u_0 &= -3.58 \text{ m/s} \\ \Delta &= 1.65 \\ h_0 &= 0.68 \text{ m}\end{aligned}$$

D_{50} becomes 0.80 m.

High dam flow:

$$q_{\max} = 1.95 (\Delta D_s)^{\frac{3}{2}} (1.9 + 0.8\phi - 3\sin\alpha)$$

With $q_{\max} = 3.16 \text{ m}^2/\text{s}$

D_{50} becomes 1.03 m.

As the the high dam flow criterion gives a higher value than the intermediate flow criterion, the value of 1.03 m. is decisive.

Phase 9:

In this phase, the sill will be constructed upto MSL +2.0, $B/d < 5$ so the equations for a sharp crested sill may be applied.

Intermediate flow: With $h_b/\Delta D = 0.81$, the intermediate flow situation is valid.

$$\frac{u_0}{\sqrt{\Delta g D}} = \sqrt{A + 0.375 \frac{h_b}{\Delta D}}$$

with: $A = 2$, (sharp crested dam)

$$u_0 = -3.3 \text{ m/s}$$

$$\Delta = 1.65$$

$$h_0 = 0.83 \text{ m}$$

D_{50} becomes 0.61 m.

High dam flow:

$$q_{\max} = 1.95 (\Delta D_s)^2 (1.9 + 0.8\phi - 3\sin\alpha)$$

With $q_{\max} = 2.67 \text{ m}^2/\text{s}$

D_{50} becomes 0.83 m.

As the the high dam flow criterion gives a higher value than the intermediate flow criterion, the value of 0.83 m. is decisive.

Phase 10:

In this phase, the sill will be constructed upto MSL +3.0 m., $B/d < 5$, so the equations for a sharp crested sill may be applied.

Intermediate flow: With $h_b/\Delta D = 1.0$, the intermediate flow situation is valid.

$$\frac{u_0}{\sqrt{\Delta g D}} = \sqrt{A + 0.375 \frac{h_b}{\Delta D}}$$

with: A = 2, (sharp crested dam)
u₀ = 3.0 m/s
Δ = 1.65
h₀ = 0.81 m

D₅₀ becomes 0.47 m.

High dam flow:

$$q_{\max} = 1.95 (\Delta D_s)^{\frac{3}{2}} (1.9 + 0.8\phi - 3 \sin \alpha)$$

With q_{max} = 0.88 m²/s

D₅₀ becomes 0.43 m.

As the the intermediate flow criterion now gives a higher value than the high dam flow criterion, the value of 0.47 m. is decisive.

Phase 11:

In this phase, the sill will be constructed upto MSL +4.0 m., B/d < 5, so the equations for a sharp crested sill may be applied.

Intermediate flow: With h_v/ΔD = 1.15, the intermediate flow situation is valid.

$$\frac{u_0}{\sqrt{\Delta g D}} = \sqrt{A + 0.375 \frac{h_b}{\Delta D}}$$

with: A = 2, (sharp crested dam)
u₀ = -3.58 m/s
Δ = 1.65
h₀ = 1.68 m

D₅₀ becomes 0.80 m.

High dam flow:

$$q_{\max} = 1.95 (\Delta D_s)^{\frac{3}{2}} (1.9 + 0.8\phi - 3\sin\alpha)$$

With $q_{\max} = 3.51 \text{ m}^2/\text{s}$

D_{50} becomes 1.10 m.

As the the high dam flow criterion gives a higher value than the intermediate flow criterion, the value of 1.10 m. is decisive.

Phase 12:

In phase 12, the flow velocities become zero because the crest level is risen above the maximum tidal level. The closure is completed.

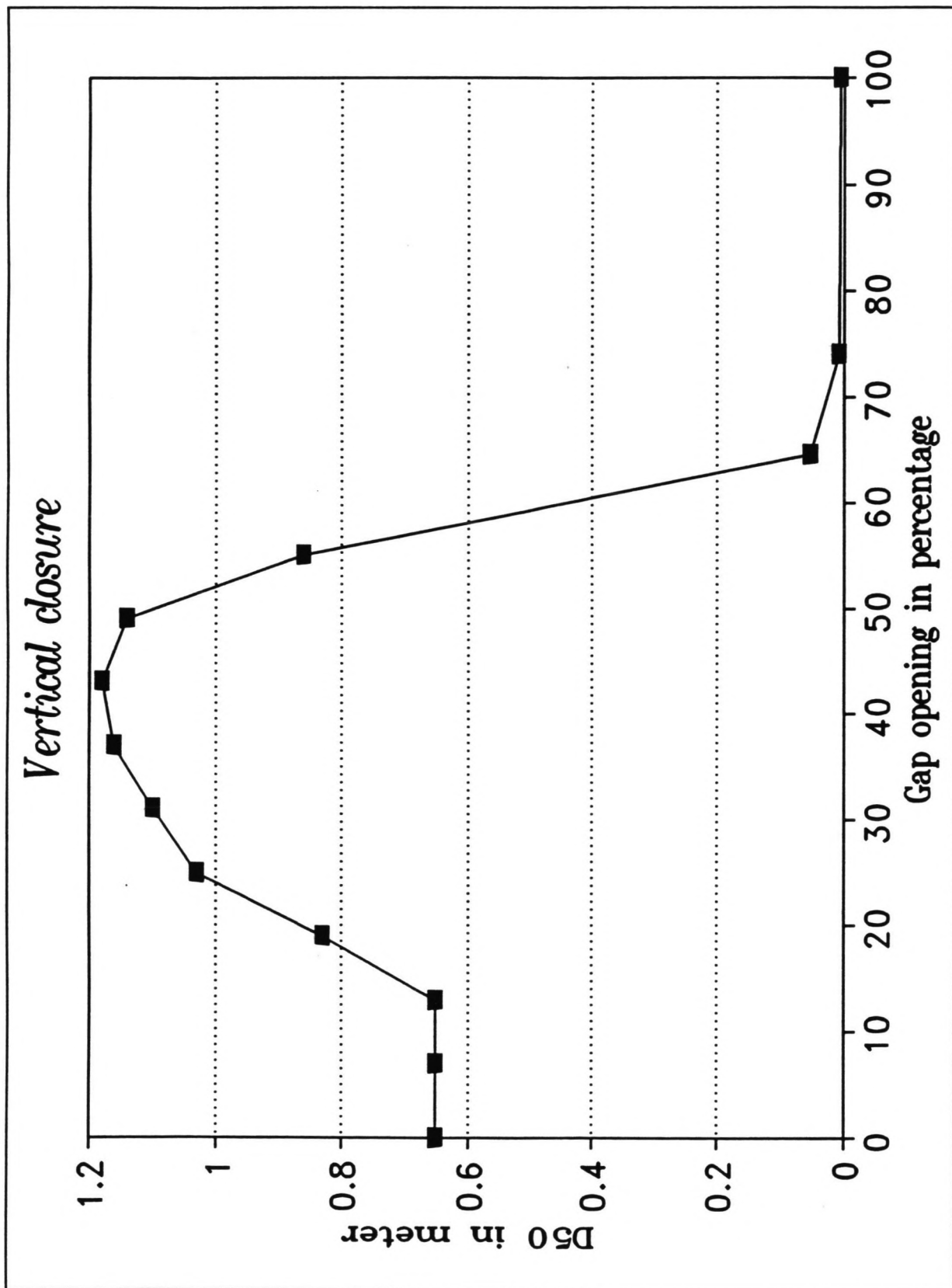


Figure C3: Resulting D_{50} for a vertical closure method

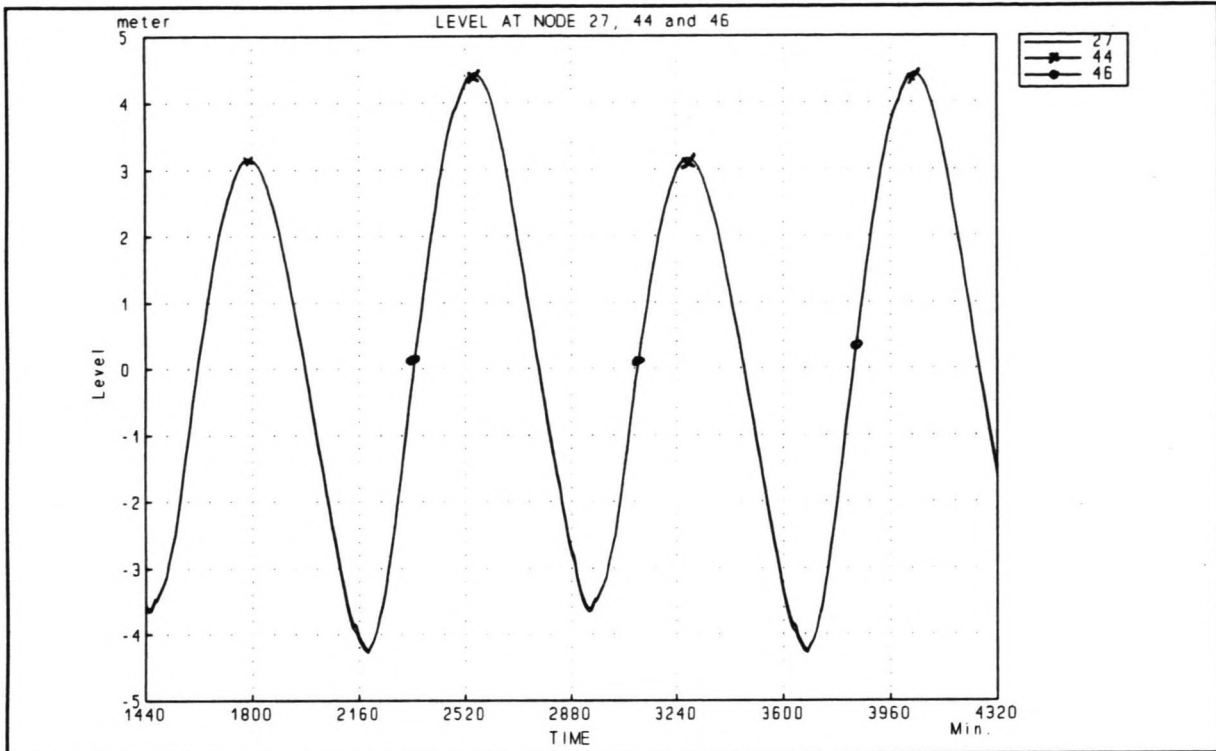


Figure C4: Water level during phase 1

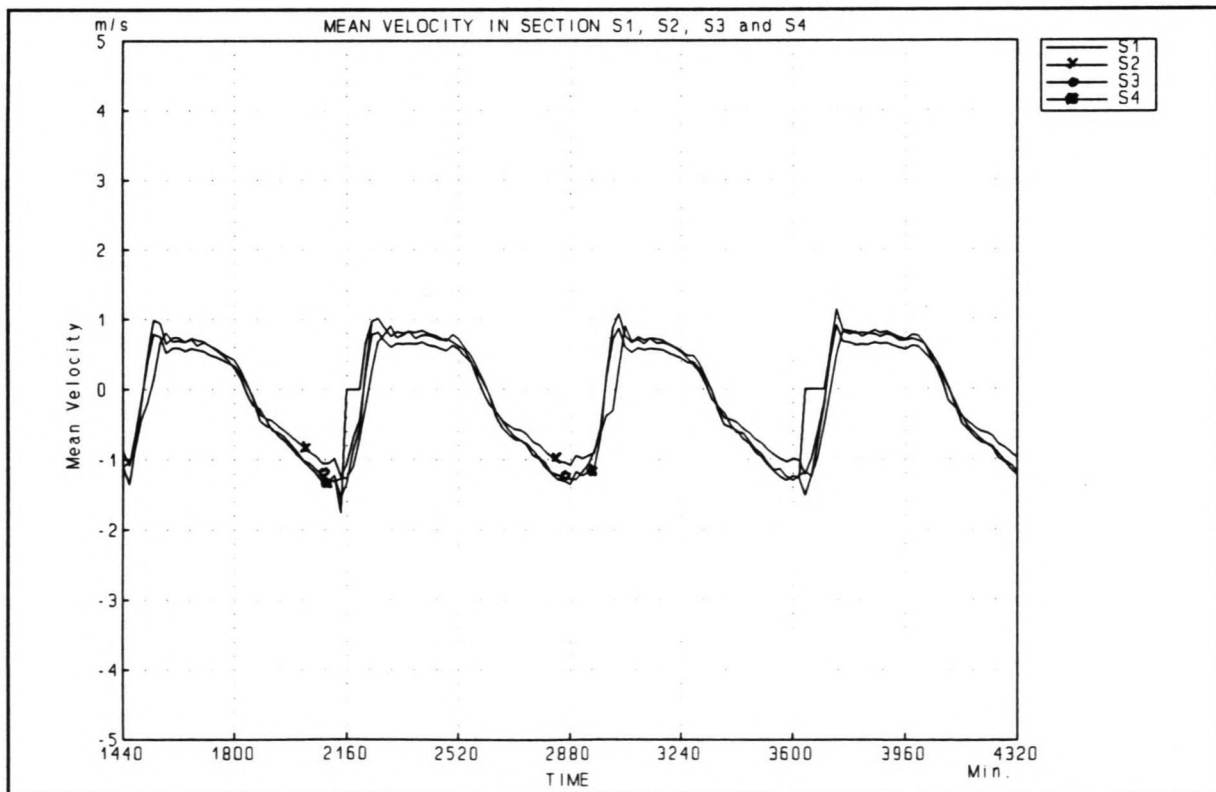


Figure C5: Flow velocities during phase 1

Closure of the Shiwa Tidal Basin

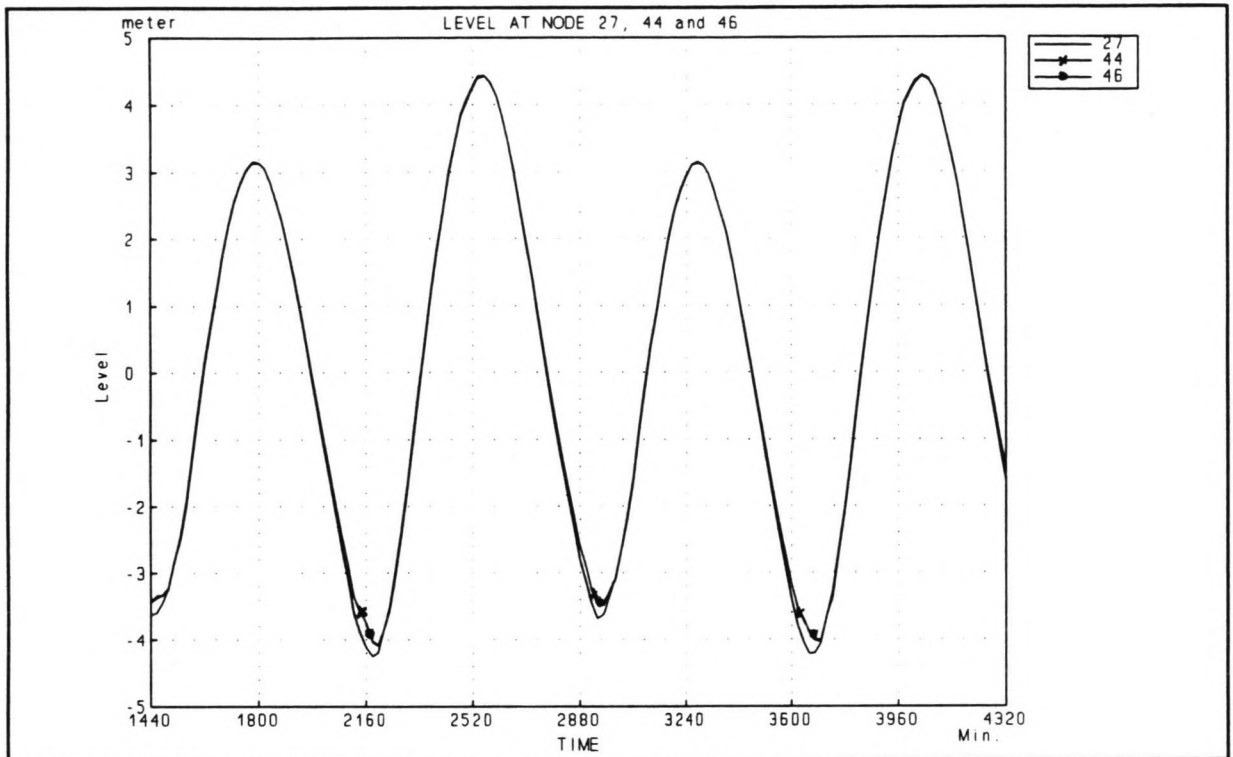


Figure C6: Water level during phase 2

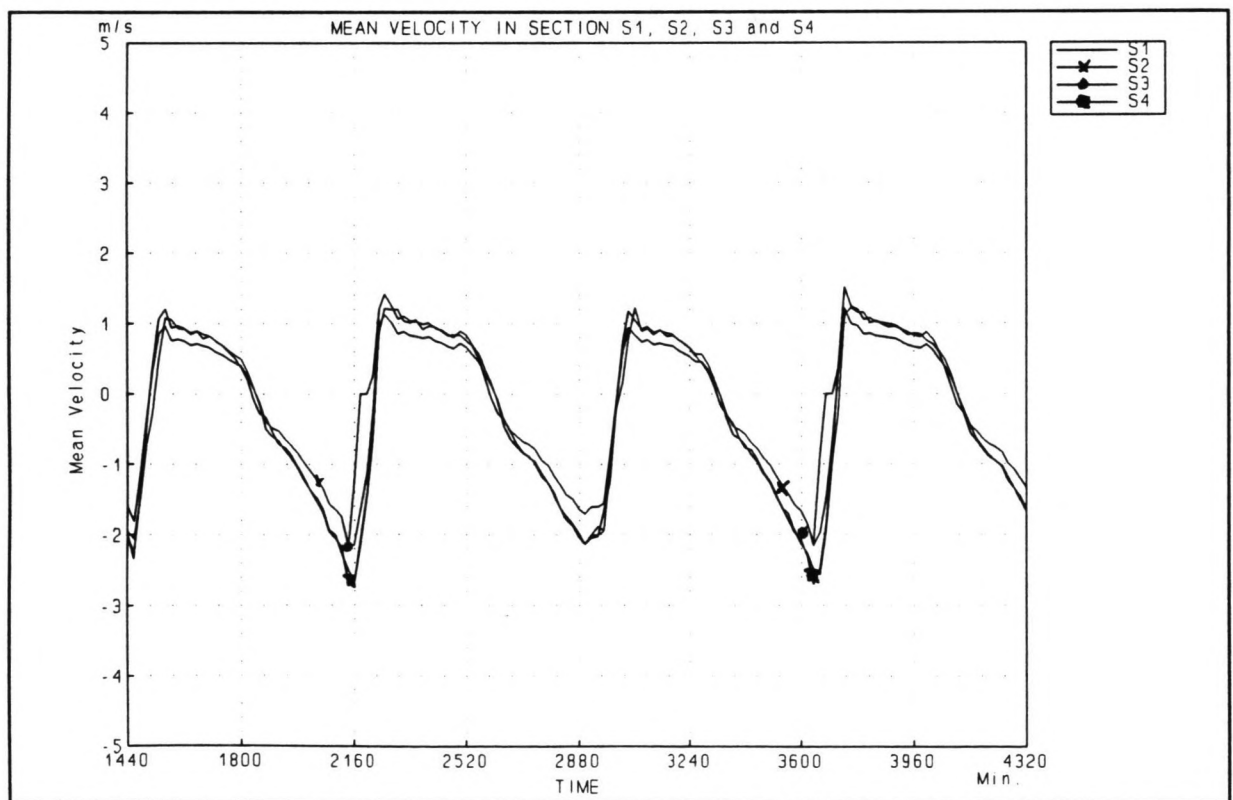


Figure C7: Flow velocities during phase 2

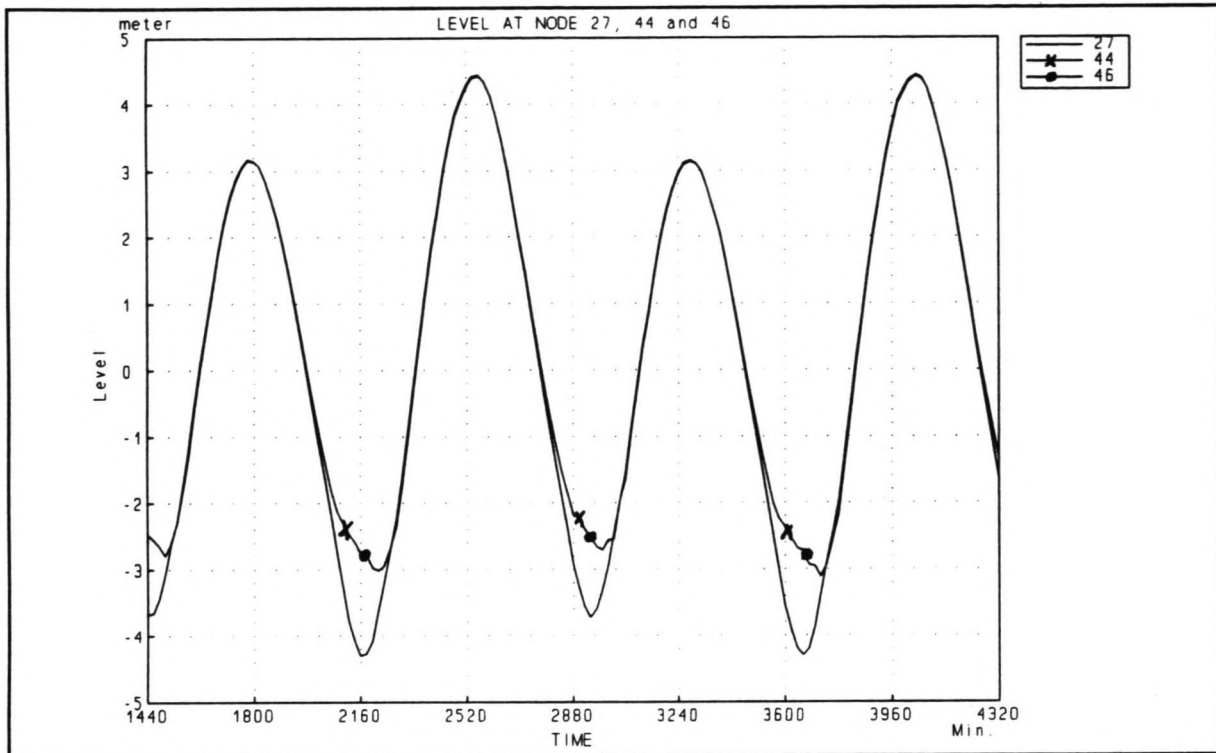


Figure C8: Water level during phase 3

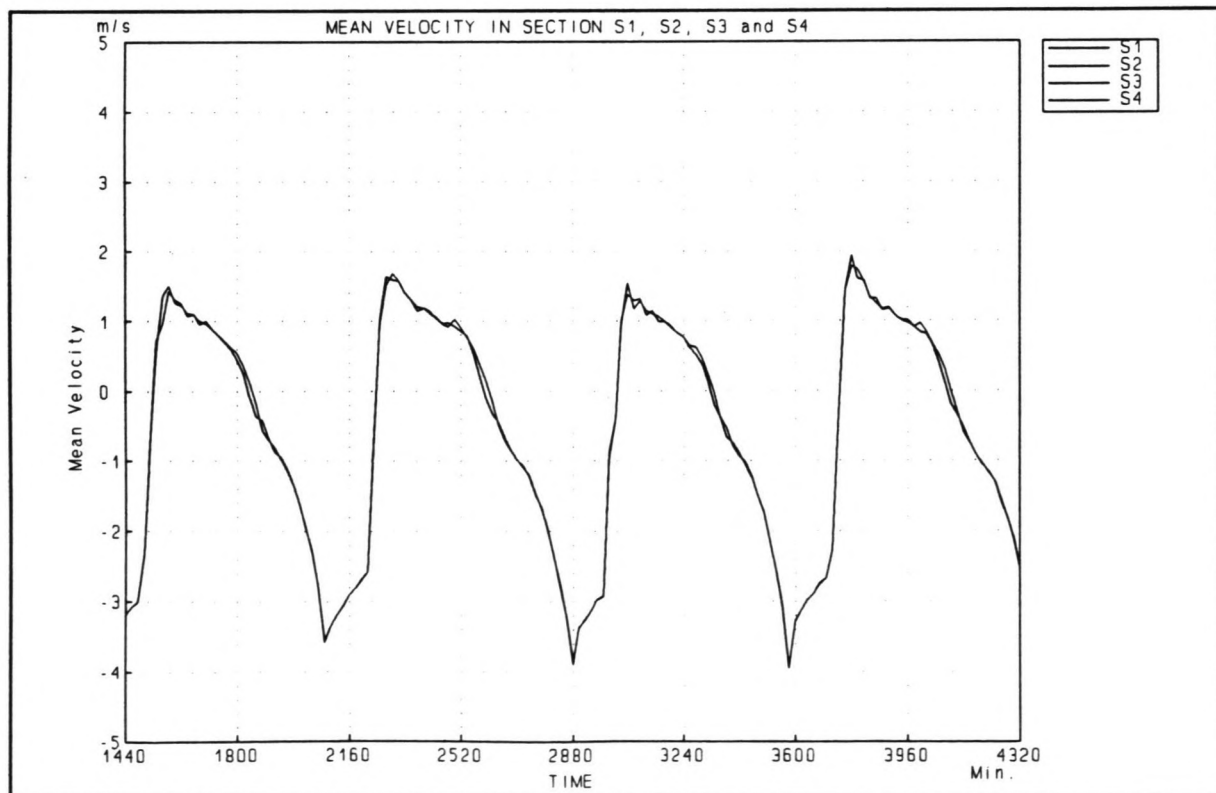


Figure C9: Flow velocities during phase 3

Closure of the Shiwa Tidal Basin

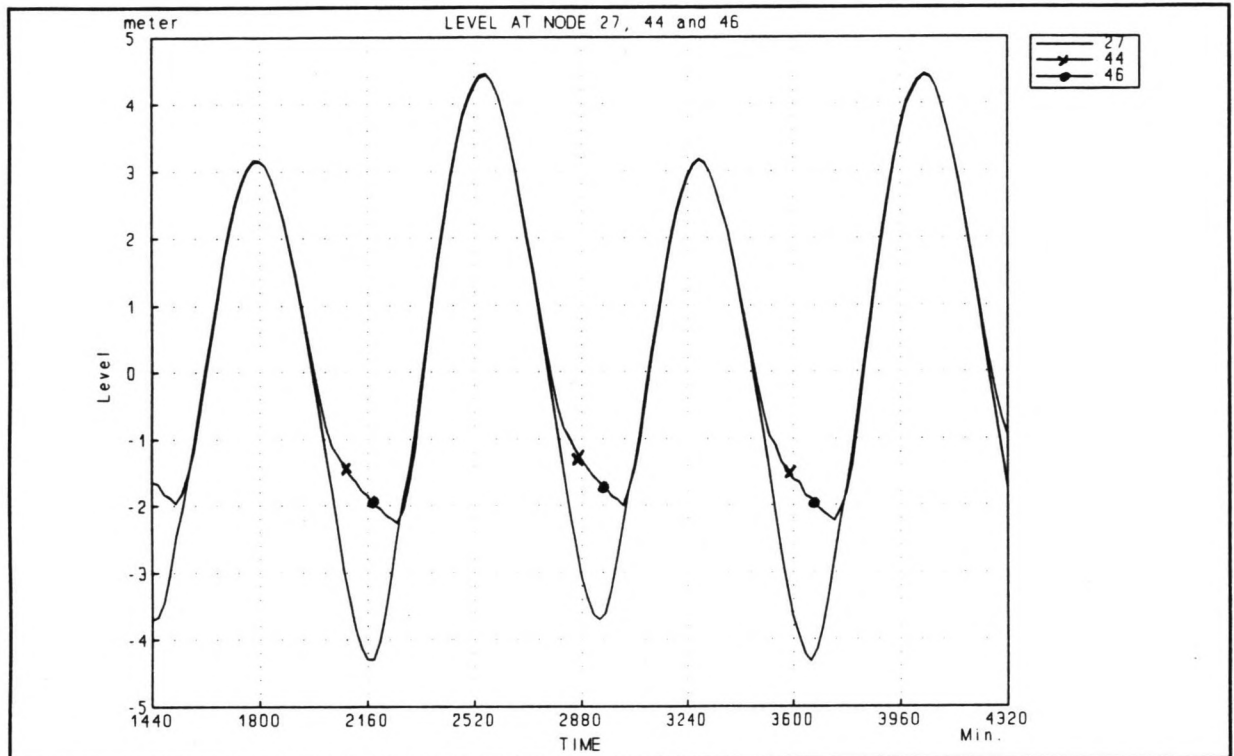


Figure C10: Water level during phase 4

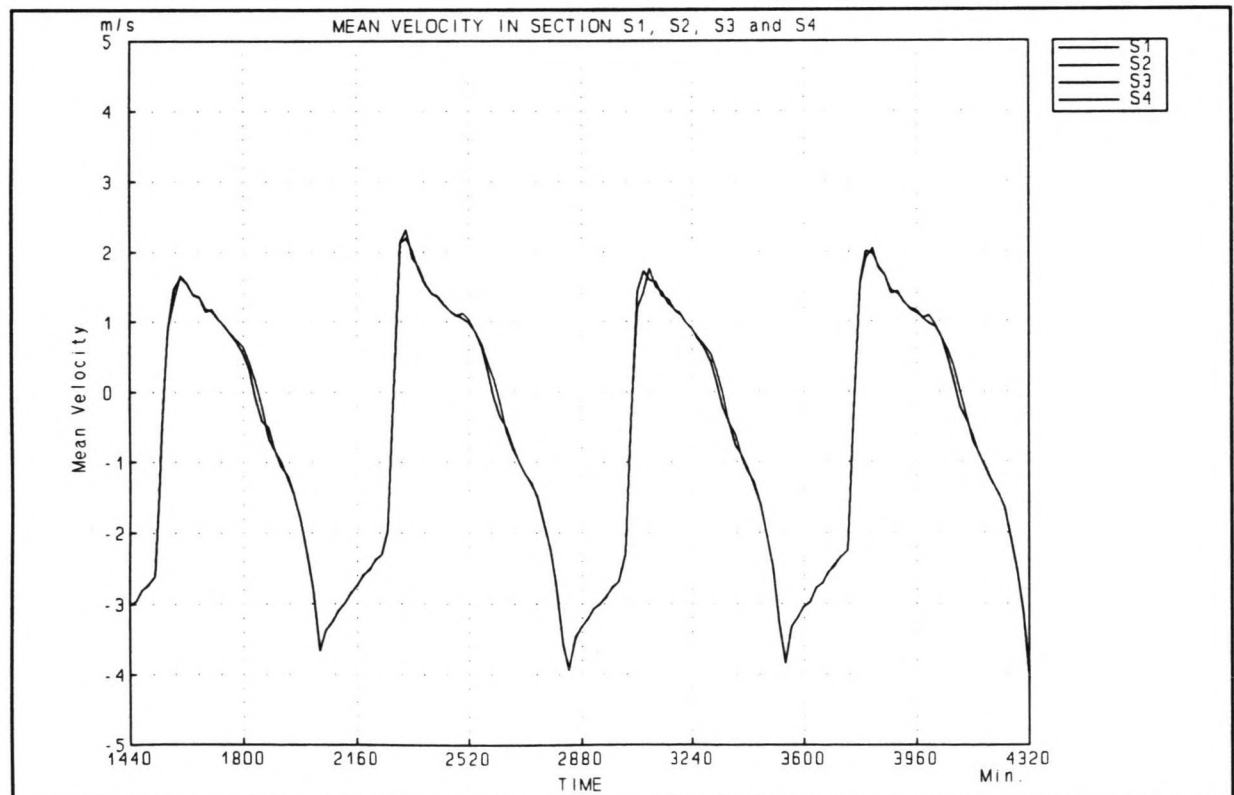


Figure C11: Flow velocities during phase 4

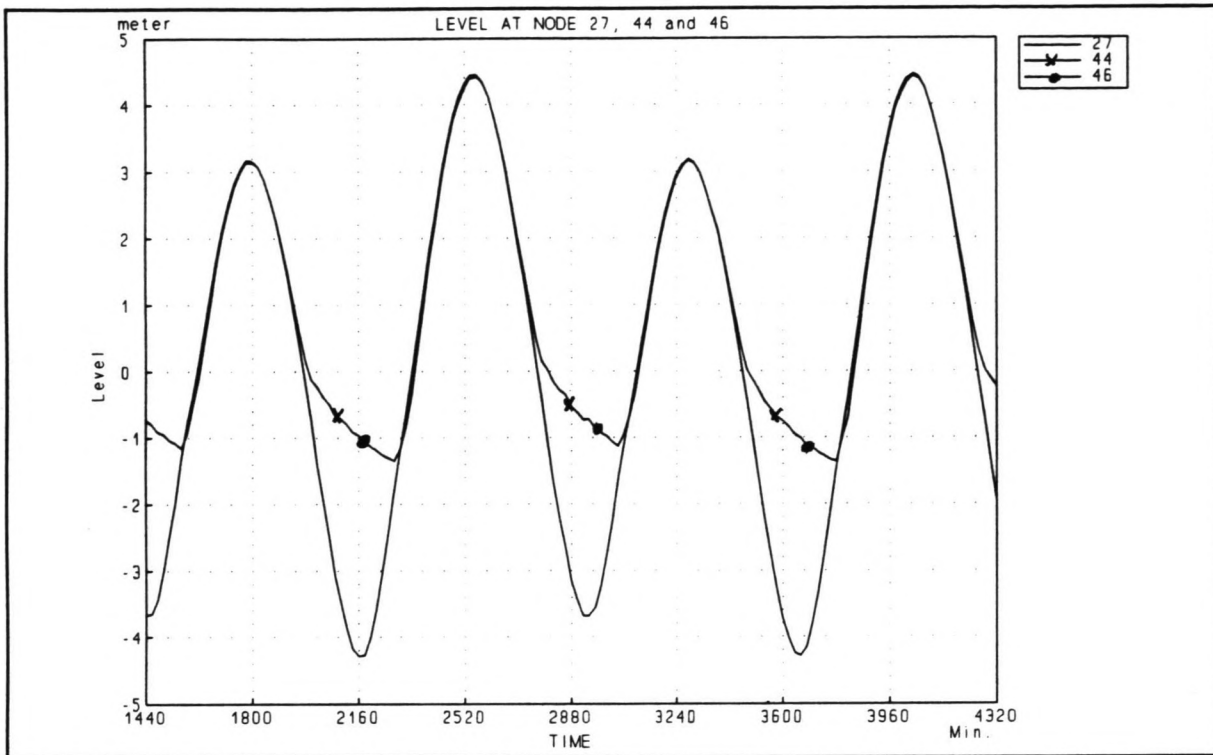


Figure C12: Water level during phase 5

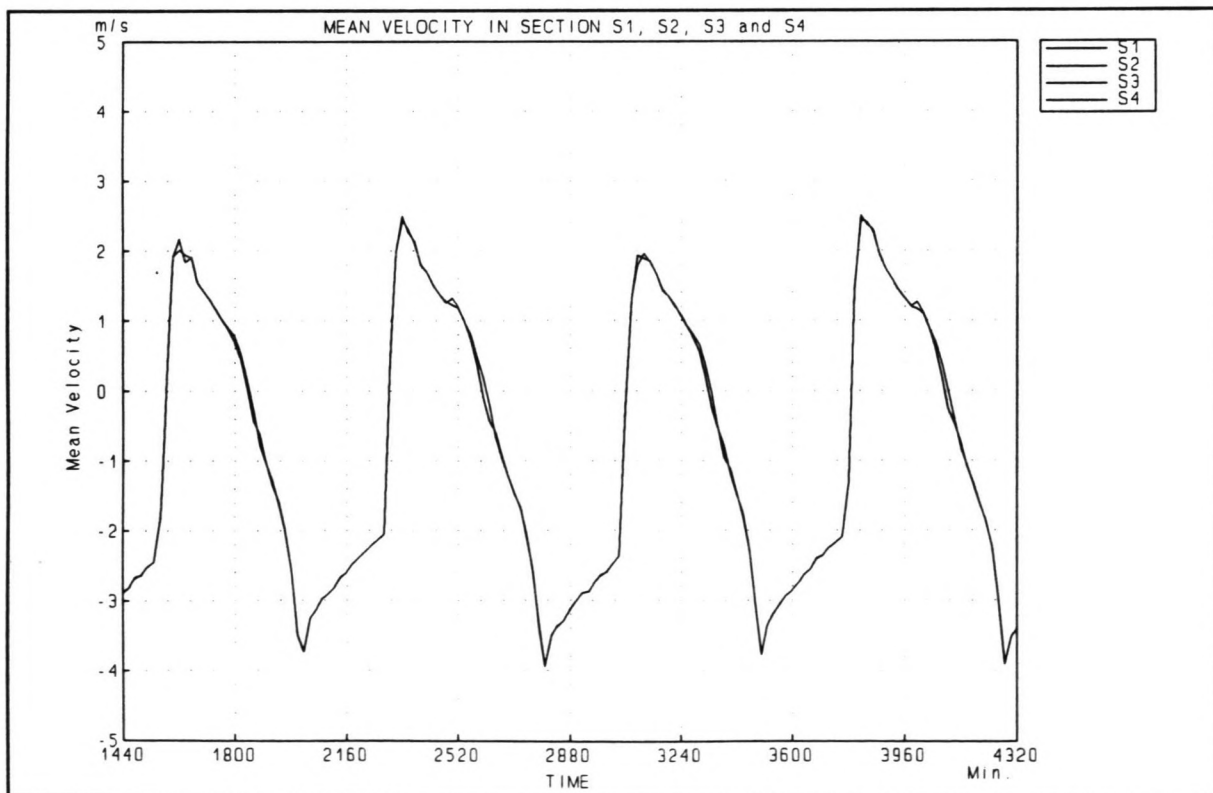


Figure C13: Flow velocities during phase 5

Closure of the Shiwa Tidal Basin

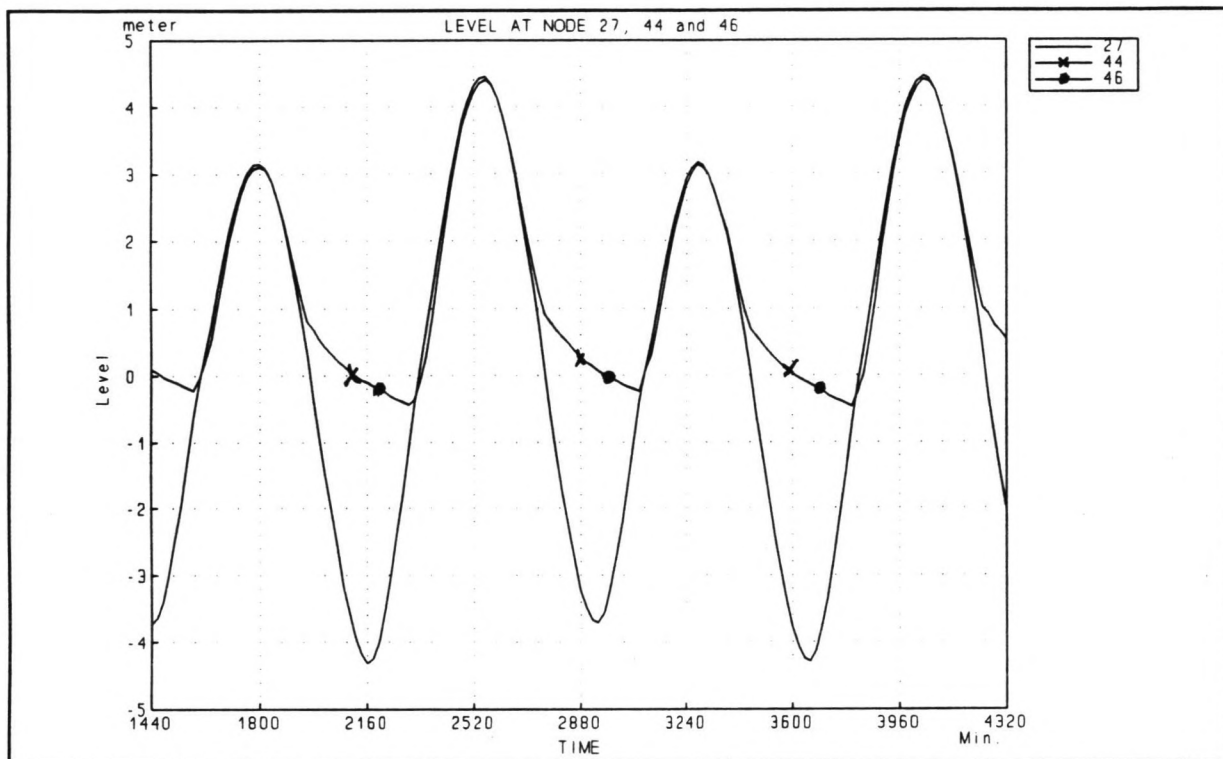


Figure C14: Water level during phase 6

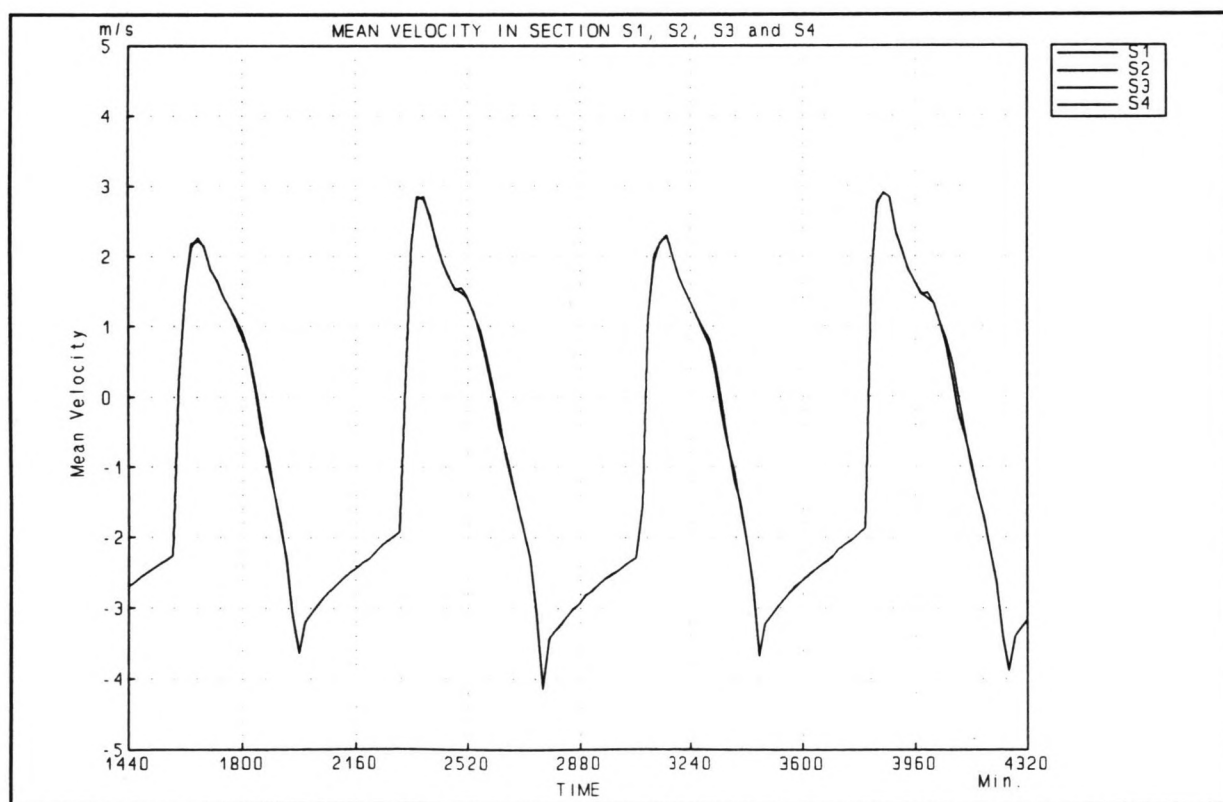


Figure C15: Flow velocities during phase 6

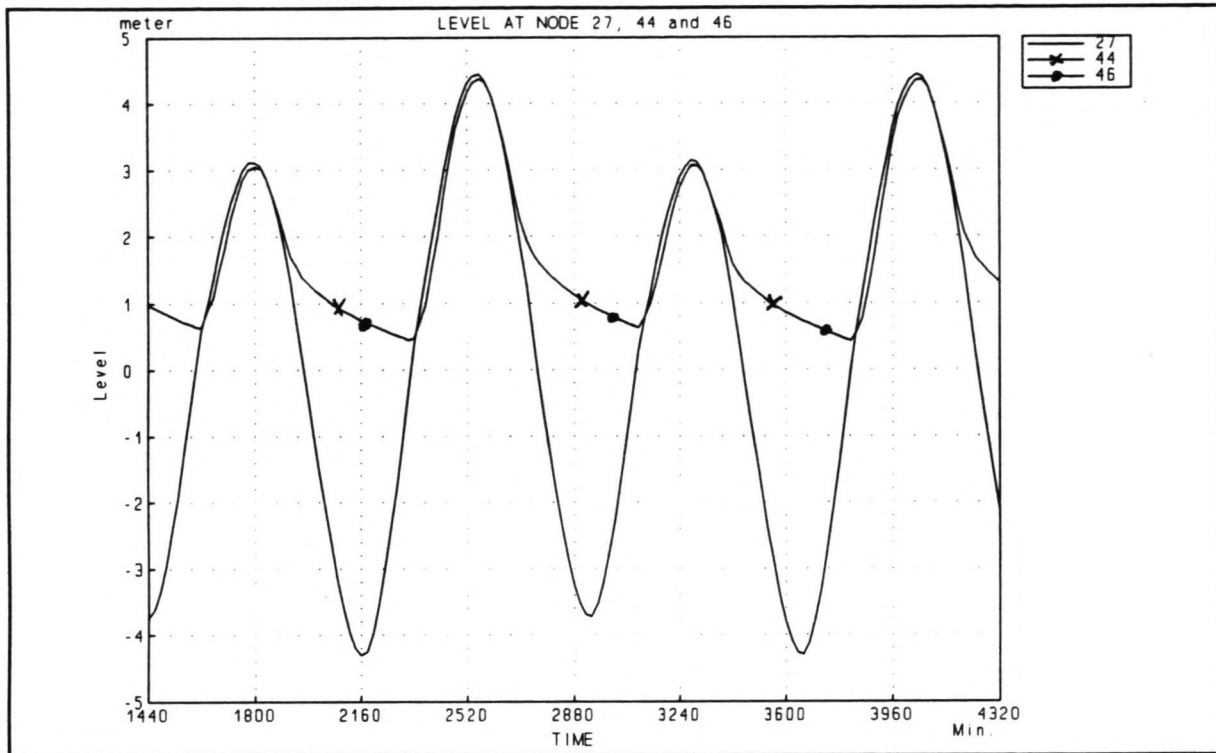


Figure C16: Water level during phase 7

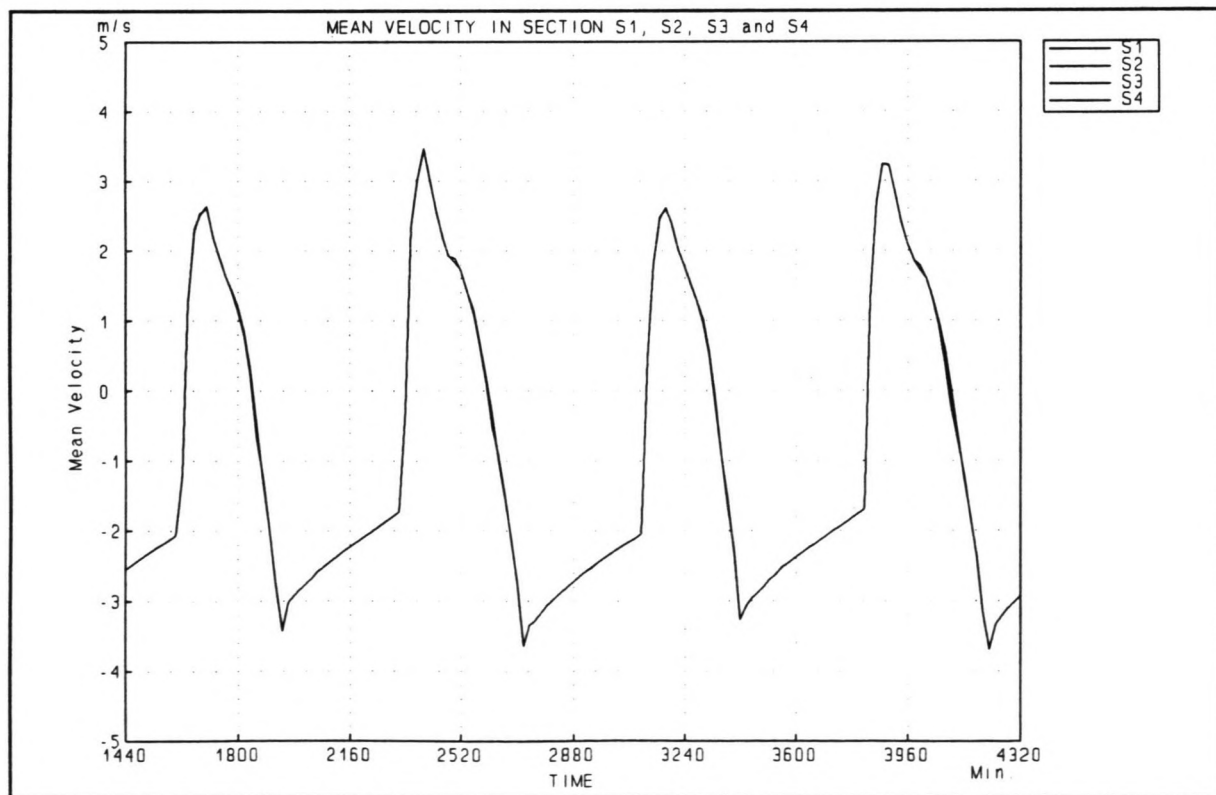


Figure C17: Flow velocities during phase 7

Closure of the Shiwa Tidal Basin

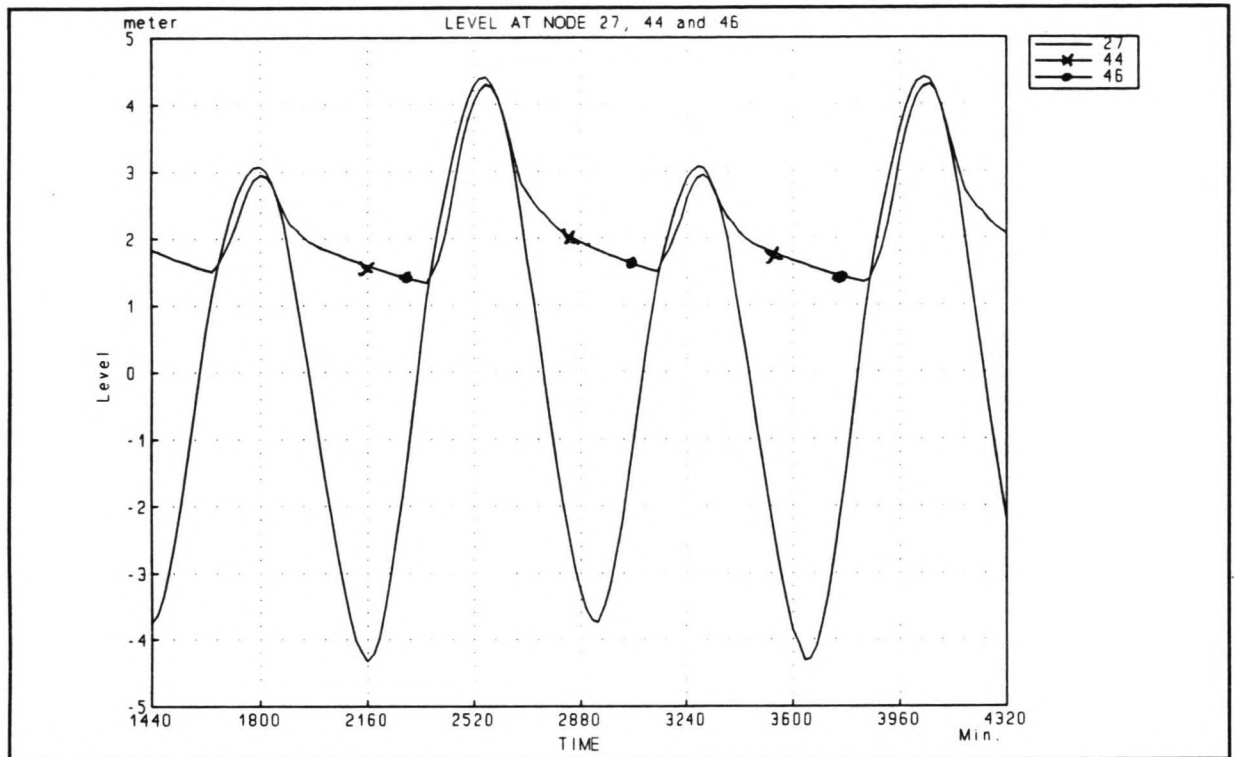


Figure C18: Water level during phase 8

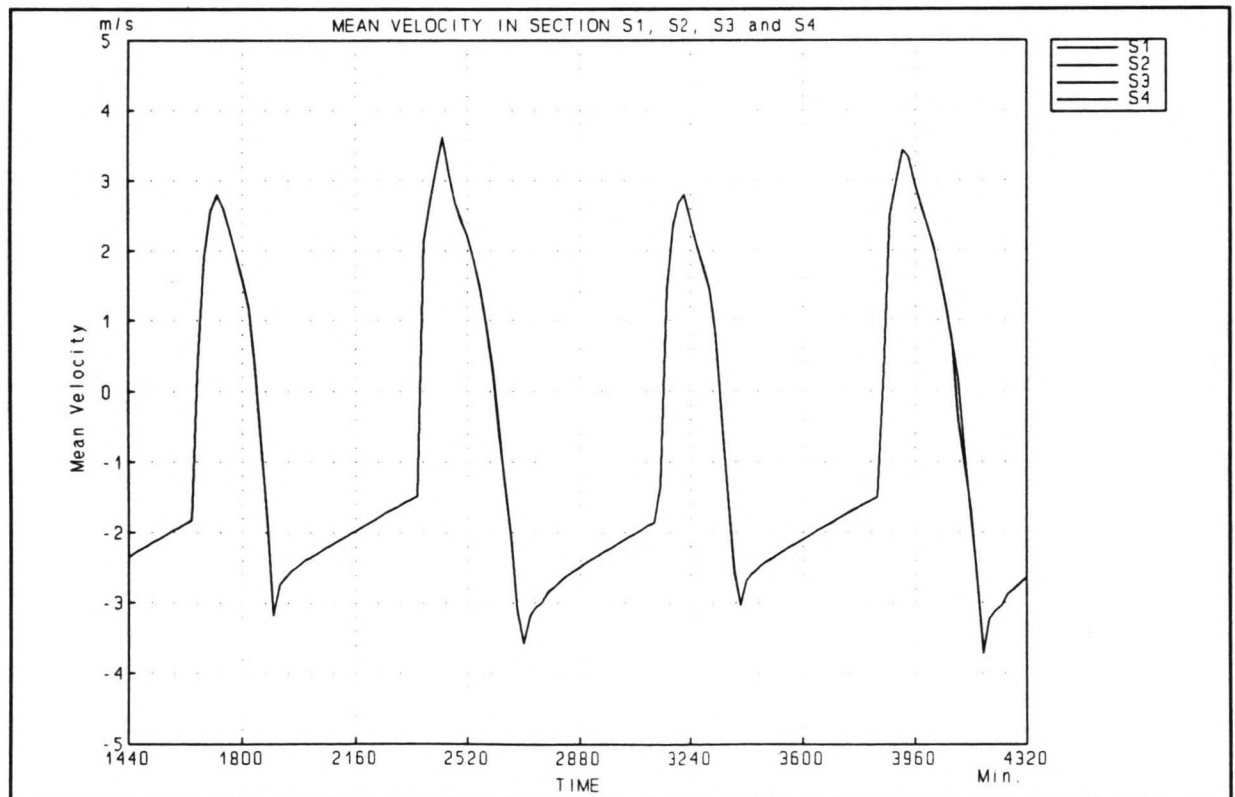


Figure C19: Flow velocities during phase 8

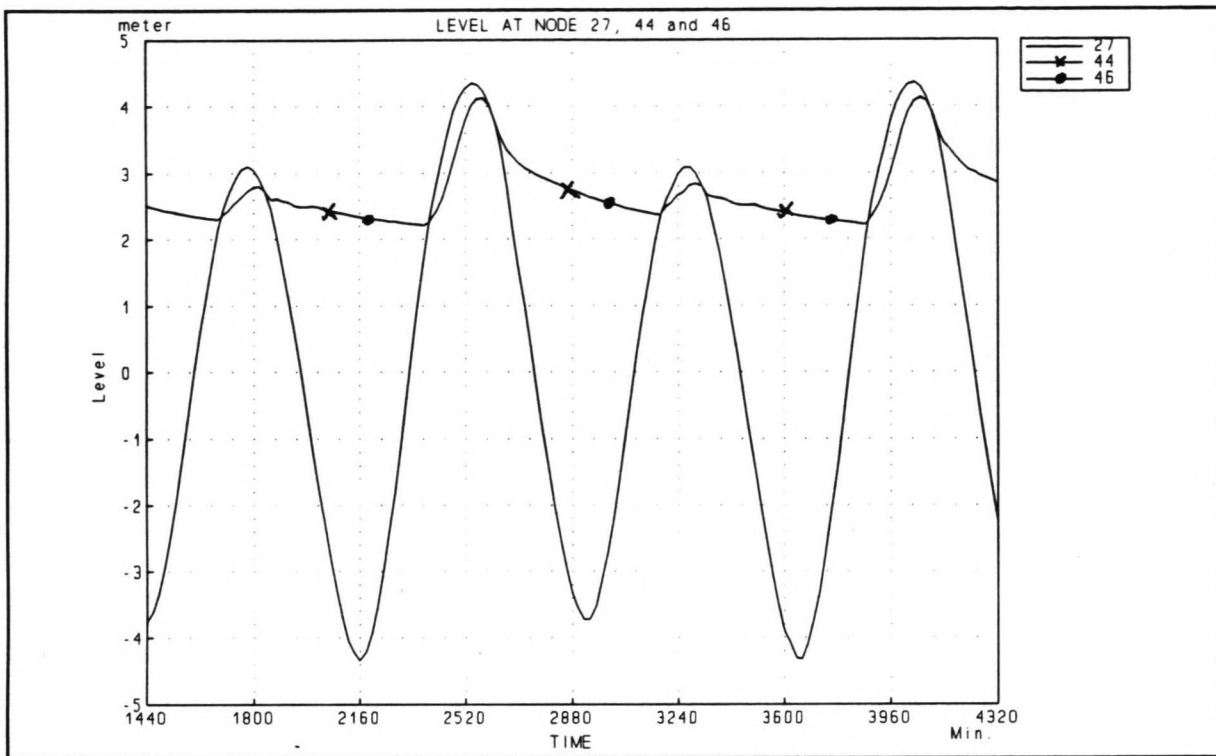


Figure C20: Water level during phase 9

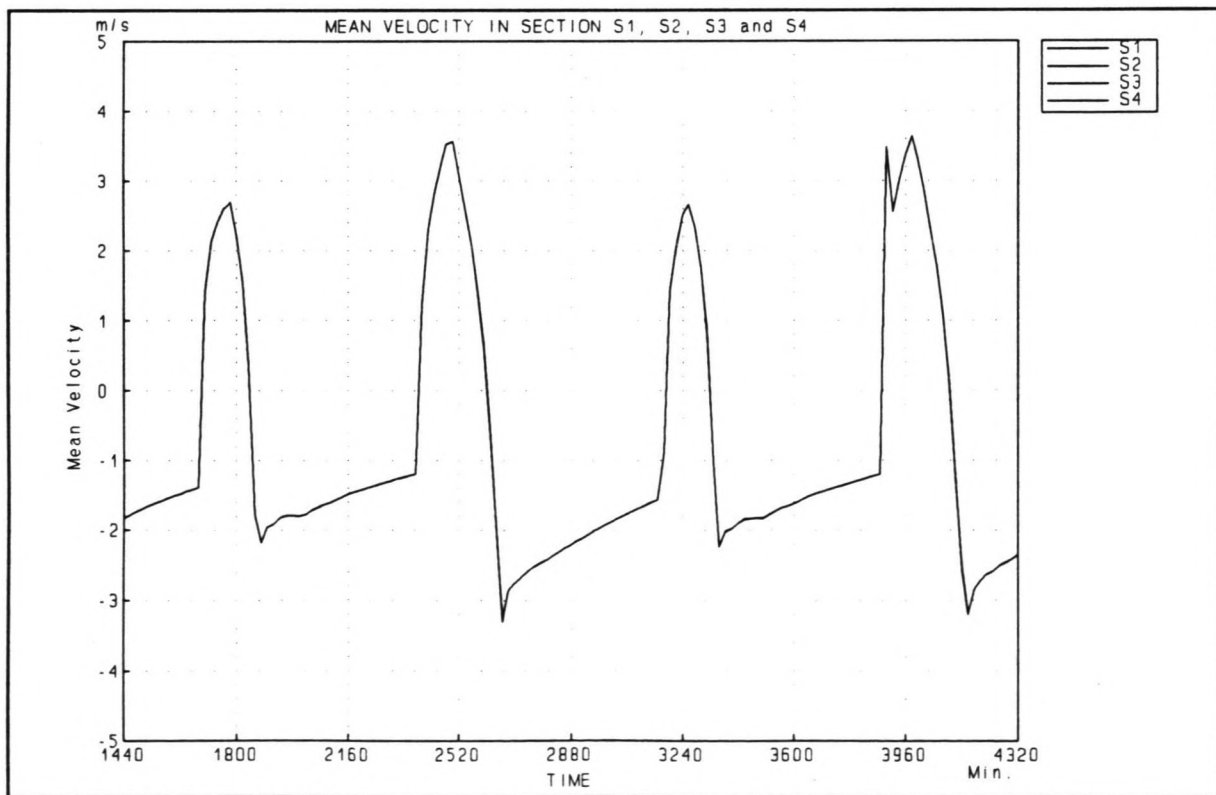


Figure C21: Flow velocities during phase 9

Closure of the Shiwa Tidal Basin

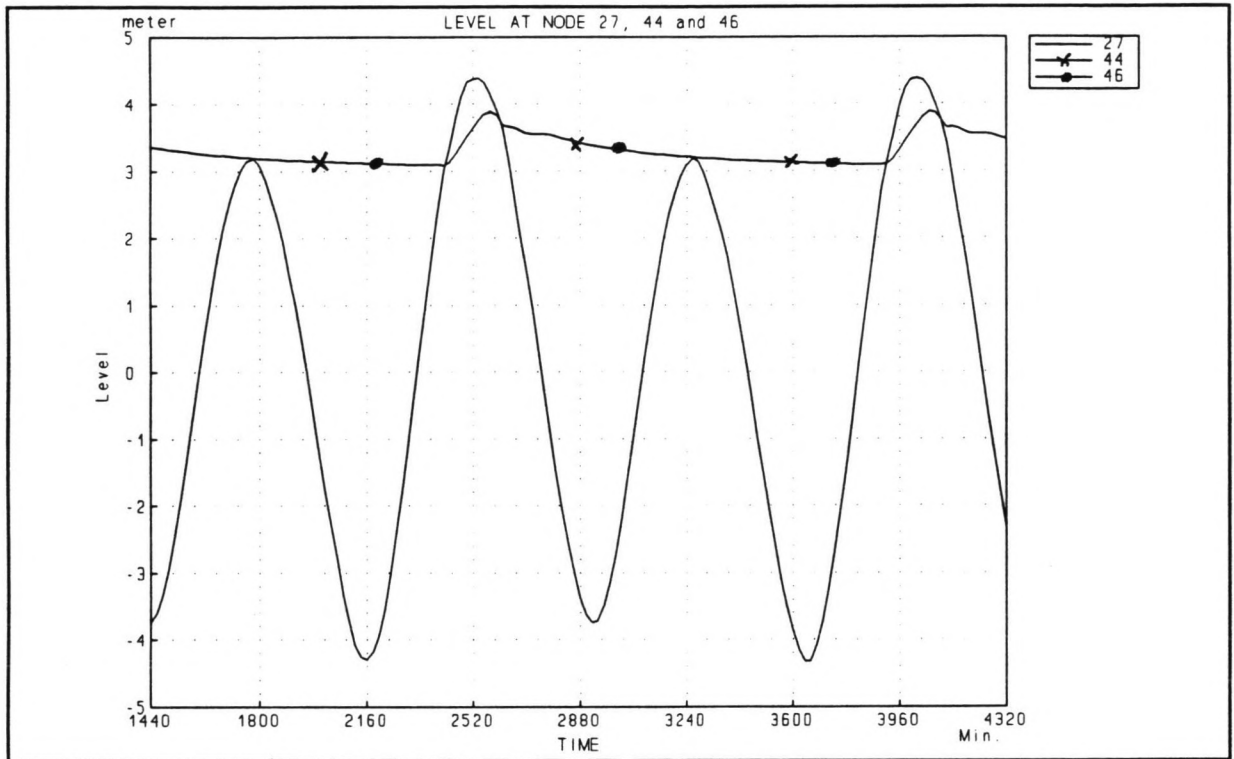


Figure C22: Water level during phase 10

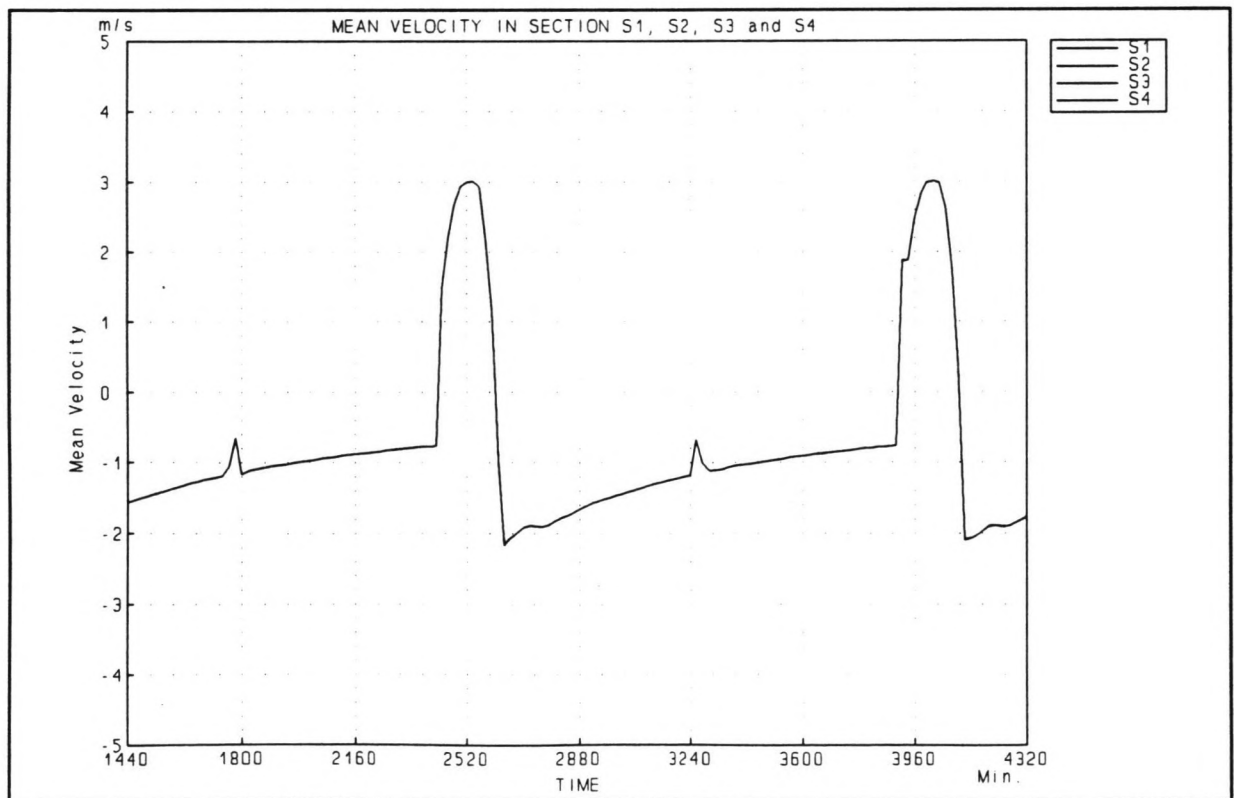


Figure C23: Flow velocities during phase 10

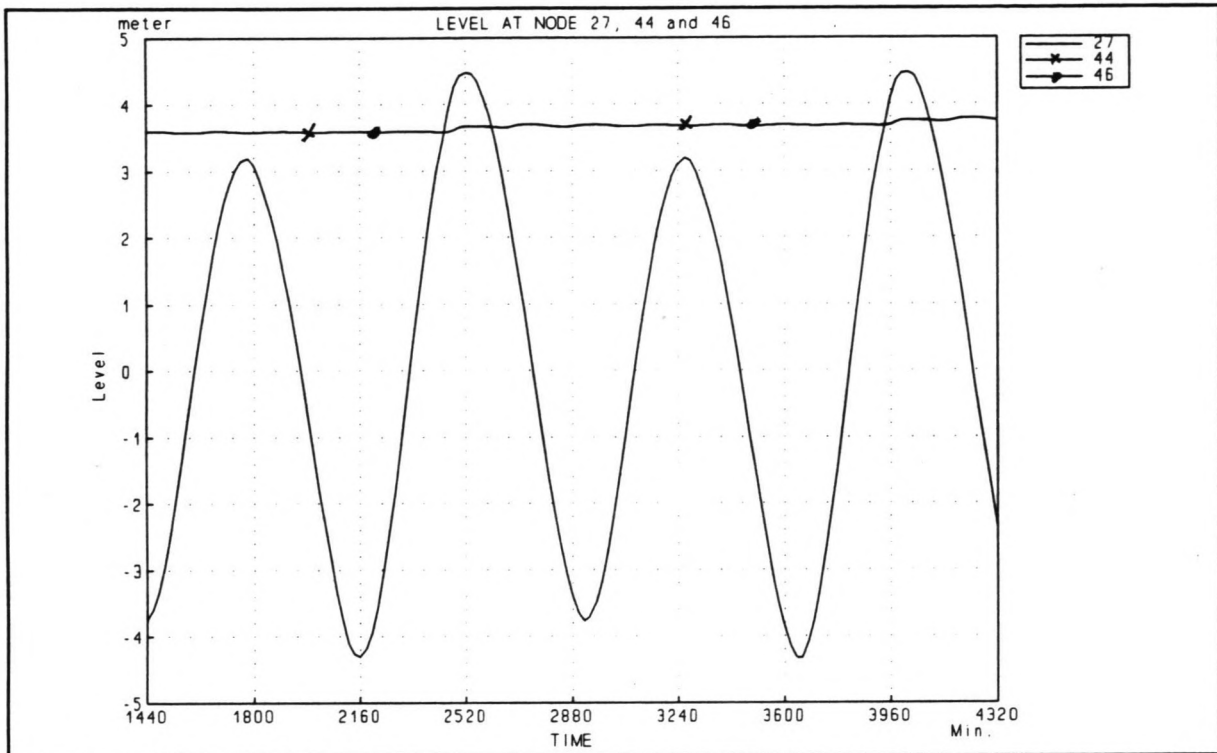


Figure C24: Water level during phase 11

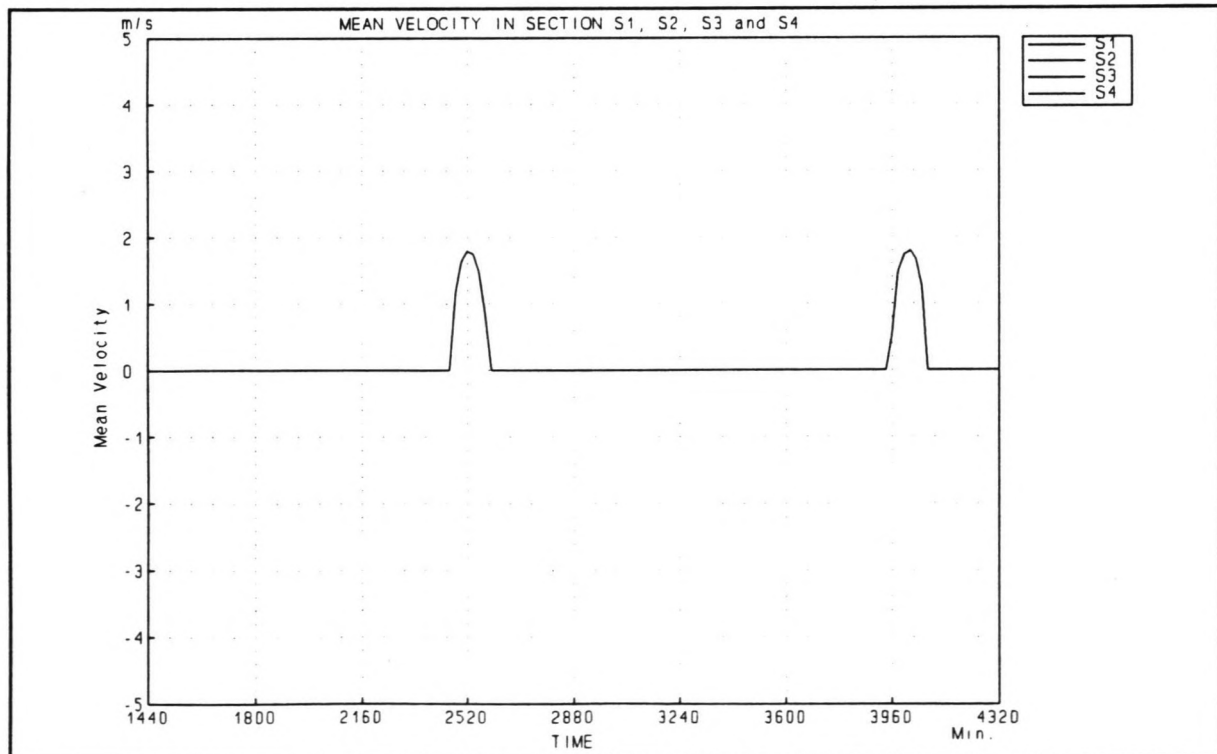


Figure C25: Flow velocities during phase 11

Closure of the Shiwa Tidal Basin

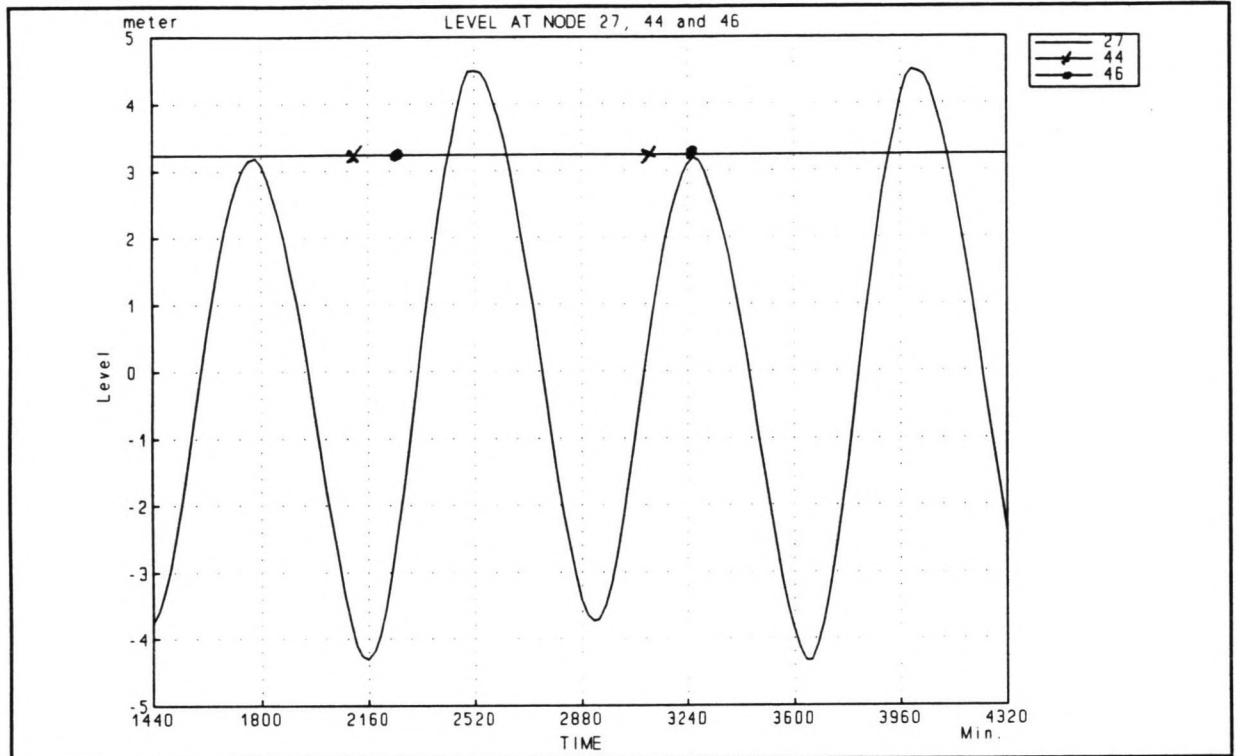


Figure C26: Water level during phase 12

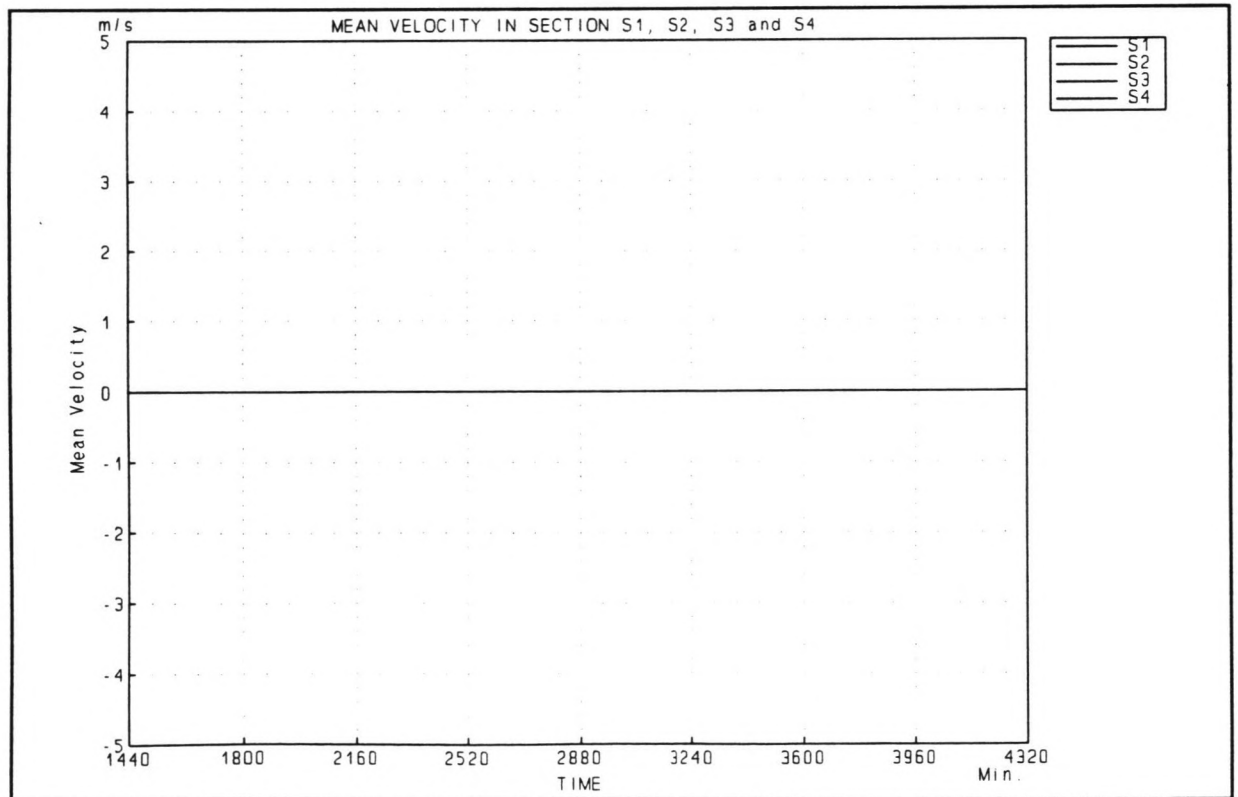


Figure C27: Flow velocities during phase 12

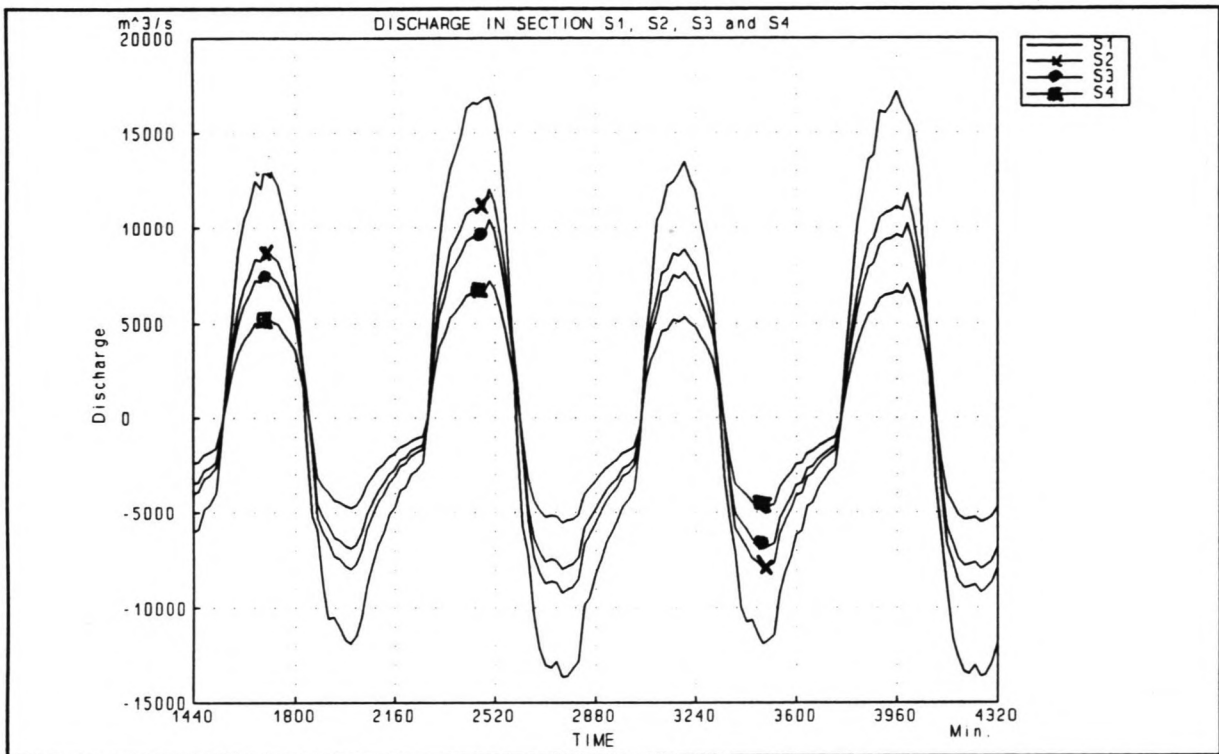


Figure C28: Discharges during phase 4

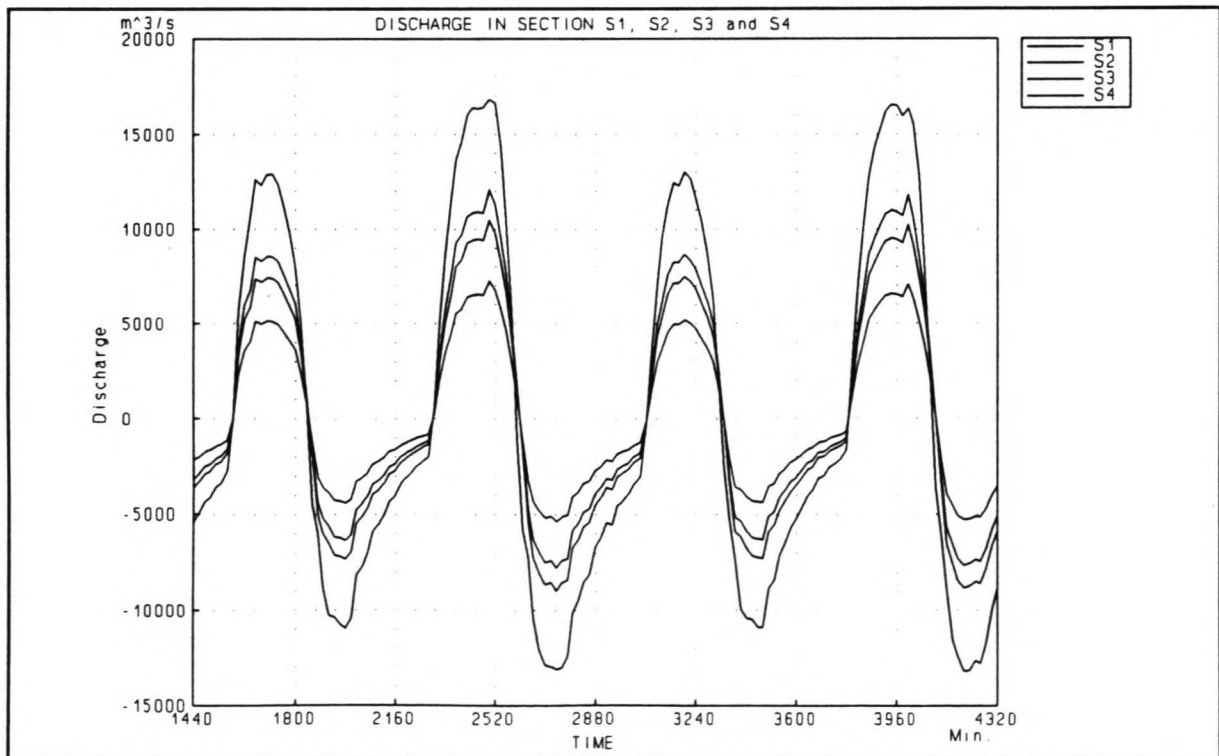


Figure C29: Discharges during phase 5.

Closure of the Shiwa Tidal Basin

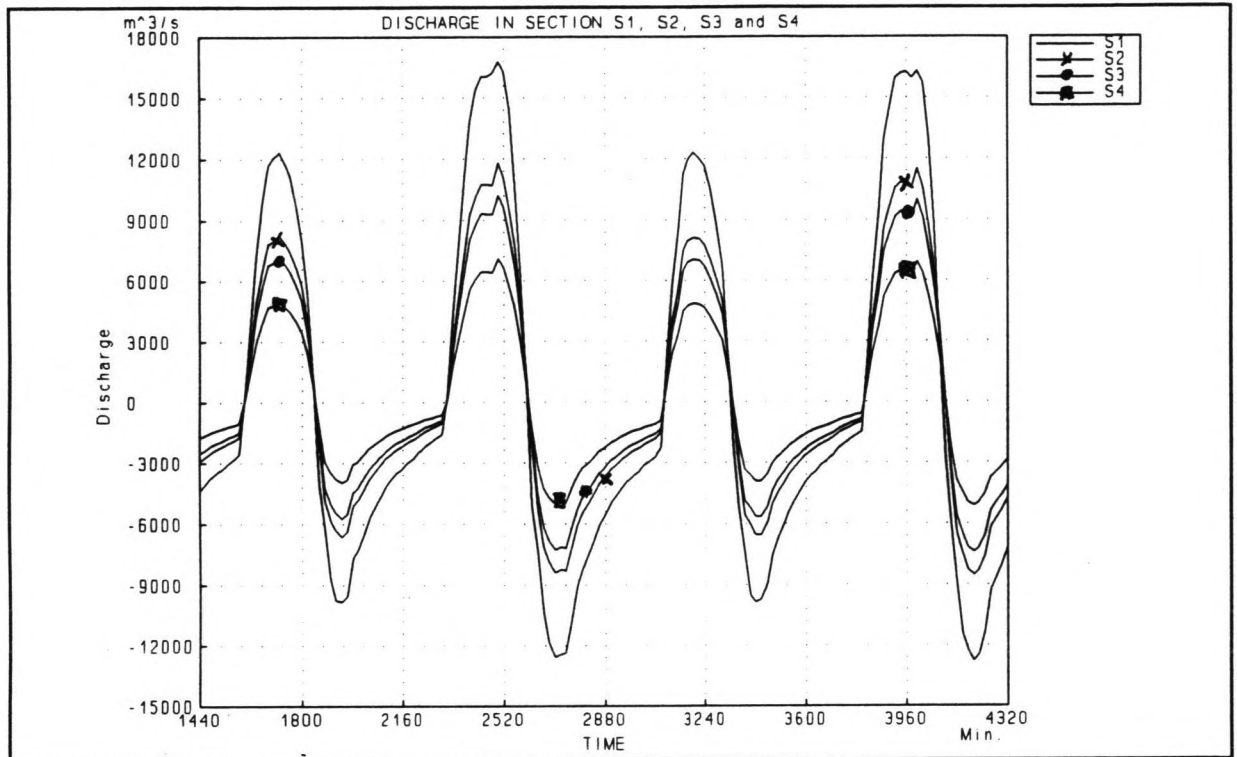


Figure C30: Discharges during phase 6

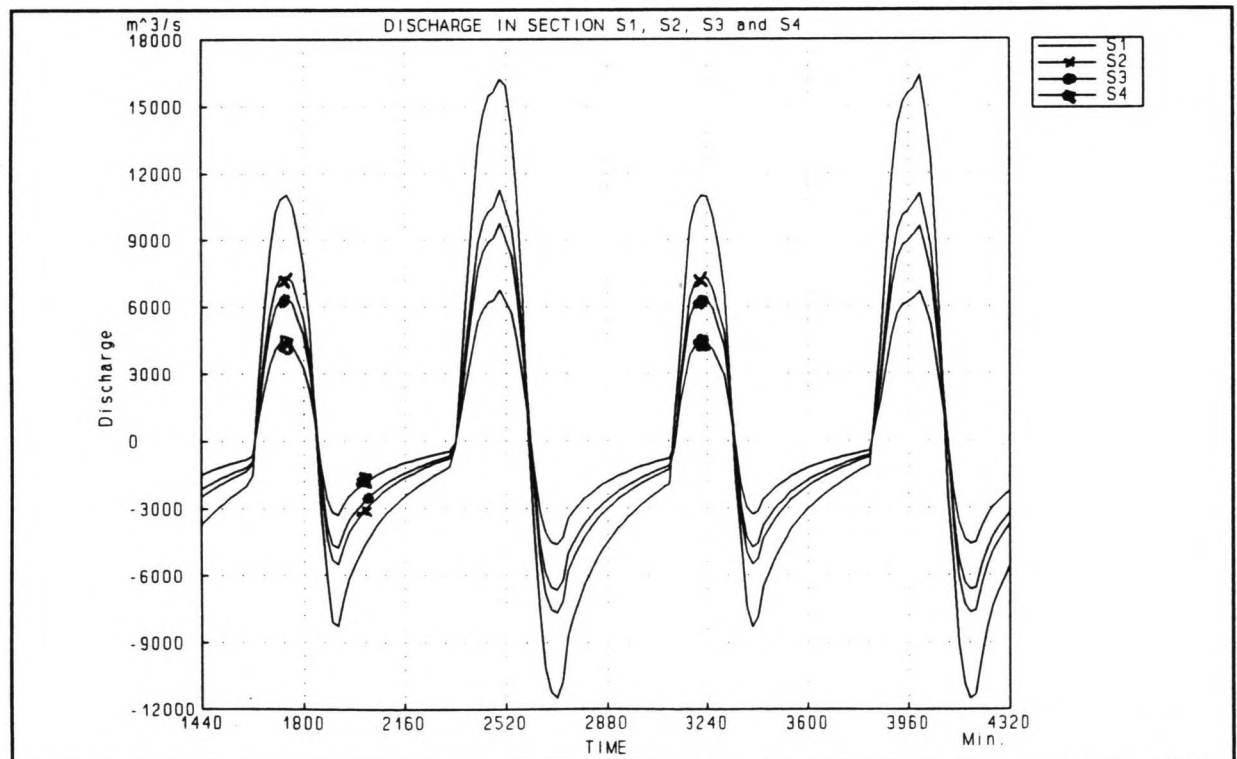


Figure C31: Discharges during phase 7

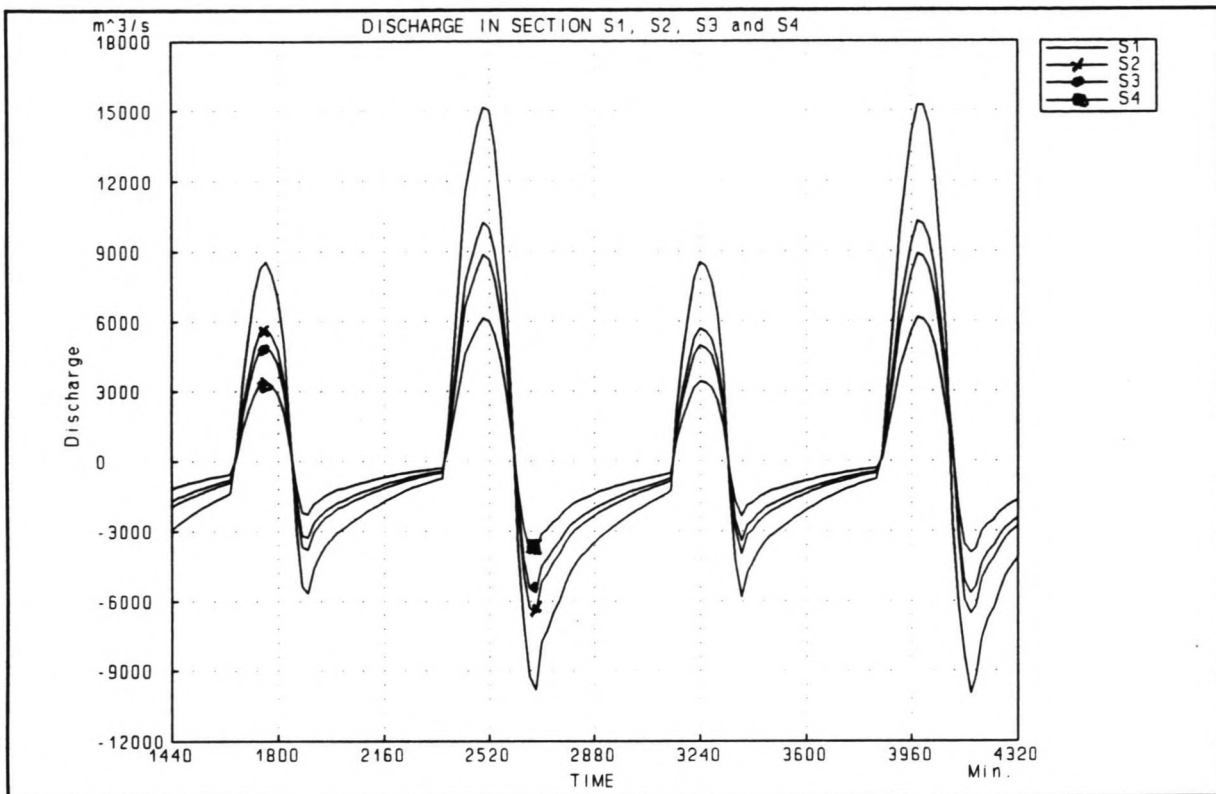


Figure C32: Discharges during phase 8

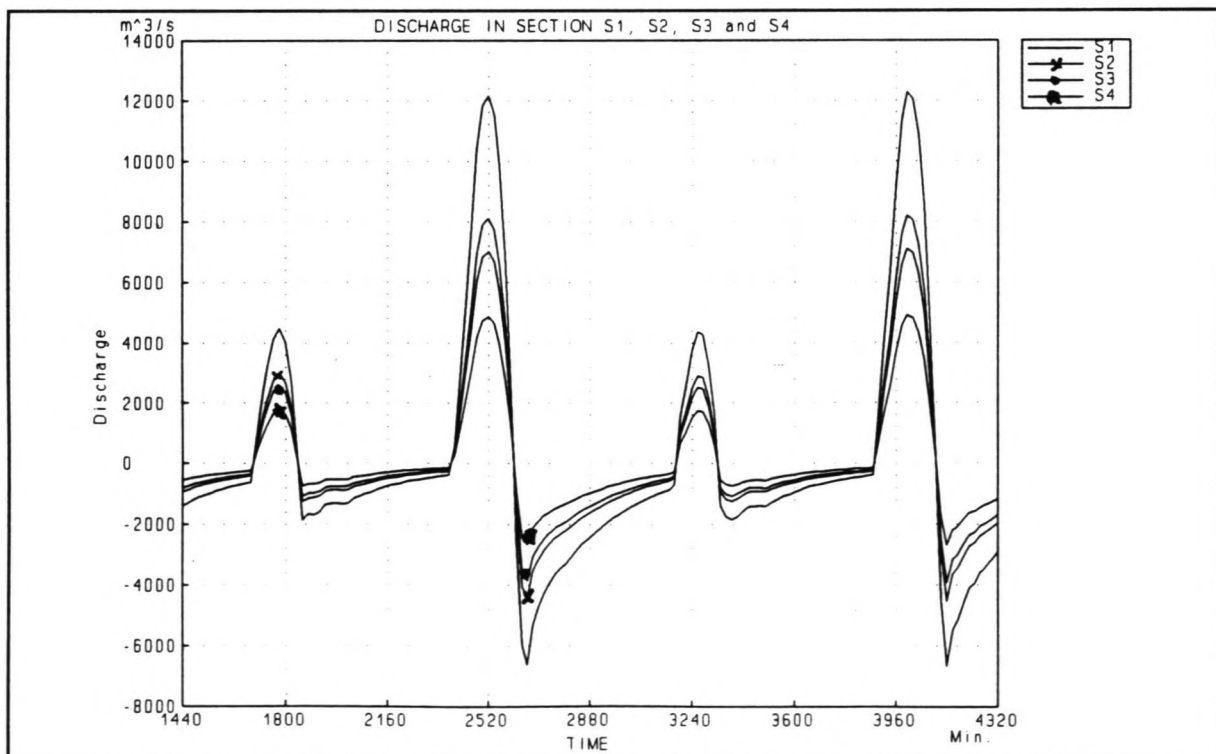


Figure C33: Discharges during phase 9

Closure of the Shiwa Tidal Basin

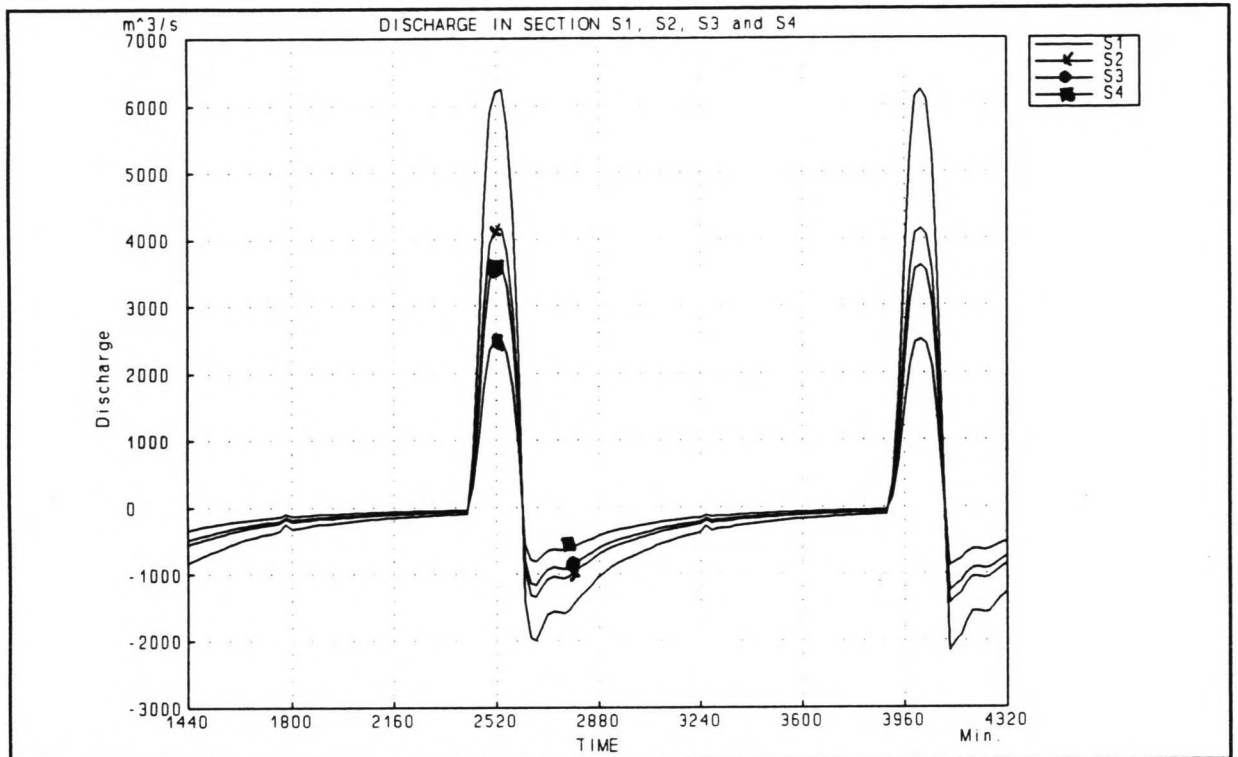


Figure C34: Discharges during phase 10

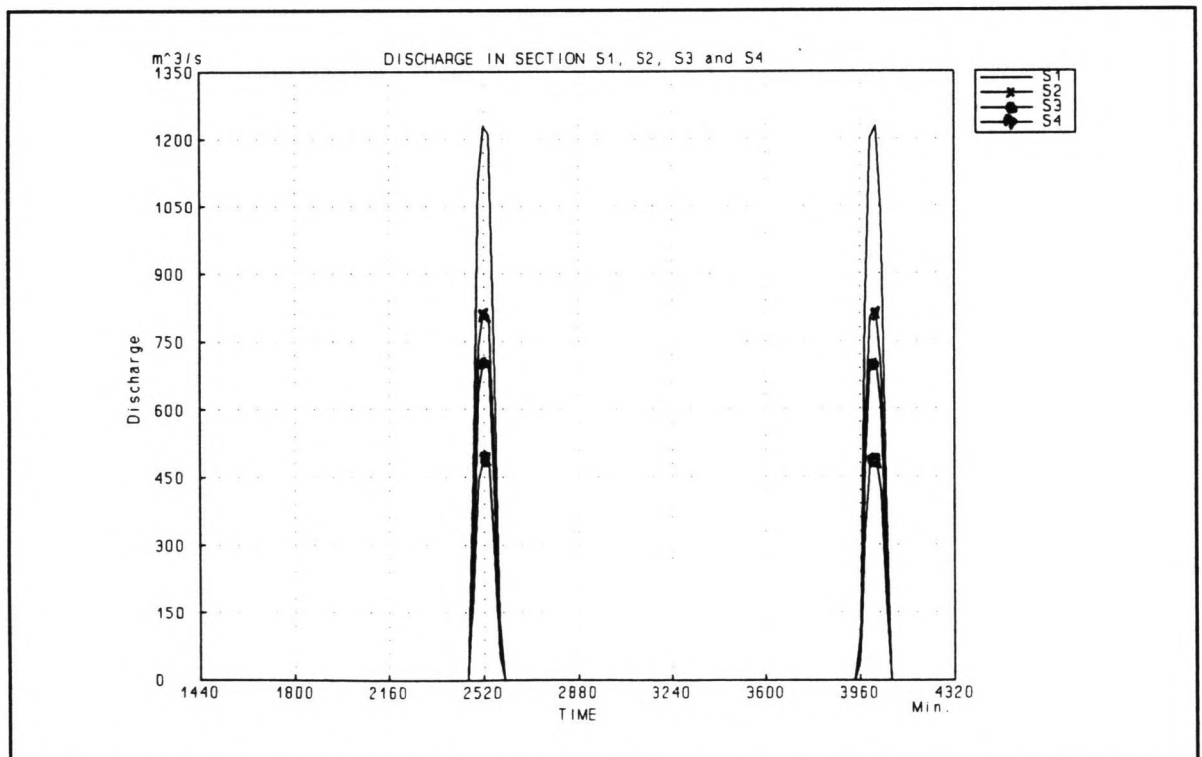


Figure C35: Discharges during phase 11

Annex C2:

D₅₀ during a horizontal closure

Applying a horizontal closure method, 12 phases can be distinguished, see Figure 35 :

Phase 1:	$B_1 = 1800$ m.
Phase 2:	$B_1 = 1350$ m.
Phase 3:	$B_1 = 900$ m.
Phase 4:	$B_1 = 450$ m.
Phase 5:	$B_1 = 0$ m.
Phase 6:	$B_2 = 1000$ m.
Phase 7:	$B_2 = 500$ m.
Phase 8:	$B_2 = 0$ m.
Phase 9:	$B_3 = 0$ m.
Phase10:	$B_4 = 700$ m.
Phase11:	$B_4 = 100$ m.
Phase12:	$B_4 = 0$ m.

With the Duflow model, the flow velocities as a function of time and the water level at the beginning and at the end of the weirs as a function of time are calculated. The results of these calculations are displayed figure to on the next pages.

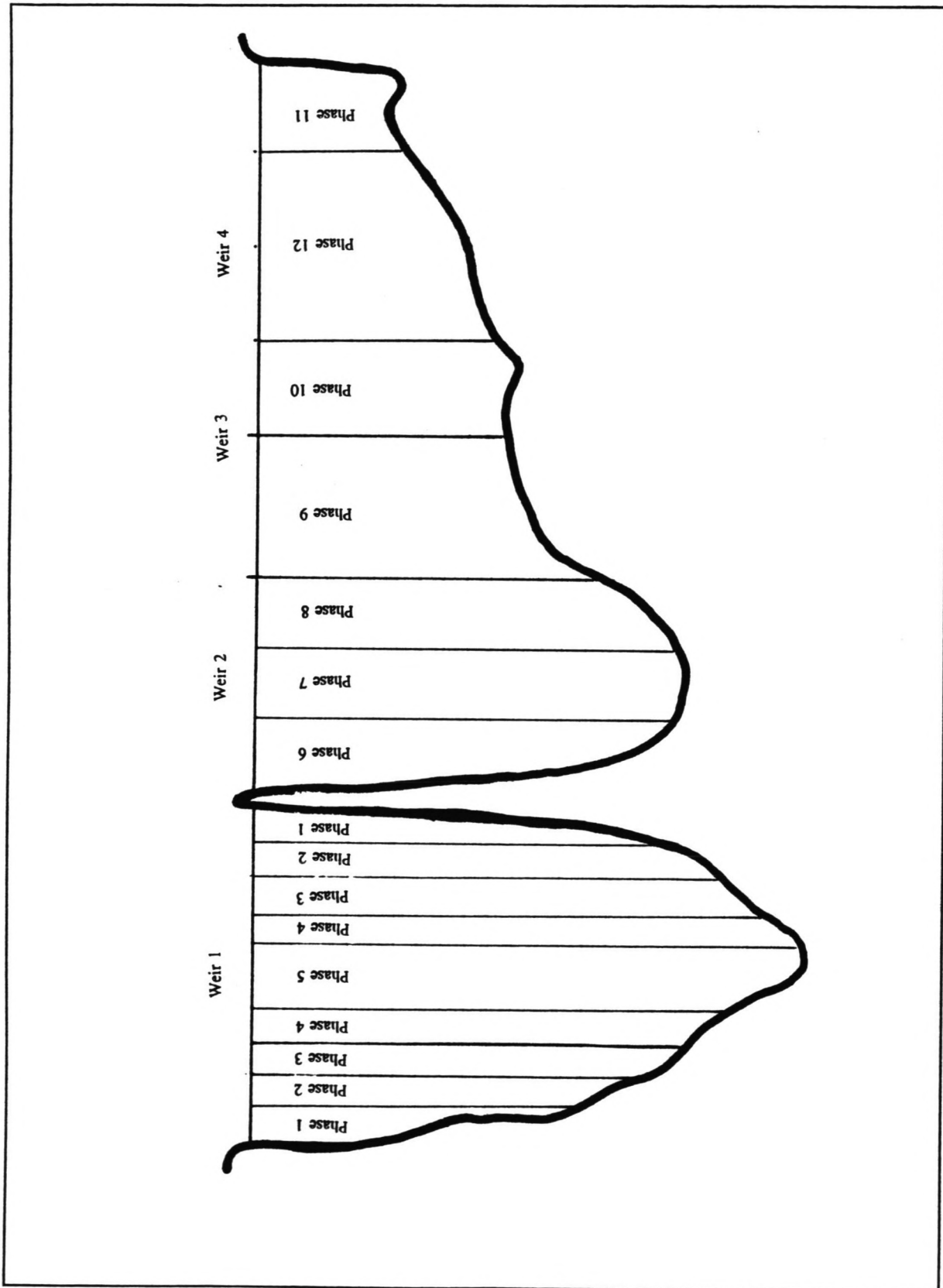


Figure C36: Phases of a horizontal closure

When applying a horizontal closure, the desisive D_{50} of every phase can be determined by using the following formula:

$$\frac{u_{cr}}{\sqrt{g\Delta D_s}} = 6\sqrt{\psi_{cr}} \left(\frac{h}{D_s}\right)^{\frac{1}{6}} \quad (1)$$

where ψ_{cr} is taken as 0.06 so limited stone transport is accepted.

Table 1 shows the resulting D_{50} for every closure phase and in every structure.

Table I

Phase	S1			S2		
	u (m/s)	h (m)	D_{50} (m)	u (m/s)	h (m)	D_{50} (m)
1	-0.8	12.5	0.0016	-0.8	9.5	0.0016
2	-0.86	12.5	0.002	-0.86	9.5	0.002
3	-1.0	12.5	0.0031	-1.0	9.5	0.0031
4	-1.3	12.5	0.007	-1.3	9.5	0.007
5				-1.5	9.0	0.012
6				-2	8.75	0.029
7				-2.9	9.0	0.088

Phase	S3			S4		
	u (m/s)	h (m)	D_{50} (m)	u (m/s)	h (m)	D_{50} (m)
1	-0.8	4.5	0.0016	-0.8	3.0	0.0016
2	-0.86	4.5	0.002	-0.86	3.0	0.002
3	-1.0	4.5	0.0031	-1.0	3.0	0.0031
4	-1.3	4.5	0.007	-1.3	3.0	0.007
5	-1.5	4.0	0.012	-1.5	3.0	0.012
6	-2.0	3.75	0.029	-2.0	2.75	0.029
7	-2.9	4.0	0.088	-2.9	3.0	0.088
8	-4.0	4.5	0.68	-4.0	2.0	0.68
9	-5.7	4.5	1.1	-5.7	2.0	1.1
10				-6.1	2.0	1.64
11				-6.5	2.0	2.47
12				-7.0	2.0	2.47

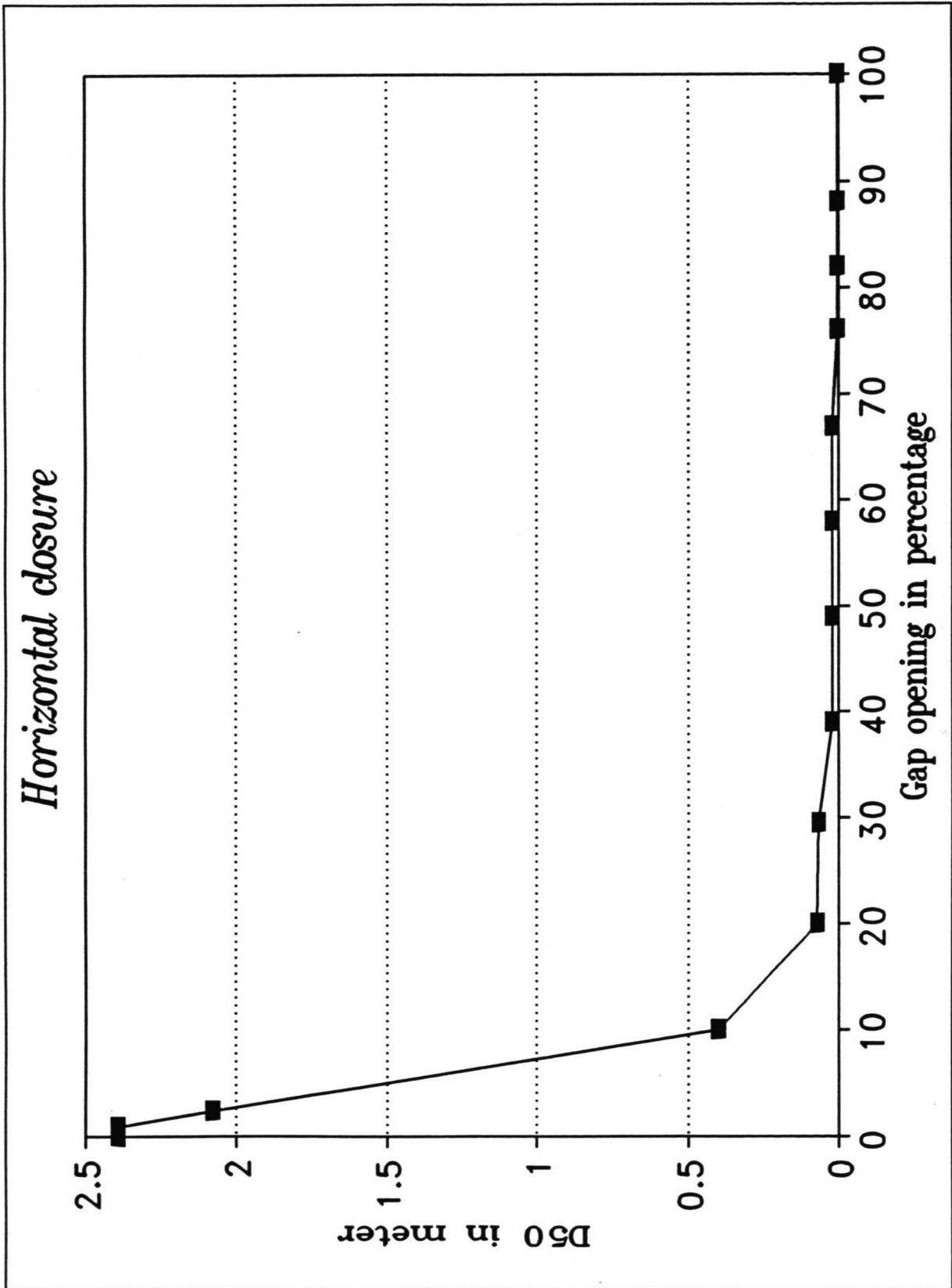


Figure C37: Resulting D_{50} for a horizontal closure method

Closure of the Shiwa Tidal Basin

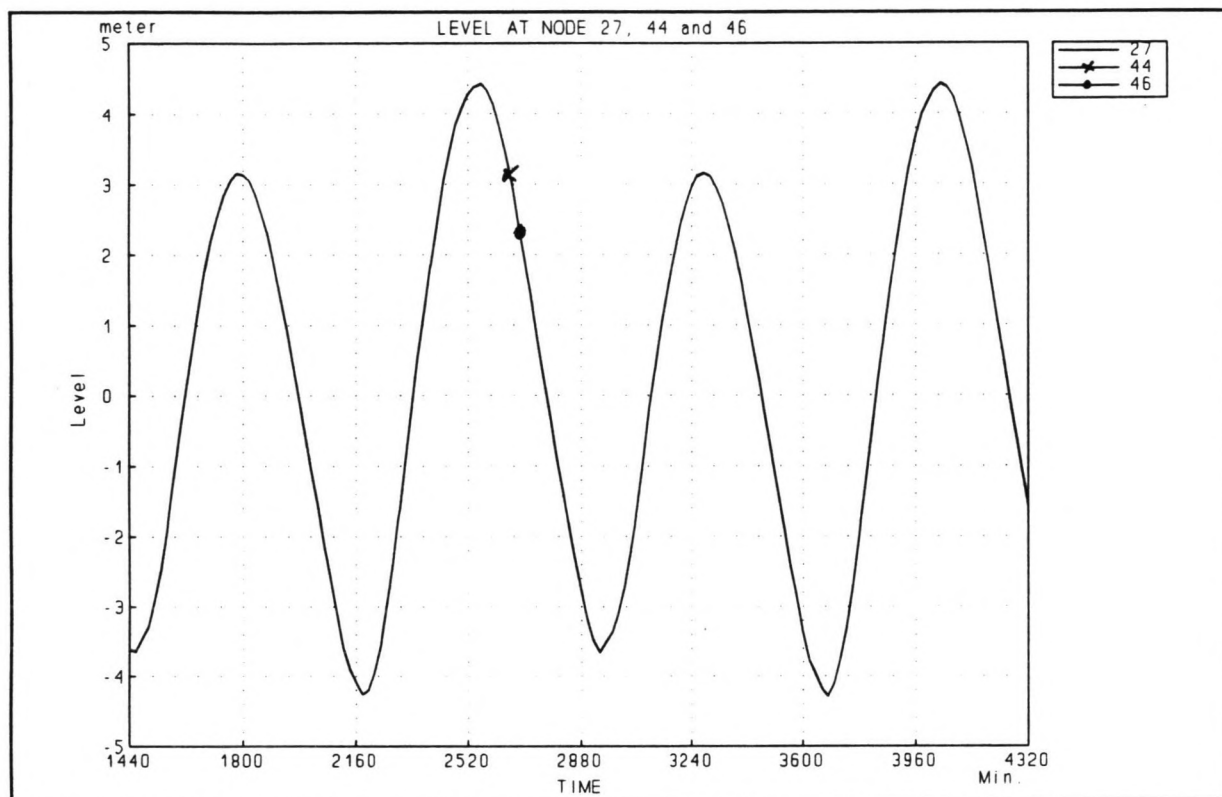


Figure C38: Water level during phase 1

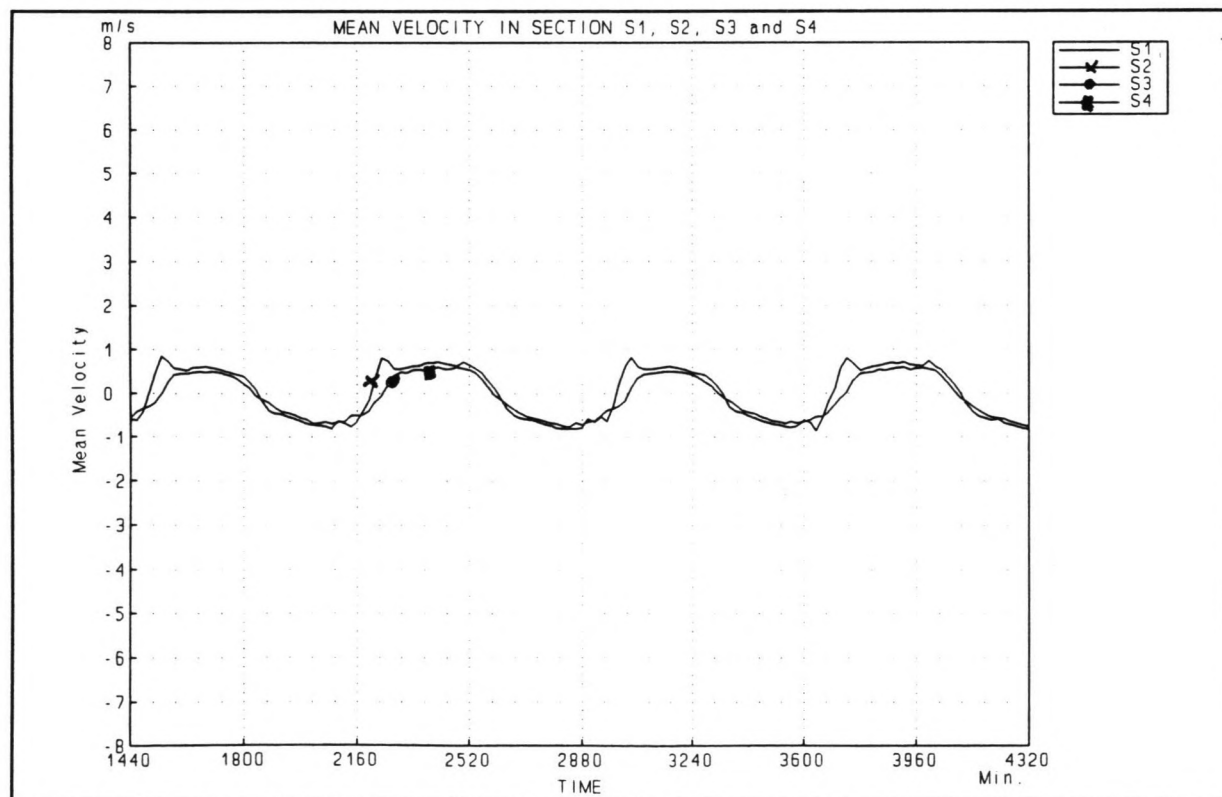


Figure C39: Flow velocities during phase 1

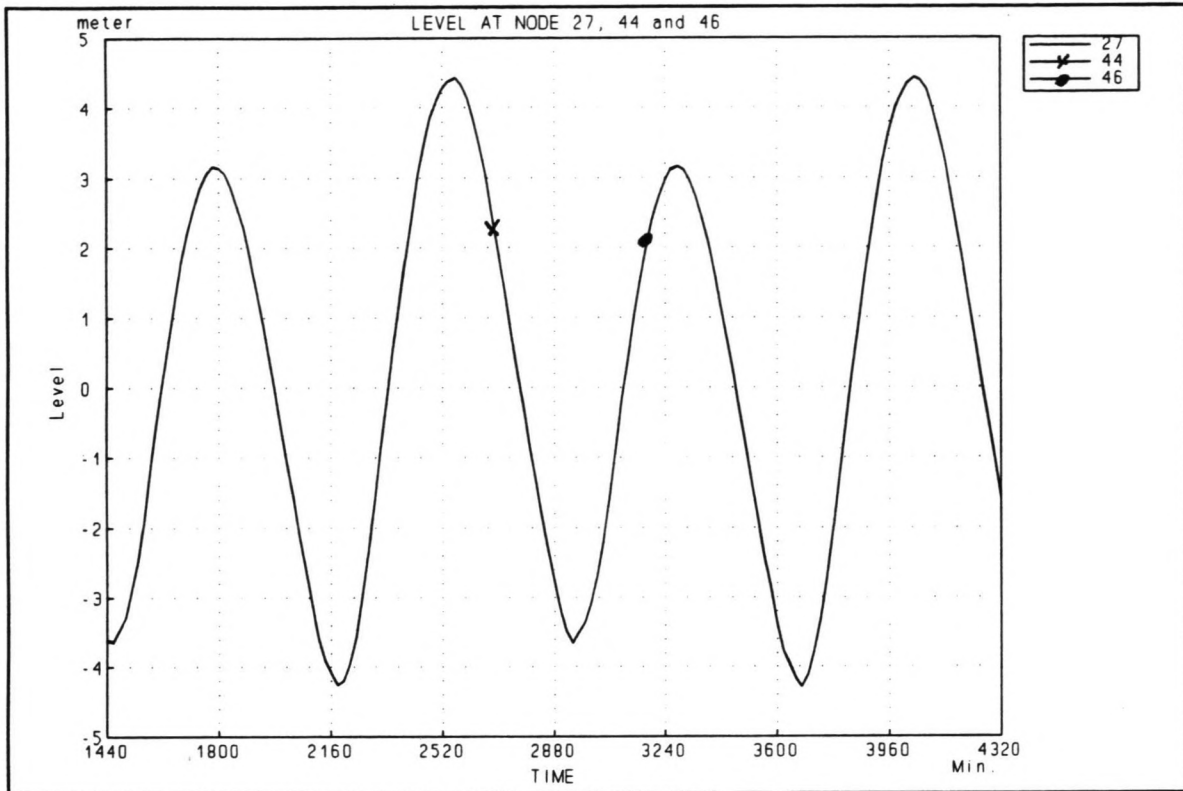


Figure C40: Water level during phase 2

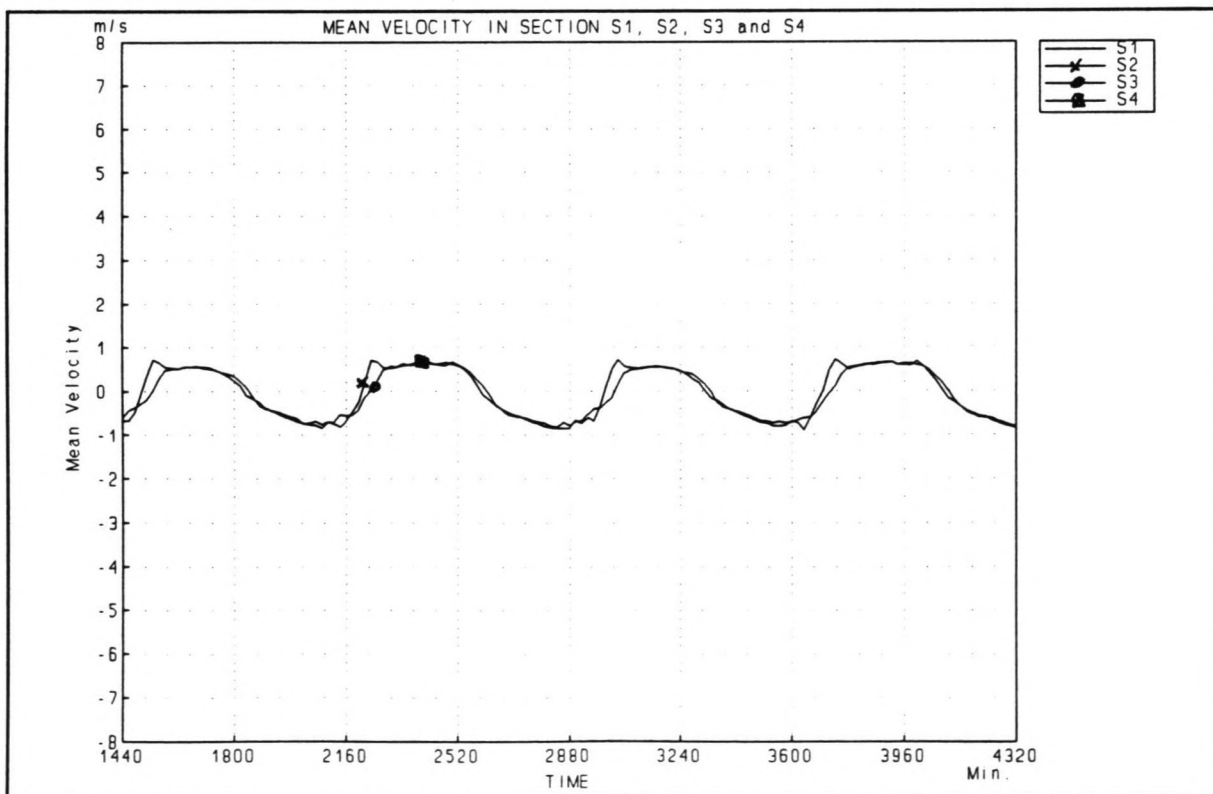


Figure C41: Flow velocities during phase 2

Closure of the Shiwa Tidal Basin

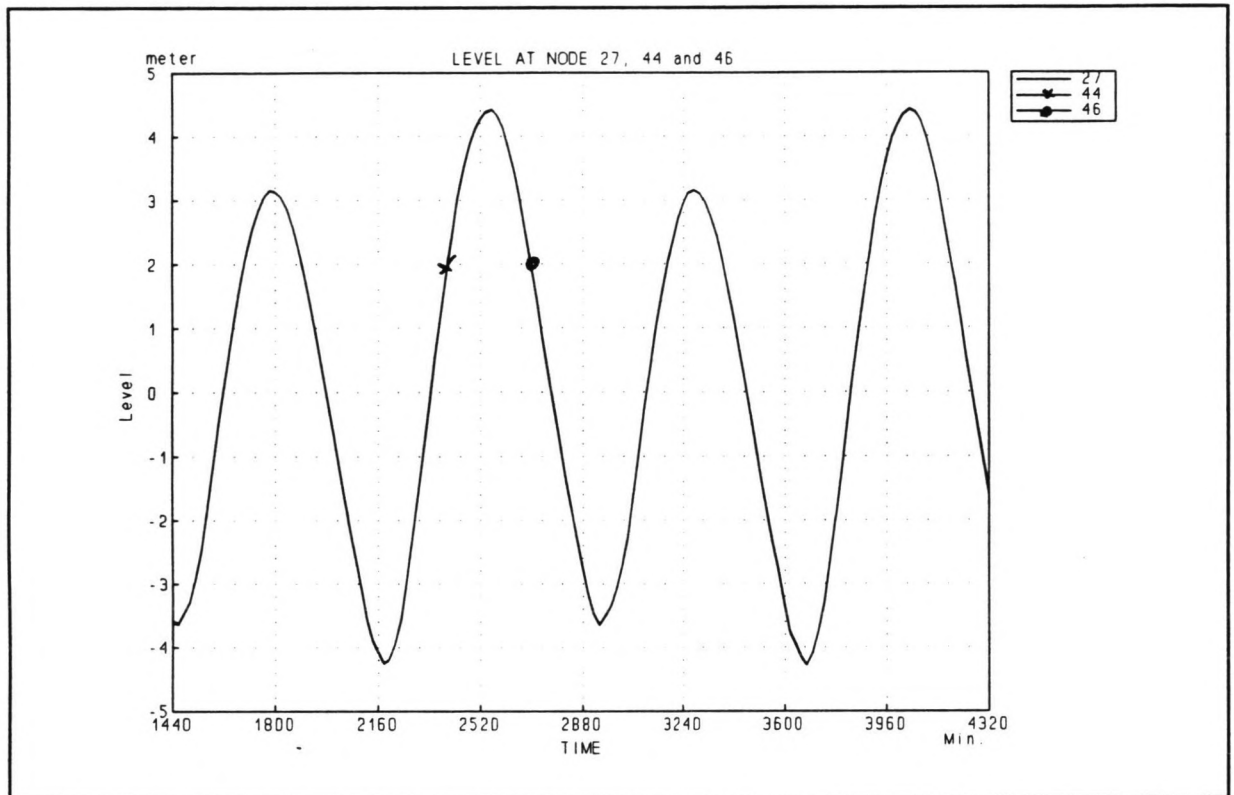


Figure C42: Water level during phase 3

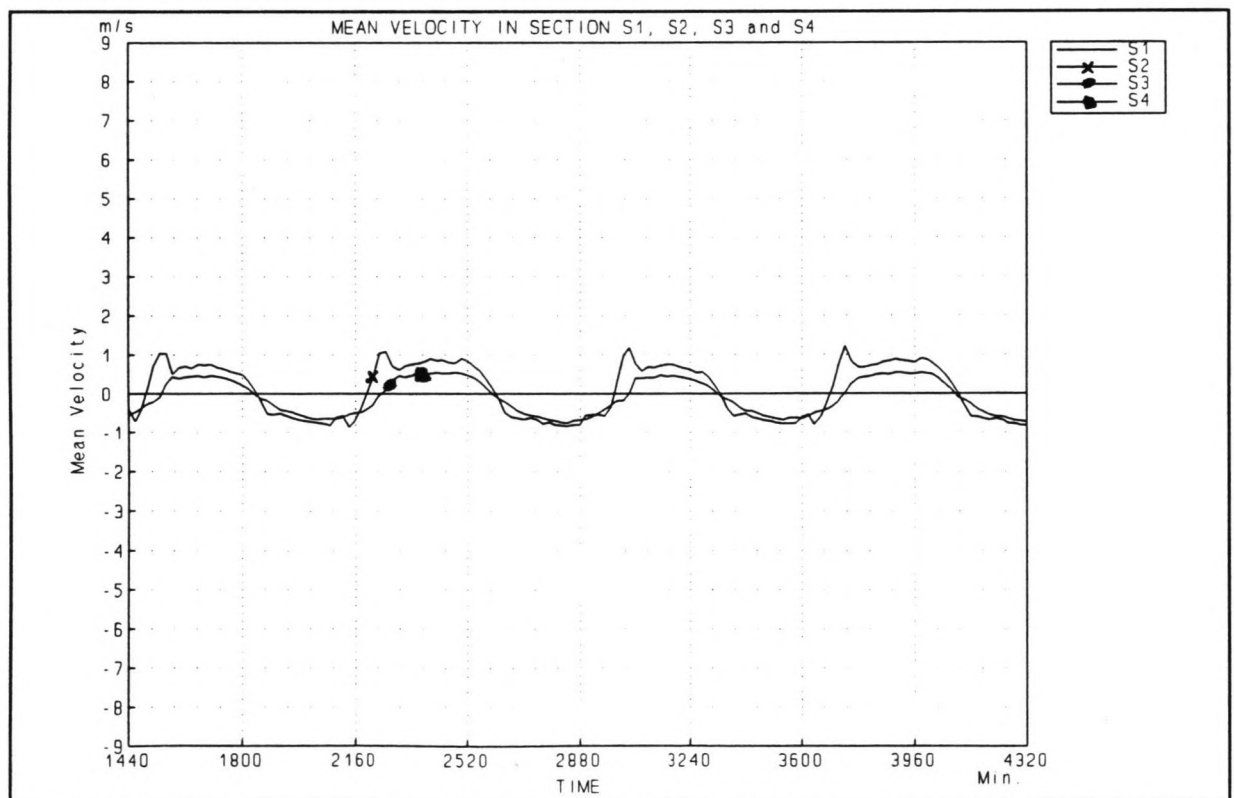


Figure C43: Flow velocities during phase 3

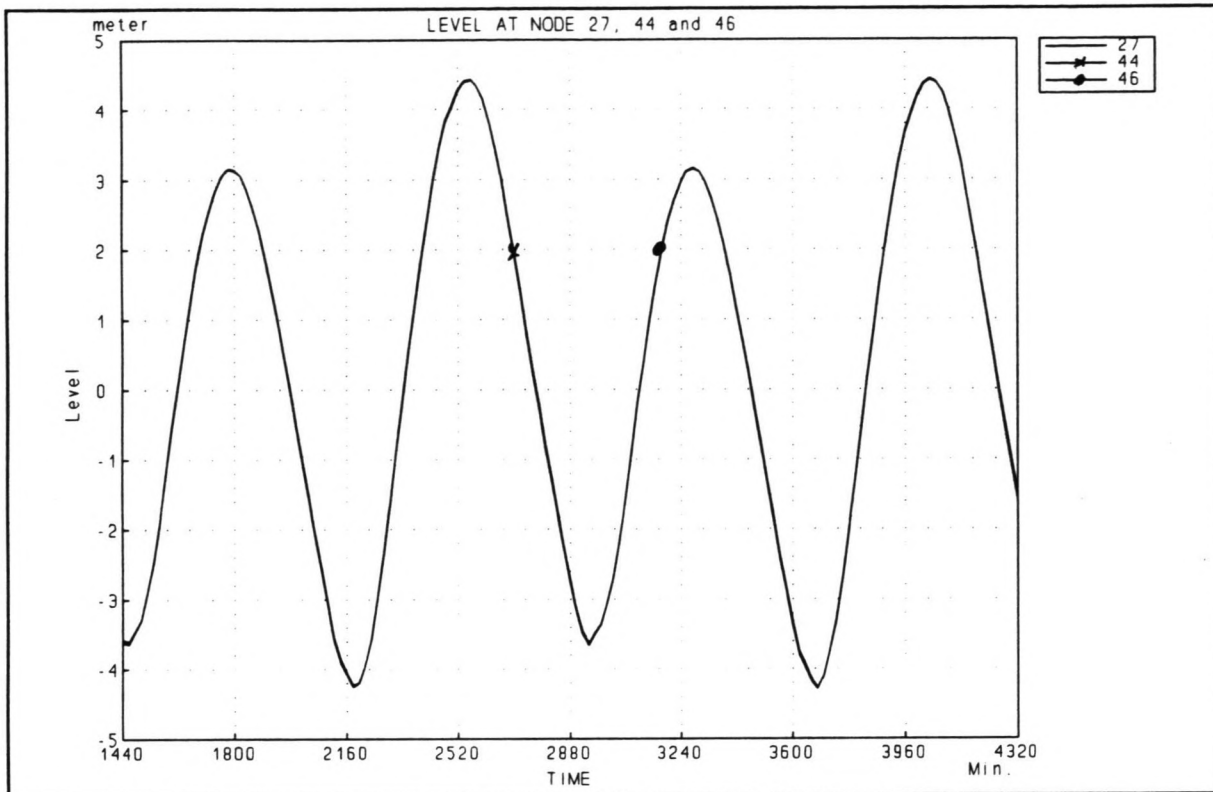


Figure C44: Water level during phase 4

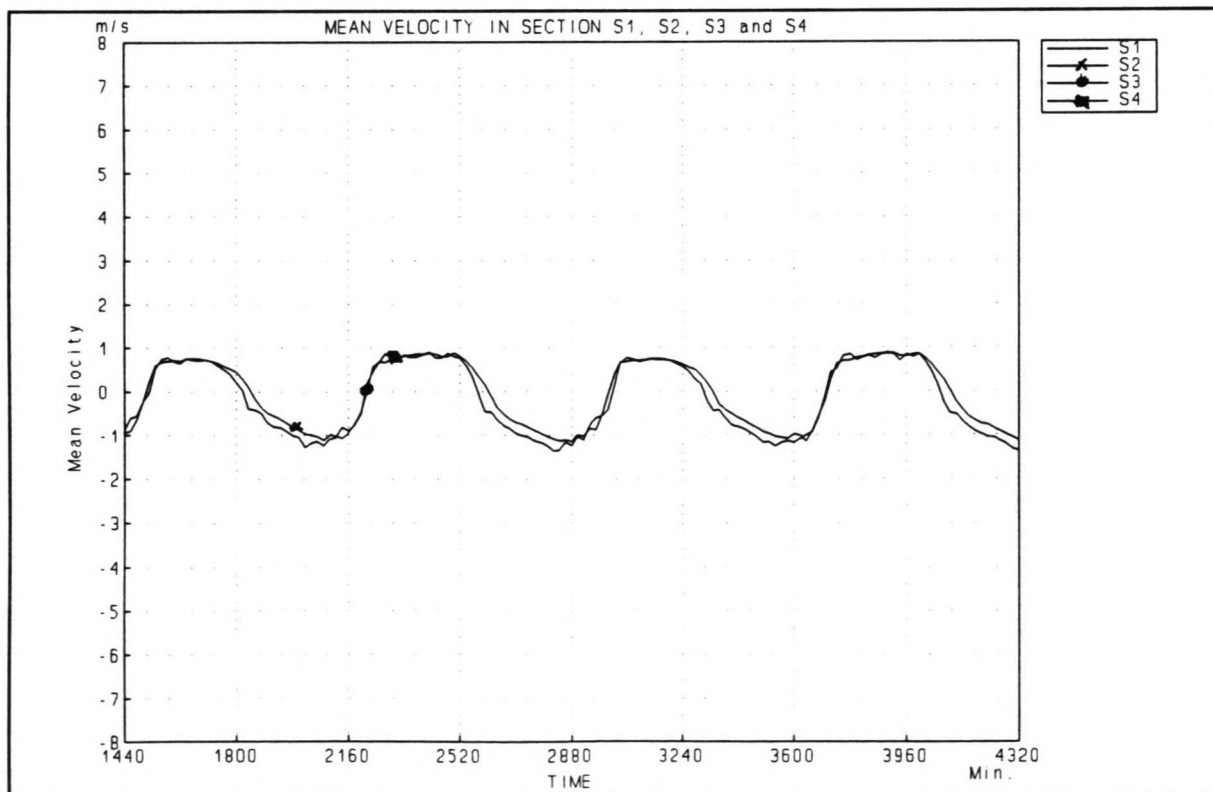


Figure C45: Flow velocities during phase 4

Closure of the Shiwa Tidal Basin

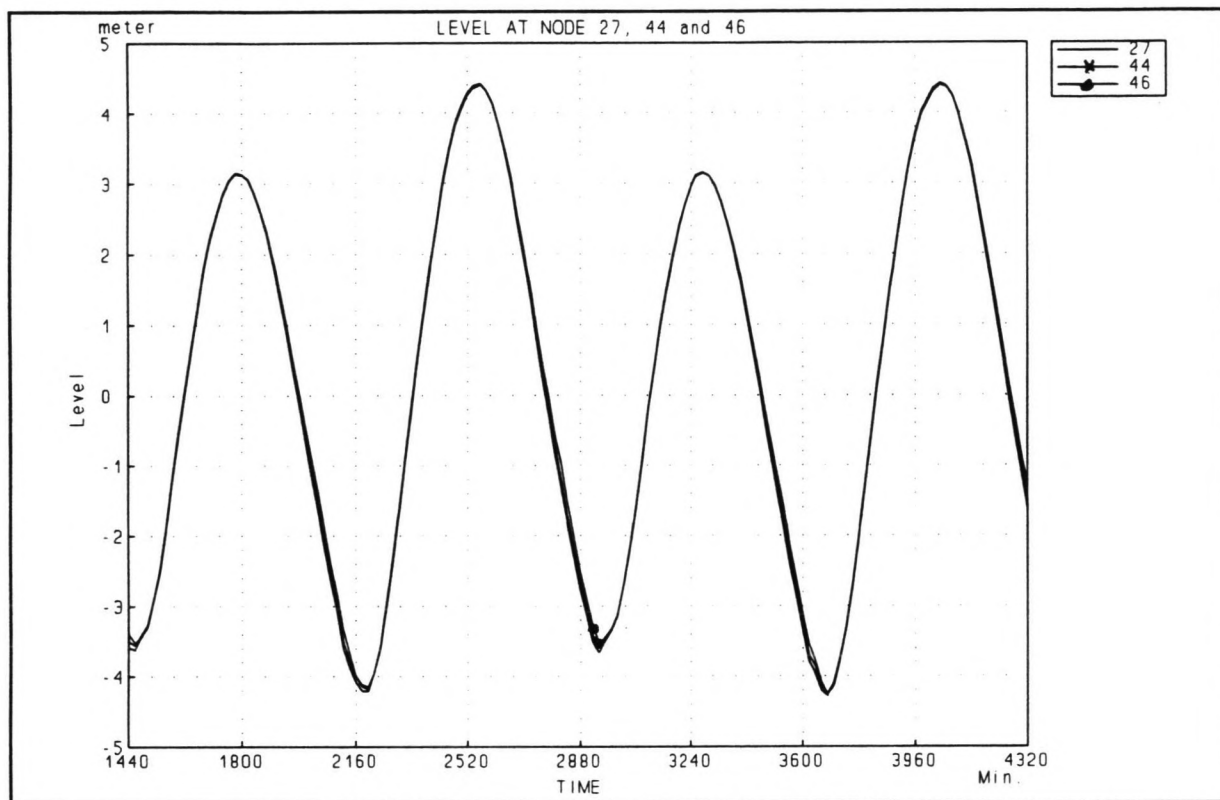


Figure C46: Water level during phase 5

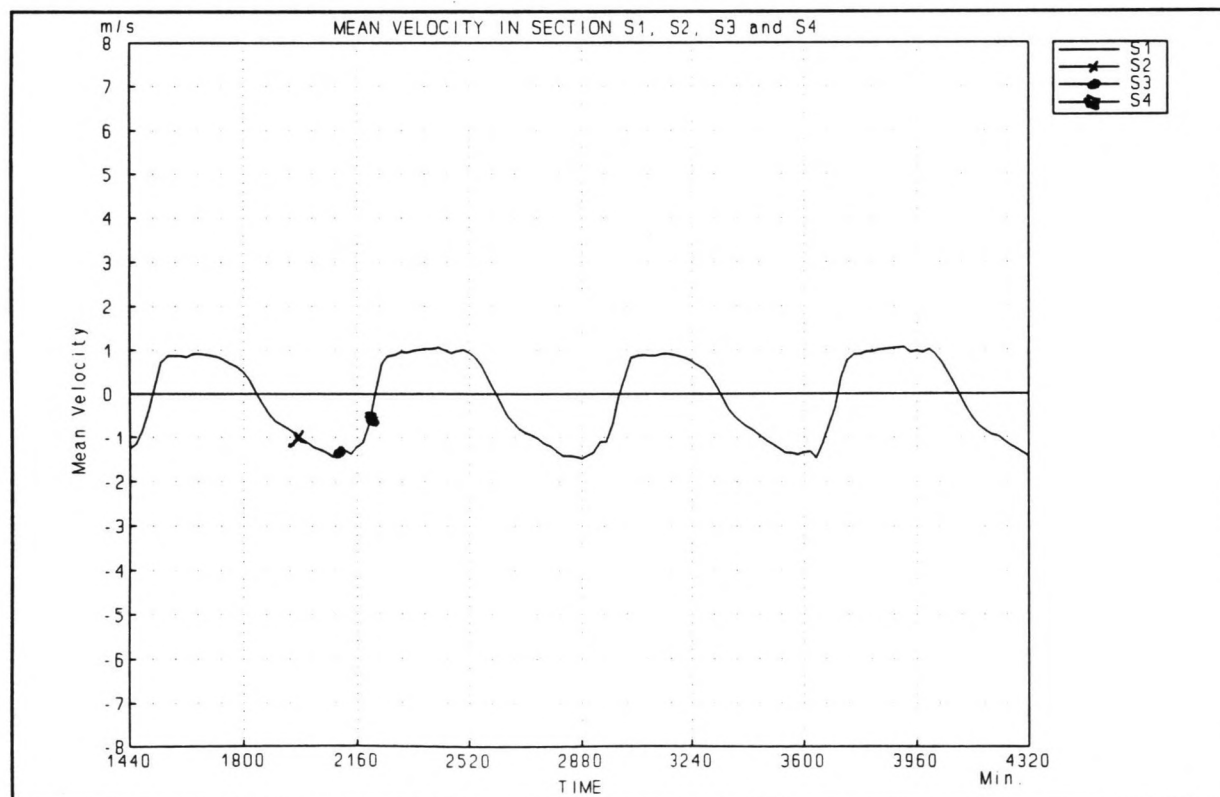


Figure C47: Flow velocities during phase 5

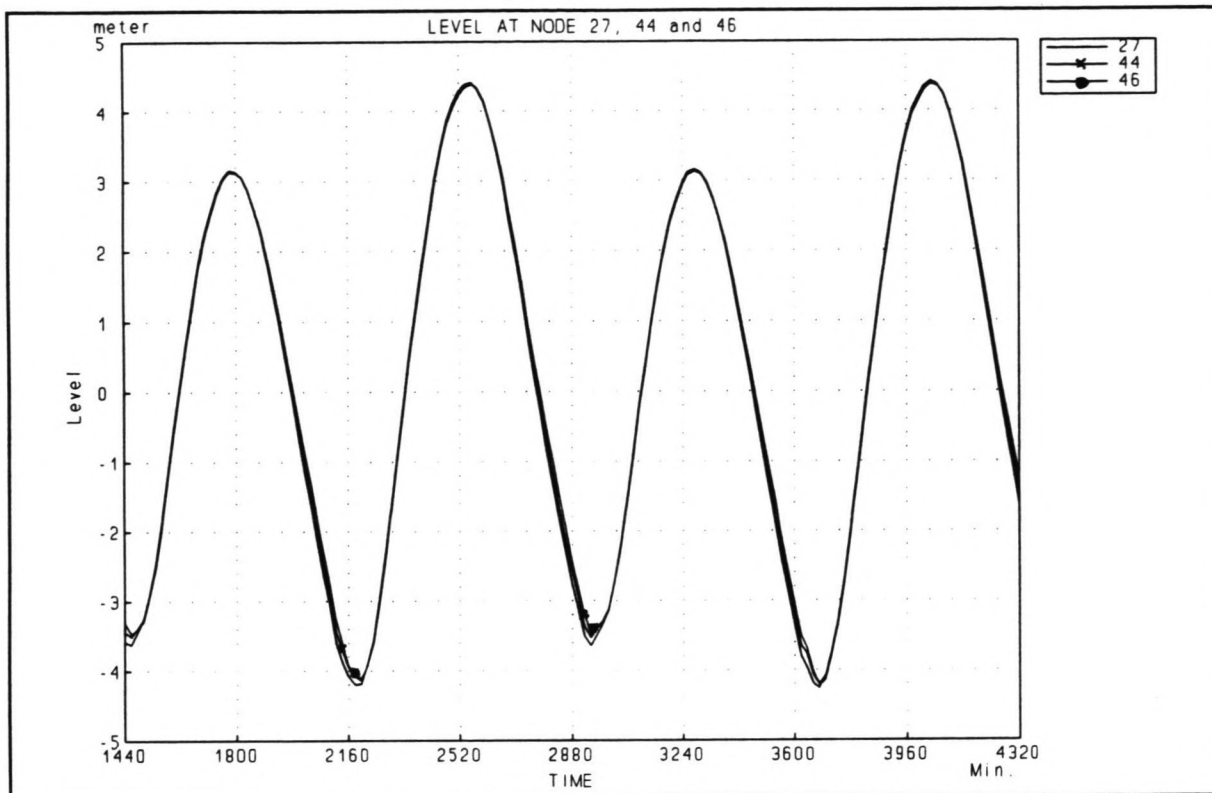


Figure C48: Water level during phase 6

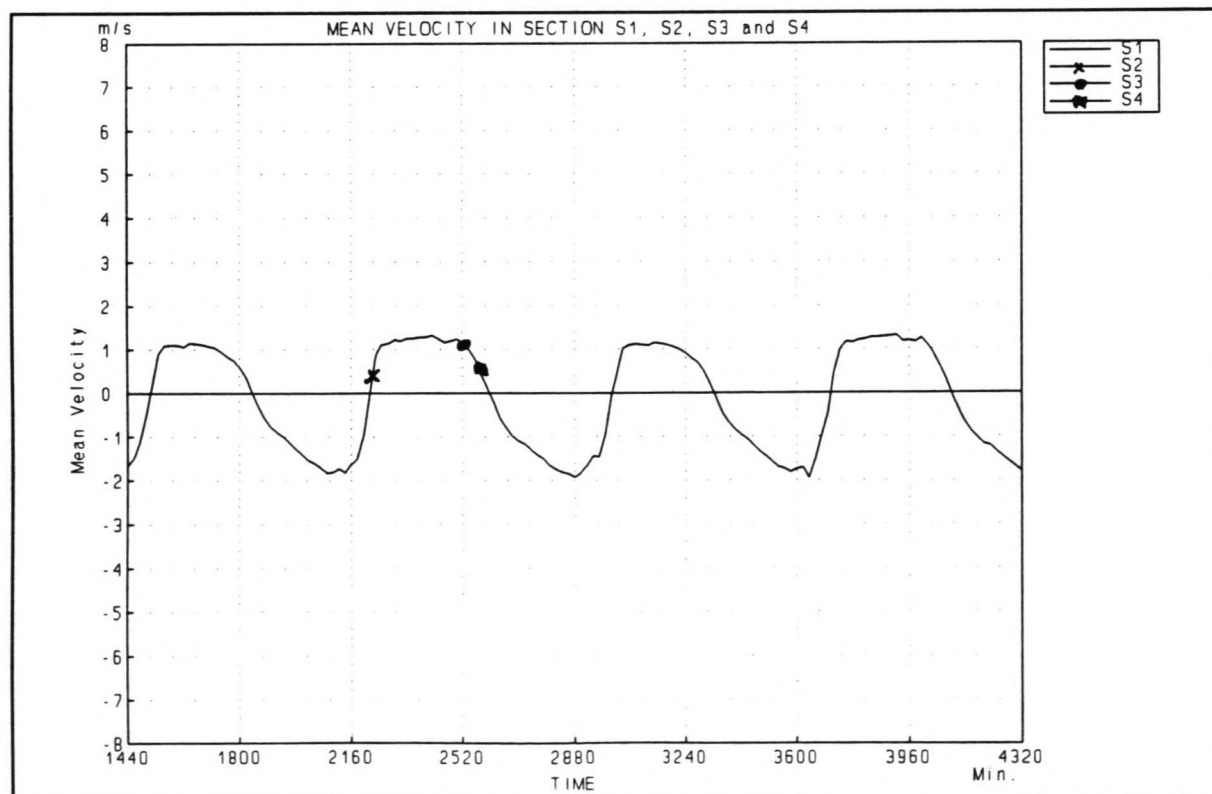


Figure C49: Flow velocities during phase 6

Closure of the Shiwa Tidal Basin

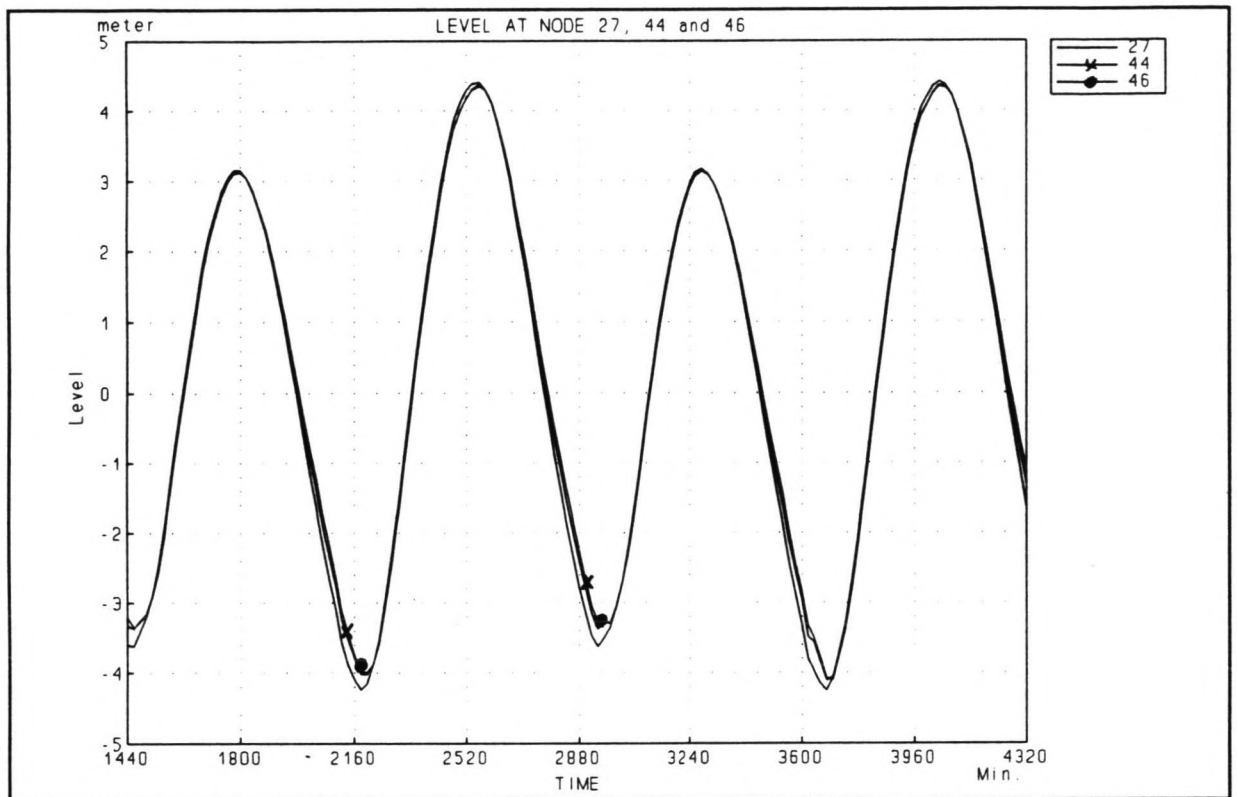


Figure C50: Water level during phase 7

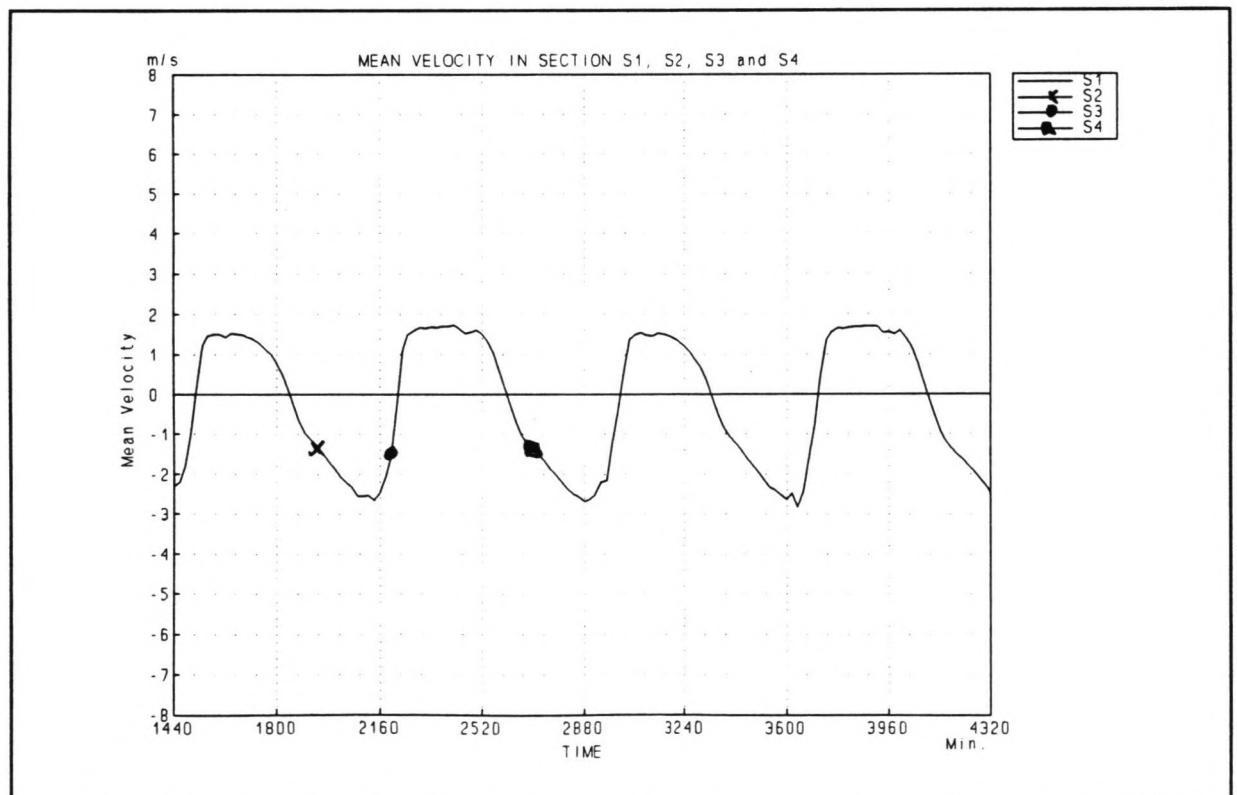


Figure C51: Flow velocities during phase 7

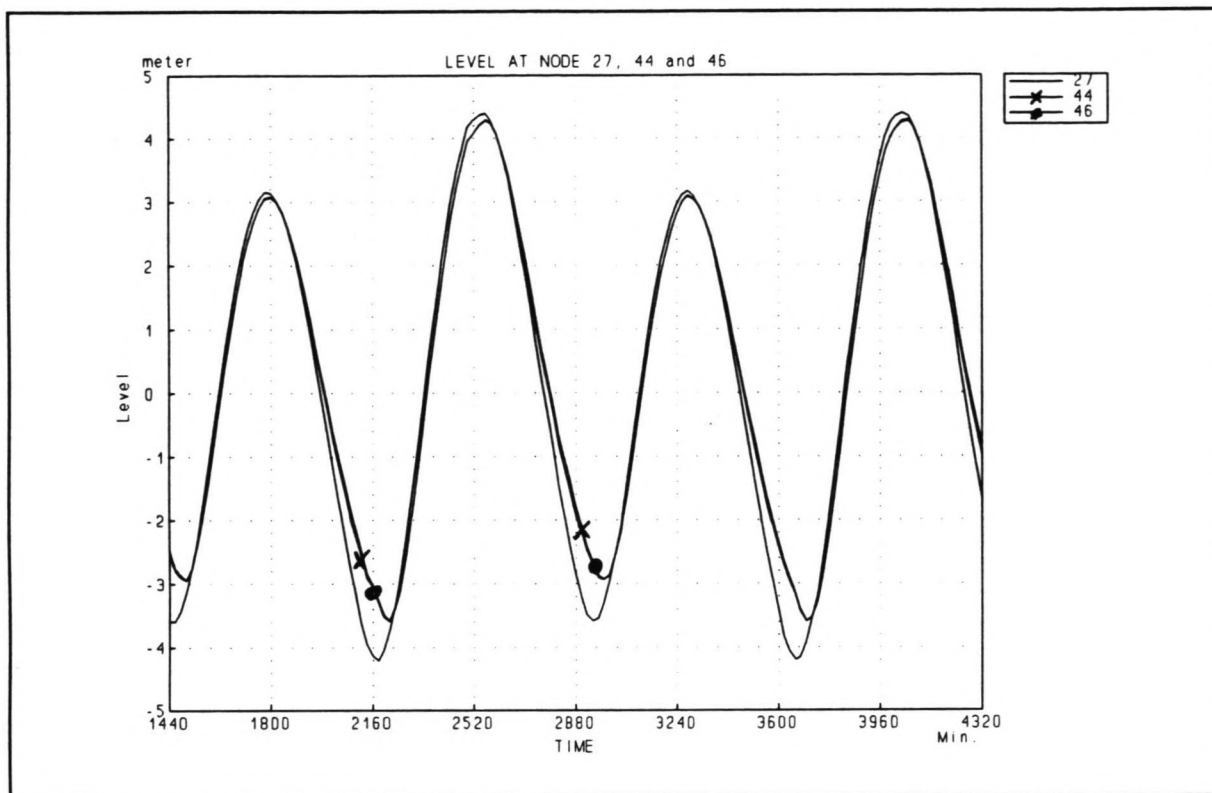


Figure C52: Water level during phase 8

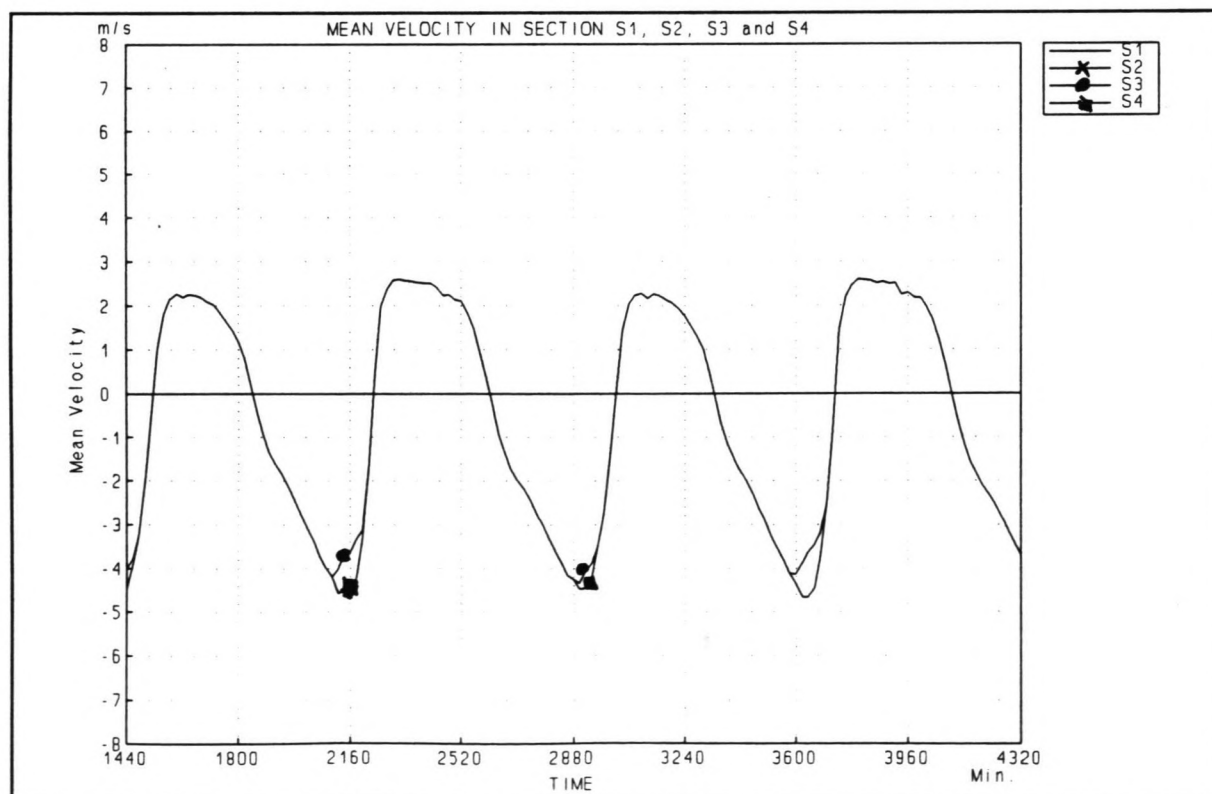


Figure C53: Flow velocities during phase 8

Closure of the Shiwa Tidal Basin

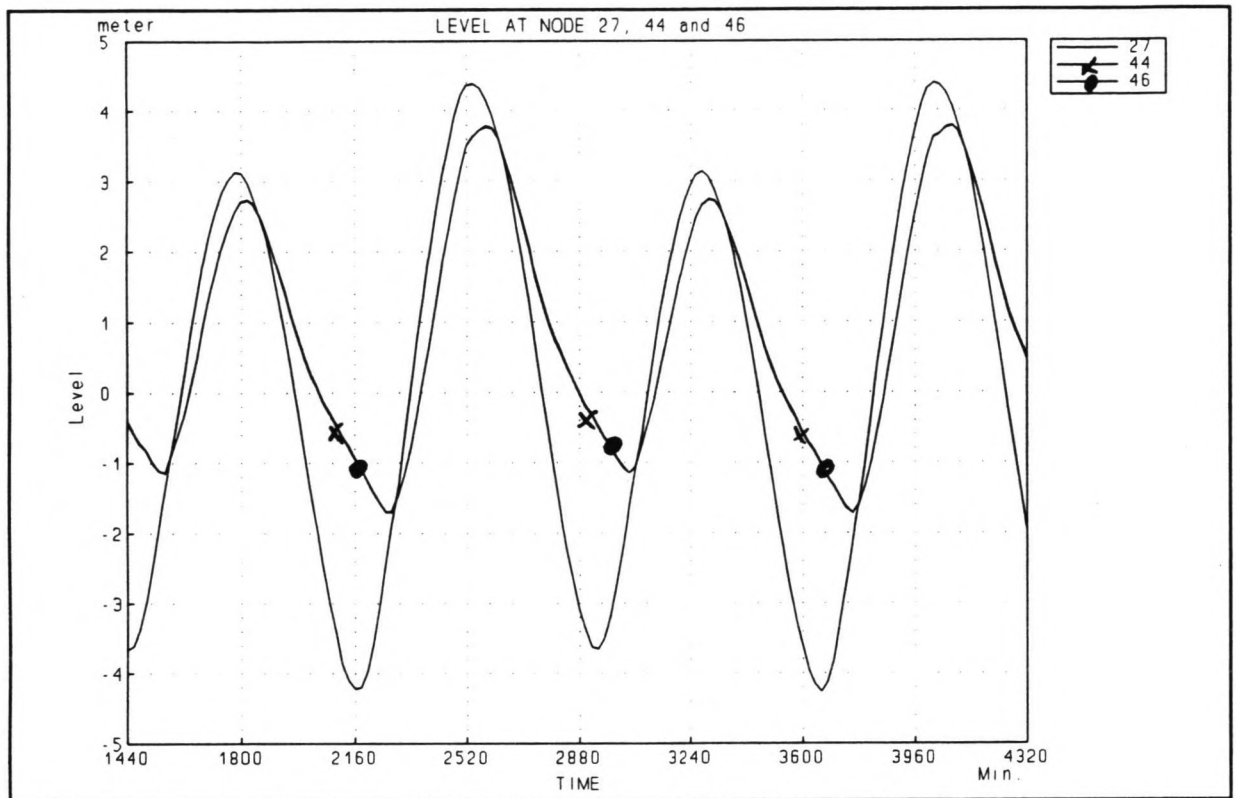


Figure C54: Water level during phase 9

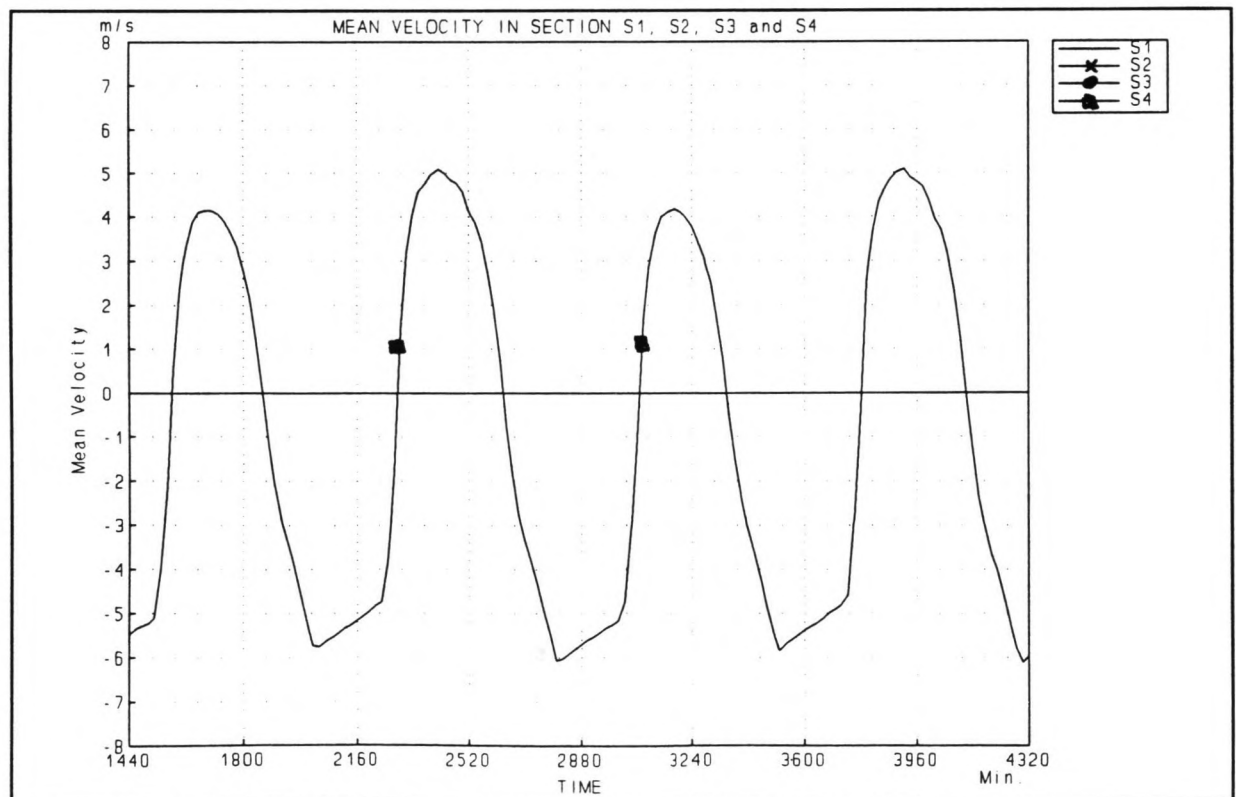


Figure C55: Flow velocities during phase 9

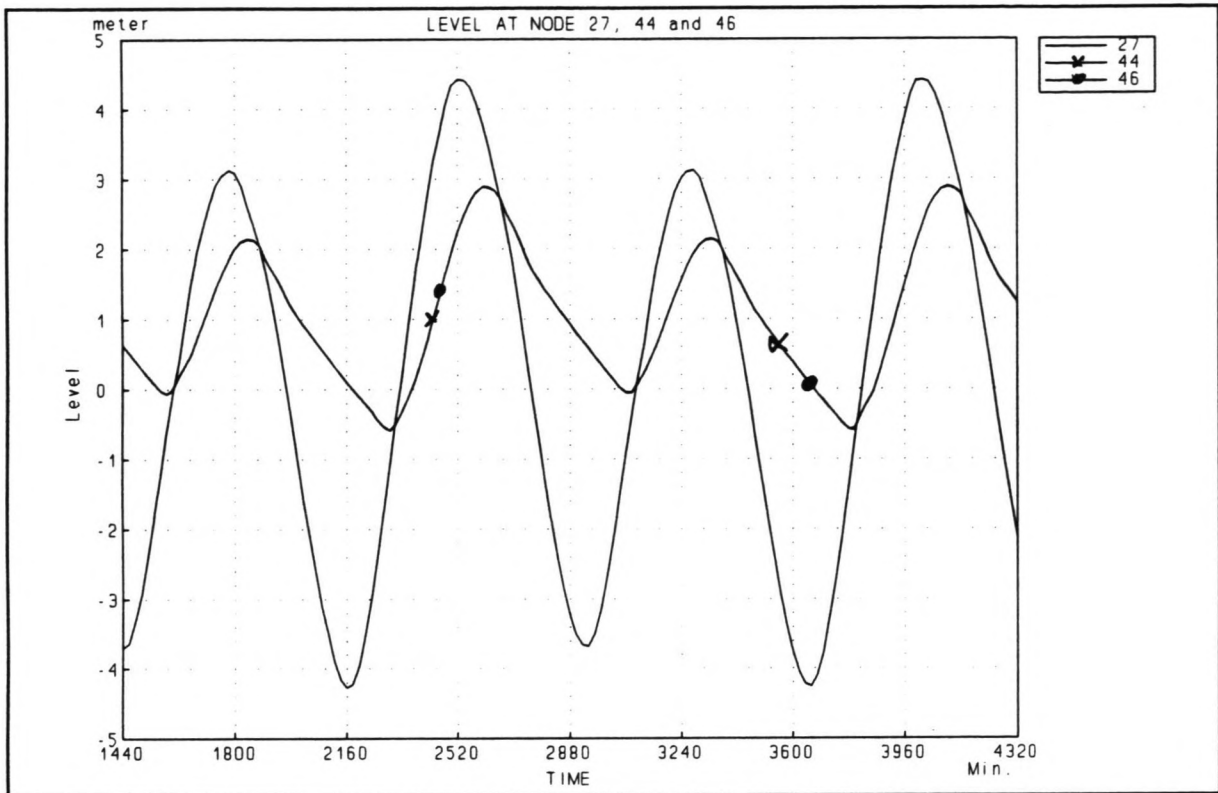


Figure C56: Water level during phase 10

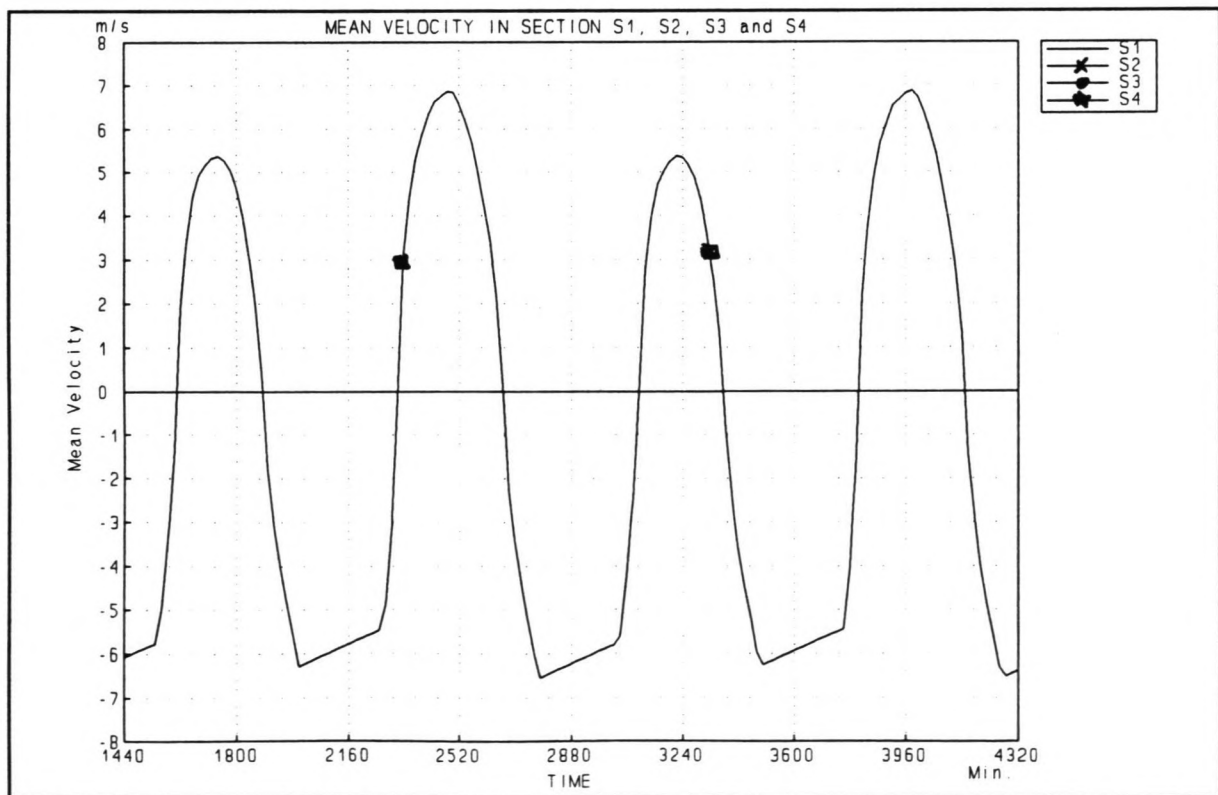


Figure C57: Flow velocities during phase 10

Closure of the Shiwa Tidal Basin

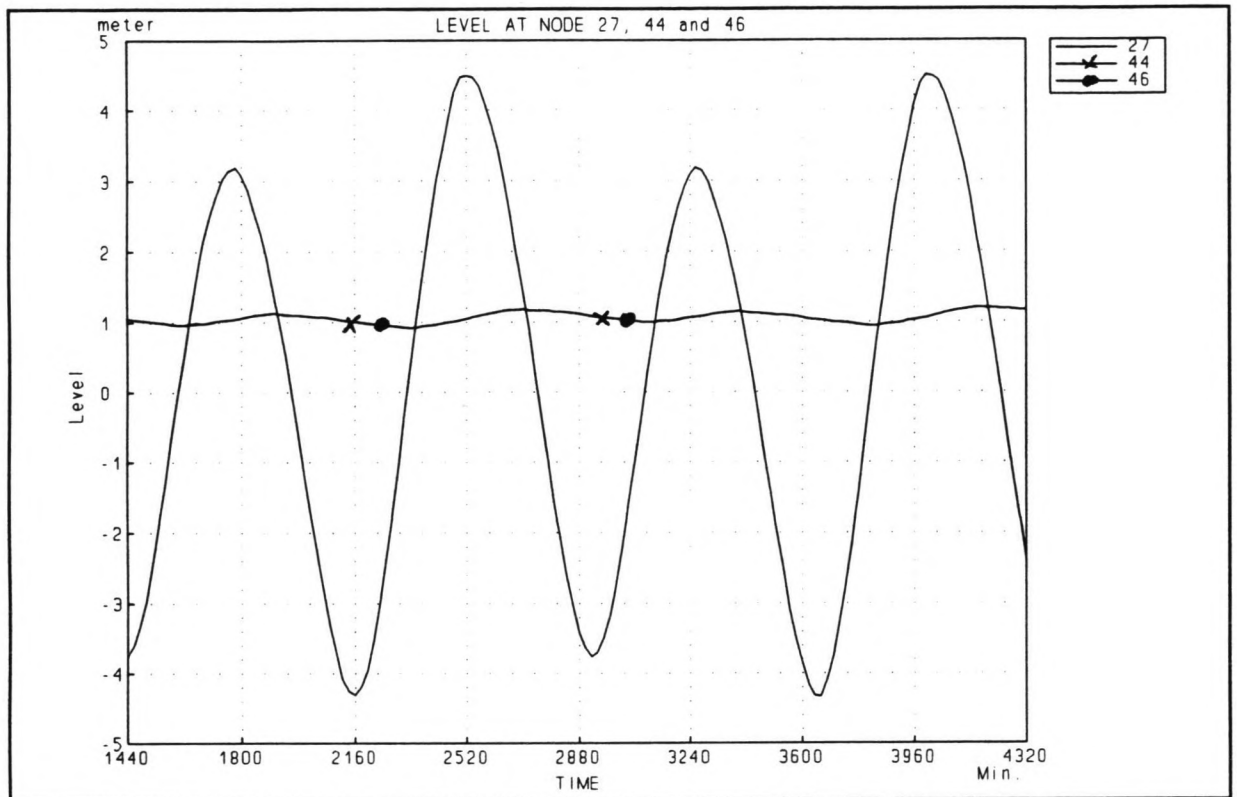


Figure C58: Water level during phase 11

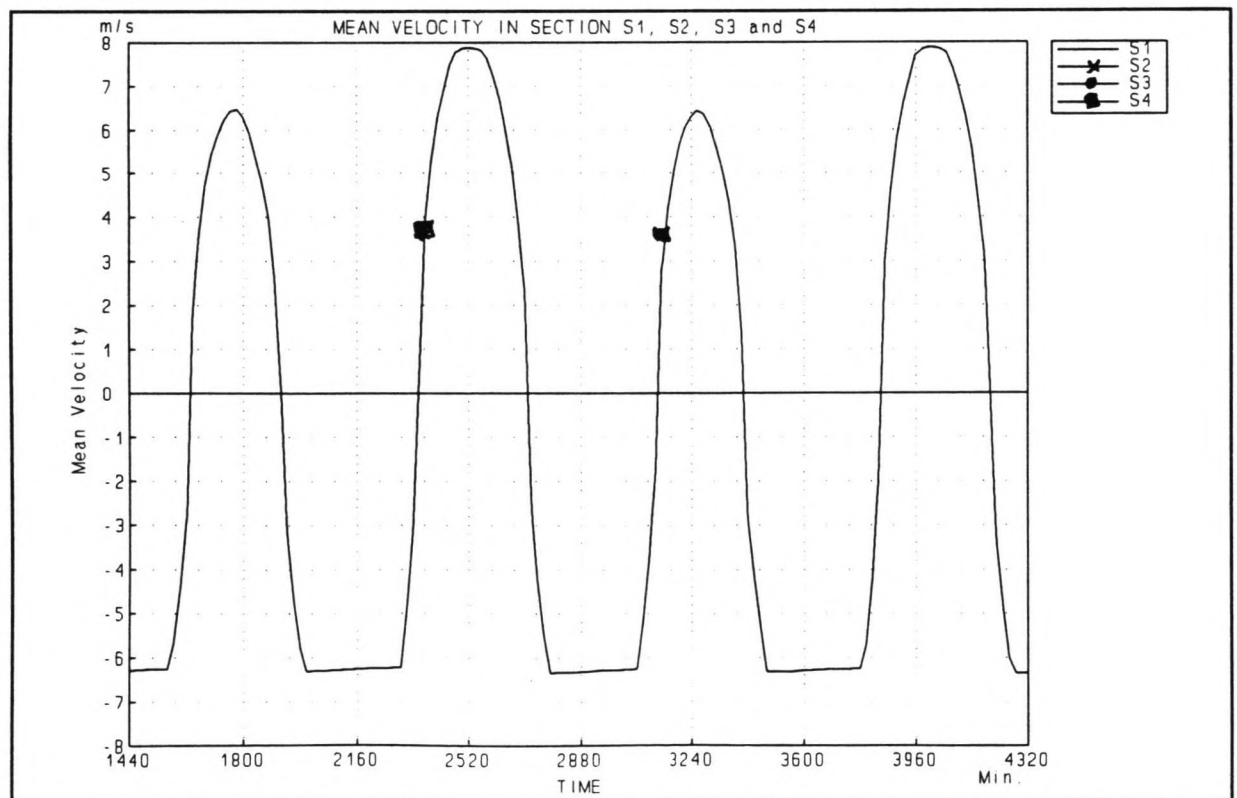


Figure C59: Flow velocities during phase 11

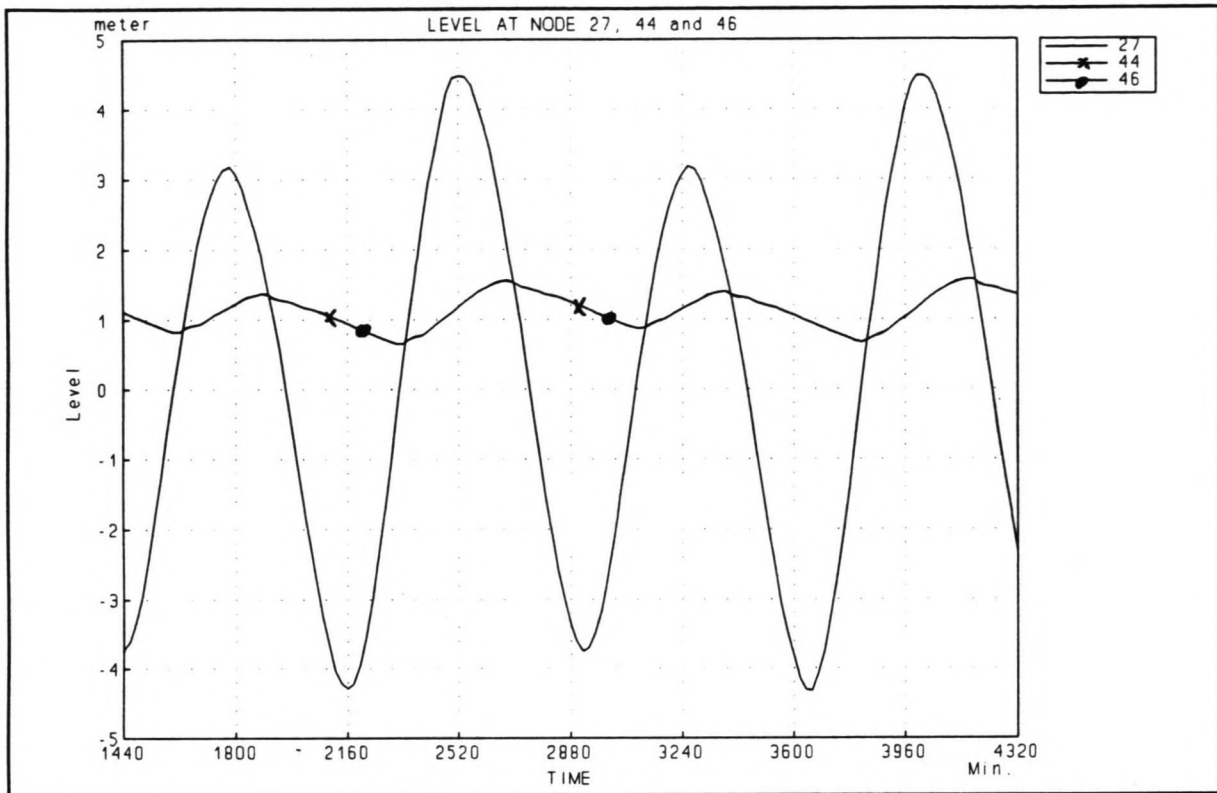


Figure C60: Water level during phase 12

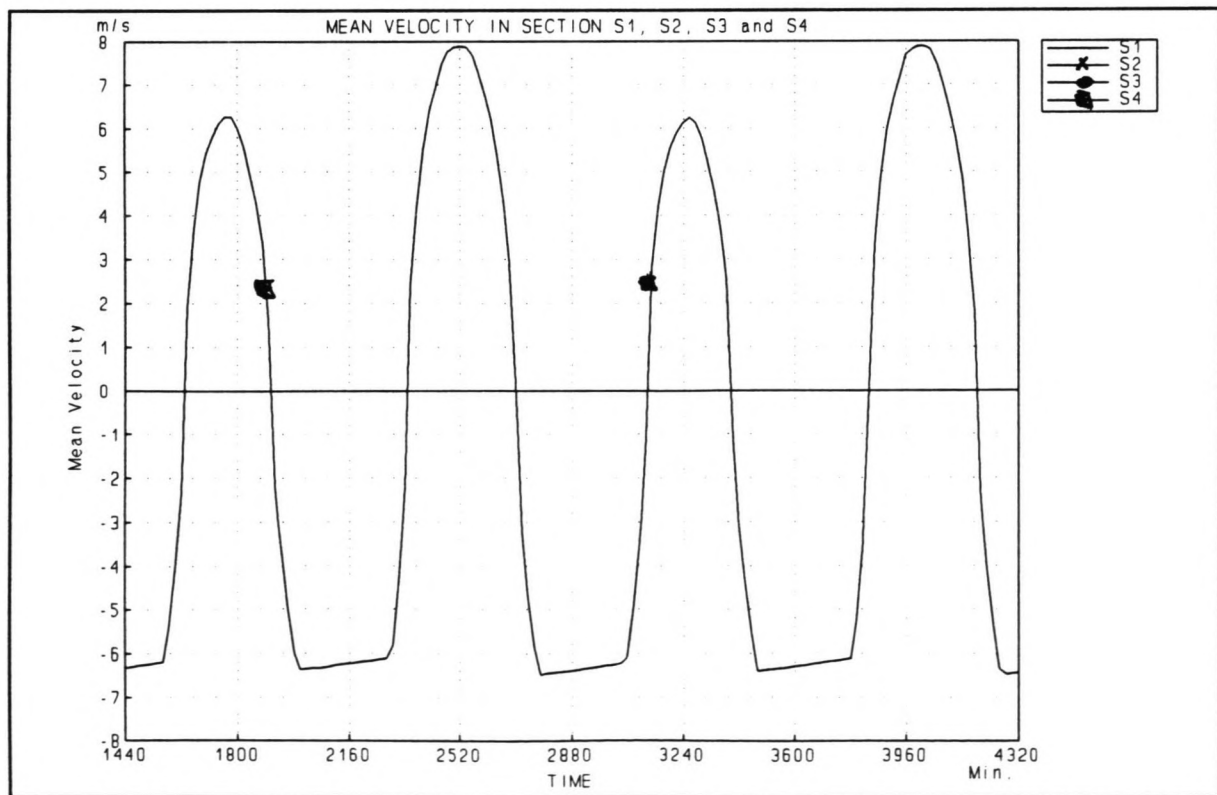


Figure C61: Flow velocities during phase 12

Annex C3:

D₅₀ during a combined closure

The combined closure consists of 13 phases, see Figure C62:

Phase 1:	S 1, 2 and 3 at MSL -8 m., sill 4 at MSL -4 m.
Phase 2:	S 1, 2 and 3 at MSL -6 m., sill 4 at MSL -4 m.
Phase 3:	All sill levels at MSL -4 m.
Phase 4:	All sill levels at MSL -3 m.
Phase 5:	All sill levels at MSL -2 m.
Phase 6:	$B_4 = 0$ m.
Phase 7:	$B_3 = 0$ m.
Phase 8:	$B_2 = 750$ m.
Phase 9:	$B_2 = 0$ m.
Phase10:	$B_1 = 1500$ m.
Phase11:	$B_1 = 1000$ m.
Phase12:	$B_1 = 500$ m.
Phase13:	$B_1 = 0$ m.

With the DufLOW model, the flow velocities as a function of time and the water level at the beginning and at the end of the weirs as a function of time are calculated. The results of these calculations are displayed at the next pages.

When determining the D_{50} in case of a combined closure method, the vertical part, (phase 1 to 5) is the same as in case of a complete vertical closure method. When closing the gap horizontally over the sill, this can be considered as a horizontal closure superimposed on a vertical closure. In this case however the waterlevel outside of the basin is sometimes lower than the sill level of MSL -2 m. Therefore this superposition is not valid and the decisive dam flow situations for a vertical closure method will be applied for the horizontal constriction as well.

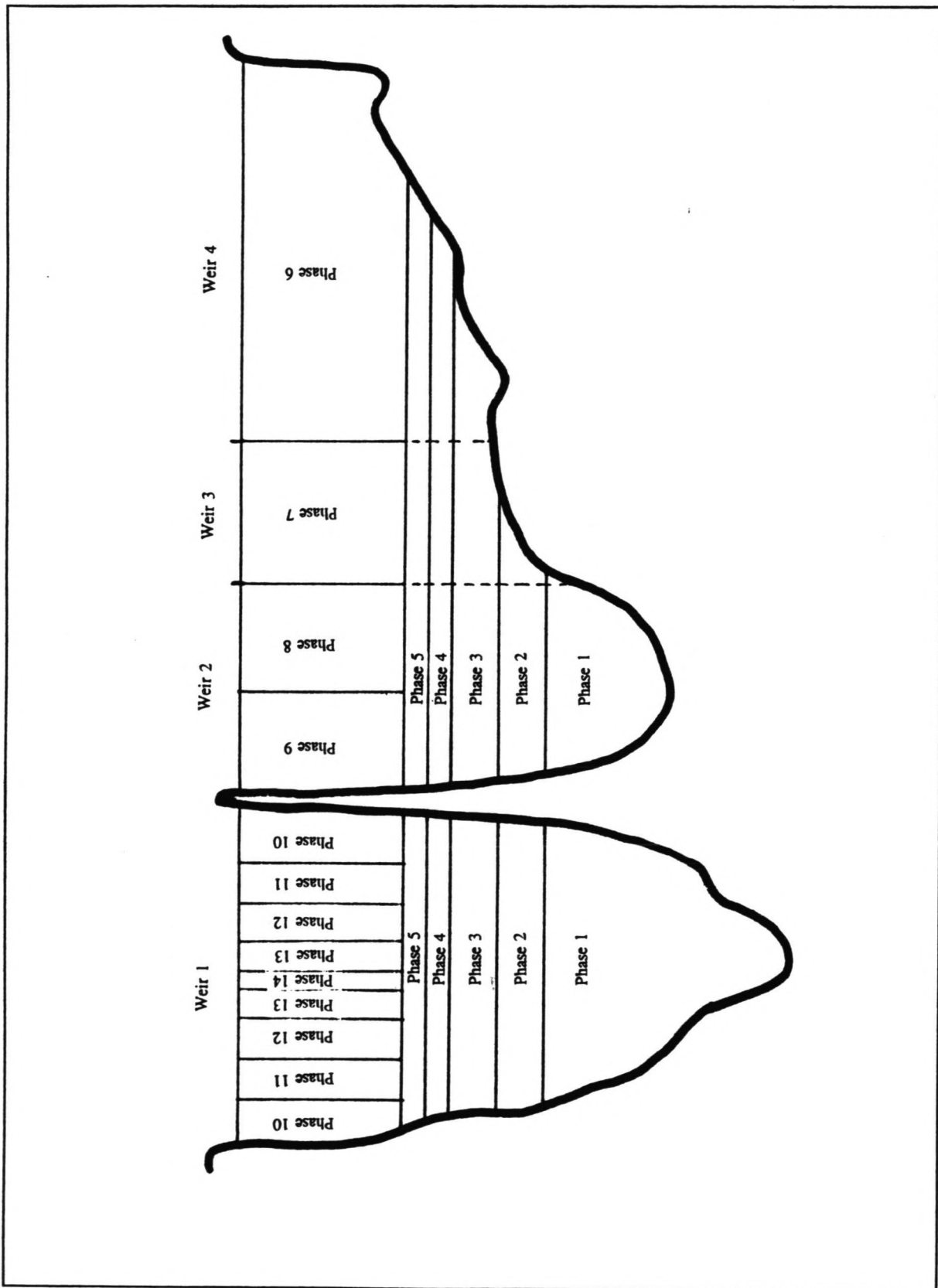


Figure C62: Phases of a combined closure method

Phase 1:

In this phase, the sill will be constructed upto MSL -8.0 m. in structure 1, 2 and 3. Assuming a crest height at MSL +5 m., and a bottom level at MSL -16 m., (see Figure C63), $B/d = 49/8 = 6.1$. This means that the equations for broad crested dams may be applied.

Low dam flow:

$$\frac{u_0}{\sqrt{g\Delta D}} = 1.4 \log \left(3.5 \frac{h_0}{D} \right)$$

with: $u_0 = -1.5$ m/s
 $\Delta = 1.65$
 $h_0 = 3.99$ m

D_{50} becomes 0.008 m.

Intermediate Flow: With $h_b/\Delta D \gg \gg 4$, intermediate flow does not occur.

Phase 2:

In this phase, the sill of structure 1,2 and 3 will be constructed upto MSL -6.0 m. $B/d = 43/10 = 34.3$. As this is smaller than 5, the equations for sharp crested sills may be applied:

Low dam flow:

$$\frac{u_0}{\sqrt{g\Delta D}} = 1.4 \log \left(1.5 \frac{h_0}{D} \right)$$

with: $u_0 = -2.7$ m/s
 $\Delta = 1.65$
 $h_0 = 2.11$ m

D_{50} becomes 0.052 m.

Intermediate Flow: With $h_b/\Delta D = 22$, intermediate flow does not occur.

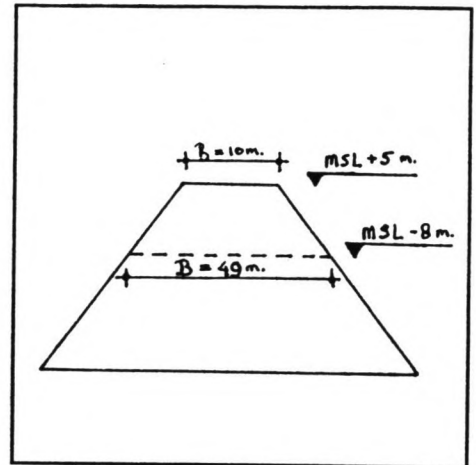


Figure C63: Crest width

Phase 3:

In this phase, the sill will be constructed upto MSL -4.0 m. , $B/d = 37/12 = 3$. As this is smaller than 5, the equations for a sharp crested sill may be applied:

Low dam flow: As $h_b/\Delta D = 0.8$, the equations who describe low dam flow are not valid anymore.

Intermediate flow: With $h_b/\Delta D = 0.8$, the intermediate flow situation is valid.

$$\frac{u_0}{\sqrt{\Delta g D}} = \sqrt{A + 0.375 \frac{h_b}{\Delta D}}$$

with: $A = 2$, (sharp crested dam)
 $u_0 = -3.86$ m/s
 $\Delta = 1.65$
 $h_0 = 1.08$ m

D_{50} becomes 0.86 m.

High dam flow: As the crest of the dam is not emerged yet, high dam flow does not occur.

Phase 4:

In this phase, the sill will be constructed upto MSL -3.0 m., $B/d = 28/13 = 2.15$. As this is smaller than 5, the equations for a sharp crested sill may be applied.

Intermediate flow: With $h_b/\Delta D = 0.57$, the intermediate flow situation is valid.

$$\frac{u_0}{\sqrt{\Delta g D}} = \sqrt{A + 0.375 \frac{h_b}{\Delta D}}$$

with: $A = 2$, (sharp crested dam)
 $u_0 = -3.93$ m/s
 $\Delta = 1.65$
 $h_0 = 1.11$ m

D_{50} becomes 0.95 m.

High dam flow:

$$q_{\max} = 1.95 (\Delta D_s)^{\frac{3}{2}} (1.9 + 0.8\phi - 3\sin\alpha)$$

with $q_{\max} = 3.44 \text{ m}^2/\text{s}$

D_{50} becomes 1.14 m.

As the the high dam flow criterion gives a higher value than the intermediate flow criterion, the value of 1.14 m. is decisive.

Phase 5:

In this phase, the sill will be constructed upto MSL -2.0 m., $B/d < 5$, so the equations for a sharp crested sill may be applied.

Intermediate flow: with $h_b/\Delta D = 0.58$, the intermediate flow situation is valid.

$$\frac{u_0}{\sqrt{\Delta g D}} = \sqrt{A + 0.375 \frac{h_b}{\Delta D}}$$

with: $A = 2$, (sharp crested dam)

$$u_0 = -3.96 \text{ m/s}$$

$$\Delta = 1.65$$

$$h_0 = 0.92 \text{ m}$$

D_{50} becomes 0.96 m.

High dam flow:

$$q_{\max} = 1.95 (\Delta D_s)^{\frac{3}{2}} (1.9 + 0.8\phi - 3\sin\alpha)$$

with $q_{\max} = 3.9 \text{ m}^2/\text{s}$

D_{50} becomes 1.18 m.

As the the high dam flow criterion gives a higher value than the intermediate flow criterion, the value of 1.18 m. is decisive.

Phase 6:

This is the first phase where the closure gap is constricted horizontally by closing structure 4.

Intermediate flow: With $h_b/\Delta D = 1.14$, the intermediate flow situation is valid.

$$\frac{u_0}{\sqrt{\Delta g D}} = \sqrt{A + 0.375 \frac{h_b}{\Delta D}}$$

with: $A = 2$, (sharp crested dam)
 $u_0 = -4.0$ m/s
 $\Delta = 1.65$
 $h_0 = 1.53$ m

D_{50} becomes 0.812 m.

High dam flow:

$$q_{\max} = 1.95 (\Delta D_s)^{\frac{3}{2}} (1.9 + 0.8\phi - 3\sin\alpha)$$

with $q_{\max} = 4.04$ m²/s

D_{50} becomes 1.21 m.

As the the high dam flow criterion gives a higher value than the intermediate flow criterion, the value of 1.21 m. is decisive.

Phase 7:

In this phase, structure 3 will be closed.

Intermediate flow: with $h_b/\Delta D = 0.8$, the intermediate flow situation is valid.

$$\frac{u_0}{\sqrt{\Delta g D}} = \sqrt{A + 0.375 \frac{h_b}{\Delta D}}$$

with: $A = 2$, (sharp crested dam)
 $u_0 = -4.39$ m/s
 $\Delta = 1.65$

$$h_0 = 1.45 \text{ m}$$

D_{50} becomes 1.1 m.

High dam flow:

$$q_{\max} = 1.95 (\Delta D_s)^2 (1.9 + 0.8\phi - 3\sin\alpha)$$

with $q_{\max} = 5.77 \text{ m}^2/\text{s}$

D_{50} becomes 1.53 m.

As the the high dam flow criterion gives a higher value than the intermediate flow criterion, the value of 1.53 m. is decisive.

Phase 8:

In this phase, the width of structure 2 will be reduced to 750 m.

Intermediate flow: With $h_b/\Delta D = 0.77$, the intermediate flow situation is valid.

$$\frac{u_0}{\sqrt{\Delta g D}} = \sqrt{A + 0.375 \frac{h_b}{\Delta D}}$$

with: $A = 2$, (sharp crested dam)

$$u_0 = -4.54 \text{ m/s}$$

$$\Delta = 1.65$$

$$h_0 = 1.4 \text{ m}$$

D_{50} becomes 1.21 m.

High dam flow:

$$q_{\max} = 1.95 (\Delta D_s)^2 (1.9 + 0.8\phi - 3\sin\alpha)$$

with $q_{\max} = 6.71 \text{ m}^2/\text{s}$

D_{50} becomes 1.69 m.

As the the high dam flow criterion gives a higher value than the intermediate flow criterion,

the value of 1.69 m. is decisive.

Phase 9:

In this phase, structure 2 will be closed.

Intermediate flow: with $h_v/\Delta D = 0.93$, the intermediate flow situation is valid.

$$\frac{u_0}{\sqrt{\Delta g D}} = \sqrt{A + 0.375 \frac{h_b}{\Delta D}}$$

with: $A = 2$, (sharp crested dam)

$$u_0 = -4.85 \text{ m/s}$$

$$\Delta = 1.65$$

$$h_0 = 1.97 \text{ m}$$

D_{50} becomes 1.28 m.

High dam flow:

$$q_{\max} = 1.95 (\Delta D_s)^{\frac{3}{2}} (1.9 + 0.8\phi - 3 \sin \alpha)$$

with $q_{\max} = 8.26 \text{ m}^2/\text{s}$

D_{50} becomes 1.95 m.

As the the high dam flow criterion gives a higher value than the intermediate flow criterion, the value of 1.95 m. is decisive.

Phase 10:

In this phase, the width of structure 1 will be reduced to 1500 m.

Intermediate flow: With $h_v/\Delta D = 1.1$, the intermediate flow situation is valid.

$$\frac{u_0}{\sqrt{\Delta g D}} = \sqrt{A + 0.375 \frac{h_b}{\Delta D}}$$

with: $A = 2$, (sharp crested dam)

$$u_0 = -5.24 \text{ m/s}$$

$$\begin{aligned}\Delta &= 1.65 \\ h_0 &= 2.57\text{m}\end{aligned}$$

D_{50} becomes 1.4 m.

High dam flow:

$$q_{\max} = 1.95 (\Delta D_s)^{\frac{3}{2}} (1.9 + 0.8\phi - 3\sin\alpha)$$

with $q_{\max} = 10.43 \text{ m}^2/\text{s}$

D_{50} becomes 2.27 m.

As the the high dam flow criterion gives a higher value than the intermediate flow criterion, the value of 2.27 m. is decisive.

Phase 11:

In this phase, the width of structure 1 will be reduced to 1000 m..

Intermediate flow: with $h_b/\Delta D = 1.45$, the intermediate flow situation is valid.

$$\frac{u_0}{\sqrt{\Delta g D}} = \sqrt{A + 0.375 \frac{h_b}{\Delta D}}$$

with: $A = 2$, (sharp crested dam)
 $u_0 = 6.1 \text{ m/s}$
 $\Delta = 1.65$
 $h_0 = 4.09 \text{ m}$

D_{50} becomes 1.7 m.

High dam flow:

$$q_{\max} = 1.95 (\Delta D_s)^{\frac{3}{2}} (1.9 + 0.8\phi - 3\sin\alpha)$$

with $q_{\max} = 12.06 \text{ m}^2/\text{s}$

D_{50} becomes 2.50 m.

As the the high dam flow criterion gives a higher value than the intermediate flow criterion, the value of 2.50 m. is decisive.

Phase 10:

In this phase, the width of structure 1 will be reduced to 500 m.

Intermediate flow: With $h_b/\Delta D = 1.05$, the intermediate flow situation is valid.

$$\frac{u_0}{\sqrt{\Delta g D}} = \sqrt{A + 0.375 \frac{h_b}{\Delta D}}$$

with: $A = 2$, (sharp crested dam)
 $u_0 = 6.5$ m/s
 $\Delta = 1.65$
 $h_0 = 3.84$ m

D_{50} becomes 2.23 m.

High dam flow:

$$q_{\max} = 1.95 (\Delta D_s)^{\frac{3}{2}} (1.9 + 0.8\phi - 3\sin\alpha)$$

with $q_{\max} = 12.56$ m²/s

D_{50} becomes 2.575 m.

As the the high dam flow criterion gives a higher value than the intermediate flow criterion, the value of 2.575 m. is decisive.

Phase 11:

In this phase, the width of structure 1 will be reduced to 50 m.

Intermediate flow: with $h_b/\Delta D = 0.88$, the intermediate flow situation is valid.

$$\frac{u_0}{\sqrt{\Delta g D}} = \sqrt{A + 0.375 \frac{h_b}{\Delta D}}$$

with: $A = 2$, (sharp crested dam)
 $u_0 = 6.5$ m/s
 $\Delta = 1.65$
 $h_0 = 3.84$ m

D_{50} becomes 2.36 m.

High dam flow:

$$q_{\max} = 1.95 (\Delta D_s)^{\frac{3}{2}} (1.9 + 0.8\phi - 3 \sin \alpha)$$

with $q_{\max} = 7.68$ m²/s

D_{50} becomes 1.85 m.

Here the D_{50} of intermediate flow is higher than in case of high dam flow, therefore the value of 2.36 m. is decisive.

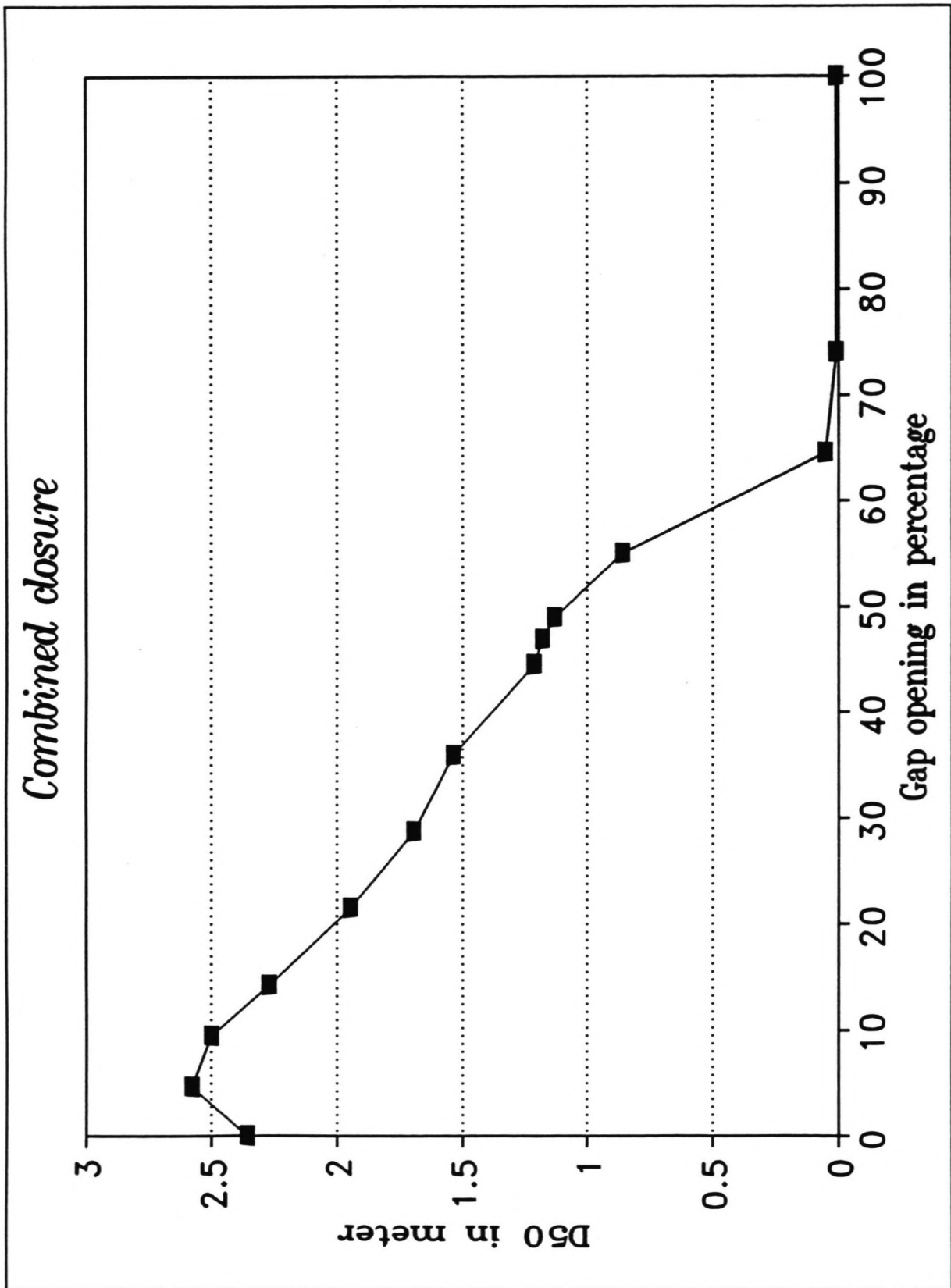


Figure C64: Resulting D_{50} for a combined closure method

Closure of the Shiwa Tidal Basin

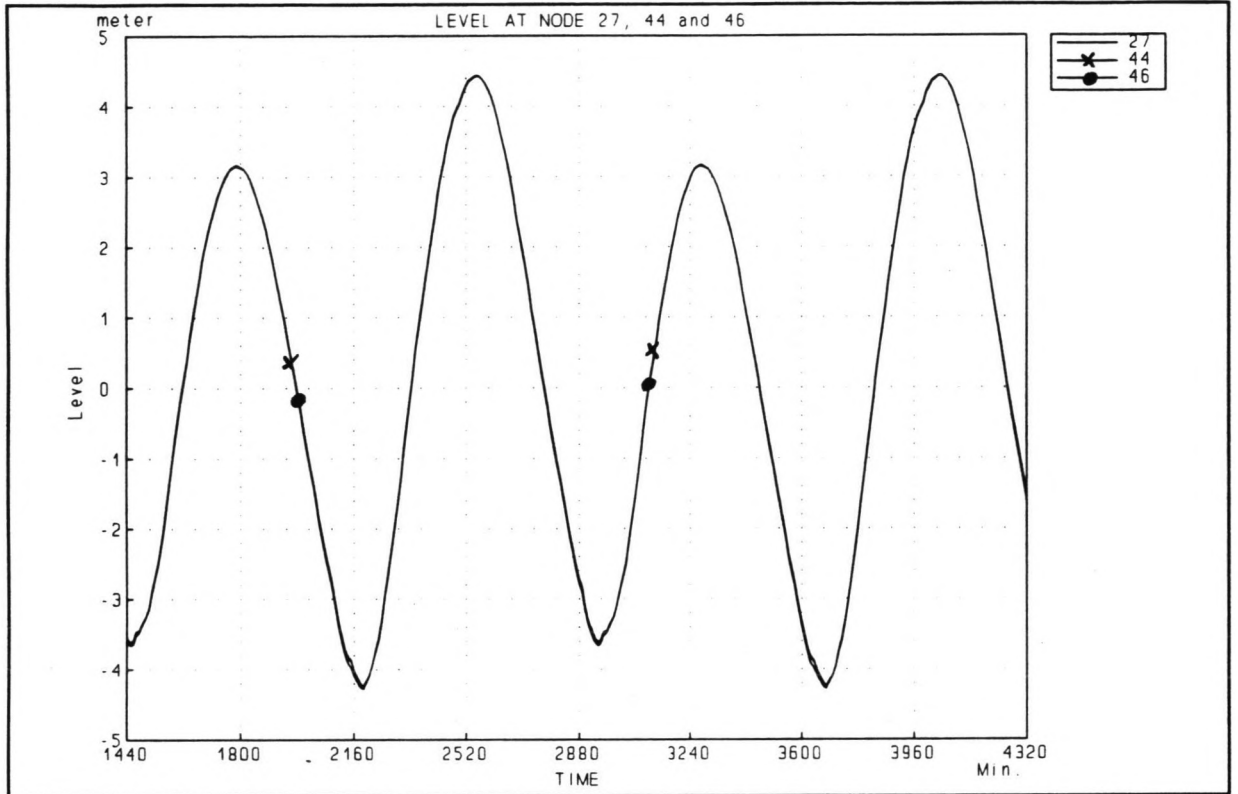


Figure C65: Water level during phase 1

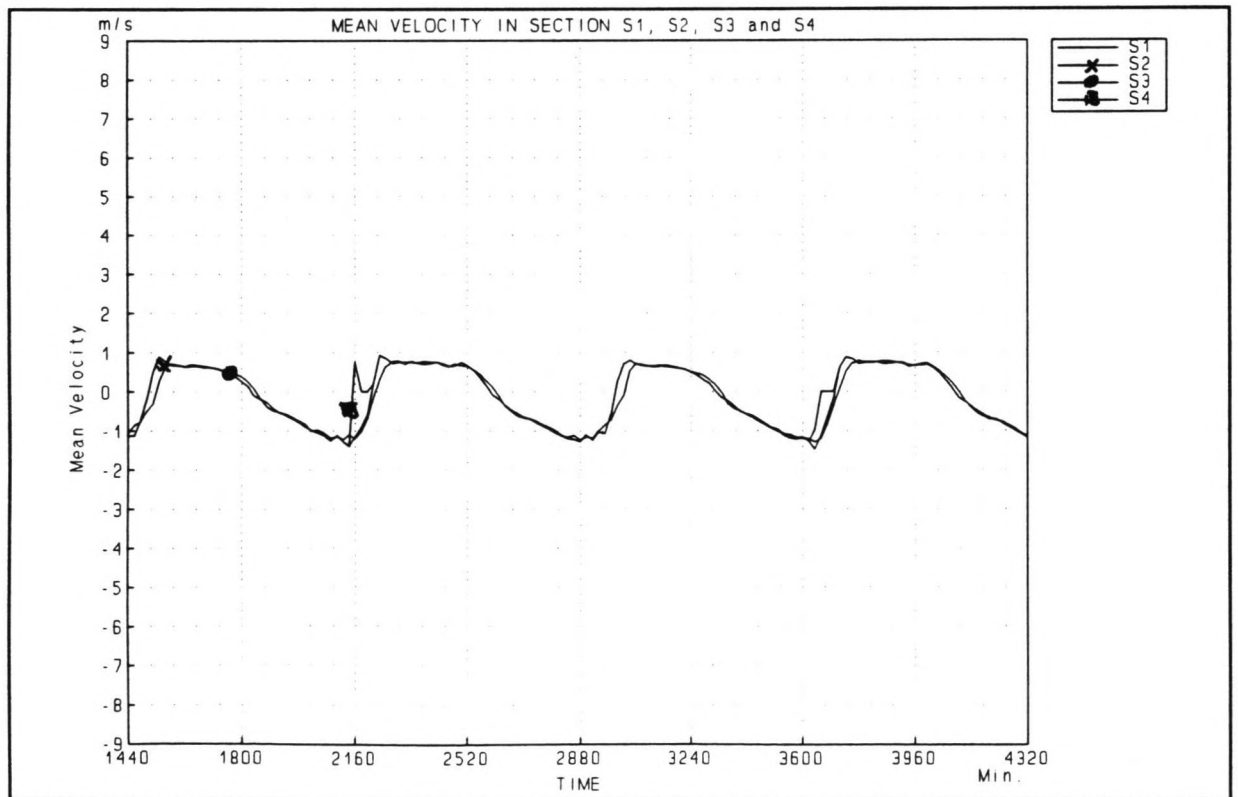


Figure C66: Flow velocities during phase 1

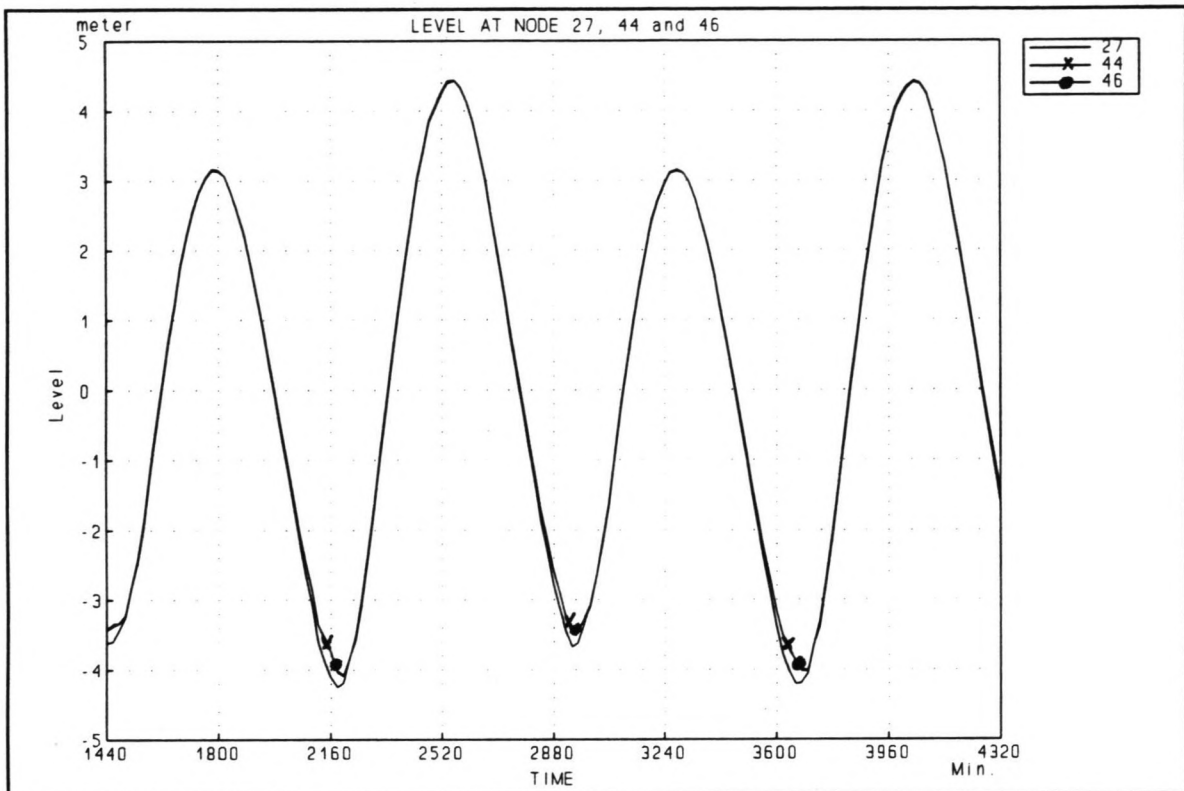


Figure C67: Water level during phase 3

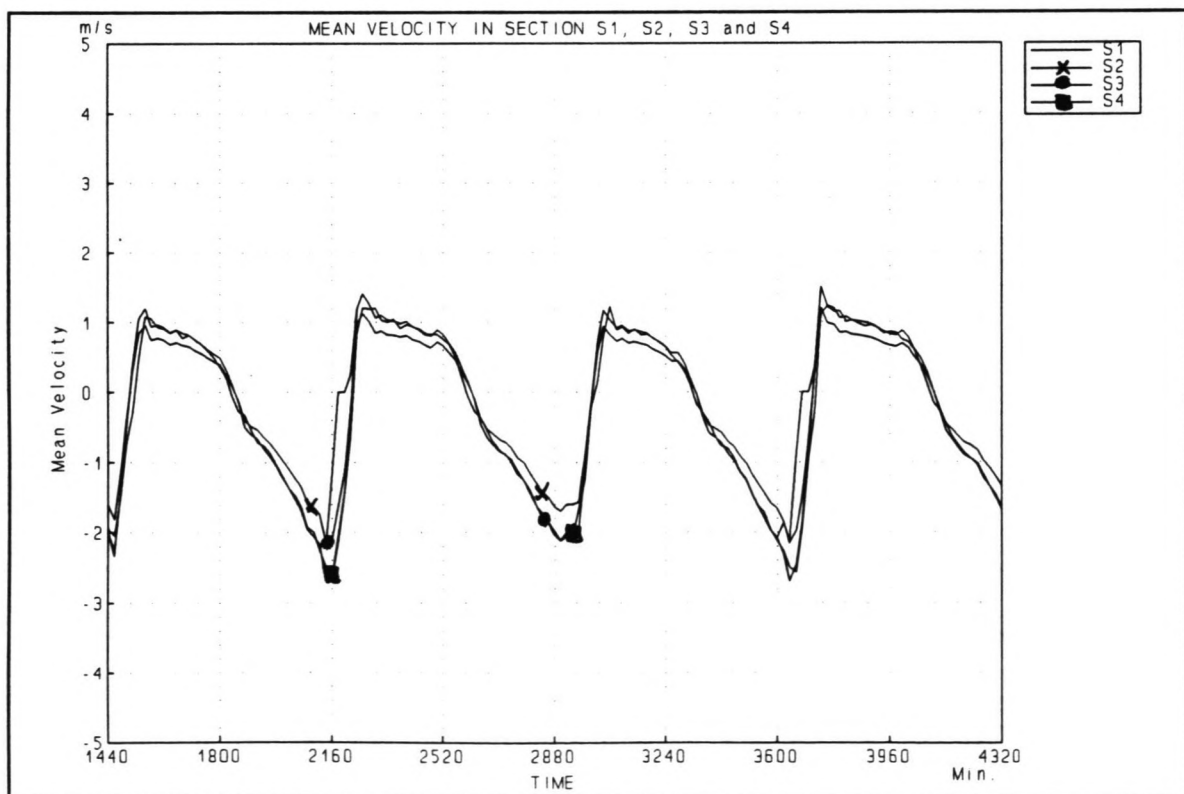


Figure C68: Flow velocities during phase 2

Closure of the Shiwa Tidal Basin

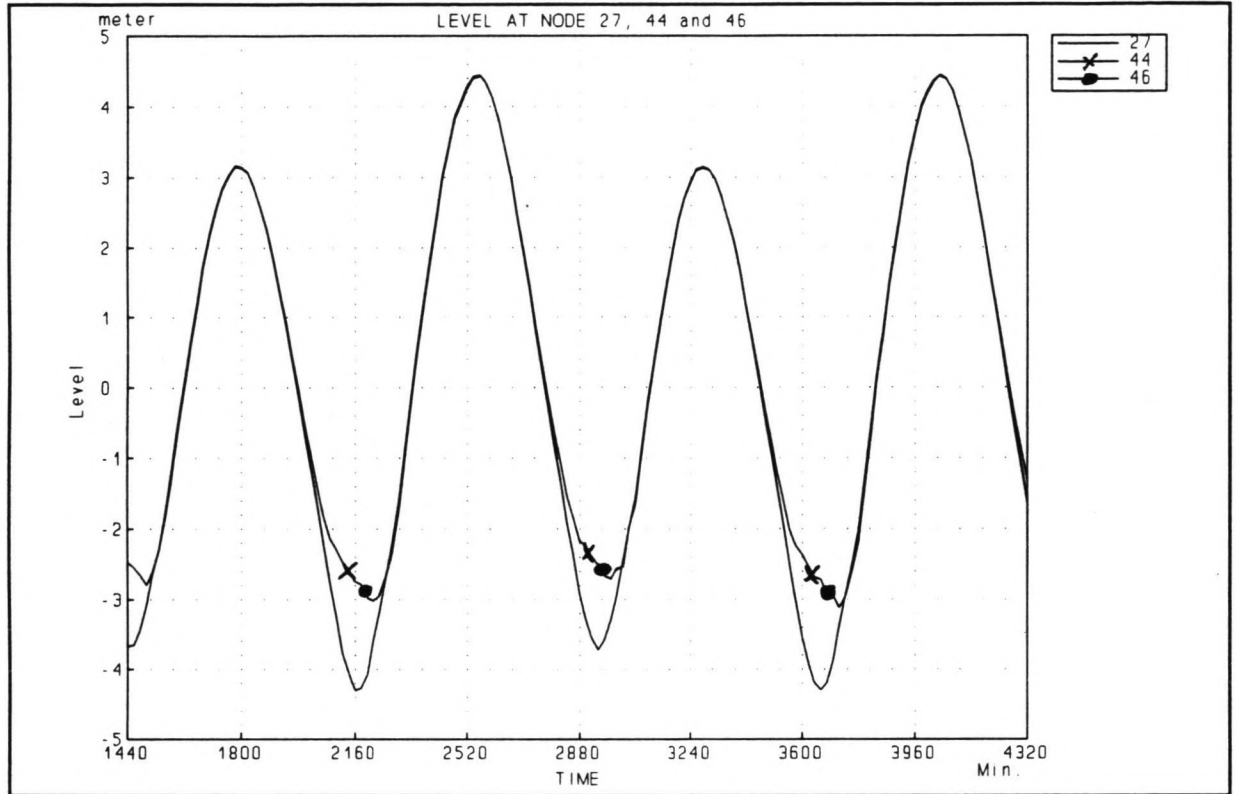


Figure C69: Water level during phase 3

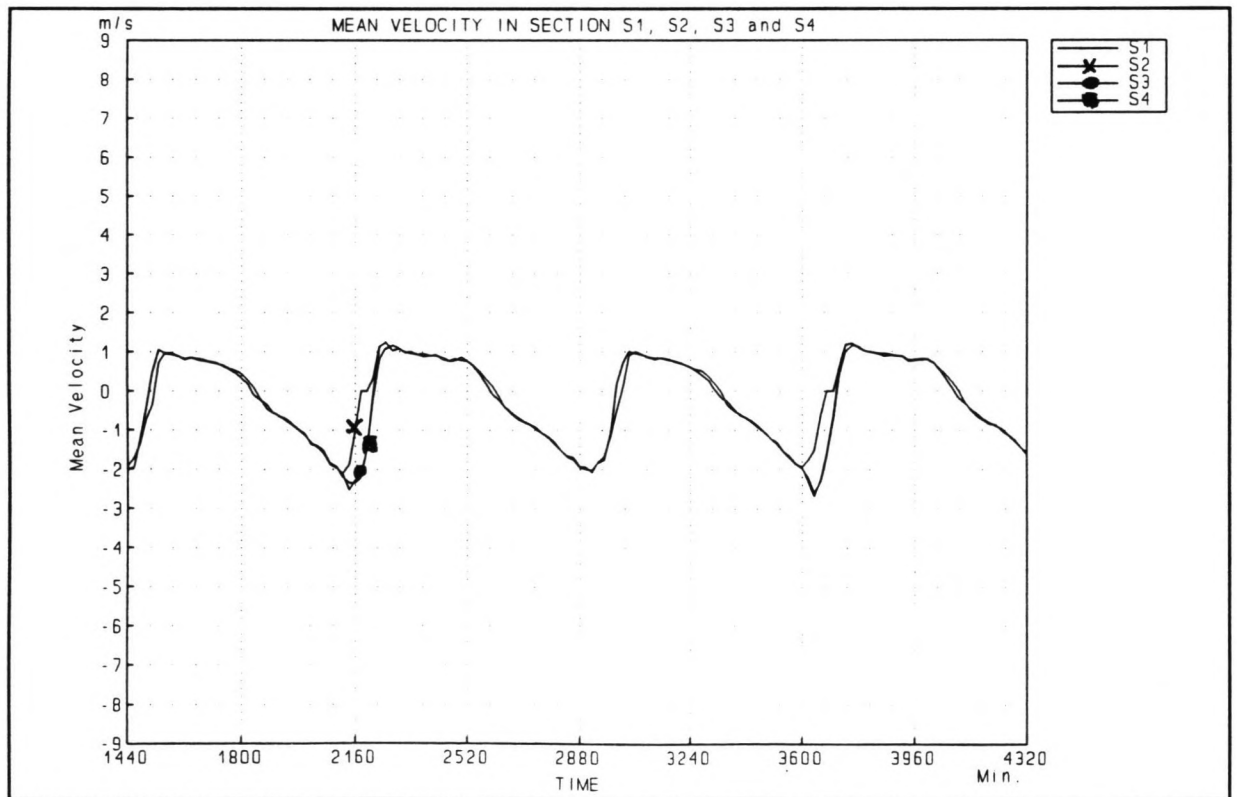


Figure C70: Flow velocities during phase 3

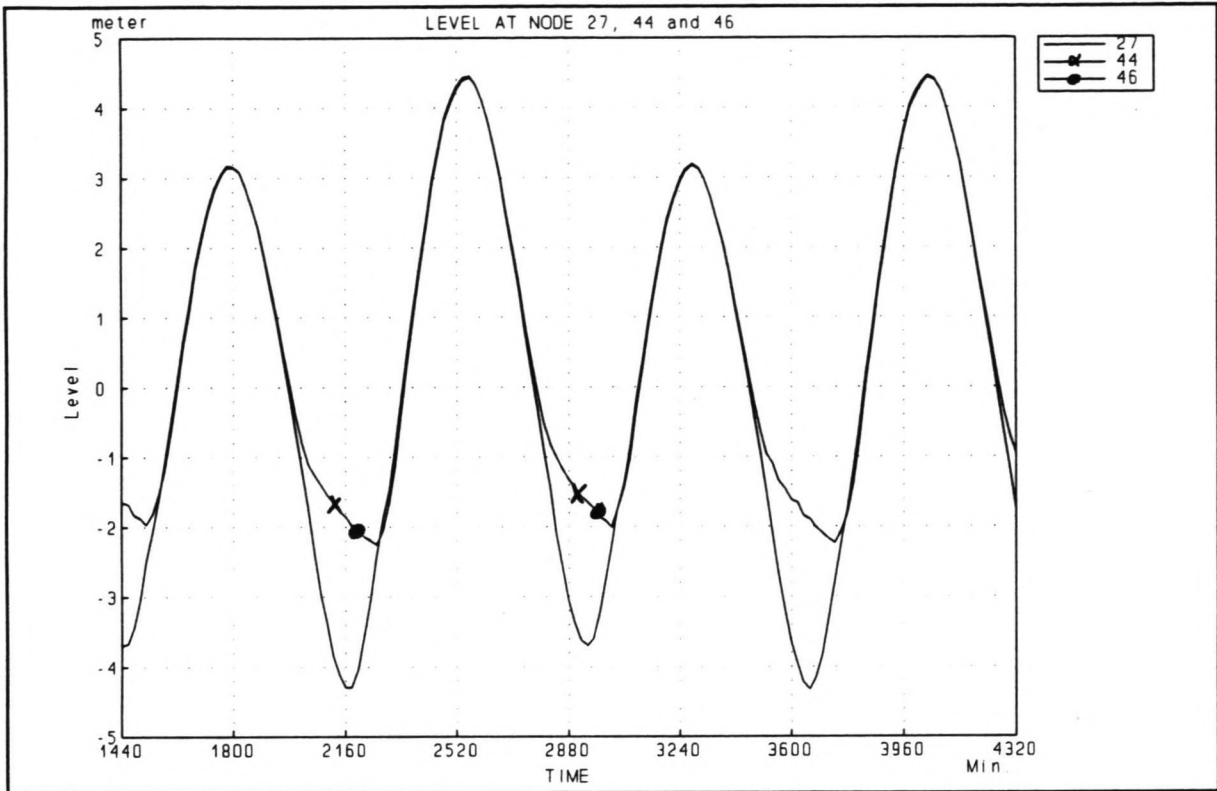


Figure C71: Water level during phase 4

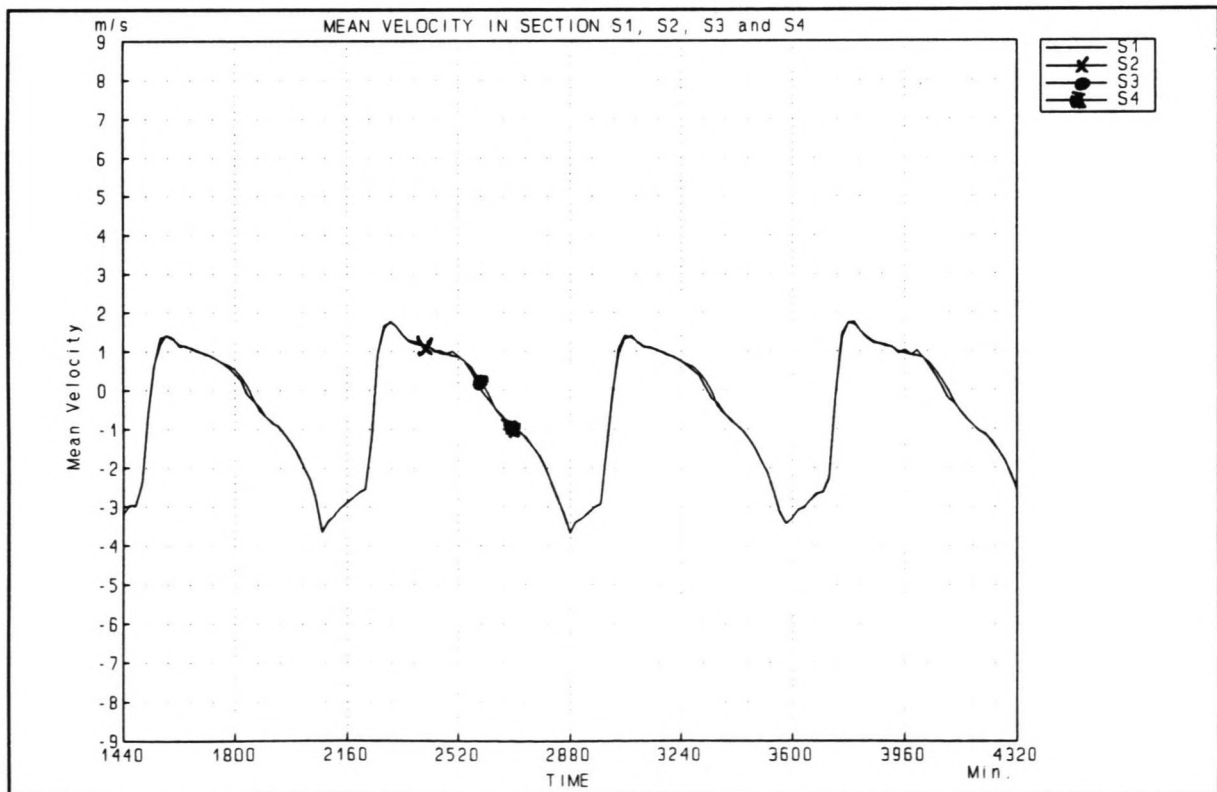


Figure C72: Flow velocities during phase 4

Closure of the Shiwa Tidal Basin

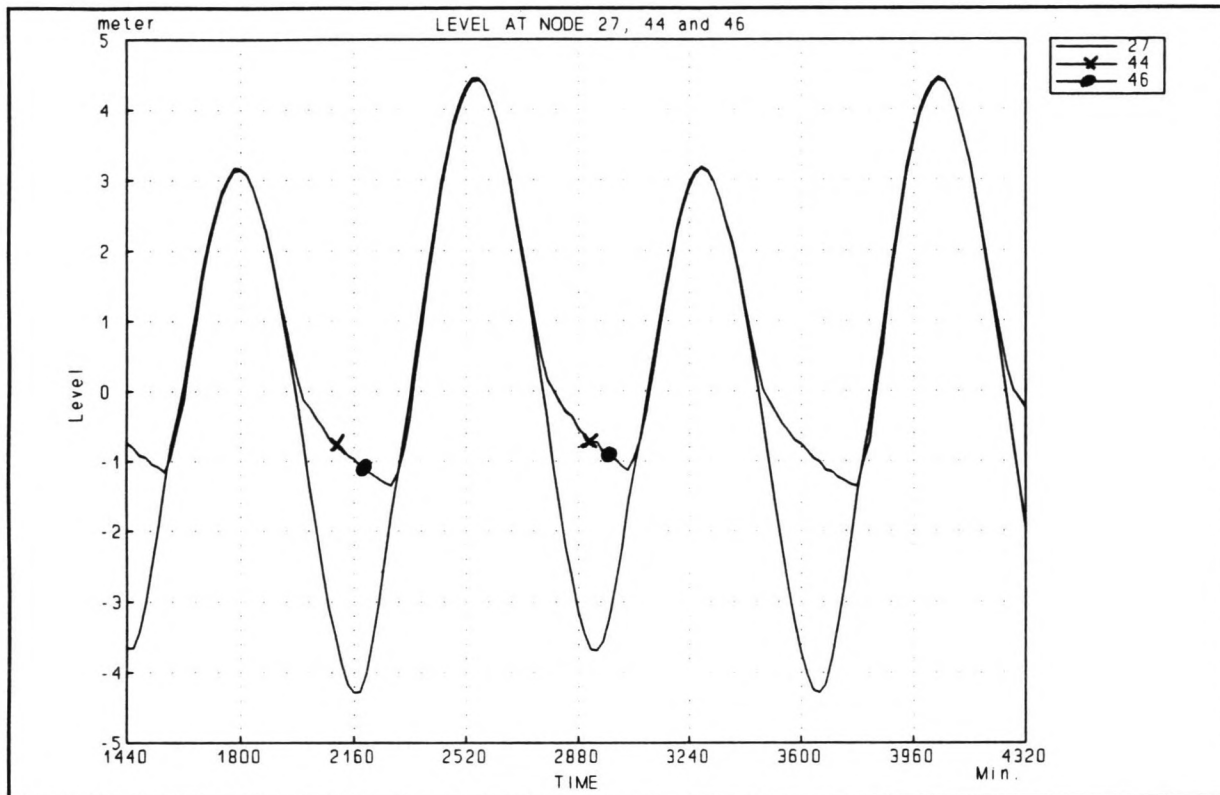


Figure C73: Water level during phase 5

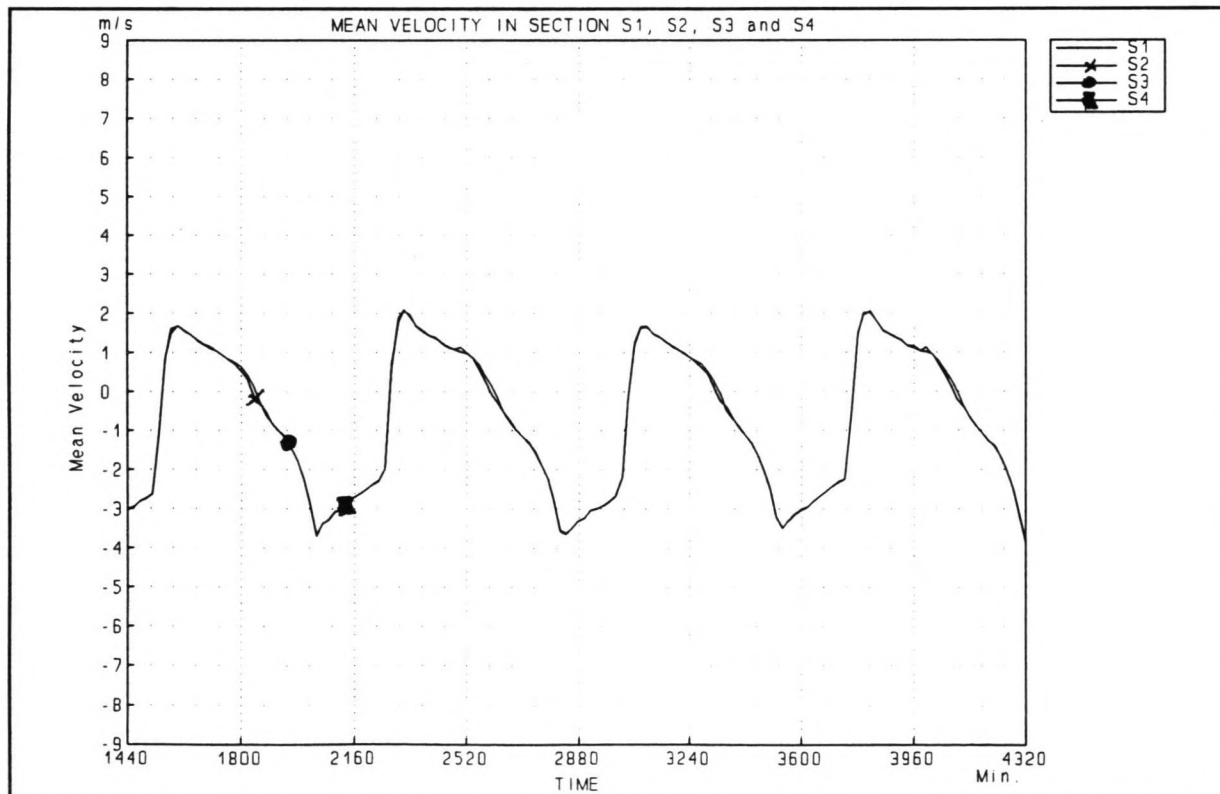


Figure C74: Flow velocities during phase 5

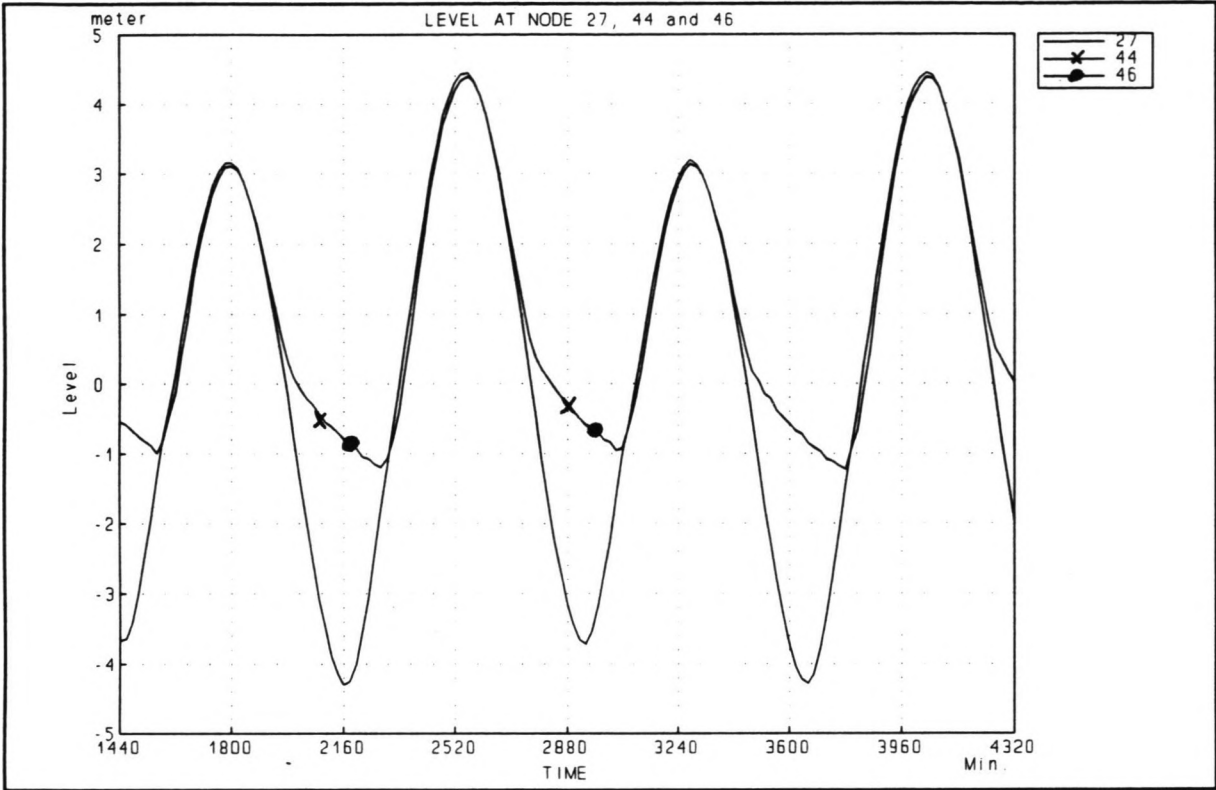


Figure C75: Water level during phase 6

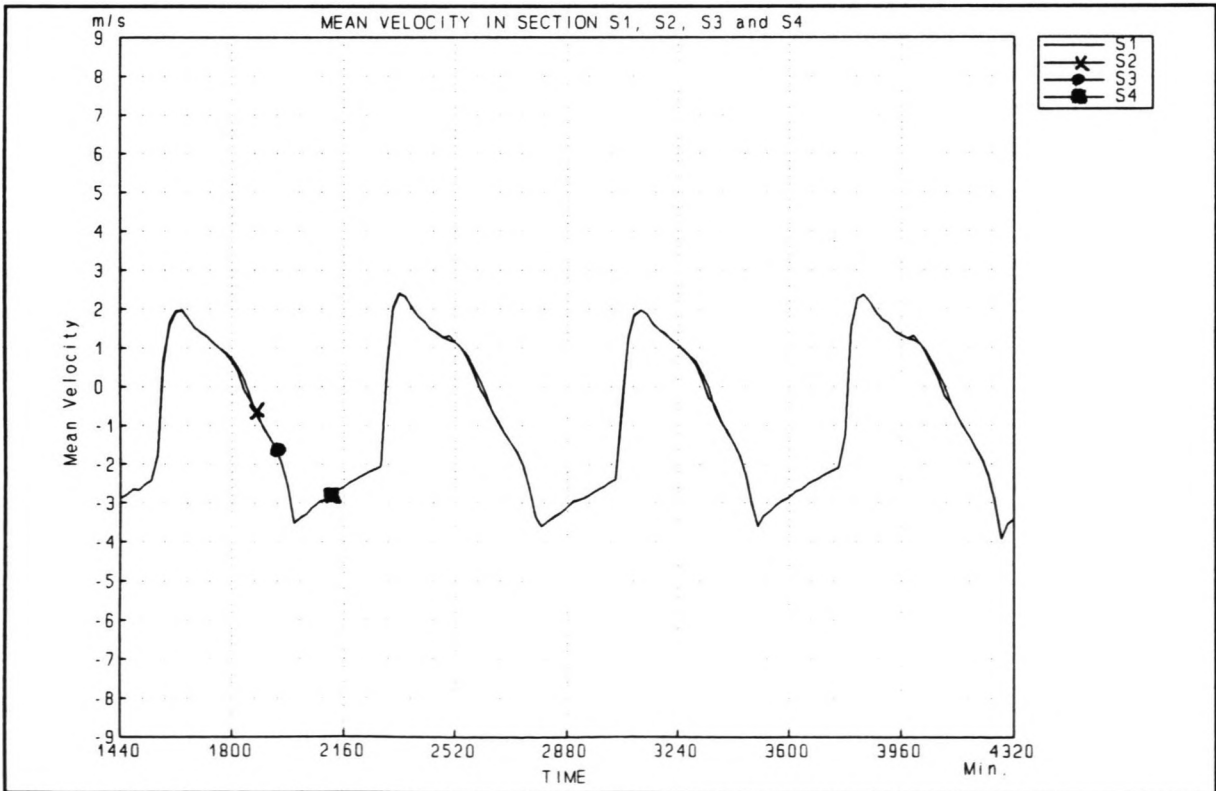


Figure C76: Flow velocities during phase 6

Closure of the Shiwa Tidal Basin

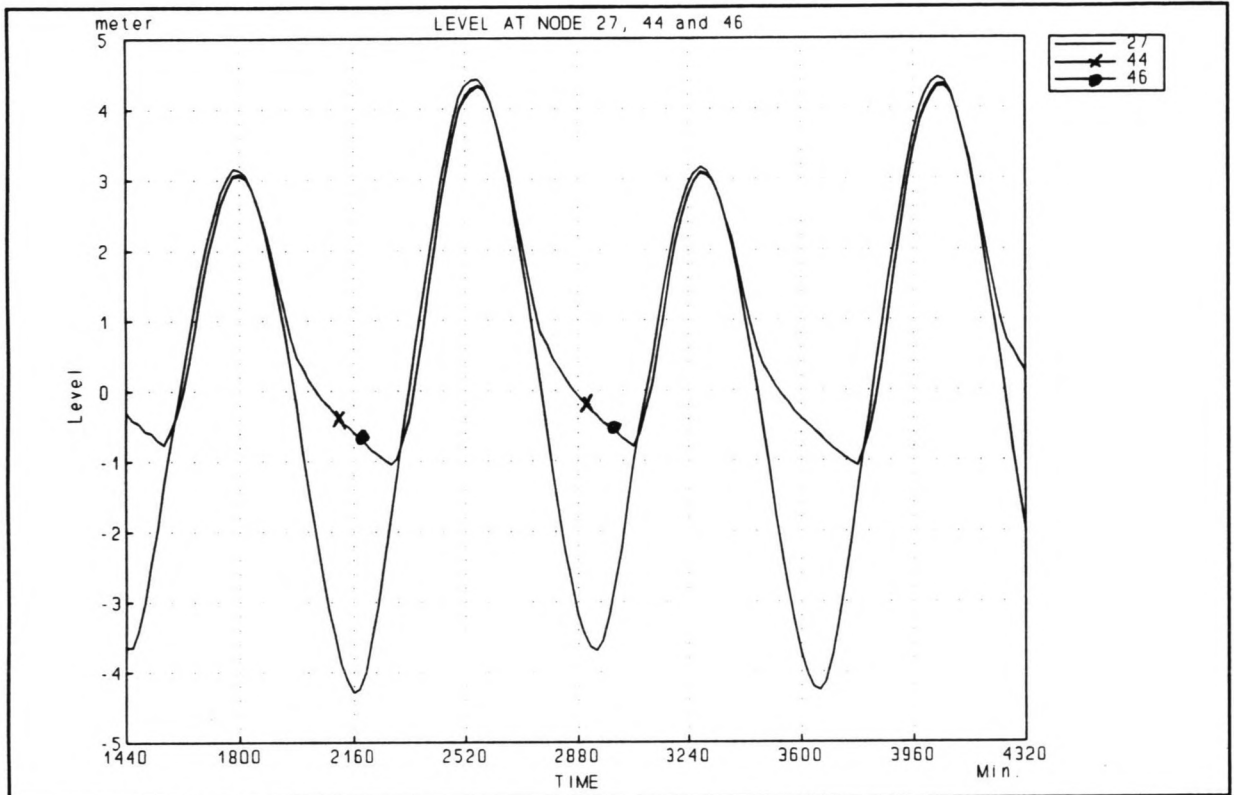


Figure C77: Water level during phase 7

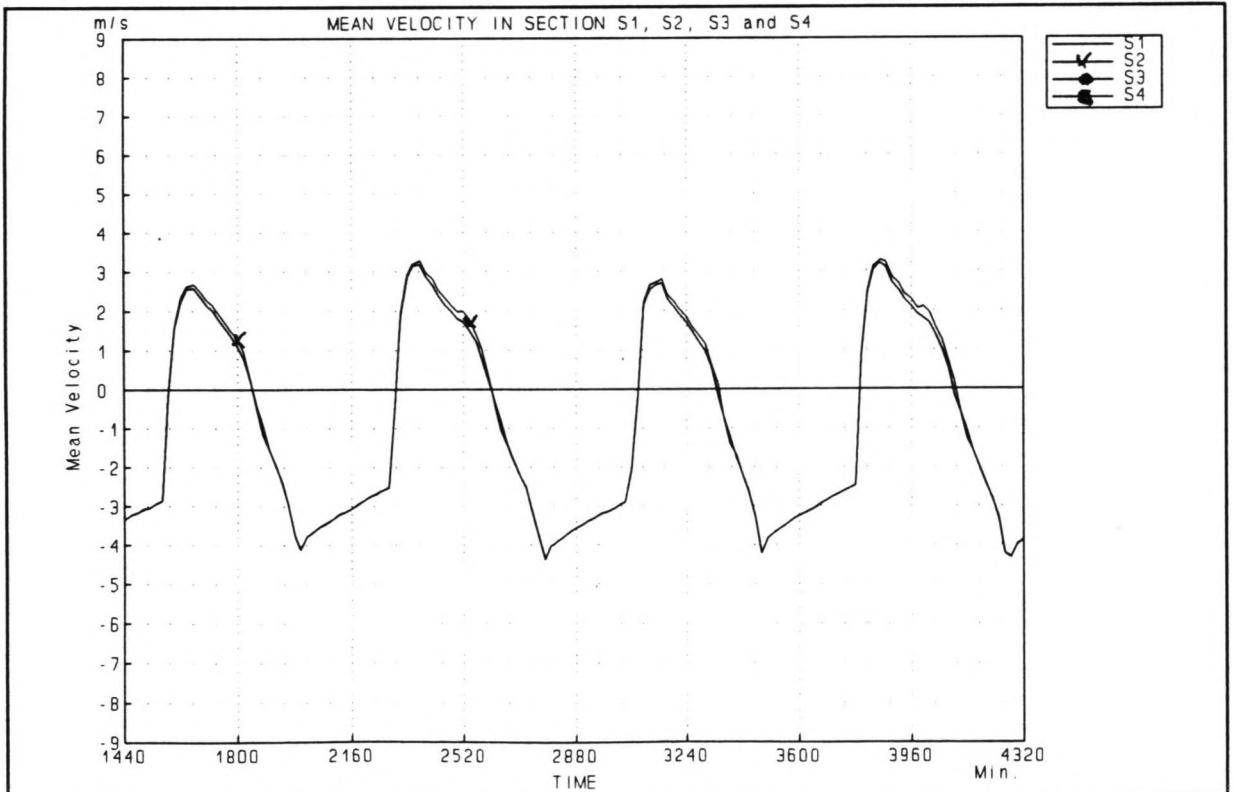


Figure C78: Flow velocities during phase 7

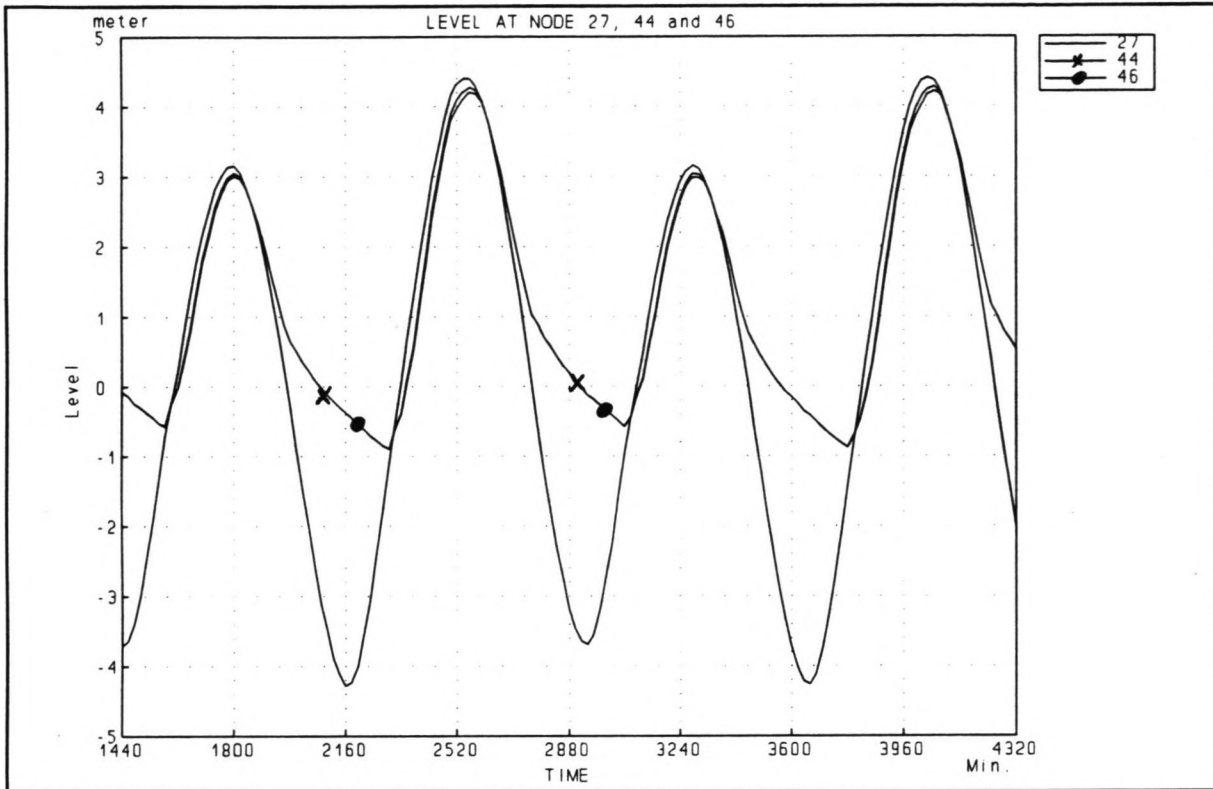


Figure C79: Water level during phase 8

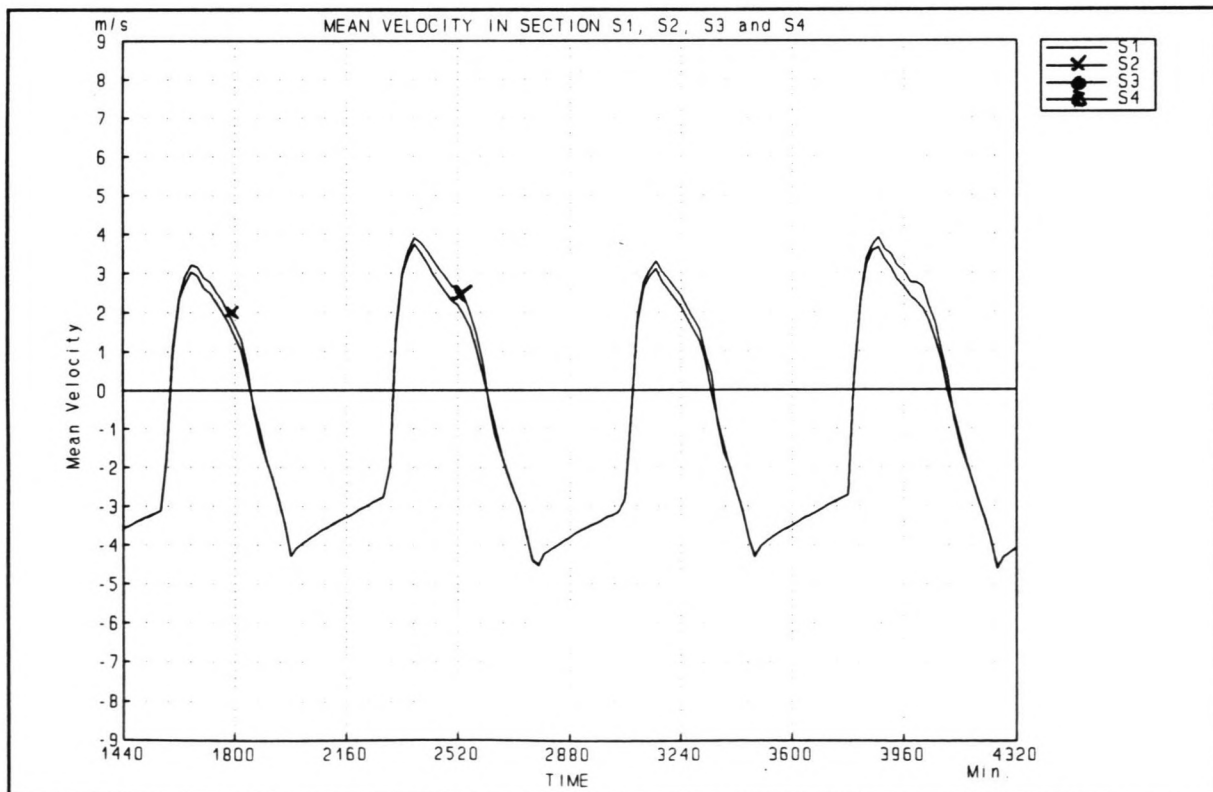


Figure C80: Flow velocities during phase 8

Closure of the Shiwa Tidal Basin

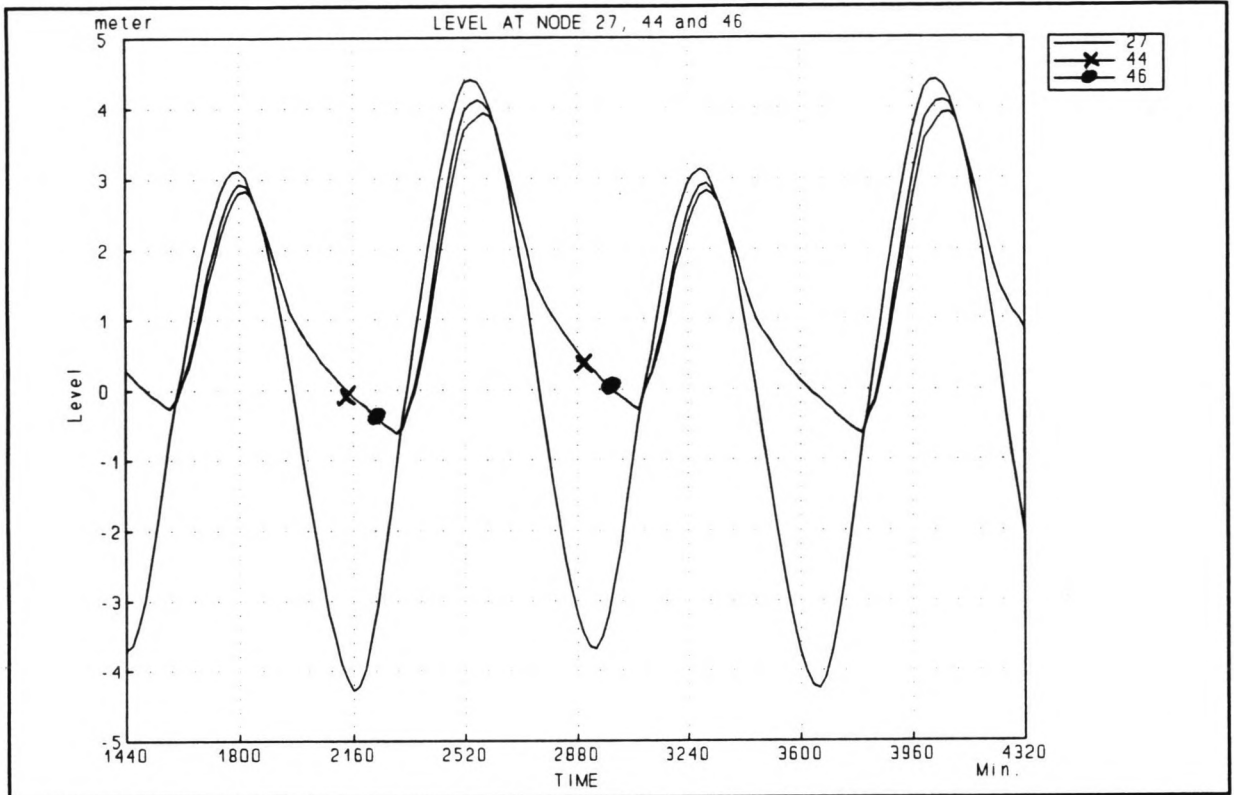


Figure C81: Water level during phase 9

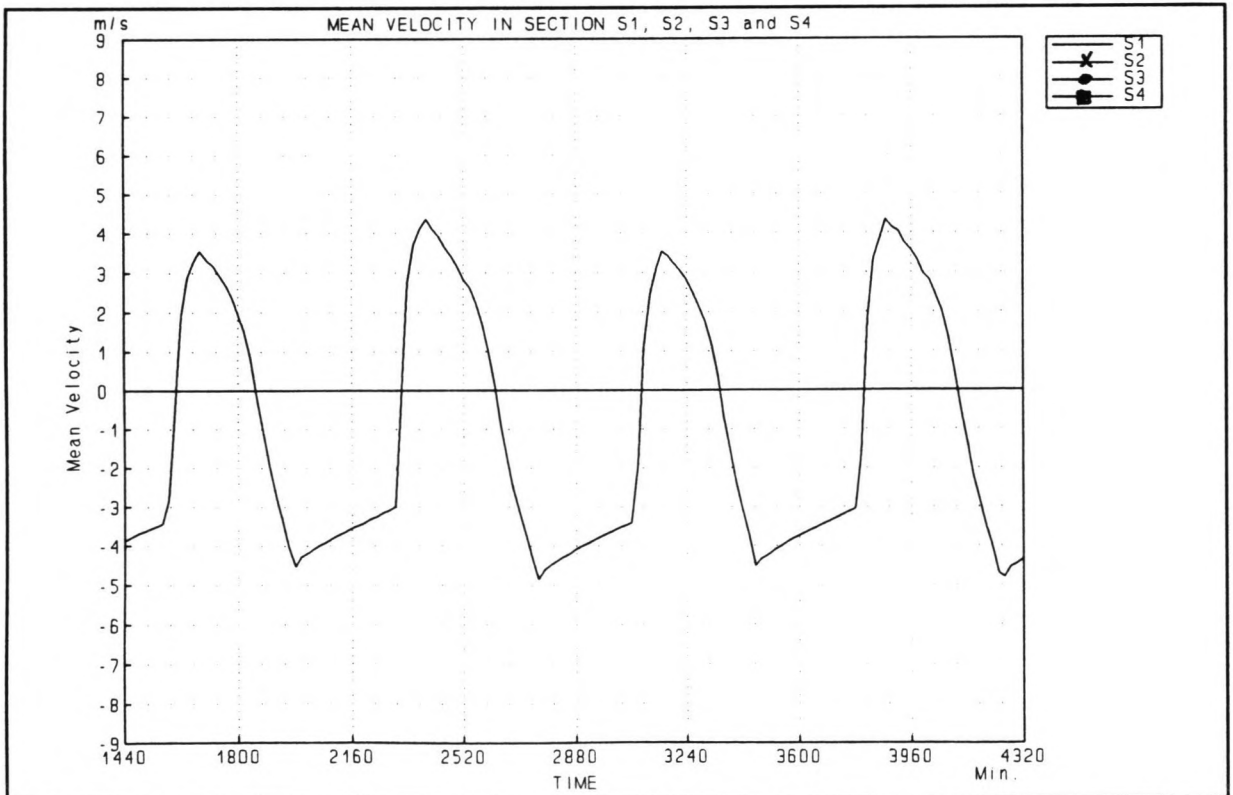


Figure C82: Flow velocities during phase 9

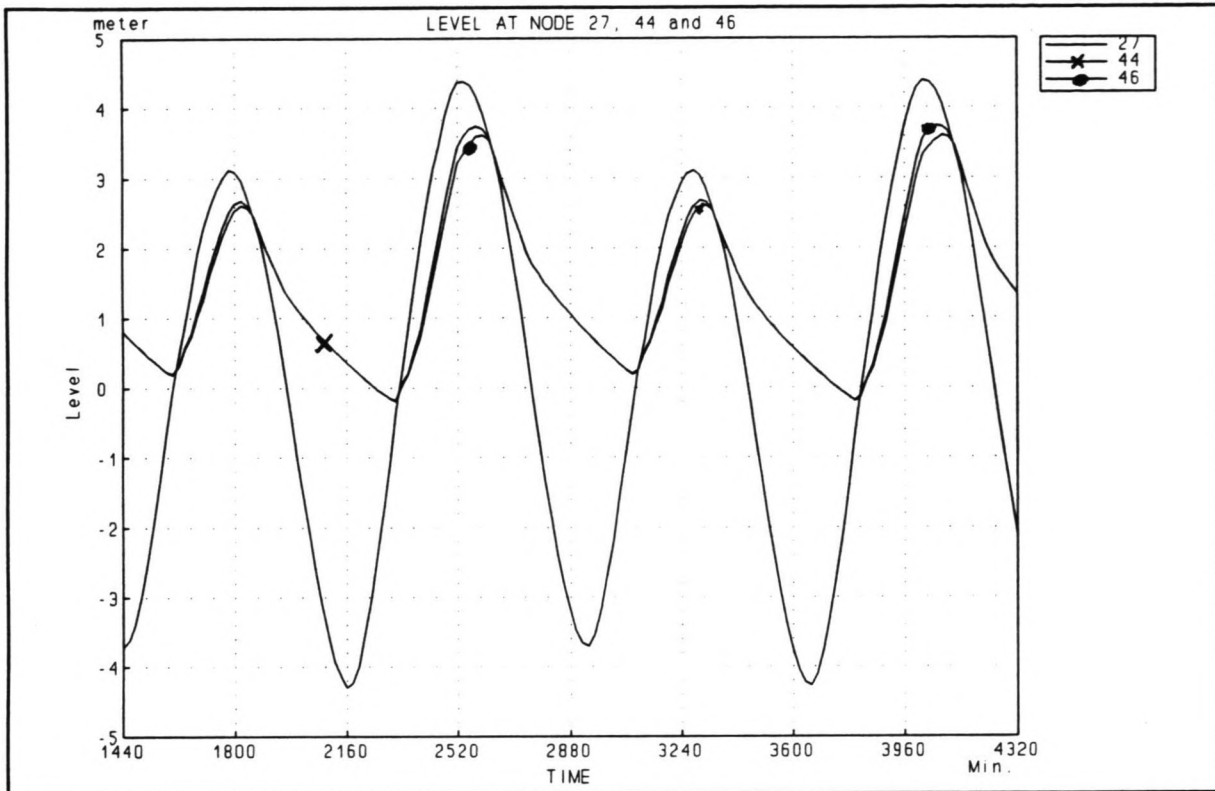


Figure C83: Water level during phase 10

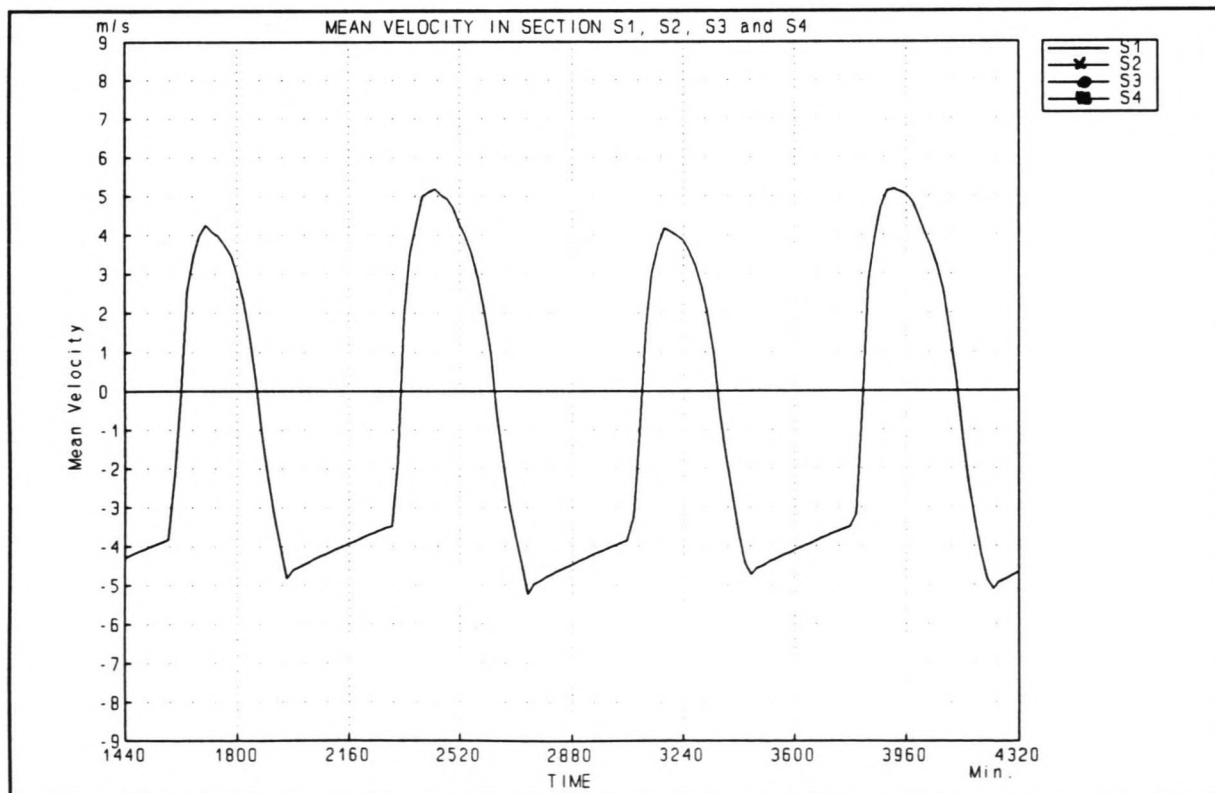


Figure C84: Flow velocities during phase 10

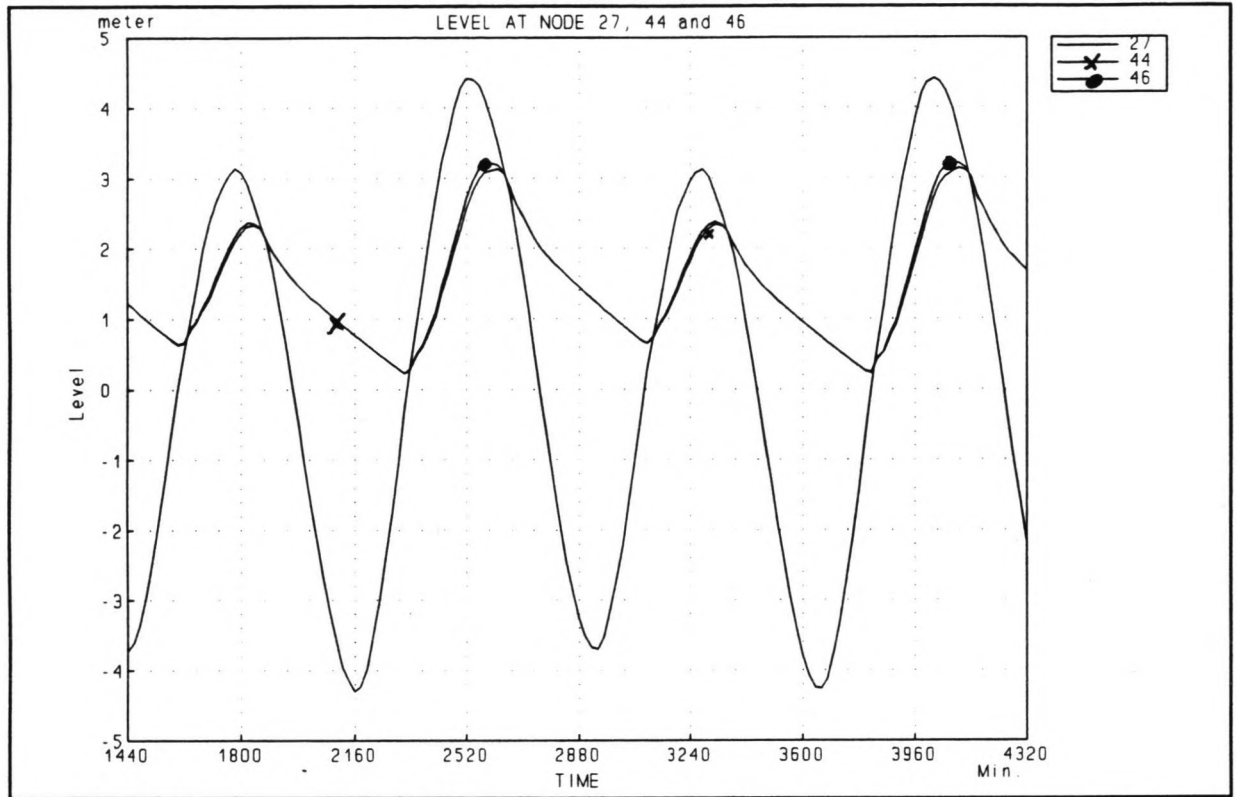


Figure C85: Water level during phase 11

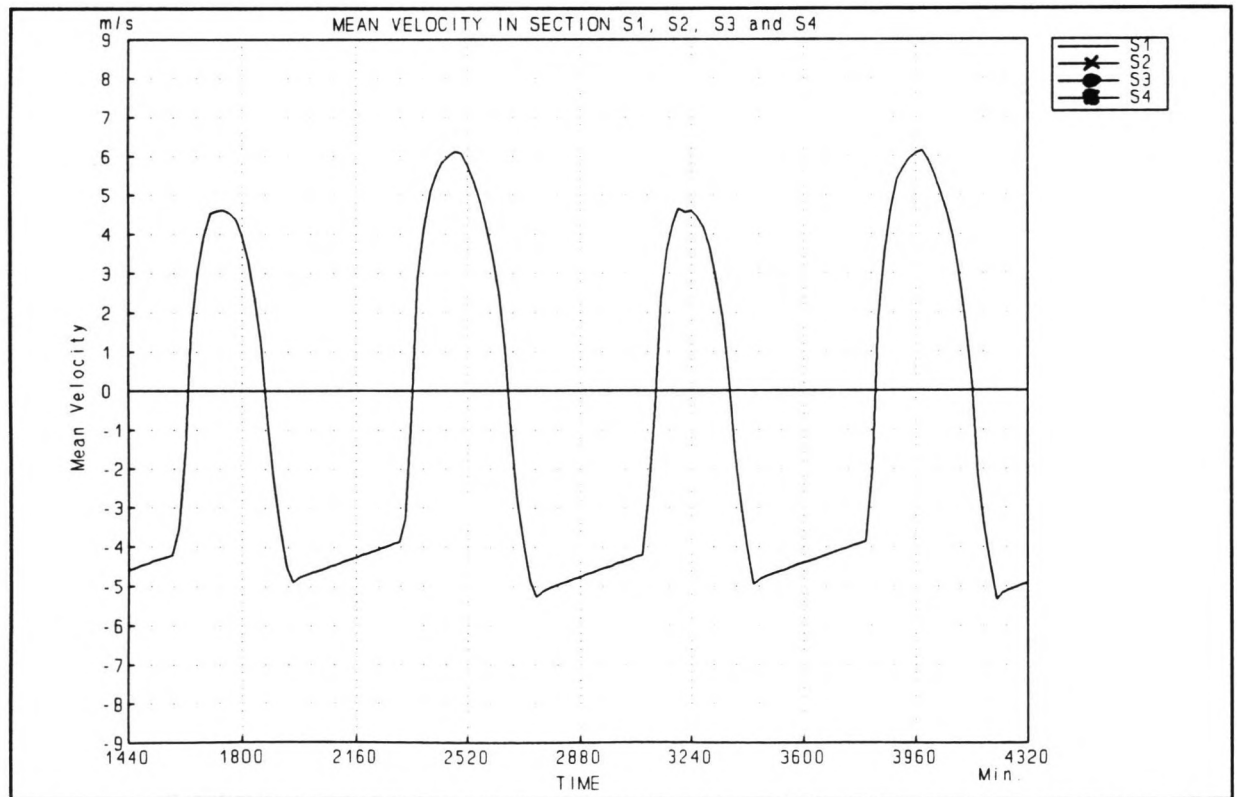


Figure C86: Flow velocities during phase 11

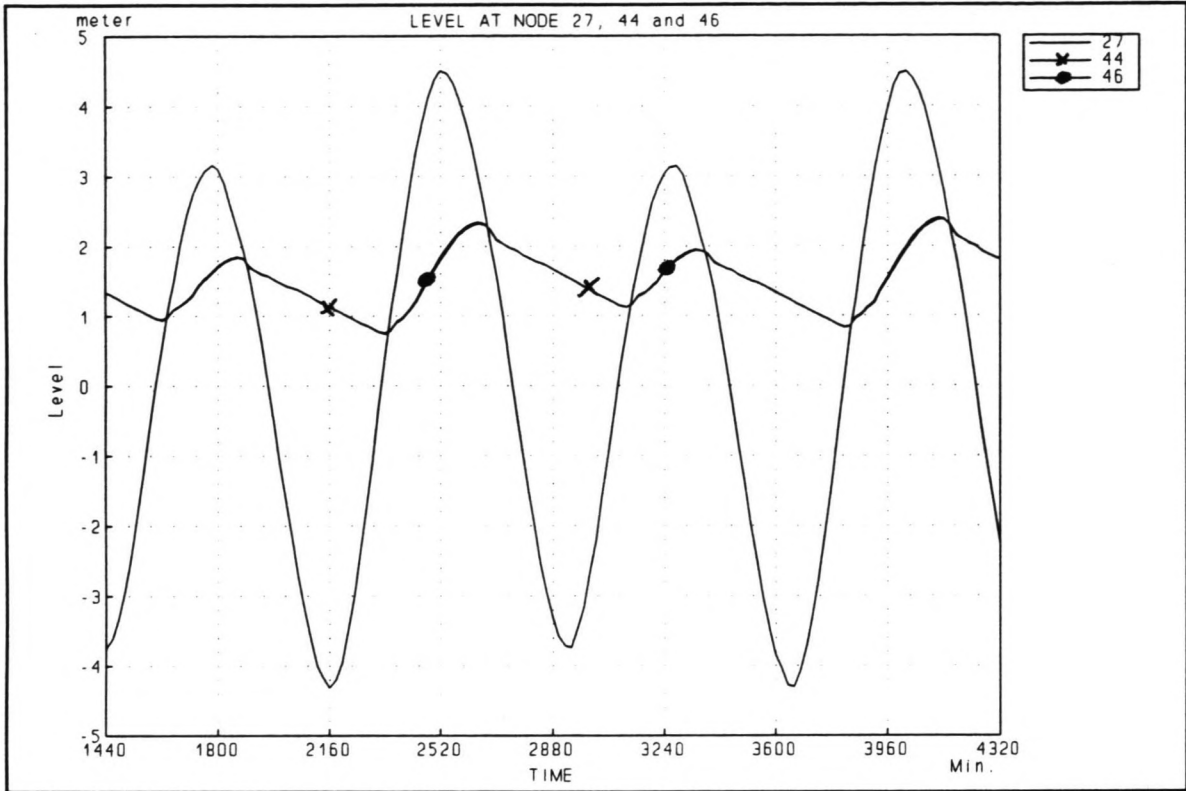


Figure C87: Water level during phase 12

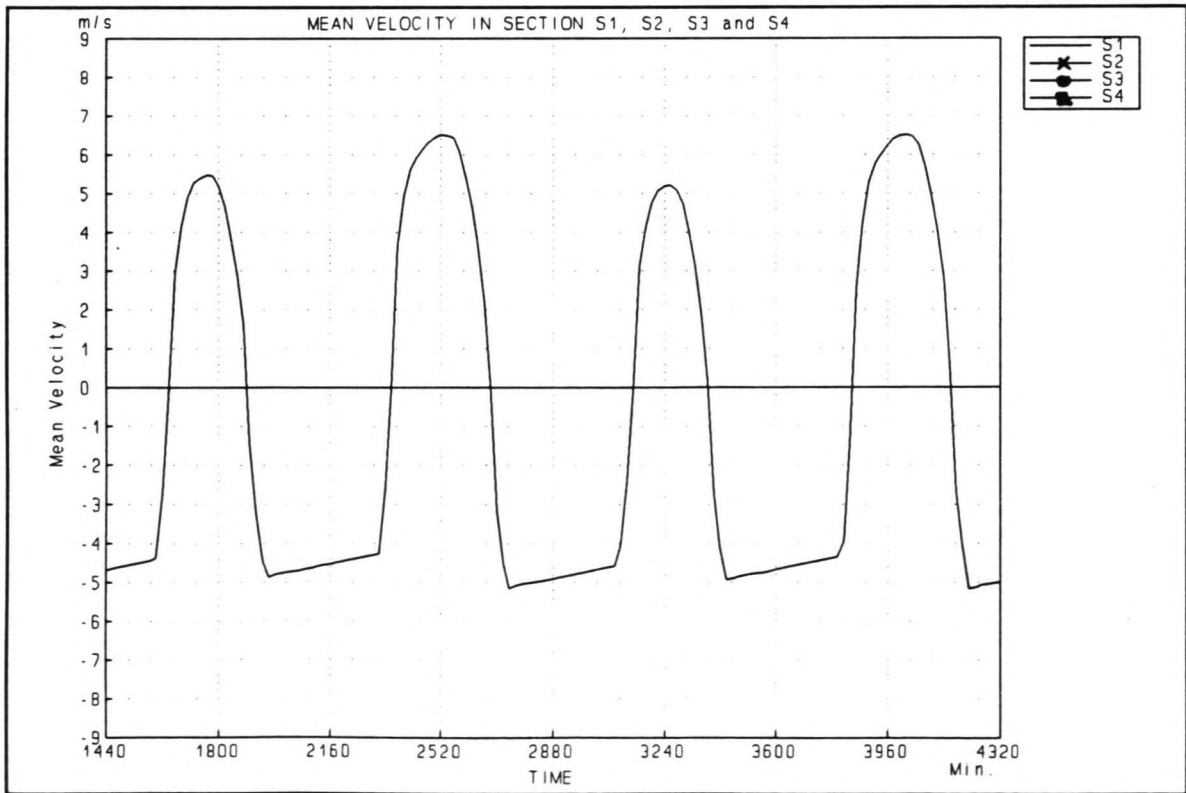


Figure C88: Flow velocities during phase 12

Closure of the Shiwa Tidal Basin

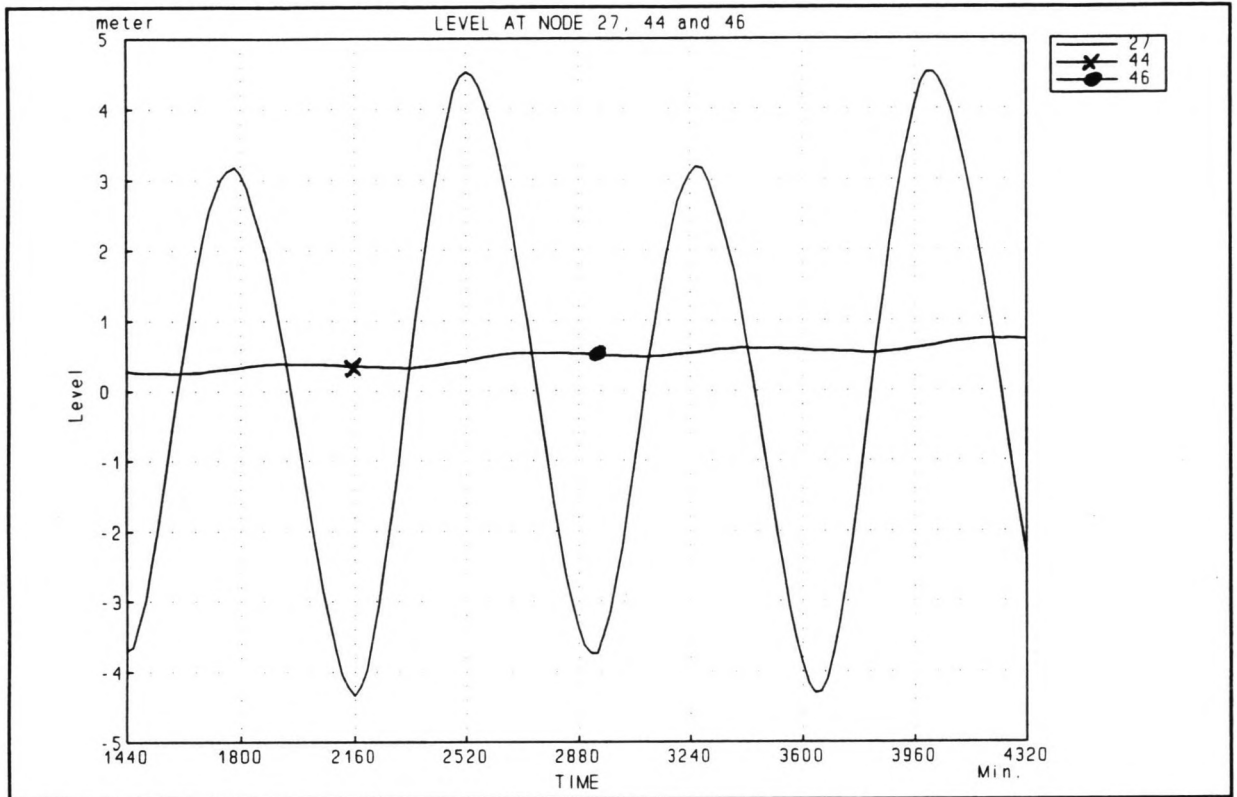


Figure C89: Water level during phase 13

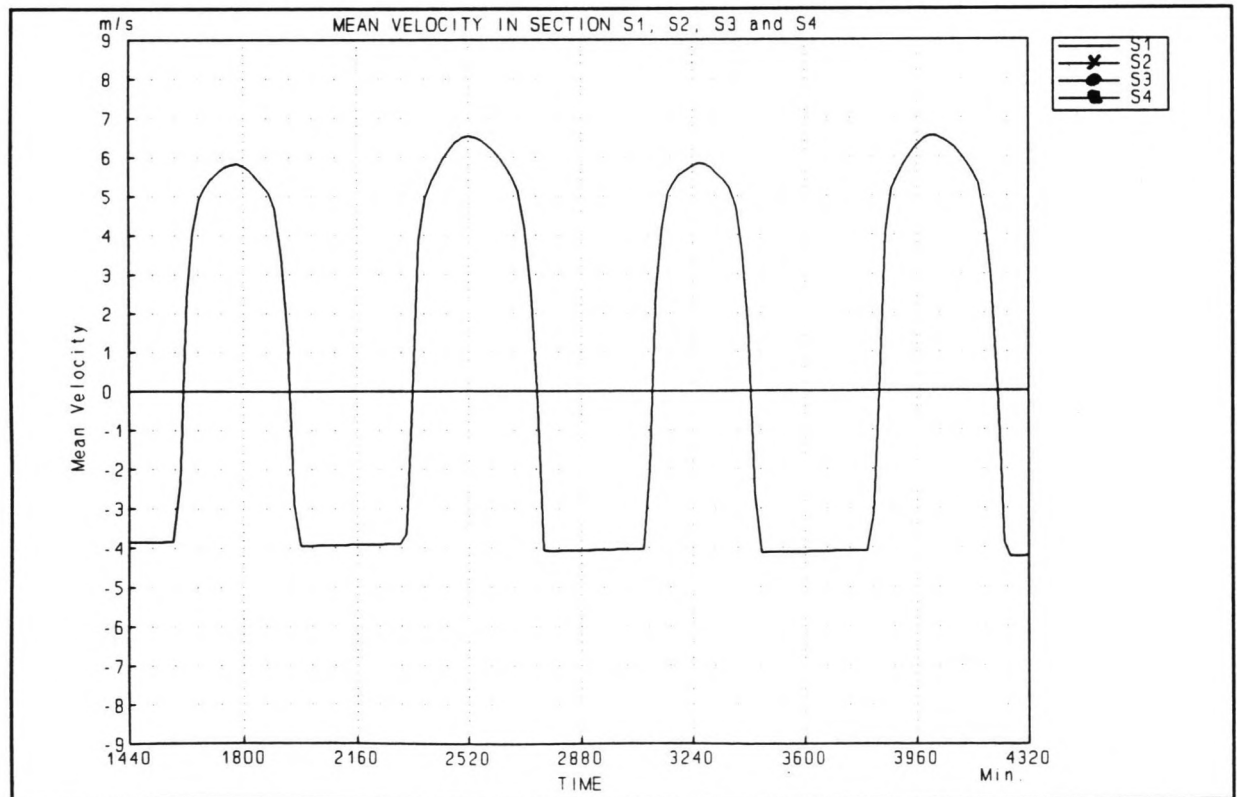


Figure C90: Flow velocities during phase 13

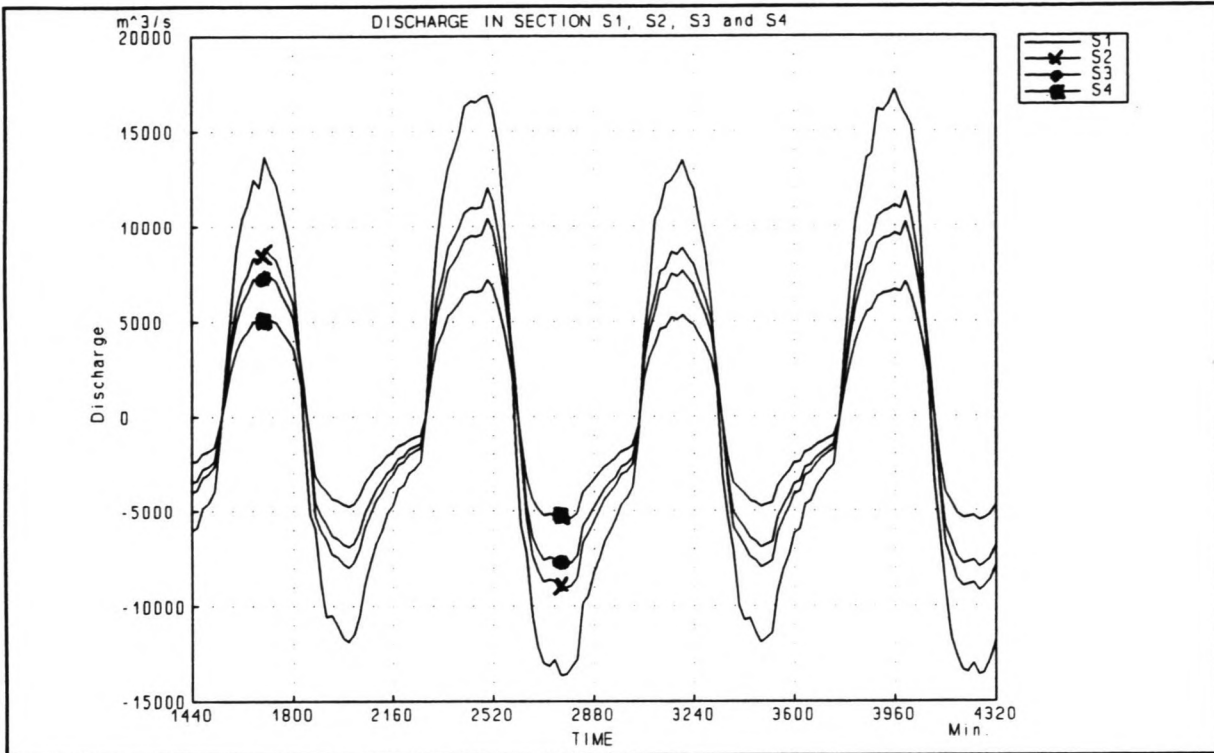


Figure C91: Discharges during phase 4

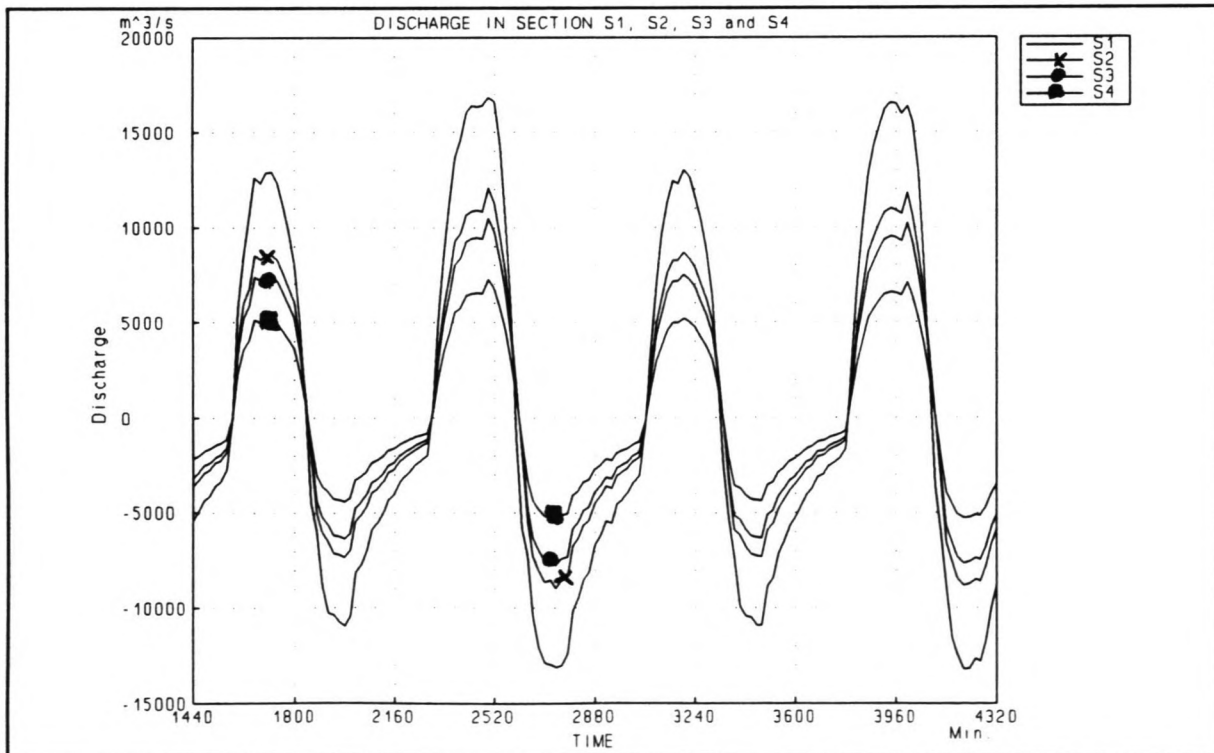


Figure C92: Discharges during phase 5.

Closure of the Shiwa Tidal Basin

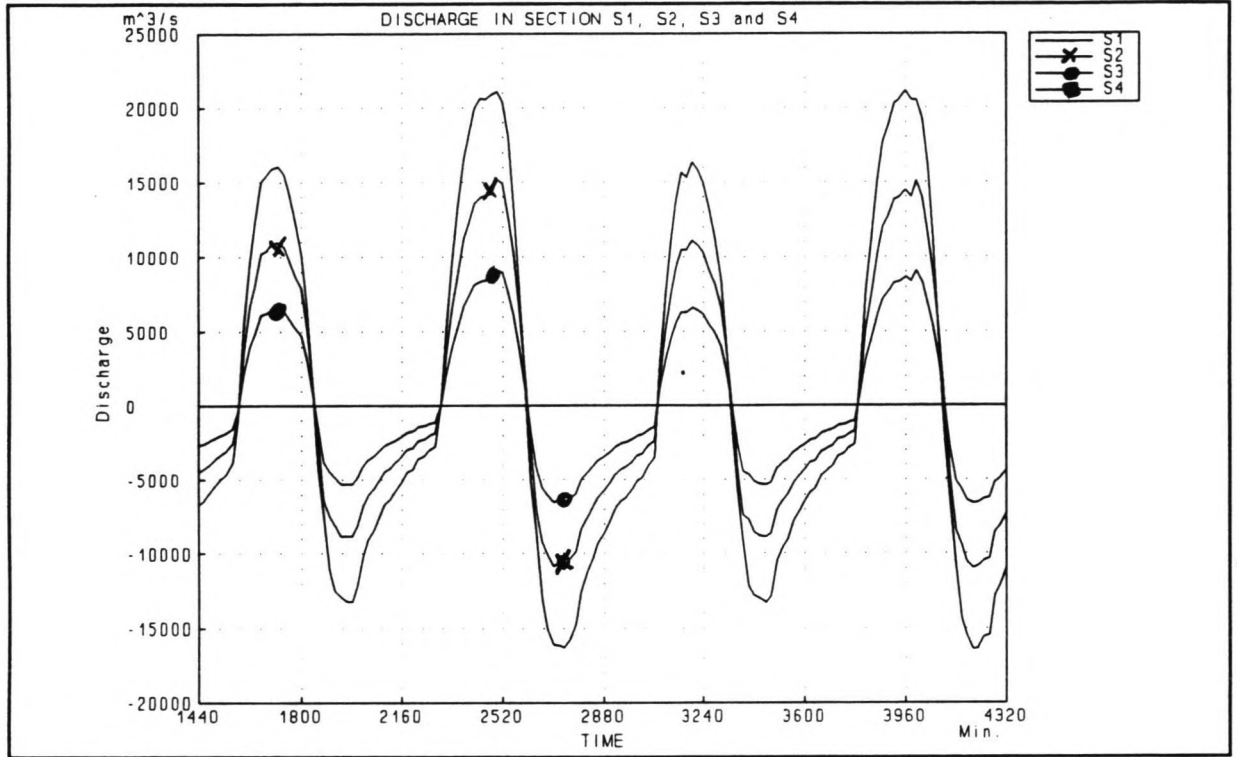


Figure C93: Discharges during phase 6

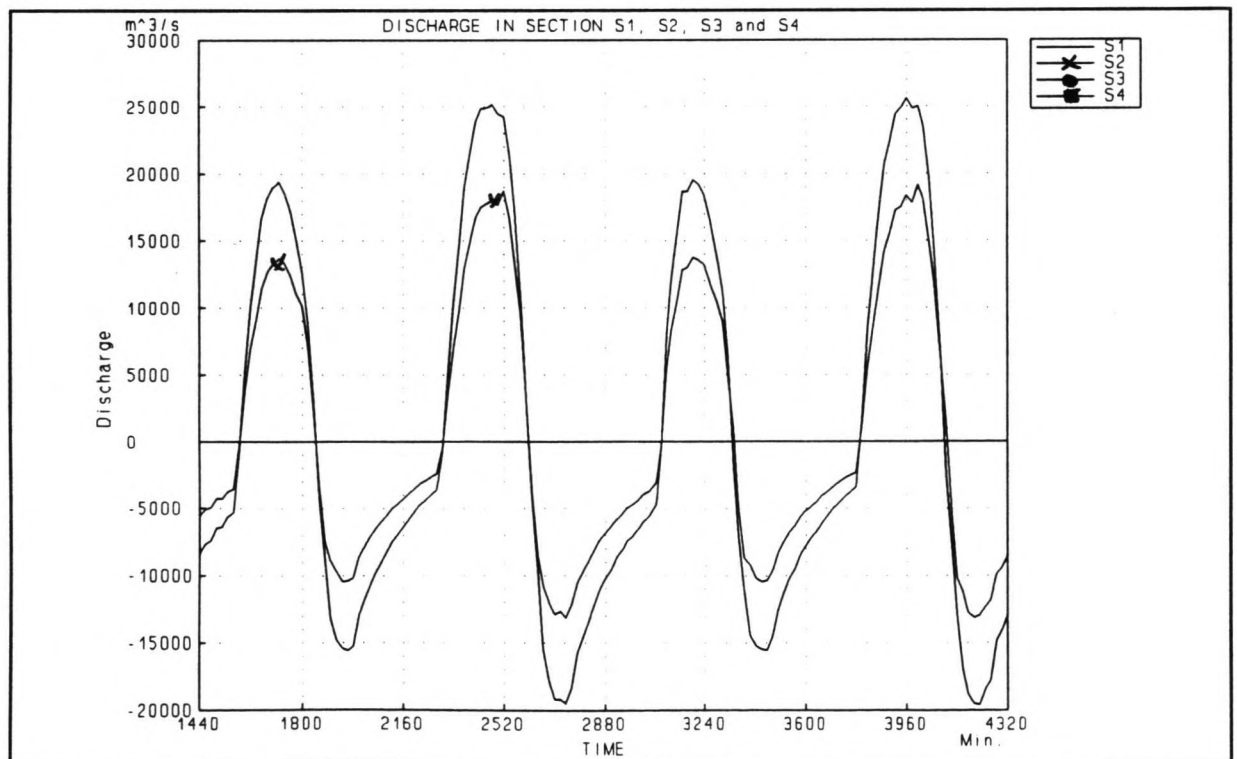


Figure C94: Discharges during phase 7

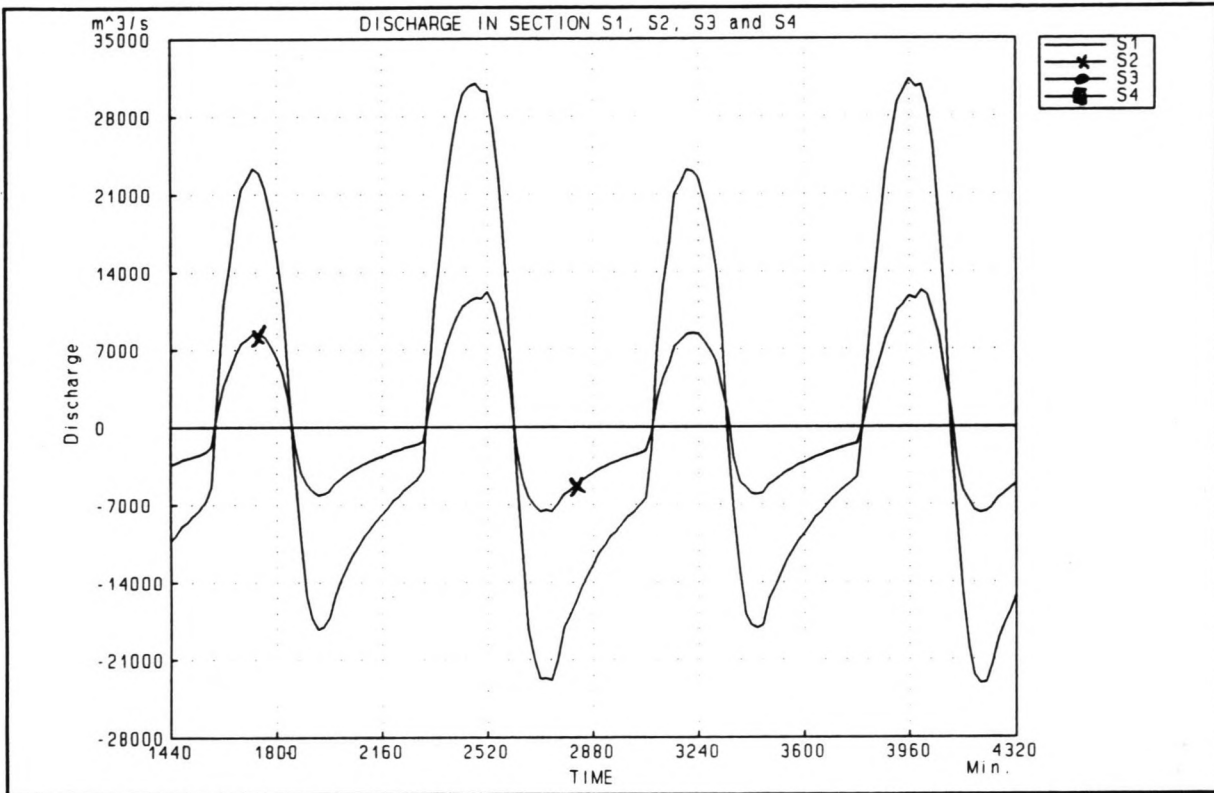


Figure C95: Discharges during phase 8

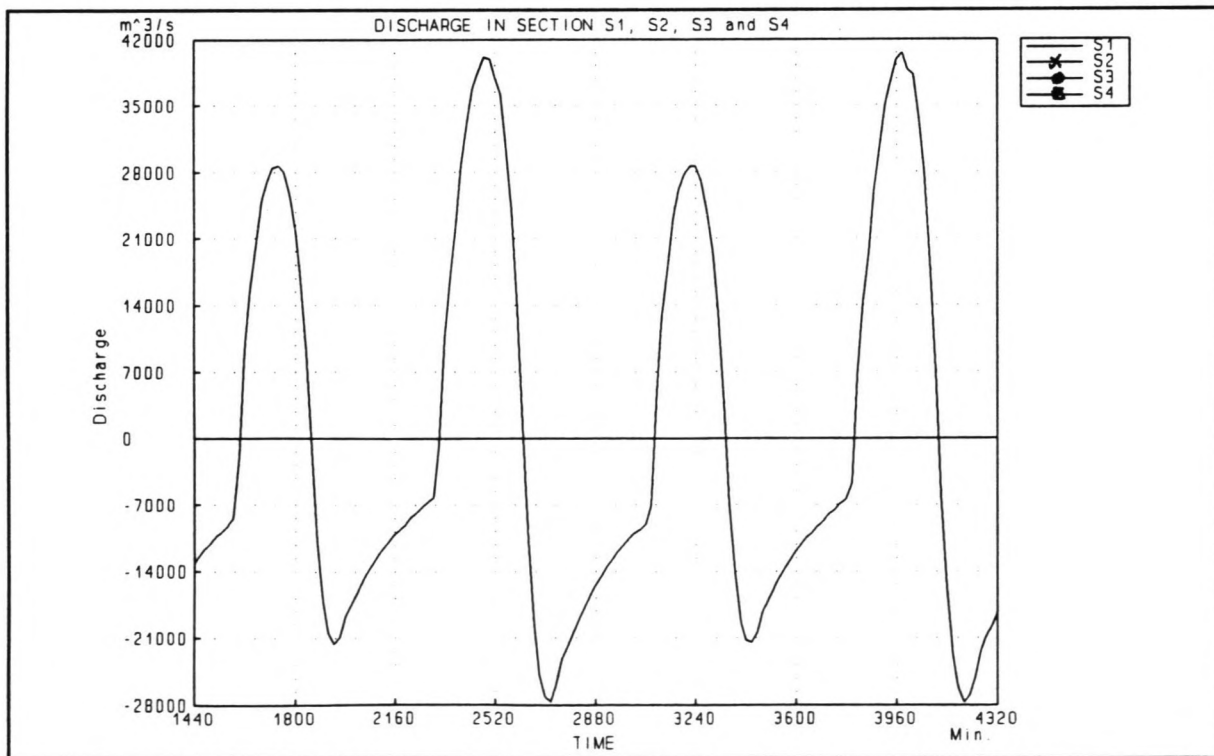


Figure C96: Discharges during phase 9

Closure of the Shiwa Tidal Basin

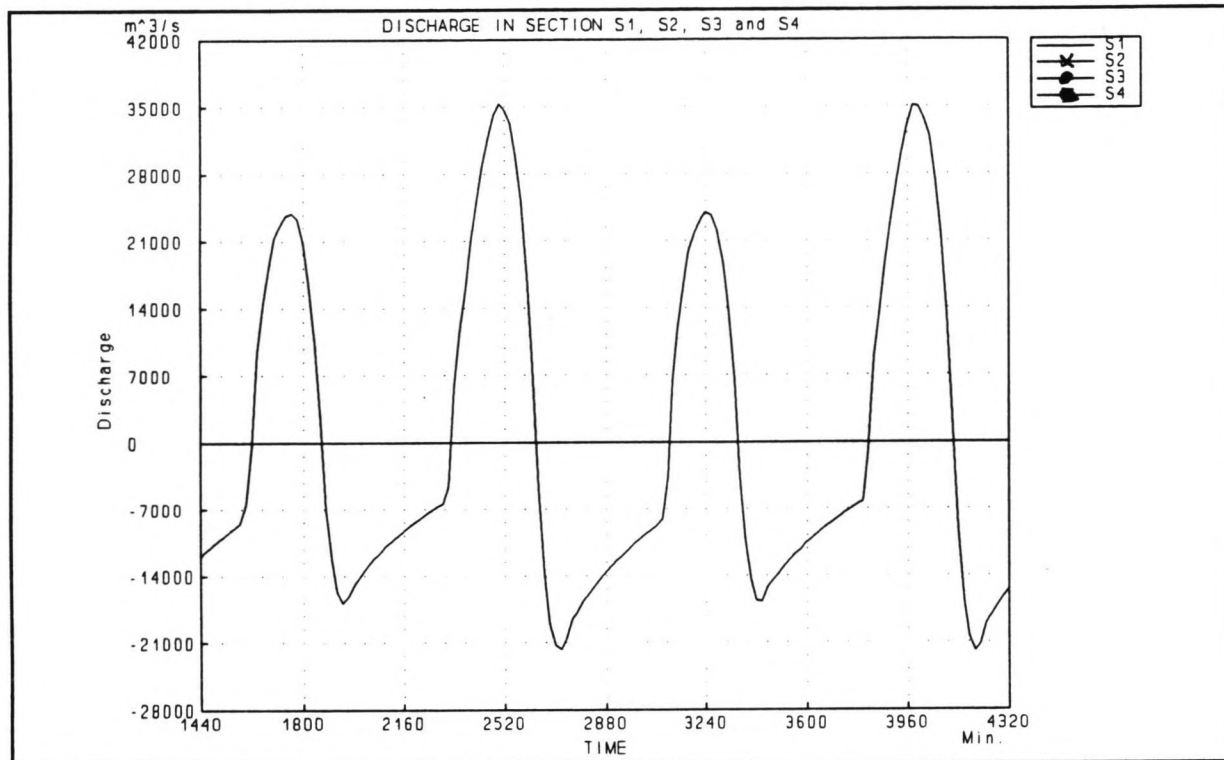


Figure C97: Discharges during phase 10

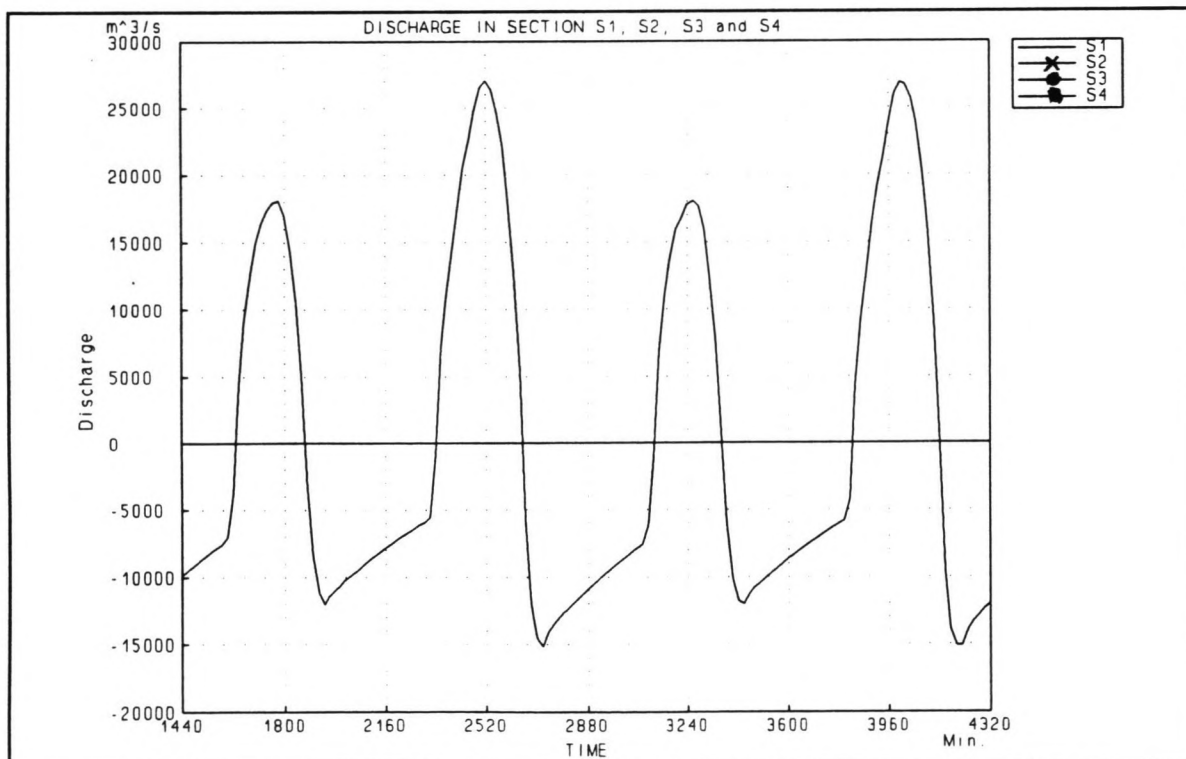


Figure C98: Discharges during phase 11

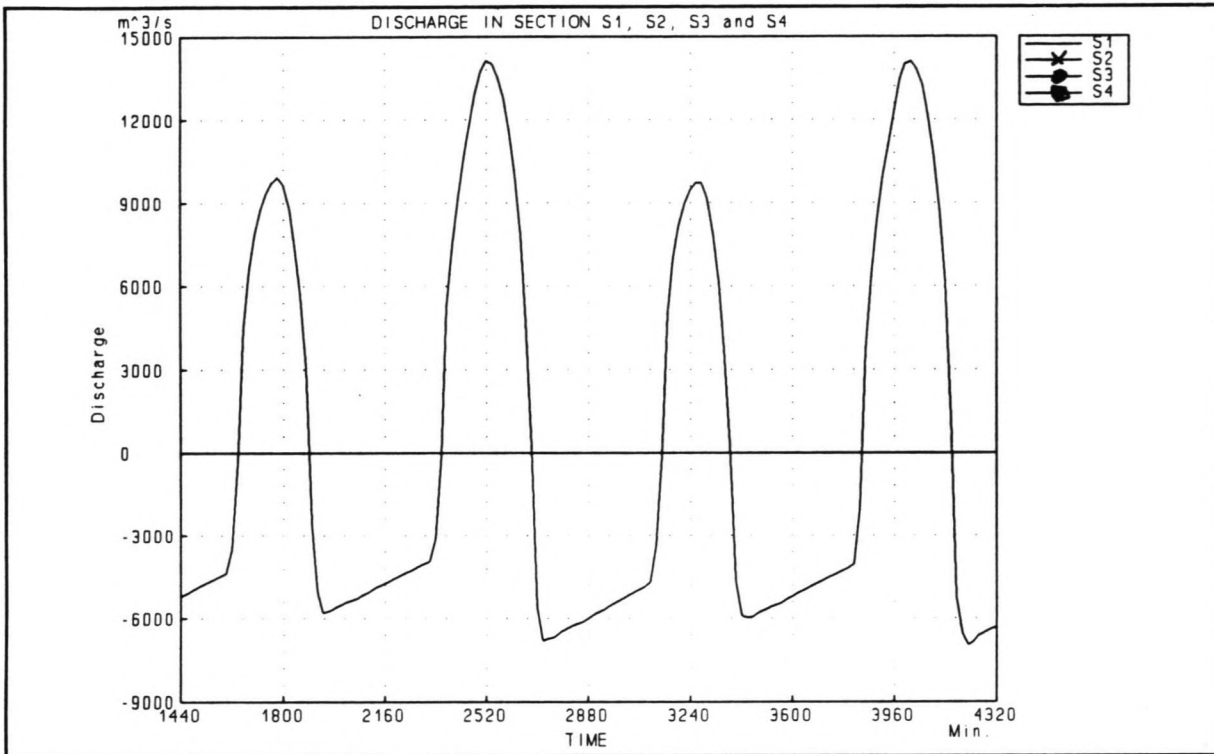


Figure C99: Discharges during phase 12

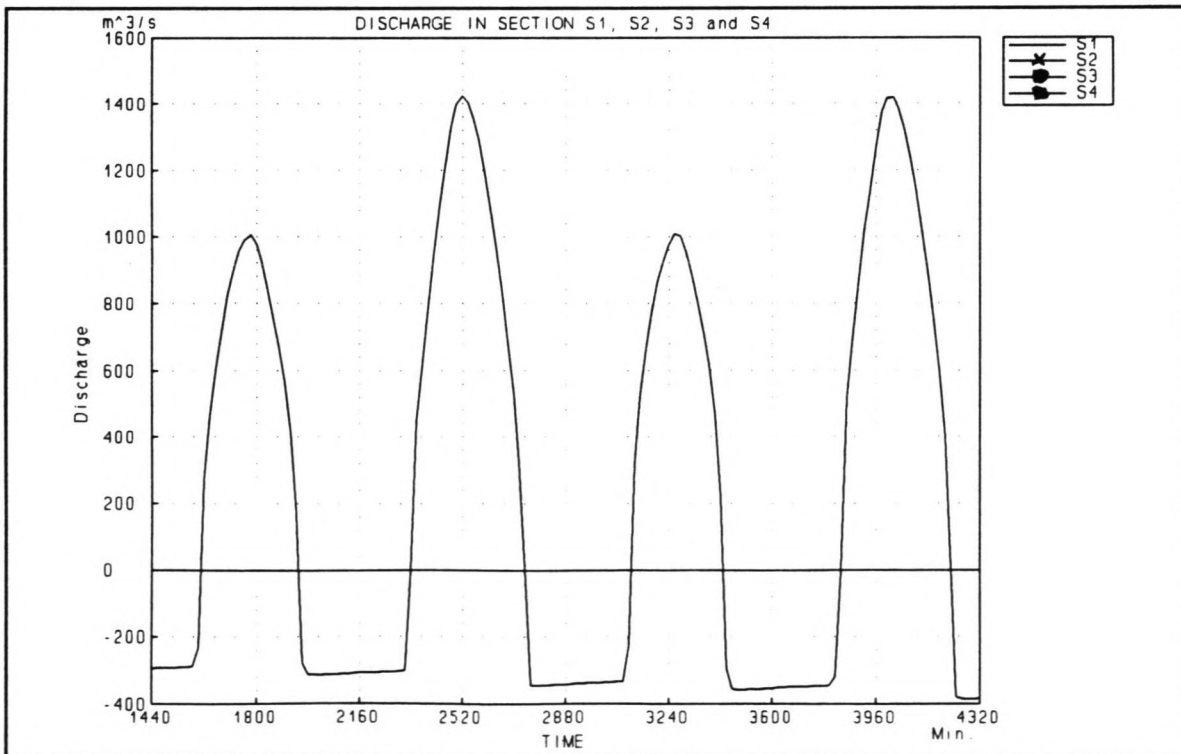


Figure C100: Discharges during phase 13

Annex D

This Annex contains

- D1: Calculation of the scour depth during a vertical closure
- D2: Calculation of the scour depth during a horizontal closure
- D3: Calculation of the scour depth during a combined closure

Annex D1		vertical closure method			
phase:	weir number:	1	2	3	4
1	α	2.9	2.55	1.5	1.5
	μ	0.5	0.651	1	1
	u_{cr}	0.118	0.118	0.116	0.116
	Σ Flood	7.71	8.97	9.59	9.93
	Σ Ebb	11.54	13.36	13.26	13.23
	t	4159.9	4159.9	4159.9	4159.9
	Hmax Flood	0.71	0.79	0.8	0.7
	Hmax Ebb	1.05	1.17	1.04	0.9
2	α	3.11	2.78	1.7	1.5
	μ	0.375	0.462	0.75	1
	u_{cr}	0.132	0.118	0.115	0.111
	Σ Flood	8.11	11.25	10.82	15.425
	Σ Ebb	14.81	18.91	19.08	25.5
	t	1659.6	1659.6	1659.6	1659.6
	Hmax Flood	0.77	0.8	0.94	0.95
	Hmax Ebb	1.32	1.53	1.38	1.43
3	α	3.6	3.35	2.3	1.5
	μ	0.25	0.31	0.5	1
	u_{cr}	0.132	0.118	0.111	0.118
	Σ Flood	9.56	13.25	16.53	26.86
	Σ Ebb	29.4	39.6	48.48	77.46
	t	1133.5	1133.5	1133.5	1133.5
	Hmax Flood	0.82	0.89	1.07	1.37
	Hmax Ebb	1.94	2.42	2.54	3.36

Closure of the Shiwa Tidal Basin

phase:	weir number:	vertical closure method			
		1	2	3	4
4	α	3.76	2.87	2.41	1.52
	μ	0.21	0.26	0.41	0.77
	u_{cr}	0.132	0.118	0.111	0.115
	Σ Flood	7.33	9.98	12.38	16.96
	Σ Ebb	23.77	30.36	36.88	49.84
	t	834.1	834.1	834.1	834.1
	Hmax Flood	0.86	0.94	1.16	2.08
	Hmax Ebb	2.13	2.65	2.81	3.64
5	α	3.73	3.57	2.7	1.7
	μ	0.167	0.2	0.32	0.58
	u_{cr}	0.132	0.118	0.111	0.115
	Σ Flood	10.69	12.93	18.71	41.21
	Σ Ebb	31.13	40.82	58.09	166.92
	t	737.4	737.4	737.4	737.4
	Hmax Flood	0.91	0.99	1.26	2.46
	Hmax Ebb	2.42	3.01	3.41	6.47
6	α	3.76	3.45	2.81	1.8
	μ	0.13	0.15	0.24	0.42
	u_{cr}	0.118	0.111	0.115	0.118
	Σ Flood	10.11	9.45	15.48	38.66
	Σ Ebb	21.48	24.26	39.39	191.165
	t	644.4	644.4	644.4	644.4
	Hmax Flood	0.97	1.02	1.33	2.64
	Hmax Ebb	2.54	3.11	3.61	8.38

phase:	weir number:	vertical closure method			
		1	2	3	4
7	α	3.9	3.56	2.94	1.99
	μ	0.1	0.12	0.18	0.3
	u_{cr}	0.125	0.118	0.115	0.118
	Σ Flood	7.78	7.81	11.93	33.04
	Σ Ebb	12.89	15.68	23.81	241.13
	t	551.2	551.2	551.2	551.2
	Hmax Flood	0.98	1.04	1.35	2.77
	Hmax Ebb	2.56	3.14	3.65	8.39
8	α	3.9	3.73	2.96	2.06
	μ	0.055	0.07	0.11	0.17
	u_{cr}	0.132	0.125	0.132	0.118
	Σ Flood	1.91	3.01	4.67	29.48
	Σ Ebb	2.34	3.942	6.31	261.84
	t	457.6	457.6	457.6	457.6
	Hmax Flood	0.98	1.04	1.36	2.86
	Hmax Ebb	2.56	3.14	3.65	10.52
9	α	3.96	3.8	3.08	2.27
	μ	0.027	0.032	0.048	0.077
	u_{cr}	0.145	0.145	0.145	0.145
	Σ Flood	0	0	0	0
	Σ Ebb	0	0	0	0
	t				
	Hmax Flood				
	Hmax Ebb				

Annex D2		horizontal closure phase			
phase:	weir number:	1	2	3	4
1	α	4	4	4	4
	μ	1	1	1	1
	u_{cr}	0.118	0.118	0.118	0.118
	Σ Flood	24.68	39.718	39.718	39.718
	Σ Ebb	30.44	38.85	38.85	38.85
	t	1553	1553	1553	1553
	Hmax Flood	1.58	2.44	2.2	1.92
	Hmax Ebb	1.95	2.38	2.16	1.88
2	α	3.4	4	4	4
	μ	1	1	1	1
	u_{cr}	0.118	0.118	0.118	0.118
	Σ Flood	26.1	43.03	43.03	43.03
	Σ Ebb	30.16	46.5	46.5	46.5
	t	1553	1553	1553	1553
	Hmax Flood	2.11	3.29	2.99	2.6
	Hmax Ebb	2.5	3.4	3.09	2.7
3	α	3	4	4	4
	μ	1	1	1	1
	u_{cr}	0.118	0.118	0.118	0.118
	Σ Flood	27.7	52.197	52.197	52.197
	Σ Ebb	34.01	58.125	58.125	58.125
	t	1553	1553	1553	1553
	Hmax Flood	2.53	4.22	3.83	3.33
	Hmax Ebb	3.07	4.52	4.1	3.57

Closure of the Shiwa Tidal Basin

		horizontal closure method			
phase:	weir number:	1	2	3	4
4	α	2.4	4	4	4
	μ	1	1	1	1
	u_{cr}	0.11	0.11	0.11	0.11
	Σ Flood	25.07	68.75	68.75	68.75
	Σ Ebb	40.13	75.77	75.77	75.77
	t	1553	1553	1553	1553
	Hmax Flood	2.81	5.47	4.97	4.32
	Hmax Ebb	3.69	5.95	5.4	4.7
5	α		4	4	4
	μ		1	1	1
	u_{cr}		0.11	0.11	0.11
	Σ Flood		96.48	96.48	96.48
	Σ Ebb		118.25	118.25	118.25
	t		1553	1553	1553
	Hmax Flood		7.4	6.7	5.84
	Hmax Ebb		8.6	7.8	6.8
6	α		3.5	4	4
	μ		1	1	1
	u_{cr}		0.11	0.11	0.11
	Σ Flood		112.5	112.5	112.5
	Σ Ebb		143.16	180.8	180.8
	t		1300	1300	1300
	Hmax Flood		9.02	9.13	7.95
	Hmax Ebb		10.9	11.17	9.72

phase:	weir number:	horizontal closure method			
		1	2	3	4
7	α		2.8	4	4
	μ		1	1	1
	u_{cr}		0.11	0.11	0.11
	Σ Flood		125.37	234.02	234.02
	Σ Ebb		172.15	320.03	320.03
	t		1300	1300	1300
	Hmax Flood		10.65	13.92	12.12
	Hmax Ebb		13.5	18.37	16
8	α			2.8	4
	μ			1	1
	u_{cr}			0.118	0.118
	Σ Flood			244.34	244.34
	Σ Ebb			392.542	726.27
	t			1300	1300
	Hmax Flood			19.9	28.94
	Hmax Ebb			28.85	44.67
9	α				4
	μ				1
	u_{cr}				0.125
	Σ Flood				1261.23
	Σ Ebb				2028.8
	t				1903.2
	Hmax Flood				104
	Hmax Ebb				108

Closure of the Shiwa Tidal Basin

phase:	weir number:	horizontal closure method			
			2	3	4
10	α				3.4
	μ				1
	u_{cr}				0.125
	Σ Flood				1612.8
	Σ Ebb				2072.45
	t				397
	Hmax Flood				109
	Hmax Ebb				116
11	α				2
	μ				1
	u_{cr}				0.13
	Σ Flood				903.5
	Σ Ebb				1128.7
	t				397
	Hmax Flood				110
	Hmax Ebb				117
12	α				2
	μ				1
	u_{cr}				0.13
	Σ Flood				858.52
	Σ Ebb				1198.4
	t				132
	Hmax Flood				146
	Hmax Ebb				158

Annex D3		combined closure method			
phase:	weir number:	1	2	3	4
1	α	2.9	2.55	1.5	1.5
	μ	0.5	0.651	1	1
	u_{cr}	0.118	0.118	0.116	0.116
	Σ Flood	7.71	8.97	9.59	9.93
	Σ Ebb	11.54	13.36	13.26	13.23
	t	5718.6	5718.6	5718.6	5718.6
	Hmax Flood	0.8	0.93	1.05	1.05
	Hmax Ebb	1.2	1.39	1.38	1.38
2	α	3.11	2.78	1.7	1.5
	μ	0.375	0.462	0.75	1
	u_{cr}	0.132	0.118	0.115	0.111
	Σ Flood	8.11	11.25	10.82	15.425
	Σ Ebb	14.81	18.91	19.08	25.5
	t	1313.5	1313.5	1313.5	1313.5
	Hmax Flood	0.88	1.1	1.29	1.55
	Hmax Ebb	1.38	1.7	1.81	2.19
3	α	3.6	3.35	2.3	1.5
	μ	0.25	0.31	0.5	1
	u_{cr}	0.132	0.118	0.111	0.118
	Σ Flood	9.56	13.25	16.53	26.86
	Σ Ebb	29.4	39.6	48.48	77.46
	t	543.65	543.65	543.65	543.65
	Hmax Flood	0.92	1.2	1.57	2.21
	Hmax Ebb	1.71	2.24	2.67	3.99

Closure of the Shiwa Tidal Basin

phase:	weir number:	combined closure method			
		1	2	3	4
4	α	3.76	2.87	2.41	1.52
	μ	0.21	0.26	0.41	0.77
	u_{cr}	0.132	0.118	0.111	0.115
	Σ Flood	7.33	9.98	12.38	16.96
	Σ Ebb	23.77	30.36	36.88	49.84
	t	510.03	510.03	510.03	510.03
	Hmax Flood	0.94	1.29	1.83	2.95
	Hmax Ebb	1.85	2.5	3.25	5.44
5	α	3.73	3.57	2.7	1.7
	μ	0.167	0.2	0.32	0.58
	u_{cr}	0.132	0.118	0.111	0.115
	Σ Flood	10.69	12.93	18.71	41.21
	Σ Ebb	31.13	40.82	58.09	166.92
	t	468.1	468.1	468.1	468.1
	Hmax Flood	0.99	1.39	2.15	4.04
	Hmax Ebb	2.08	2.87	4.12	8.97
6	α	3.45	3.34	3.04	
	μ	0.125	0.154	0.25	
	u_{cr}	0.111	0.111	0.111	
	Σ Flood	5.14	10.29	21.42	
	Σ Ebb	19.62	27.35	55.8	
	t	1526.2	1526.2	1526.2	
	Hmax Flood	1.01	1.52	2.67	
	Hmax Ebb	2.27	3.26	5.48	

phase:	weir number:	combined closure method			
		1	2	3	4
7	α	3.46	3.35		
	μ	0.136	0.17		
	u_{cr}	0.111	0.111		
	Σ Flood	11.11	17.54		
	Σ Ebb	27.63	39.38		
	t	1038.63	1038.63		
	Hmax Flood	1.11	1.73		
	Hmax Ebb	2.55	3.76		
8	α	3.45	3.36		
	μ	0.15	0.185		
	u_{cr}	0.111	0.111		
	Σ Flood	17.64	28.98		
	Σ Ebb	38.45	53.87		
	t	546.84	546.84		
	Hmax Flood	1.24	2.04		
	Hmax Ebb	2.82	4.27		
9	α	3.47			
	μ	0.16			
	u_{cr}	0.111			
	Σ Flood	28.4			
	Σ Ebb	52.56			
	t	546.84			
	Hmax Flood	1.58			
	Hmax Ebb	3.32			

Closure of the Shiwa Tidal Basin

phase:	weir number:	combined closure method			
		1	2	3	4
10	α	3.48			
	μ	0.176			
	u_{cr}	0.111			
	Σ Flood	51.69			
	Σ Ebb	76.47			
	t	341.2			
	Hmax Flood	2.2			
	Hmax Ebb	3.94			
11	α	3.48			
	μ	0.18			
	u_{cr}	0.118			
	Σ Flood	72.66			
	Σ Ebb	91.2			
	t	341.2			
	Hmax Flood	3.07			
	Hmax Ebb	4.68			
12	α	3.4			
	μ	0.19			
	u_{cr}	0.118			
	Σ Flood	97.1			
	Σ Ebb	106.08			
	t	341.2			
	Hmax Flood	4.19			
13	Hmax Ebb	5.52			
	α	3.4			
	μ	0.2			
	u_{cr}	0.118			

	Σ Flood	142.63			
	Σ Ebb	85.25			
	t	307			
	Hmax Flood	5.81			
	Hmax Ebb	5.89			

